

Fall 2013

Evaluating airborne laser data on steeply sloping terrain

Bob Champoux

University of New Hampshire, Durham

Follow this and additional works at: <https://scholars.unh.edu/thesis>

Recommended Citation

Champoux, Bob, "Evaluating airborne laser data on steeply sloping terrain" (2013). *Master's Theses and Capstones*. 816.
<https://scholars.unh.edu/thesis/816>

This Thesis is brought to you for free and open access by the Student Scholarship at University of New Hampshire Scholars' Repository. It has been accepted for inclusion in Master's Theses and Capstones by an authorized administrator of University of New Hampshire Scholars' Repository. For more information, please contact nicole.hentz@unh.edu.

EVALUATING AIRBORNE LASER DATA
ON STEEPLY SLOPING TERRAIN

BY

BOB CHAMPOUX

Bachelor of Science in Forestry (BSF), University of New Hampshire, 1982

THESIS

Submitted to the University of New Hampshire
in Partial Fulfillment of
the Requirements for the Degree of

Master of Science

in

Natural Resources

September, 2013

UMI Number: 1524445

All rights reserved

INFORMATION TO ALL USERS

The quality of this reproduction is dependent upon the quality of the copy submitted.

In the unlikely event that the author did not send a complete manuscript and there are missing pages, these will be noted. Also, if material had to be removed, a note will indicate the deletion.



UMI 1524445

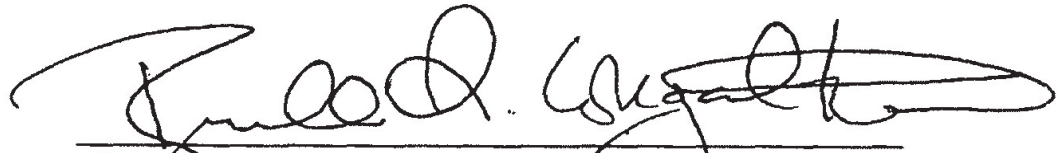
Published by ProQuest LLC (2014). Copyright in the Dissertation held by the Author.
Microform Edition © ProQuest LLC.

All rights reserved. This work is protected against
unauthorized copying under Title 17, United States Code.

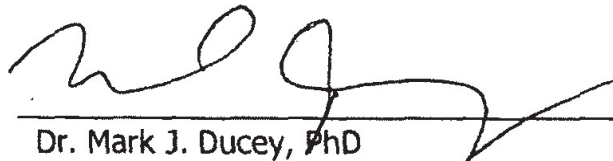


ProQuest LLC
789 East Eisenhower Parkway
P.O. Box 1346
Ann Arbor, MI 48106-1346

This thesis has been examined and approved.



Thesis Director, Dr. Russell G. Congalton, PhD
Professor of Remote Sensing and GIS



Dr. Mark J. Ducey, PhD
Professor of Forest Biometrics



Prof. Robert G. Moynihan, MBA, PE, LLS
Professor of Civil Technology-Surveying and Mapping

May 22, 2013
Date

To Jen Smith

Acknowledgments

Without reservation, I need to acknowledge the time, effort, and sincere support my committee members have offered me: Dr. Russ Congalton, for all the assistance over many, many months. Little did he know what he signed up for when he offered to take me on as a graduate student. To Dr. Mark Ducey for pulling me out of the statistical whirlpools, when no results were forthcoming, explaining it all in plain English, and getting me back on track. To Bob Moynihan, who has been a colleague for twelve years, a mentor, and friend for 30 solid years. To my old colleagues in the Civil Technology program at the University of New Hampshire, Guy Petty, Ken Flesher, and Tom March: Thank you for all your encouragement. To Bruce and Heidi Bonenfant who kept me fed and sheltered. And, to another old colleague at the university, Rene Gingras, who, seeing me in the throes of writing this, commented that his thesis was only 26 pages long. Thanks for that, Rene...

Table of Contents

| | |
|--------------------------------------------------------|------|
| Acknowledgments | iv |
| List of Tables | viii |
| List of Figures | ix |
| Abstract | xii |
| Chapter 1 Introduction..... | 1 |
| Research Questions and Approach..... | 5 |
| Chapter 2 Literature Review | 7 |
| Introduction to Airborne Laser Terrain Mapping | 8 |
| General ALTM Principles | 8 |
| Primary Benefits of ALTM | 14 |
| Uses of ALTM Data | 15 |
| Diversity of Applications | 15 |
| Primary ALTM Product: Digital Terrain Models..... | 17 |
| ALTM Errors, Accuracies, and Precisions..... | 18 |
| Error Budget of the System | 22 |
| Global Navigation Satellite System Unit | 23 |
| Inertial Measurement Unit | 28 |
| Scanning Mirror Unit | 30 |
| LiDAR Unit..... | 33 |
| Integration of Components..... | 36 |
| Flying Height Influence on ALTM Errors | 38 |
| ALTM Horizontal Accuracies | 43 |
| ALTM Accuracies as stated by System Manufacturers..... | 45 |

| | |
|-----------------------------------------------------------------------------------|--------|
| ALTM Vertical Accuracies from an ALTM service provider..... | 46 |
| ALTM Vertical Accuracies from Independent Studies | 48 |
| Accuracies, Errors and Causes for Error on Sloping Terrain | 51 |
| ALTM Vertical Accuracies on Sloping Terrain | 51 |
| Effect of Horizontal Error on Vertical Error | 55 |
| Incidence Angle..... | 58 |
| Footprint Reflectivity | 61 |
| Footprint Size..... | 64 |
| Limitations of Digital Terrain Model Errors on ALTM Accuracy | 69 |
| Filtering..... | 69 |
| Interpolation..... | 73 |
| Reference Data Errors, Accuracies, and Precisions | 75 |
| Reference Points Established using Traditional or Real Time Kinematic Methods.... | 76 |
| Reference Points Established using Line Transects..... | 80 |
| Proximal to Reference Points | 80 |
| Reference points Established precisely at Laser Strikes | 82 |
| Summary of Errors and Accuracies | 83 |
| Chapter 3 Data and Methodology..... | 87 |
| Study Site..... | 87 |
| ALTM Data | 94 |
| Data Collection | 94 |
| ALTM Data Assembly | 98 |
| Determination of Terrain Slope..... | 101 |
| GNSS used to establish Reference Data..... | 103 |
| GNSS, more In-Depth | 103 |
| Testing and Accuracy of GNSS Equipment and Procedures | 108 |
| Establishment of GNSS Control Points for Reference Data | 112 |
| Validation of ALTM Planimetric Coordinates..... | 116 |
| Field Test..... | 119 |
| Determination of Sample Size..... | 120 |
| Field Work..... | 122 |

| | |
|------------------------------------------------------------------------------------------------------|-----|
| Additional Data Collected in the Field | 126 |
| Chapter 4 Results and Discussion | 131 |
| Normality of the ALTM-derived Elevations | 131 |
| Flat Terrain ALTM Vertical Errors and Block Correction | 139 |
| Influence of Sloping Terrain on ALTM-derived Elevations..... | 145 |
| Influence of Scan Angle on ALTM-derived Elevations..... | 157 |
| Influence of Flying Height on ALTM-derived Elevations..... | 163 |
| Influence of Horizontal Inaccuracy on ALTM-derived Elevations..... | 164 |
| Influence of Laser’s Footprint Size on ALTM-derived Elevations | 173 |
| Exploration of Varying Elevations within Laser’s Footprint due to Sloping Terrain | 188 |
| Horizontal Displacement combined with Elevation Spread across the Footprint on Sloping Terrain | 200 |
| Influence of Incidence Angle on ALTM-derived Elevations..... | 203 |
| Influence of Slope Aspect on ALTM-derived Elevations | 213 |
| Influence on Ground Elevation on ALTM-derived Elevations | 219 |
| Influence of Laser Range on ALTM-derived Elevations | 222 |
| Determination of Most Influential Factors on ALTM-derived Elevations..... | 227 |
| Chapter 5 Summary of Results | 240 |
| Chapter 6 Conclusions..... | 250 |
| Uses for this Study | 253 |
| Limitations of this Study | 255 |
| Future Investigations..... | 256 |
| Appendix | 258 |
| Appendix A ALTM Flight Conditions..... | 259 |
| Appendix B GNSS Postprocessing with OPUS..... | 262 |
| Appendix C Breakdown of Conflicting Reasons for Range Measurement Error on Sloping Terrain | 264 |
| List of References | 266 |

List of Tables

| | | |
|-----------|---------------------------------------------------------------------------------------|-----|
| Table 1 | <i>ALTM System Accuracies as Stated by Manufacturer</i> | 45 |
| Table 2 | <i>Vertical Accuracies of Select Projects of an ALTM Data Provider</i> | 47 |
| Table 3 | <i>Descriptive Statistics of Errors for Slopes less than 5°</i> | 142 |
| Table 4 | <i>Descriptive Statistics of Errors (n=351)</i> | 145 |
| Table 5 | <i>Descriptive Statistics of Errors by Slope Strata</i> | 146 |
| Table 6 | <i>Significance Levels for Errors Between Slope Strata</i> | 151 |
| Table 7 | <i>Errors After Adjustment by Horizontal Displacement</i> | 169 |
| Table 8 | <i>Descriptive Statistics of Footprint Sizes by Slope Strata</i> | 179 |
| Table 9 | <i>Descriptive Statistics of Footprint Elevation Spreads by Slope Strata</i> | 192 |
| Table 10 | <i>Errors Comparing Reference Elevation to Footprint Elevations</i> | 197 |
| Table 11 | <i>Errors After Adjustment Using Footprint Elevations and Horizontal Displacement</i> | 201 |
| Table 12 | <i>Descriptive Statistics of Incidence Angles by Slope Strata</i> | 205 |
| Table 13 | <i>Akaike Information Criterion for linear regression models</i> | 236 |
| Table A-1 | <i>Climatological Data for ALTM Mapping</i> | 259 |
| Table B-1 | <i>Results with OPUS Processing of GNSS Data</i> | 262 |
| Table B-2 | <i>Results Using Different GNSS Software and Base Stations</i> | 263 |
| Table C-1 | <i>Appraisal of Origins for Observed Vertical Errors</i> | 264 |

List of Figures

| | |
|---------------------------------------------------------------------------------------|-----|
| Figure 1. Multiple return signals from one laser pulse. | 12 |
| Figure 2. ALTM point cloud created by a discrete pulse system. | 13 |
| Figure 3. Graphical representation of accuracy and precision. | 19 |
| Figure 4. Variations in horizontal and vertical accuracies due to flying height. | 40 |
| Figure 5. Categorized horizontal and vertical errors. | 43 |
| Figure 6. Profile view of change in elevation due to horizontal displacement. | 56 |
| Figure 7. Change in pulse duration due to reflection off an inclined surface. | 59 |
| Figure 8. Influence of scan angle, slope, and slope aspect on incidence angle. | 60 |
| Figure 9. Relative power distribution of an emitted laser pulse. | 62 |
| Figure 10. Errors in range measurements due to scan angle. | 67 |
| Figure 11. Errors in range measurements due to sloping terrain. | 68 |
| Figure 12. Locus map of Pawtuckaway State Park. | 87 |
| Figure 13. Topographic map showing ring dike of Pawtuckaway Mountains. | 88 |
| Figure 14. Aerial photograph showing ring dike of Pawtuckaway Mountains. | 89 |
| Figure 15. Typical forest cover and terrain of Pawtuckaway State Park. | 91 |
| Figure 16. Typical terrain of study area in Pawtuckaway State Park. | 92 |
| Figure 17. Oblique view of Mount Pawtuckaway ridgeline. | 93 |
| Figure 18. Plan view of ALTM ground strikes in study area. | 99 |
| Figure 19. Geometry of ALTM laser beam which defined footprint size. | 101 |
| Figure 20. Degree of slopes from ALTM-derived TIN in study area. | 102 |
| Figure 21. Photograph of GNSS receiver stationed at a control point. | 113 |
| Figure 22. GNSS receiver establishing a horizontal position. | 118 |
| Figure 23. Typical configuration of GNSS base receiver. | 120 |
| Figure 24. Digital carpenter's level attached to 1.62 m long dowel. | 127 |
| Figure 25. Digital level in use measuring terrain slope. | 128 |

| | |
|--------------------------------------------------------------------------------------|-----|
| Figure 26. ALTM ground strike location on moderately sloping terrain. | 129 |
| Figure 27. ALTM ground strike location on steeply sloping terrain. | 130 |
| Figure 28. Histogram of the vertical errors (n=351). | 134 |
| Figure 29. Boxplot of the vertical errors (n=351). | 135 |
| Figure 30. Quantile-Quantile plot of the vertical errors (n=351). | 137 |
| Figure 31. Plan view of the vertical errors coded by magnitude (n=351). | 138 |
| Figure 32. Histogram of the errors for slopes less than 5° (n=85). | 141 |
| Figure 33. Scatterplot of errors for slopes less than 5° (n=85). | 143 |
| Figure 34. Scatterplot of errors for all slopes. | 153 |
| Figure 35. Scatterplot of errors for all slopes fitted with curvilinear line. | 155 |
| Figure 36. Scatterplot of absolute errors for all slopes. | 156 |
| Figure 37. Scatterplot of errors for all scan angles. | 159 |
| Figure 38. Scatterplot of errors for all scan angles on slopes <10°. | 160 |
| Figure 39. Scatterplot of absolute errors for all scan angles on slopes <10°. | 162 |
| Figure 40. Change in error due to horizontal displacement. | 166 |
| Figure 41. Change in elevation due to horizontal displacement of one meter. . | 168 |
| Figure 42. Scatterplot of errors for slopes with lines representing change. | 171 |
| Figure 43. Influence of scan angle, slope and slope aspect on footprint size. ... | 176 |
| Figure 44. Scatterplot of footprint sizes relative to slopes. | 180 |
| Figure 45. Scatterplot of errors for all footprint sizes. | 182 |
| Figure 46. Scatterplot of errors for footprint sizes on slopes <20.0°. | 184 |
| Figure 47. Scatterplot of absolute errors for all footprint sizes. | 185 |
| Figure 48. Scatterplot of footprint sizes relative to scan angles. | 186 |
| Figure 49. Calculation of slope of the line tangent to the footprint. | 190 |
| Figure 50. Scatterplot of footprint elevations relative to slopes. | 193 |
| Figure 51. Scatterplot of footprint elevations relative to footprint sizes. | 195 |
| Figure 52. Elevation of laser strike footprint relative to reference elevation. | 196 |
| Figure 53. Scatterplot of errors for all footprint elevations. | 199 |
| Figure 54. Scatterplot of incidence angles relative to slopes. | 206 |
| Figure 55. Scatterplot of footprint sizes relative to incidence angles. | 207 |

| | |
|-----------------------------------------------------------------------------------|-----|
| Figure 56. Scatterplot of errors for all incidence angles. | 208 |
| Figure 57. Scatterplot of absolute errors for all incidence angles. | 210 |
| Figure 58. Scatterplot of errors for all recoded slope aspects. | 213 |
| Figure 59. Orientation of slope to the flight Line. | 214 |
| Figure 60. Scatterplot of slopes relative to recoded slope aspects. | 216 |
| Figure 61. Scatterplot of footprint sizes relative to recoded slope aspects. | 218 |
| Figure 62. Scatterplot of errors for all ALTM-derived elevations..... | 219 |
| Figure 63. Scatterplot of errors for all laser ranges..... | 222 |
| Figure 64. Scatterplot of laser ranges to scan angles..... | 224 |
| Figure 65. Scatterplot of footprint sizes relative to laser ranges. | 226 |
| | |
| Figure A-1. Aeromagnetic map of study area | 260 |
| Figure A-2. GPS satellite geometry at the time of the ALTM flight..... | 261 |

Abstract

EVALUATING AIRBORNE LASER DATA ON STEEPLY SLOPING TERRAIN

by

Bob Champoux

University of New Hampshire, September, 2013

Accuracy of Airborne Laser Terrain Mapping (ALTM) elevations is not well known on steeply sloping terrain. A unique method was used whereby, the planimetric location of ALTM ground strikes were located in the field and reference elevations measured at these points. Survey-grade Global Navigation Satellite System (GNSS) and rigorous techniques accurately established vertical heights to 0.010 meters, Root Mean Squared Error (RMSE). Sampled slopes range from 0.5 degrees to 50.6 degrees. A positive quadratic relationship exists between slope and vertical error. Error is negligible on slopes less than twenty degrees. Incidence angle, footprint size, and elevation spread from the upper reach of the footprint to the lower reach for each laser strike were also determined. An increase in each results in an increase in ALTM elevation imprecision. Elevation spread within the footprint and horizontal error could account for high percentages of vertical error on steeper slopes.

Chapter 1

Introduction

Researchers and resource managers are among many users enticed by Airborne Laser Terrain Mapping (ALTM). This mapping method has transformed the way data are collected in forest stands and other natural resource environments. The accuracy and detail of the data surpass that of traditional methods for large areas. Impressive work with this technology includes measurements of forest biomass (e.g., Ferraz et al., 2012), forest canopy (e.g., Kato et al., 2009), individual stem diameter and volume (e.g., Ene, Næsset, & Gobakken, 2012), and even individual tree species identification (e.g., Kim, McGaughey, Andersen, & Schreuder, 2009). The prevailing use however, continues to be terrain mapping and modeling (Flood, 2004). ALTM can produce hundreds of thousands of discrete laser pulses per second, each one a representation of a unique point on the ground. The resulting detail is beyond the realm of any other mapping methods available. Without limitations of other methods, it has the ability to map inhospitable terrain such as steeply sloping terrain or under thick forest canopy. Terrain models too cost prohibitive to create using traditional methods, can be produced with ALTM providing more definitive data for geologic, hydrologic, and archaeological studies, among others (e.g., Baruch & Filin, 2011; Hopkinson,

Crasto, Marsh, Forbes, & Lesack, 2011; Lasaponara & Masini, 2011).

Investigators continue to study the ALTM system attributes while others incorporate the technology to assist in the continual studying of natural resources and manmade systems.

From the onset, numerous studies focused on the overall accuracies and precisions of this mapping system (e.g., Bolstad & Stowe, 1994; Lemmens, 1997; Kraus & Pfeiffer, 1998; Cowen, Jensen, Hendrix, Hodgson, & Schili, 2000; Ahokas, Kaartinen, & Hyyppä, 2003), while others concentrated on system component errors (e.g., Huising & Gomes Pereira, 1998; Baltasvias 1999a; Schenk, 2001; Morin, 2002). Subsequent studies highlighted system accuracy for specific terrain conditions and/or vegetative cover such as, forested areas (e.g., J. Hyyppä, Pyysalo, H. Hyyppä, Haggrén, & Ruppert, 2000; Reutebuch et al., 2000; Lang & McCarty, 2009), rain forest landscape (M. Clark, D. Clark, & Roberts, 2004), saltmarsh (Montané & Torres, 2006; C. Wang et al., 2009). With regards to sloping terrain, many of the accuracy studies were limited to flat or gently sloping terrain (e.g., Cobby, Mason, & Davenport, 2001; Adams & Chandler, 2002; Bowen & Waltermire, 2002; Hodgson, Jensen, Schmidt, Schill, & Davis, 2003; Hodgson & Bresnahan, 2004; Hodgson et al., 2005). Recent works also spotlighted ALTM accuracies but they too, were limited to modest slopes (e.g., Su & Bork, 2006; Xhardé, Long, & Forbes, 2006; Haneberg, 2008; Aguilar et al., 2010; Glenn et al., 2010; Vaze, Teng, & Spencer, 2010; White, Dietterick, Mastin, & Strohman, 2010; Spaete et al., 2011). A small number of these studies

noted possible degraded accuracies on steeper slopes but insufficient analysis resulted from very small datasets or other limitations (e.g., Yu et al., 2005; Hollaus, Wagner, Eberhöfer, & Karel, 2006; Peng & Shih, 2006; Kobler et al., 2007; Stewart et al., 2009; Burns, Coe, Kaya, & Ma, 2010; Estornell, Ruiz, Velázquez-Martí, & Hermosilla, 2011). Thus, one area of ALTM accuracy and precision not well known is how well this technology maps the ground on steeply sloping terrain.

Since ALTM has proven successful at mapping inhospitable terrain (Flood, 2004), its use to map steep terrain continues to increase. Given this growth, the accuracy and precision of ALTM on steeply sloping terrain are necessary facets for users of the data. This study offers a detailed look at and presents accuracies and precisions of ALTM in steeply sloping terrain.

Furthermore, the reference data in this study are more accurate and more precise than the vast majority of studies, due to the methods employed. Since ALTM laser strikes on the ground rarely coincide with reference points, some method is typically used other than a direct comparison: Certain studies compared the elevation of the laser ground strike closest to reference point on the ground (e.g., Daniels, 2001; Webster, 2005; Liu, 2011). While this form of comparison is reasonably accurate on level ground, it is severely deficient in steeply sloping terrain where a laser strike one or five meters away may have a significantly different elevation than the reference point. Many studies have created and compared a Digital Terrain Model (DTM) of the ALTM-derived data

to reference points on the ground (e.g., J. Hyypä et al., 2000; Clark et al., 2004; Schmid, Hadley, & Wijekoon, 2011). A DTM, inherent in its design, degrades accuracy by requiring interpolation of the model's elevation corresponding to a reference point. Other studies (e.g., Hodgson et al., 2003; Yu et al., 2005; Aguilar & Mills, 2008) used less rigorous methods or techniques resulting in less precise reference data. This study is rather unique in that survey-grade GNSS (Global Navigation Satellite System) equipment provided for an accurate navigation to the actual locations of laser strikes on the ground. At each point, high accuracy and redundant methods insured reliable ground elevations. In addition to a higher level of accuracy and precision of reference data, this technique allowed for direct comparison of ALTM-derived elevations to reference data without any interpolation.

Thus, this study provides a robust and definitive comparison between the accuracy and precision of ALTM elevations on varying degrees of terrain slope. Additionally, this investigation involved several other factors that affect ALTM accuracy and precision, such as slope aspect and incidence angle¹, as well as their interrelationships.

¹ Incidence angle is the angle between two vectors originating where a laser strikes the ground. One vector runs from this point along the laser's path back to laser. The other vector is normal to the terrain.

Research Questions and Approach

ALTM is used to map less hospitable areas, such as steeply sloping terrain since these areas typically are harder to map accurately using other methods.

However, numerous studies indicated that as terrain slope increases, vertical accuracy decreases (e.g., Baltsavias, 1999a; Huising & Gomes Pereira, 1998; Kraus & Pfeifer, 1998; Hodgson & Bresnahan, 2004; Hodgson et al., 2005; H. Hyypä et al., 2005; Xhardé et al., 2006; Kobler et al., 2007). Of these, very few have made conclusive assessments of elevation accuracy on slopes greater than ten degrees. For users of these data, a greater understanding of the accuracy is required.

Hence, the questions this study addressed:

- Do ALTM-derived elevations have greater inaccuracies on steeper slopes than on flat terrain or gentle slopes?
- If so, is the relationship between increasing vertical inaccuracy and increasing slope linear?
- Does incidence angle increase as slope increases? If so, what is the relationship between incidence angle and ALTM elevation error?

So as make the most definitive comparison between ALTM and reference elevations, the planimetric coordinates derived from the ALTM data were used to navigate to actual strike locations in the field using survey-grade GNSS equipment. At each strike location, rigorous RTK GNSS techniques measured

ground elevations. This may be the first study using enhanced RTK GNSS methods resulting in the least amount of reference data error. Direct comparison of the RTK GNSS elevations and the ALTM elevations eliminated the use and errors of DTMs. Furthermore, these techniques significantly reduced errors caused by the misclassification of laser strikes.

Prior to assessment of accuracies on steep slopes, a supporting presentation of ALTM concepts and error sources would prove beneficial.

Chapter 2

Literature Review

Many factors affect the accuracy and precision of ALTM on sloping terrain. An ALTM system is comprised of several components, each with its own inaccuracies. Outside of the system, other variables such as, flying height, incidence angle, and robustness of the reference data also affect accuracy. Accuracy results are also conflicting: independent researchers and users of ALTM have found accuracies quoted by system manufacturers far too optimistic. These findings in addition to the amount and sources of error are examined in this section.

First, is an introduction to ALTM basic components, principles, and uses, highlighting the use of the system for DTM creation. This is followed by the errors and accuracies of the main system components, accuracies as stated by system manufacturers, and those reported by independent studies.

Subsequently, variables outside of the system which affect vertical accuracy are presented such as, horizontal system inaccuracies, incidence angle, reflectivity of ground objects, and the size (area) of the laser beam when it intersects the ground. The end of this section includes discussions regarding the limitations of

DTMs created from the ALTM data for accuracy studies and errors in the reference data.

Introduction to Airborne Laser Terrain Mapping

General ALTM Principles

Airborne Laser Terrain Mapping (ALTM) is still evolving such that a common name for this technology has yet to be agreed upon. Other commonly used names of the technology include: Airborne Laser Scanning (ALS), Light Detection And Ranging (LIDAR or LiDAR), Airborne Laser Detection and Ranging (LADAR), laser altimetry, and Airborne Laser Swath Mapping (ALSM). Regardless of the name, the concept and technology are the same whereby a laser, GNSS unit, and Inertial Measurement Unit (IMU) are the main components of the system mounted onboard a fixed or rotary wing aircraft.

Congruent to most lasers, the laser unit produces a narrow beam of light emitted in pulses. For most units, the monochromatic light is in the near infrared portion of the electromagnetic spectrum, typically in the range of 900 nm to 1550 nm (Lemmens, 2007). The unit directs each pulse of light at the earth's surface. The unit also precisely measures the elapsed time from emission of the pulse until the integral optical receiver observes returning light returning reflected off the ground (i.e., the return). Onboard software converts this time of flight, based on the speed of light, into a distance from the laser unit to the ground. ALTM units are capable of emitting and measuring several hundred thousand pulses per

second (Leica Geosystems, 2011), thus providing the inordinate amount of detail which eclipses other mapping systems.

Since this system generates and emits its own electromagnetic radiation, it is an active sensor versus a passive one, the latter being dependent on the subject's response to the sun (e.g., aerial photography). A laser, by definition, generates a highly focused beam of light with little divergence as it moves outward from the source (Siegman, 1986). Given this coherent, extremely collimated beam, the emitted pulse strikes a relatively small area on the ground. These properties provide for determining elevations of specific points on the terrain. The light produced, typical of most lasers, is quite pure spectrally, meaning the light uses only a very narrow band of the wavelength spectrum. This purity equates to less interference and easier modeling as the light passes through the atmosphere.

The collective elements of the laser, receiver, and timer technically comprise the LiDAR unit. This unit is one of the three major components of the ALTM system.

The second main component of the ALTM system is the GNSS unit. This integrated unit provides the coordinates (e.g., latitude, longitude, and elevation) of the LiDAR unit. Onboard software determines these coordinates for each pulse. With the distance known from the LiDAR unit to the ground, software calculates the coordinates for each laser strike.

The third major element of the system is the Inertial Measurement Unit (IMU) that monitors the climb, roll, and heading (e.g., attitude or orientation) of the

LiDAR unit. Additional calculations incorporate these data into the laser strike coordinates, since any climb or roll values other than zero causes the laser to be skew relative to the ground, resulting in erroneous coordinates assigned to the laser strikes. The product of the ALTM system is an assemblage of unique geographic coordinates corresponding to each laser strike.

On the first ALTM systems, the laser emitted pulses downward towards the ground directly below the aircraft. This configuration resulted in a string of laser strikes producing a profile of elevations along the flight line. These systems are termed Profiling Airborne Laser System (PALS). As ALTM technology evolved, manufacturers incorporated a rotating or oscillating mirror. This mirror continually redirects each laser pulse off of nadir with each successive pulse further away than the last across the flight line up to a predetermined limit. When reaching the limit, the mirror then redirects subsequent pulses back towards and across nadir, to the limit on the opposite side of the flight line. This combination of scanning and the forward movement of the aircraft results in rows of laser strikes extending out on both sides of the aircraft.

The type of mirror used varies between ALTM systems resulting in different laser scanning patterns but they all function similarly in that, an encoder determines the orientation of the mirror for each laser pulse. Additional software incorporates this precisely measured scan angle into the calculation of the geographic X, Y and Z coordinates for each laser strike. With the laser's ability to generate hundreds of thousands of pulses per second and given the relatively

low speed of the aircraft, the mirror provides for a more effective and efficient use of the profusion of laser pulses. Even with a large maximum scan angle, the ALTM system can create a swath of dense laser strikes where the distance between rows of strikes equals or is less than the distance between successive laser strikes. Pre-flight planning controls density between laser strikes to meet the user's needs. Frequency of laser pulses (repetition rate), maximum scan angle, scanning rate, flying height of the aircraft, overlap between swaths, and flying speed control the ground spacing between laser strikes (Sapeta, 2000).

Since the ALTM system produce extraordinary amounts of data during a flight, another key physical component of the system is the hardware required for storage. Since the laser of some systems can emit up to 500,000 pulses per second (Leica Geosystems, 2011), exceptionally large hard drives are required.

Thus, an ALTM system, in addition to the three main components (i.e., LiDAR, GNSS, and IMU), typically incorporates a scanning mirror unit, computer hardware, software, and data storage.

Pulsed (also known as discrete) lasers emit individual pulses of radiation. With each emission, several returns are possible. As depicted in Figure 1 with a tree for an example, the upper leaves intercept part of the light beam of each pulse. This portion reflects back towards the ALTM receiving sensor, which then observes the return and the additional processing results in a set of coordinates for this return. The rest of the pulse's light beam continues down through the

tree with other branches and leaves reflecting portions of the beam back towards the ALTM sensor, resulting in additional signal returns with differing geographical coordinates. Branches closer to the base of the tree or low-level shrubs cause more reflection of the beam until the ground reflects back the last of the radiation.

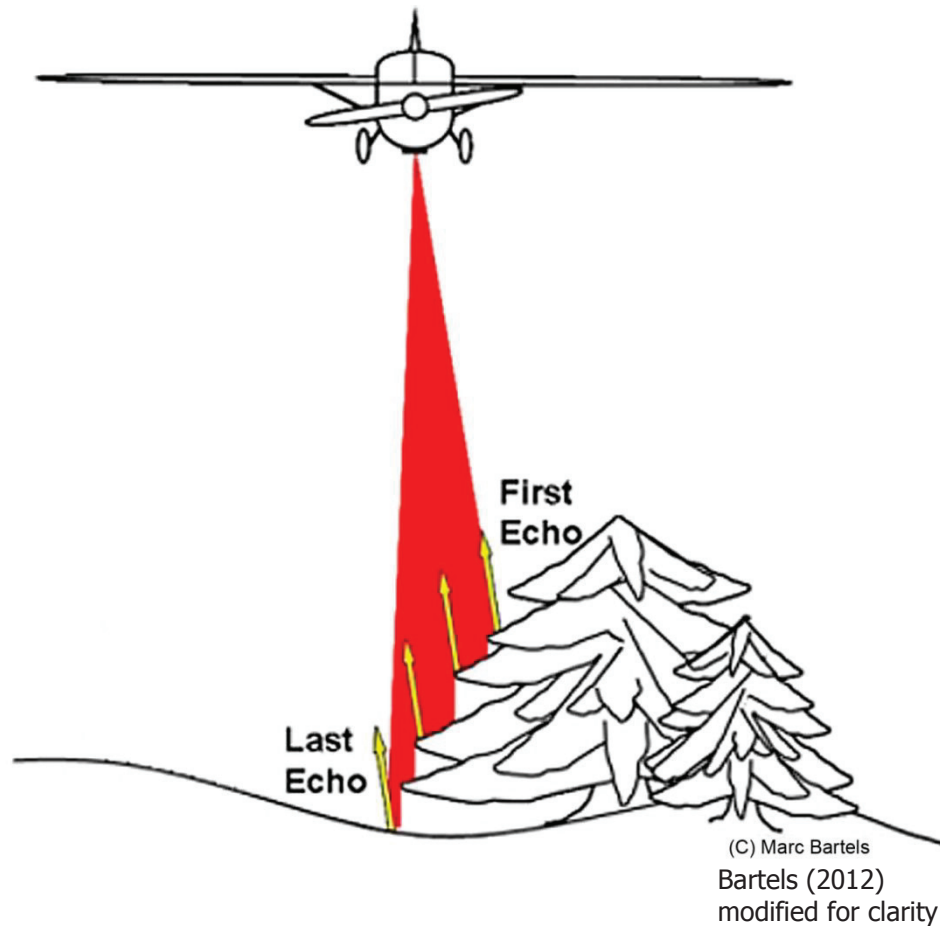


Figure 1. Multiple return signals from one laser pulse.

Thus, each pulse of the laser can result in several return signals, each representing a different portion of the tree and each assigned a unique northing, easting, and elevation. This profuse collection of returns is termed a point cloud

due to the collective three-dimensional shape of these data when viewed graphically (see Figure 2). In this figure, the view is a low oblique. The dense cluster of points at the bottom depicts ground returns while those above it correspond to returns from various portions of a forest canopy.



-adapted from Treitz (2012)

Figure 2. ALTM point cloud created by a discrete pulse system.

Discrete sensors are capable of observing limitless returns from one laser pulse (Leica Geosystems, 2011) but for natural resource studies, three to five returns is typical (Renslow, Greenfield, & Guay, 2000) . These returns are commonly

referred to as first, second, and third or last return, with the first return representing the intercepting object closest to the sensor and the last return being the ground (Baltsavias, 1999b; Hudak, Evans, & Stuart Smith, 2009).

Another common ALTM system employs a full waveform LiDAR unit. Since a discrete sensor was used in this study, all discussion and references are limited to the latter type of system.

Primary Benefits of ALTM

Use of an ALTM system results in a vast quantity of elevation data that is orders of magnitude greater than obtained by other technologies. While terrestrial surveys are more precise, methods typically result in an elevation measurement every three square meters (Ghilani & Wolf, 2010). A discrete pulse ALTM survey can easily best this with densities of one ground point every 0.5 square meters or better (Reutebuch et al., 2000; Bao et al., 2008).

In addition to the amount of detail gathered, the ALTM data collection and processing are considerably faster. The costs are also significantly less than terrestrial surveys and photogrammetric mapping (Flood, 2004). Numerous studies have compared ALTM to photogrammetric methods for terrain mapping. Petzold, Reiss, and Stössel (1999) noted that the ALTM data collection required only 25 percent to 33 percent of the budget needed for a typical photogrammetric project. Huising and Gomes Pereira (1998) constructed a DTM

from ALTM data with the time required to generate the terrain map being much shorter compared to photogrammetric methods.

Other significant benefits of ALTM over photogrammetric and other traditional methods are the result of using a laser. Sun angle must be considered with many other methods as shadows can severely limit the ability to map. For ALTM, sun angle is not a concern. Since the sensor creates its own energy, nighttime forays are possible with no loss in performance (Baltsavias, 1999a; Flood, 2004). In addition, it has wider latitude weather wise (Flood, 2004; Goulden, 2009).

With fewer restrictions, equitable time and monetary costs, users and researchers continue to opt for mapping with ALTM (Flood, 2004; Leigh, Thomas, & Kidner, 2009).

Uses of ALTM Data

Diversity of Applications. Coupled with reasonable cost, many researchers employ discrete pulse ALTM systems to assist in their work based on its ability to provide closely spaced ground elevations. Töyrä, Pietroniro, Hopkinson, and Kalbfleisch (2003) used the technology to study river deltas while Thoma, Gupta, Bauer, and Kirchoff (2005) used ALTM to analyze river channel bank erosion. Cobby et al. (2001) was one of several research groups to use the high density of ALTM laser strikes to create maps of the slopes and aspects of drainage channels and to develop surface roughness coefficients for hydrologic models. Hopkinson et al. (2011) used the technology to investigate the spatial

distribution of water levels in a river delta. Beyond hydrology, Baruch and Filin (2010) were able to identify well-developed and subtle gullies, while Davenport, Holden, and Gurney (2004) used ALTM to determine soil roughness. Fornaciai, Pareschi, and Mazzarini (2010) were successful in creating detailed maps of the 2001 lava flows on Mount Etna, in Italy.

Maxwell, in his thesis (2010), used ALTM to identify and map boulder landforms, while Lasaponara and Masini (2011) and Corns and Shaw (2009) successfully documented archaeological monuments. Stewart et al. (2009) reported the use of ALTM to monitor ground movement in earthquake prone areas. From a review of current literature, new uses of ALTM to map project sites have become a regular occurrence.

As identified previously, not all of the emitted laser pulses strike the ground. A unique feature of ALTM is the ability to map the top of forest canopies. While the previous example focused on singular trees (see Figure 1), ALTM can map complete forest stands. With returns from the uppermost leaves of trees, comparison of these elevations to ground elevations yields canopy heights. ALTM continues to be used for studies of forest structure, biomass measurements, and carbon stocks (e.g., Hollaus et al., 2009; Kato et al., 2009; Kim et al., 2009; Van Leeuwen, Coops, & Wulder, 2010; Ene et al., 2012; Ferraz et al., 2012; Wulder et al., 2012). Metrics that tend to be time intensive to collect and, in some locales, difficult to obtain are now readily collected using ALTM (Flood, 2004).

Reference is made to Hudak et al. (2009) for a compilation of natural resource-based uses for ALTM data.

Primary ALTM Product: Digital Terrain Models. While varying types of work and studies use ALTM, mapping of ground topography was the primary purpose leading to its development (Wagner, Ullrich, Melzer, Briese, & Kraus, 2004). Lloyd and Atkinson (2002) noted ALTM has been used extensively for terrain mapping since its inception. Even with the 100 percent canopy cover, discrete pulse ALTM systems have the ability to penetrate dense forest and other vegetative canopies (Clark et al., 2004). L. James, Watson, and Hansen (2007) reported that maps based on ALTM data are far more accurate and complete than those that from other sources under dense forest cover. Several researchers have indicated that it is becoming the preferred method for terrain mapping over traditional techniques such as photogrammetry (Sapeta, 2000; Hodgson & Bresnahan, 2004). For many ALTM projects, the three-dimensional coordinates of laser strikes reaching the ground are used to build DTMs as DTMs continue to be one of the most commonly used, basic spatial information products (Hudak et al., 2009; Vaze, et al., 2010).

These models typically serve a foundation for research and design projects. With designs, further modeling and evaluations stemming from the underpinning model, it is essential to know the accuracy and precision of the underlying ALTM data used to build them.

ALTM Errors, Accuracies, and Precisions

With any detailed discussion of errors and accuracies, some descriptive terms require definition and comprehension. For this study, those terms were *error*, *accuracy*, *precision*, and associated statistical descriptors. While apparent definitions of these tend to be common knowledge, differences between them are not always clear in an in-depth discussion.

Accuracy is the closeness of a measurement or measurements to the actual (true) value (see Figure 3). The inaccuracy of a measurement, regardless of magnitude, is synonymous with error. Two common accuracy descriptors used in ALTM are mean signed error and mean absolute error. Since the actual or true value is never known, there is some uncertainty associated with the stated values of the descriptors. A common descriptor for this is confidence interval of the mean. Again, since the true value is never known, the confidence interval of the mean values is qualified at 95 percent (in this study). This uncertainty appears in Figure 3 labeled as "Error of the Mean."

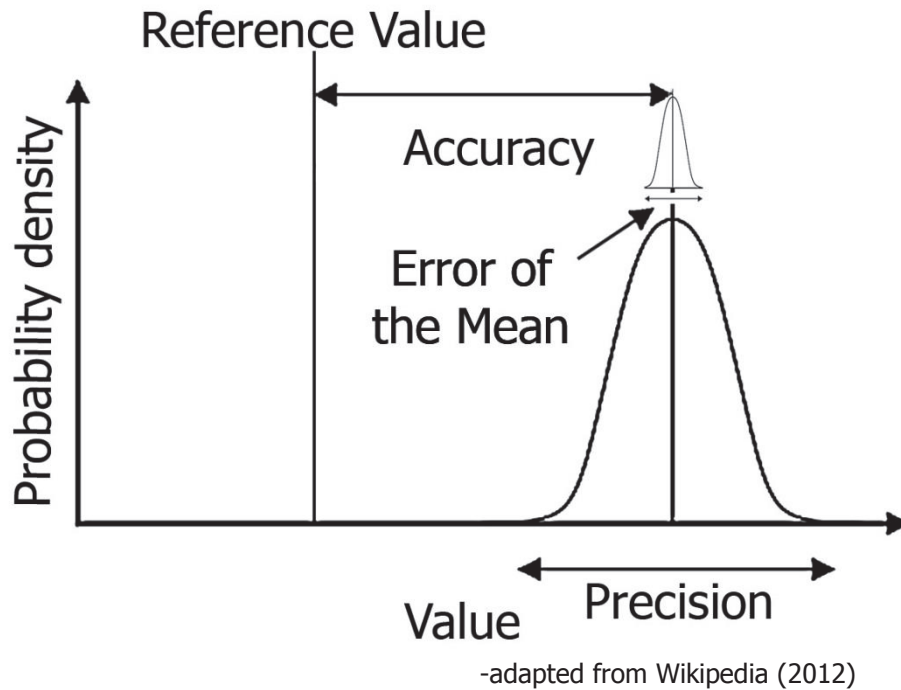


Figure 3. Graphical representation of accuracy and precision.

Systematic errors, sometimes called determinate errors, are comprised of component, operator, software, method, etc. errors. *Bias* describes any of these errors if they are unidirectional. A large number of measurements are required to determine if systematic errors and bias exist. These terms are typically associated with accuracy with the elimination of predictable or constant errors resulting in an increase in accuracy. However, some level of inaccuracy remains since the true value is unknown.

Precision describes the closeness of measurements to one another and corresponds to the repeatability or reliability of obtaining similar results. It is completely independent of the true value. Therefore, there is no systematic error

or bias involved. With ALTM, precision and repeatability can be described via two different scenarios:

1. The closeness of several measurements to each other (e.g., the similarity of elevations from laser strikes in close proximity to one another on level terrain).
2. The closeness of measurements from a second mapping foray to the first over the same area.

In order to assess precision, several measurements are required. Using only one or two measurements defines accuracy, not precision. Range, absolute deviation, inter-quartile distance, variance, and standard deviation typically describe precision (or imprecision). These descriptors indicate the amount of variation about a mean or expected value.

Random errors are commonly associated with precision since these types of errors are unknown, unpredictable, and variable. These types of errors are typically due to system insensitivity, procedures, and noise. Therefore, the descriptors of precision depend on the distribution of random errors. The collective of measurements however, have an expected value of zero.

The generic term, *error*, can be used to describe systematic error, random error or both. Therefore, it can also be used to define inaccuracy, imprecision, or both. *Total Error* is typically comprised of both systematic and random errors, defining the combination of both. Thus, *total error* incorporates inaccuracy or imprecision.

Neither *error* nor *total error* includes mistakes as the latter should be identified and excluded from the data prior to analysis. *Root Mean Square Error* (RMSE) is a descriptor for total error. Therefore, RMSE incorporates systematic and random error (i.e., bias and variability; accuracy and precision). From this, RMSE does not describe accuracy or precision singly. Additionally, it does not differentiate between the two types of error, meaning, the relative proportions of bias and variability is unknown.

For additional information regarding these terms, refer to Foote and Huebner (1995), Royal Society of Chemistry (2003), Joint Committee for Guides in Metrology (2008), Buccianti, Cibien, Mari, and Rebaglia (2009), and NDT Resource Center (2013).

From the literature, most studies used the term, *error* loosely. For many, error defined inaccuracy, and other times, imprecision. Given this, citations from literature used throughout this study, were replicated using the author's own words.

Outside of these citations, accuracy was distinguished from precision when using the word, *error*, when deemed significant. Additionally, to add clarity, the terms, *dispersion* and *variability* were used only when describing precision. Lastly, the terms *predictor*, *outcome*, and *residual* pertain to modeling such as with linear regression and were used only in this context. *Residual*, it should be noted, is

commonly referred to as an error but more specifically describes the difference between a model's predicted and observed values.

Following is an overview of the error budget of the ALTM system responsible for the accuracy and precision limitations of the data.

Error Budget of the System

As noted, the ALTM system is a combination of three major components: LiDAR, GNSS, and IMU, each with their own errors, both systematic and random, which limit accuracy and precision. Similarly, the scanning mirror, being an optical-mechanical device, introduces errors. Augmenting these, are errors due to the interfacing of the components. Other variables such as flying speed and altitude also have their effect. Among the ALTM error investigations, Baltsavias (1999a) provided the seminal study that scrutinized each element of the ALTM system and identified potential error sources of each. While there are numerous errors and biases, most of these can be corrected (Bethel, van Gelder, Cetin, & Sampath, 2006). The focus of this thesis was on those errors not eliminated via calibration and standard procedures. And while the emphasis was on vertical error, this study included horizontal error when it affected vertical accuracy and precision.

From previous ALTM accuracy investigations, each researcher arranged and categorized the errors depending on their focus. While all are valid, the breakdown of error sources given by Schenk (2001) and further refined by

Goulden and Hopkinson (2010) was basic, straightforward, and applicable for this study:

- Global Navigation Satellite System Unit (GNSS)
- Inertial Measurement Unit (IMU)
- Scanning Mirror Unit
- Laser Ranging Unit (LiDAR)
- Integration of components

Discussions of the error sources follow this order.

Global Navigation Satellite System Unit. The precision of the GNSS receiver is dependent on a multitude of variables. Fortunately, standard practices easily remove many errors. However, the system is dynamic and the amount of error varies during a mapping project.

Part of the system precision is dependent on the number of satellites transmitting GNSS-specific signals above the horizon available to the receiver. The relative location of the satellites about the sky is also quite important. Accurate geographic coordinates (e.g., latitude, longitude, and elevation) via GNSS requires receiving signals from a minimum of four satellites with each of these satellites in different quadrants of the sky. As the satellites are continually orbiting the Earth, their locations are not fixed relative to each other and continually varying. Theoretically, the most accurate GNSS measurements occur when four satellites positioned about the horizon, are 90 degrees to each other

with another satellite overhead, relative to the observer's position. These five satellites create the strongest geometric figure from which to calculate the location of the GNSS receiver (Van Sickle, 1996). This arrangement however, has a flaw since satellite signals originating at or near the horizon suffer serious degradation, as they must propagate through a significantly greater amount of atmosphere. Therefore, satellites must be higher in the sky allowing for greater signal to noise ratios and more accurate modeling of the atmosphere affecting the signals. Thus, there is always a trade-off in precision between geometry and atmospheric effects.

A second GNSS receiver is required as a base station sited at a control point with known coordinates. The geographic coordinates assigned to the laser strikes are constructed from this receiver's data. The distance between this GNSS base receiver and the ALTM GNSS receiver is limited since errors increase as the two receivers move further apart. As the distance increases, Errors occur since the satellite signals pass through diverging parts of the ionosphere and troposphere to reach each receiver. The signals are affected by these parts of the atmosphere and currently, atmospheric modeling can only correct the errors when the receivers are close to one another. These errors, resulting in degraded geographic coordinates of the observer's position increases linearly with distance. One GNSS receiver manufacturer, Trimble Navigation, states that the accuracy for their survey-grade system as $0.008 \text{ m} + \text{one part per million (ppm; RMSE)}$,

horizontal) and $0.015 \text{ m} + \text{one ppm (RMSE vertical)}^2$ (Trimble Navigation Limited, 2012). One part per million describes the error incurred relative to the distance between the two receivers. Practitioners consider the distance between receivers a when planning the mapping. With large projects, precision can vary from one end of the site to the other.

Additionally, both GNSS receivers must be receiving signals from the same set of satellites during the mapping session. With long distances between the receivers, one receiver may be calculating positions using a signal from a satellite low in the sky that is not available to the other receiver. This can result in inaccuracies or worse, the inability to process coordinate data requiring another mapping foray.

As for accuracy values of GNSS in ALTM systems, Applanix, a manufacturer of ALTM components and software, offered 0.03 m planimetrically and 0.05 m in elevation (Goulden, 2009).

From the accuracy values above, the planimetric coordinates typically have a higher resolution than the elevation. This disparity is primarily due to tropospheric delay error and is considered the most problematic element in the GNSS elevation error budget (Seeber, 2003). Additionally, weather fronts may

² These accuracy values pertain to when one GNSS receiver is moving, typical of ALTM applications. Accuracy is greater when both receivers are stationary.

cause a GNSS signal to be delayed, potentially leading to height errors exceeding 0.09 m (Marshall, Schenewerk, Snay, & Gutman, 2001).

Further degradation can occur when a satellite's signal bounces off a natural or manmade hard surface such as a building or exposed ledge before reaching the GNSS receiver. This reflection results in a delay before the receiver obtains the signal, known as multipath. This deferment can produce significantly erroneous coordinates and it is not always readily apparent that multipath has occurred (Kaplan, 1996; Rodríguez-Pérez, Alvarez, & Sanz-Ablanedo, 2007). Multipath episodes occur and disappear as the aircraft and satellite positions continually change. However, multipath errors should be minimal for a GNSS receiver 700 m to 1000 m above the ground (Leigh et al., 2009).

Even when these errors kept to a minimum, a current limitation is the frequency at which the GNSS receiver calculates coordinates. The receiver computes a position once every one to two seconds, although twenty hertz is possible (Topcon Positioning Systems Incorporated, 2004). Concurrently, the LiDAR unit is recording several hundred thousand laser strikes every second. Given that the aircraft is moving, the geographic coordinates of each of these laser strikes requires interpolation between the slower GNSS calculations. The assigned coordinates can be seriously affected when the aircraft is mapping during atmospheric turbulence (Schenk, 2001). Hongchao and Jianwei (2012) went further by stating that engine noise, acoustic resonance phenomena, and airframe structural motions due to maneuvers also result in vibration of the

LiDAR system. Some investigators deemed this disparity in timing the most critical part of the system (Goulden & Hopkinson, 2010).

While not speaking specifically about the timing error, Huising and Gomes Pereira (1998) believed that the GNSS component as a whole was part of the primary source of error in the ALTM system. Wehr and Lohr (1999) indicated that GNSS is responsible for 0.05 m to 0.15 m of error. From another study, the position of the sensor has an accuracy of approximately 0.1 m (J. Hyypä et al., 2000). At low elevations, where laser strikes are less than 400 m from the unit, Stebler, Stengele, Tomé, Schaer, and Skaloud (2009) found that the GNSS unit is responsible for more than half of the overall ALTM system error budget.

However, they found that as flying height increased, other errors become more predominate and the GNSS error remains uniform. Goulden and Hopkinson (2010) noted similarly that GNSS is responsible for the largest portion of vertical error but only at low scan angles and low altitudes. They observed errors of five centimeters, which remained constant. They also summarized that GNSS error is frequently perceived as the largest source of vertical error however, it is not always the case.

While GNSS is responsible for some of the error in the ALTM system, other research has indicated that error emanating from other components is also significant.

Inertial Measurement Unit. Other studies have referred to this component as the Inertial Navigation Unit or Inertial Navigation System. Technically, the IMU is an element of Inertial Navigation Unit.

Human piloting and winds influence the aircraft such that it rarely flies level. The aircraft will have varying degrees of pitch, roll, and/or heading bias. Since the ALTM system is mounted stationary in the aircraft and the LiDAR, GNSS, and scanning mirror units are oriented to nadir, having uncorrected aircraft attitude results in erroneous geographic coordinates of the laser strikes. The IMU measures the amount of variation about the three axes relative to level and the direction the plane is heading. IMU data account for these variations when the system assigns geographic coordinates. However, imprecisions in the measurement of these variations encumber coordinate accuracy and precision. Errors after calibration of the ALTM system are in the range of 0.004 degrees to 0.02 degrees for pitch and roll with the error in heading typically two times larger (Triglav-Čekada, Crosilla, & Kosmatin-Fras, 2009). Applanix, a manufacturer of IMUs, states that their most precise unit, after processing of the data, has a RMSE of 0.0025 degrees for pitch and roll and 0.0050 degrees for heading (Applanix, 2012). Hence, if the flying height is 2000 m, a roll imprecision of 0.004 degrees results in an error of 0.14 m in the planimetric (X and Y) coordinates of a laser strike. Glennie (2007) noted that a more accurate IMU is typically required for an ALTM system in a fixed wing versus a rotary wing since the former maps from a higher altitude.

The gyroscope, an integral part of IMU, is subject to biases, drift, and noise over time. While much of these errors can be eliminated or minimized, the noise remains adding error that causes the flight path, and resulting swath of laser strikes, to dip, bow, or angle. Post flight adjustments minimize this error but typically, some remains (Maas, 2002; Morin, 2002). Additionally, gravity anomalies can influence the sensors resulting in inaccuracies. These irregularities are usually located in mountainous terrain (Morin, 2002) where there are large accumulations of dense material (e.g., rock). While a model of this effect can be made, errors cannot be completely eliminated (Triglav-Čekada et al., 2009).

Similar to the GNSS unit, the IMU component measures the aircraft's orientation at a frequency less than the emission of laser pulses. The best repetition rates of IMUs currently used in ALTM systems is 200 to 400 Hz (Triglav-Čekada et al., 2009). As such, interpolation of roll, pitch, and heading is required for the several thousand laser strikes that occur between IMU measurements. Schenk (2001) added that IMU sampling rates should be high to capture sharp changes in motion due to atmospheric turbulence. Goulden and Hopkinson (2010) accented the importance of avoiding this degradation by flying in clear conditions. Under optimal conditions, the residuals of the GNSS and IMU trajectory values are between 0.05 and 0.1 m (Triglav-Čekada et al., 2009).

Apart from interpolation error due to low sampling rates, most of the effects of IMU errors are angular in nature (Goulden & Hopkinson, 2010). Angular errors

also comprise many of the inaccuracies and imprecisions emanating from the scanning mirror unit.

Scanning Mirror Unit. Mentioned previously, nomenclature for ALTM aspects and components is not standardized. As such, other names describe this unit: Scan Angle Unit, Encoder Angle Unit, or Observation Angle Unit.

Scan Angle is routinely described as: Scanning Angle, Looking Angle, Encoder Angle, Observation Angle, Pointer Angle, Pointing Angle, Swath Angle, and Sampling Angle. Maximum scan angle may refer to the angle from nadir to where the mirror is pointing at the edge of scan swath or it may describe the angle from one edge of the swath to the opposite edge, which is the same as Field of View. In this study, scan angle will indicate the angle off nadir. Baltasvias (1999b) stated that ALTM units typically have scan angles ranging from twenty to 40 degrees.

While the mirror and integrated angle-measuring device adds vastly to the capabilities of the ALTM system, its incorporation does add error affecting the geographic coordinates of the laser strikes. One source of error is any imprecision in the angle measurement. Some systems have precisions of approximately 0.001 degrees (Morin, 2002; RIEGL Laser Measurement Systems GmbH, 2012b) and others 0.001 degrees to 0.002 degrees (Goulden & Hopkinson, 2010). From this, an imprecision of 0.001 degrees and a flying height

of 2000 m, introduces an error of 0.03 m. Kumari (2011) noted that scan angle error is not constant but varies with scan angle.

Some systematic errors are difficult to observe: Manufacturing irregularities result in the mirror not redirecting the light beam at precisely 90 degrees resulting in a cross track error as reported by Schenk (2001) and Maas (2002). Similarly, imperfections in mirrors result in redirecting the laser beam to a location other than expected (Baltsavias, 1999a).

Additionally, given the environment in the aircraft, the mirror is subject to vibrations or pointing jitter, which again, result in assigning erroneous coordinates to the laser strikes (Lemmens, 1997; Maas, 2002).

Airborne 1 Corporation (2001) stated that the aggregate of these errors result in a decrease in accuracy as scan angle increases but commonly quoted system accuracies are the average of the errors between minimum and maximum scan angles. Schaer, Skaloud, Landtwin, and Legat (2007) also indicated scan angle strongly influences vertical accuracy with the best vertical accuracy obtained when laser strikes are at nadir and that accuracy decreases as scan angle increases. They defined this relationship between accuracy and scan angle as being a very homogenous pattern with no sudden changes. Baltsavias (1999a; 1999b) stated that the elevation error increases non-linearly for small to medium scan angles and increases exponentially with medium to large scan angles. He termed elevation error a relatively stable error but it is one not typically

accounted for during processing. Ussyshkin, Ravi, Ilnicki, and Pokorny (2009) saw a noticeable difference in elevation along scan edges that they attributed to the error caused by scanning geometry. Ahokas et al. (2003) found an elevation error of typically 0.10 m due to scan angle change and classified this relationship as a systematic error. They found systematic change in height differences as scanning angle increased. Some observations had a positive correlation while others were negative. They stated that random errors should generally increase as scan angle increases but their own findings were contrary to this assertion. They did not offer an explanation but did comment that the random errors seem to fluctuate as a function of scan angle. Interestingly, Su and Bork (2006) found that errors and RMSE were generally greater for the ALTM elevations of laser strikes closer to nadir (less than 3°) than those with greater scan angles. However, they suggested that this finding might be due to the presence of extreme errors caused by other sources.

As for horizontal errors due to scan angle, Airborne 1 Corporation (2001) noted a strong correlation between planimetric accuracies and scan angle precision. They quantified planimetric accuracies as being typically two to five times worse than stated vertical accuracies. Goulden and Hopkinson (2010) showed that since scan angle measurement errors are angular dependent errors, they heavily affect horizontal coordinates. They noted that the along-track (i.e., along the flight line) horizontal error is consistently lower at small scan angles due to errors in the measurement of scan angle having no effect in this direction. They did find that

horizontal error is greater in the along-track direction and surpassed the across-track horizontal error when the scan angle reached approximately thirteen degrees. They remarked that others perceive vertical error in GNSS measurements as the larger source of vertical error but this is not always the case: From their sensitivity analysis of the error magnitudes, they demonstrated that increasing scan angle results in increasing horizontal and vertical random errors.

LiDAR Unit. Many generally regard the LiDAR unit as the principal component of the ALTM system, such that the terms, LiDAR and ALTM, are commonly interchanged. A variety of internal and external factors can affect accuracy and precision of the system and hence, coordinates of the laser strikes.

The LiDAR unit (also known as the laser ranging unit) is chiefly comprised of the laser sending unit, the receiving unit, and the timer that measures time of flight from when the laser pulse is emitted until its reflection is received back at the unit.

As for errors, water vapor in the troposphere can absorb, scatter, diffract, or result in propagation delays of the laser's light (Morin, 2002). Lemmens (1997) found time delays resulting in two centimeters of error with a flying height of 1000 m above ground level. Seven centimeters of error was observed with a height of 2000 m. Baltasvias (1999a), Goulden (2009), and Goulden and Hopkinson (2010) stated that the best range performance is achieved when the

atmosphere is dry, cool, and clear. Water vapor, in the form of rain, fog, and/or humidity, and carbon dioxide in the atmosphere severely attenuates infrared energy propagation and thus, range. Dust particles and smoke also reduce detection of laser pulse returns (Baltsavias 1999a).

Not all of the laser beam's energy will reflect back towards the receiver after striking the ground. While laser energy is highly collimated, it does diverge as it radiates out from the energy source. This divergence is typically in the shape of a cone. RIEGL Laser Measurement Systems GmbH (2012b) quoted for one of their systems that a divergence of the beam amounts to a 50 cm increase in beam width per 1000 m distance. Glennie (2007), Goulden (2009), and Goulden and Hopkinson (2010) indicated that the greatest amount of energy is about the center of the beam with energy dropping off towards the edges of the beam. This divergence results in a spreading out of the energy across the footprint and follows a normal distribution. Local terrain effects such as roughness, vegetation, and other terrain features can further scatter the light beam reflecting only a marginal amount of light back towards the sensor. J. Hyyppä et al. (2000) found that under deciduous forests in summertime, the optical receiver detected only 24 to 29 percent of the emitted pulses reaching the ground.

The sensitivity of the optical receiver is crucial to observing diminished reflections and recording a strike (Morin, 2002; C. Wang et al., 2009), especially when some ground features have minimal reflective properties (e.g., water. Cowen et al., 2000; C. Wang et al., 2009) or asphalt (Huising & Gomes Pereira, 1998; Leigh et

al., 2009). Jutzi and Stilla (2003) indicate that there are several ways of measuring the return pulse. One of which was described by Baltsavias (1999a) who stated that the time measurement of the return pulse is on the rising side of the returning energy when the signal has reached a predetermined value. The shorter the pulse duration and the higher the received pulse power, the smaller the detection error. The steeper the return pulse (i.e., strength, number of photons received), the more accurate the time of flight can be measured. In flat terrain, the pulse detection accuracy should be ten to fifteen percent of the rise time (e.g., a one ns rise time, would correspond to 1.5-2.25 cm range accuracy). Johnson (2009) added that if the target surface is tilted ($\sim 45^\circ$ and with the range greater than a few km's), the received pulse is lengthened by the target's depth resulting in a reduction in range measurement precision. However, some receivers such as RIEGL Laser Measurement Systems' LMS-Q780, samples the return energy at constant time intervals. This constant sampling may negate some of these issues (RIEGL Laser Measurement Systems GmbH, 2012b). Though, Vaughn, Bufton, Krabill, and Rabine (1996) added that details determining stop times are often considered proprietary information by ALTM manufacturers.

Lemmens (1997) indicated that the size of the detector aperture, in addition to sensitivity, plays an important part in detection. Hence, the ability of the optical receiver to detect returning pulses is essential for a high success rate providing ample laser strikes to reproduce the terrain accurately.

Integration of Components. Errors also result from the combination and interaction of the units and from the inexactness of measurements of the three-dimensional space between them.

The LiDAR unit and scanning mirror unit interaction affect the accuracy of measurements such that: as scanning angle increases, the distance that the emitted radiation must travel to the target and back, increases. Morin (2002) noted atmospheric factors affect the range of the laser and thus, the resulting planimetric coordinates and elevation. He stated that the laser beam refracts as it passes through the atmosphere and the amount of deflection is based on the beam's wavelength, altitude, and scan angle, with the amount of deflection being proportional to the scan angle. He further stated that no distortion occurs at nadir and maximum curvature of the beam occurs when the scan angle is at maximum. This deflection results in the laser striking the terrain in a location that is not the same as the calculated one. Additionally, the laser pulse travels along this curved path causing a delay in the return and recording of the pulse, yielding an erroneous longer range. The amount of this delay is due to the severity of the scan angle and atmospheric conditions.

Elsewhere in the system, Baltsavias (1999b) noted that attitude errors lead to a rapid increase in elevation error with increasing scan angle.

Knowing the location and the orientation of the LiDAR, GNSS, and IMU components relative to one another is crucial for accurate laser strike

coordinates: The GNSS receiver calculates three-dimensional coordinates for a specific point in its antenna while the LiDAR unit has its own frame of reference being the point where the distance measurement equals zero. Hence, the distance and direction from the GNSS antenna to the LiDAR unit must be known to transform the coordinates to the LiDAR unit and the software can then incorporate the range and scan angle measurements to calculate laser strike coordinates. Similarly, the distance and direction to the IMU is also a requirement. An XYZ reference system typically defines each component's orientation. Lever arm distances describe the offsets in three dimensions between the components. Boresight angles describe the angular differences between the three coordinate systems, which are typically less than three degrees (Triglav-Čekada et al., 2009). The lever arm offsets and boresight angles are determined via calibration techniques, but some error still occurs. Triglav-Čekada et al. (2009) found errors of 0.01 degrees after inflight calibration. They stated that if the three components remain stationary in the aircraft, the errors could diminish to 0.003 degrees to 0.005 degrees, maximum. This reduction is due to the collective of repeated calibrations.

The ALTM system is multifaceted and many variables exist that create inaccuracies and imprecisions. As indicated previously, this study of ALTM system focused on those errors remaining after calibration and use of standard procedures. The above discussion presented those errors having the most influence.

For more in-depth explanation of ALTM component errors, refer to Lemmens (1997), Huising and Gomes Pereira (1998), Baltsavias (1999a), Schenk (2001), Maas (2002), Morin (2002), Glennie (2007), Schaer et al. (2007), Goulden (2009), Habib, Bang, Kersting, and Lee (2009), Johnson (2009), Leigh et al. (2009), Triglav-Čekada et al. (2009), and Goulden and Hopkinson (2010).

Flying Height Influence on ALTM Errors

Outside of the typical error budget of the ALTM components prescribed by many studies, is the effect on error from a greater flying height. Baltsavias (1999b) noted that flying heights could vary from twenty to 6000 m while flights from 200 m to 1000 m are more typical.

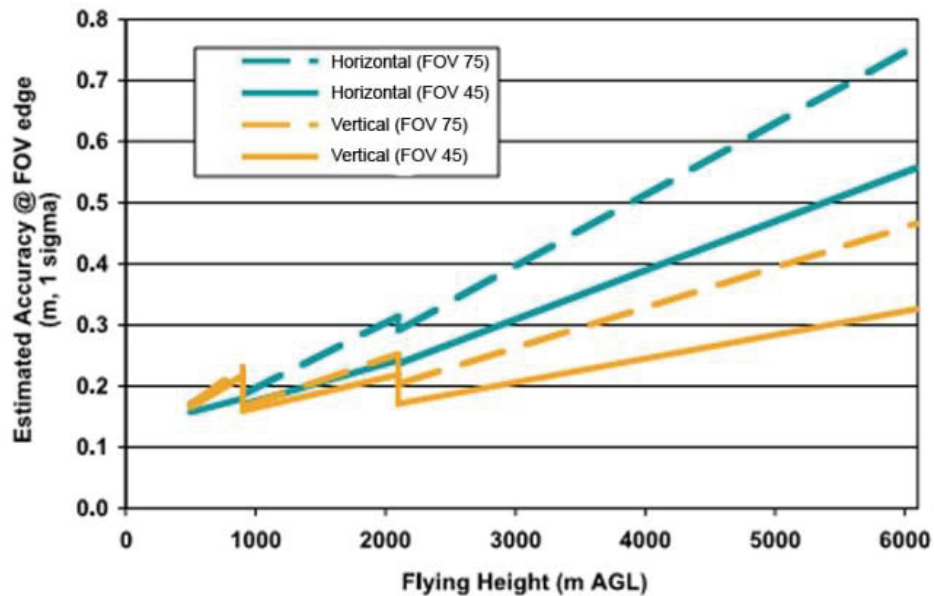
Baltsavias (1999a), stated that as flying height increases, laser pulse strength decreases resulting in a lessened ability of the LiDAR sensor to detect the reflected pulse. Thus, the power of the laser and the ability of the receiving optics to observe a signal ultimately limit maximum flying height. Additionally, temperature and aging effects of the laser signal increase range measurement errors due to the increased travel distance of the laser energy (Triglav-Čekada et al., 2009).

Baltsavias (1999b) stated that typical vertical errors range from 0.05 m to 0.20 m but increase approximately 0.005 m to 0.02 m per 100 m increase in flying height. Baltsavias (1999a), Maas (2002), and Goulden and Hopkinson (2010) noted that as flying height increases, angular measurement imprecision in the

IMU, mirror orientation, scanning mirror angle, etc., results in more uncertainty in geographic position. J. Wang, Xu, Li, and Tian (2011) noted that as flying height increases, planimetric error increases rapidly while the vertical error increases very slowly. Glennie (2007) also documented horizontal error and noted that angular errors increase proportionally to an increase in flying height. He observed that IMU and boresight errors significantly affect vertical accuracy and the amount of error is dependent on altitude: The attitude errors contribute from 25 percent to over 50 percent of the total error, depending on altitude. Attitude errors are predominately responsible for horizontal errors in fixed wing ALTM systems. Combined IMU and boresight errors contribute from 60 percent to 75 percent of the overall horizontal error, depending on flying height. He offered for a rule of thumb that horizontal accuracy is at least five times worse than the expected vertical accuracy. For systems mounted in rotary wing aircraft, the ratio of horizontal accuracy to vertical accuracy is about 2-2.5:1. Error is lower for rotary aircraft since they typically fly at lower altitudes. Ahokas et al. (2003) examined ALTM data from three study sites successively mapped from different heights. At the first site, mapping occurred at Above Ground Levels (AGLs) of 400 m and 800 m. At the second site, the ALTM system flew at AGLs of 100 m and 400 m and at the third site, the AGLs were 200 m and 550 m. They found that the higher the altitude, the larger the error in ALTM-derived elevations. Ding, Chen, King, and Liu (2011) observed a 0.37 m difference between two flights with flying heights of 2400 m and 3000 m. Triglav-Čekada et

al. (2009) found a range difference of six centimeters between measurements made at sea level and those at 2000 m (Given a pulse length of 10 ns and a nominal counter frequency of 10 GHz).

Manufacturers also indicate degradation in accuracy, both horizontal and vertical, as flying height increases. Leica Geosystems (2002) shows this graphically in Figure 4. In this figure, both horizontal and vertical inaccuracies increase as flying height increases.



FOV = Field of View (in degrees).
Upper two lines show horizontal accuracy.
Lower two lines show vertical accuracy.
-Leica Geosystems (2002)

Figure 4. Variations in horizontal and vertical accuracies due to flying height.

With all other ALTM system variables being the same, the flying height alters the density of laser strikes such that, as AGL increases, the distance between strikes is greater across the flight line, resulting in less laser strikes per unit area. This

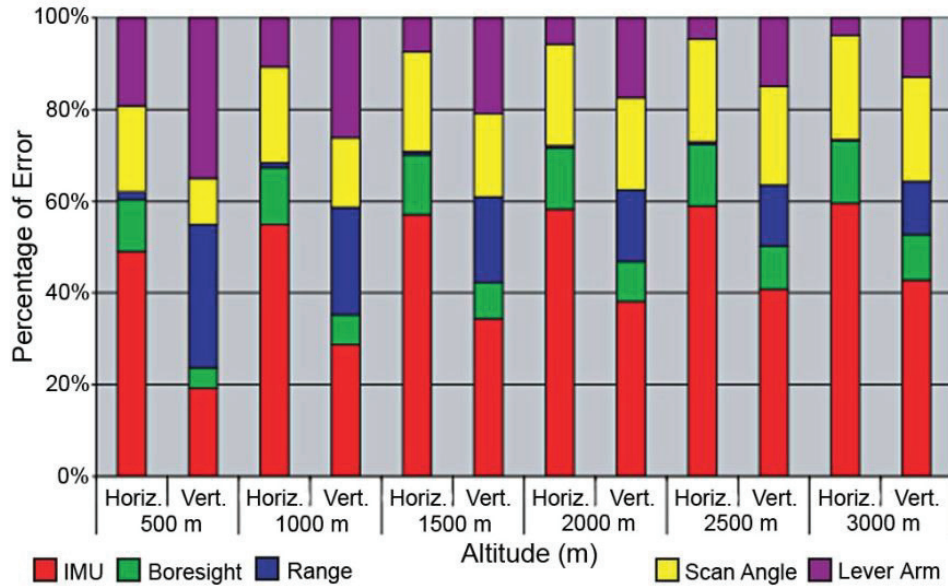
decrease in density in turn, affects the accuracy of the DTM derived from the ALTM data (Ahokas et al., 2003; H. Hyypä et al., 2005). Peng and Shih (2006), when comparing elevation from such DTMs to reference points, found that a higher flying height of 1800 m results in greater error than a height of 1100 m. They observed a mean error of -0.59 m (at the 95th percentile, RMSE 0.276)³ when the flying height was 1800 m versus -0.003 m (RMSE 0.163) when AGL was 1100 m. This change in height amounted to a 0.056 m increase in error as AGL increased 700 m. From this observation, they concluded that the lower flying altitude offers better results.

Næsset (2009) similarly found that the height metrics tended to be somewhat higher at a higher flying altitude when comparing ALTM-derived Triangulated Irregular Networks (TINs) to reference data. Overall, he found only relatively small differences between the flying heights of 1100 m and 2000 m. However, he added that with higher AGLs coupled with greater beam divergence, there is less of a tendency for the laser beam to penetrate forest canopies. Hodgson et al. (2003) had also noted this effect on penetration a few years earlier. Goodwin, Coops, and Culvenor (2006) found a reduction in the proportion of first and last return pulses with a higher AGL. With an AGL of 3000 m, they observed more than 70 percent of the pulses recorded as a single return.

³ Vertical Error = ALTM-derived Elevation - Reference Point Elevation

H. Hyyppä et al. (2005) mapped the same study sites with differing AGLs of 400 m, 800 m, and 1500 m. Comparing ALTM-derived DTMs, the increase in AGL from 400 m to 1500 m increased the random error of the DTM by 50 percent (0.12 m to 0.18 m). The degradation in DTMs as flight altitude increases is mainly due to the decrease of the pulse density and increase in planimetric error of the laser strikes. They also found systematic shifts between the DTMs. Their findings supplemented Baltsavias' (1999a) in that: as AGL varies, beam size and sensitivity of the laser system determine this systematic behavior.

Glennie (2007) also investigated how accuracy changes as AGL changes. His focus included the change in contribution of each error source as AGL increased. His results are graphically depicted in Figure 5. From the figure, he has categorized the error sources slightly different from those presented earlier (see the section, Error Budget of the System). Glennie's *Range* category strongly correlates to the above section entitled, LiDAR Unit. He did not include GNSS as a category as he deemed the errors fairly difficult to quantify. Each category represents a percentage of the total horizontal or vertical error. Percentages are given for six different flying heights. From Glennie's findings: For vertical error, Range and Lever Arm errors amount for the most error when AGL was low. As flying height increases, the effect of scan angle increases with IMU errors having the most influence. For horizontal error, IMU errors account for most of the error regardless of flying height. As AGL increases, the dominance of IMU errors continues to increase.



-Glennie (2007) Modified for clarity.

Bottom fraction of each bar: IMU
 Top fraction of each bar: Lever Arm

Figure 5. Categorized horizontal and vertical errors.

With an understanding of the ALTM system and error sources, accuracy values of other studies served as a basis for comparison of results from this study.

ALTM Horizontal Accuracies

As stated, the focus of this study was on vertical accuracy and precision of ALTM-derived elevations. However, as evidenced in the various error budget sections, some portion of vertical error is dependent on horizontal error. Most of the emphasis, based on a review of the literature, has been on vertical accuracy. Interestingly, very few studies have quantified horizontal errors.

Flood (2001) indicated that the absolute accuracy of the horizontal data is typically within tens of centimeters to one meter, depending on flying parameters.

Stewart et al. (2009) noted that horizontal accuracies range from 0.05-0.12 m from two flights with flying heights of 900 m and 210 m.

Airborne 1 Corporation, an ALTM service provider, surveyed the accuracies stated by manufacturers and supplemented this with findings of other service providers. They summarized the horizontal error as being 0.50-1.00 m (Airborne 1 Corporation, 2001). As presented previously, horizontal accuracy is less than vertical accuracy. Airborne 1 Corporation (2001) found that the former are typically two to five times worse than vertical accuracies.

Glennie (2007) also documented horizontal error. He offered for a rule of thumb that horizontal accuracy is at least five times worse than the expected vertical accuracy. Error is lower for rotary aircraft since they typically fly at lower altitudes.

Quantifying ALTM horizontal errors is difficult due to the laser strikes rarely falling on readily identifiable features on the ground. Typically, some interpolation is involved which clouds the actual accuracy values (Stewart et al., 2009). Manufacturers of ALTM systems, however, do offer horizontal accuracies of their systems.

ALTM Accuracies as stated by System Manufacturers

With the ALTM system error budget minimized by following their operating procedures, manufacturers offer the probable accuracies shown in Table 1. This table shows the accuracies of the current high-end, high altitude, discrete pulse models of the three major manufacturers of commercial ALTM systems. Leica Geosystems provides system accuracies in graph form. Interpreting their graph provided the values given in this table.

Table 1
ALTM System Accuracies as Stated by Manufacturer

| Manufacturer (Model) | Horizontal accuracy | Vertical accuracy |
|-----------------------------------------------------------------|-------------------------------------------------------|------------------------|
| Leica Geosystems (ALS70HA) ^a | 0.12 m at scan edge (1000m AGL) 0.09 m at nadir | 0.07 m (1 SD) |
| Optech, Inc. (Pegasus HD500) ^b | 1/5500 x Altitude (1 SD) ^c | <0.05-0.15 m (1 SD) |
| RIEGL Laser Measurement Systems GmbH (LMS-Q780) ^d | 0.02 m (250 m AGL) | |

Note. Data is for high altitude models from three of the ALTM LiDAR manufacturers.

^a Leica data were given in graphical form. Values scaled from the graph.

^b Nominal 50° Field of View and standard atmospheric conditions.

^c A horizontal accuracy of 0.18 m was calculated for an altitude of 1000m from formula provided.

^d RIEGL stated accuracy is solely for the range measurement and does not take into account errors due to other components. RIEGL was the only manufacturer quoting precision: 0.02 m (250 m AGL)

AGL: Flying height Above Ground Level

SD: Standard Deviation

Prior to discussing manufacturer accuracies some further explanation is required pertaining to accuracy and precision. Leica Geosystems, for example, indicates that its current high altitude mapping system has a vertical accuracy of 0.07 m at one standard deviation (see Table 1). However, standard deviation describes precision, not accuracy (see section, ALTM Errors, Accuracies, and Precisions).

For this discussion, assumptions were made that this quoted value indicates an accuracy of 0.00 m after biases are removed and the precision is plus or minus 0.07 m. From this, 68 percent of all laser strikes will have elevations within the range -0.07 to 0.07 m of their true elevation. However, for this portion of the discussion, the term, *accuracy* will be used to describe the error in keeping with manufacturer's terminology.

The Leica Geosystems data indicate an increase in horizontal inaccuracy as scan angle increases. This concurs with the findings of others presented in the section, Scanning Mirror Unit, and can be seen in the graph of horizontal and vertical accuracies for the older Leica Geosystems ALS40 system (see Figure 4)⁴.

Optech Incorporated does not indicate any loss of accuracy as scan angle increases but demonstrates that horizontal accuracy degrades as flying height increases, similar to the findings of others presented in the section, Flying Height Influence on ALTM Errors.

These manufacturer quotes served as a basis to compare accuracies obtained by others.

ALTM Vertical Accuracies from an ALTM service provider

Airborne 1 Corporation determined and reported on observable errors for five of their own projects (Airborne 1 Corporation, 2001). For each of the projects,

⁴ Reference is made to the older ALS40 unit since the study area was mapped with this system.

reference data were comprised of points and profiles on the ground with known elevations. Table 2 provides the results. Summarizing these projects, Airborne1 calculated an average mean vertical error of 0.15 m.

Table 2
Vertical Accuracies of Select Projects of an ALTM Data Provider

| Project No. | Mean Error (m) | RMSE (m) | Reference Data |
|-------------|----------------|----------|----------------|
| 1 | -0.02 | 0.05 | 400 |
| 2 | 0.01 | 0.12 | 4500 |
| 3 | 0.003 | 0.03 | 90 |
| 4 | -0.006 | 0.09 | 90 |
| 5 | -0.006 | 0.05 | 150 |

Note. The reference data were comprised of reference points and kinematic Global Navigation Satellite System (GNSS) profiles. Kinematic GNSS calculates geographic coordinates while the receiver is in motion, such as mounted in a moving vehicle, versus being stationary. With Kinematic GNSS, the result is one observation of geographic coordinates at each point.

Many researchers indicated that manufacturer and service providers list accuracy values that are optimistic (e.g., Airborne 1 Corporation, 2001; Flood, 2001).

Bethel et al. (2006) commented that most service providers would routinely quote accuracies of 0.15 m (RMSE) during the initial years of ALTM. Bowen and Waltermire (2002) stated that observed errors can be twice as large as typical accuracy specifications. Goulden (2009) noted that quotes from manufacturers tend to be simplified and that they do not provide observation conditions. Leigh et al. (2009) criticized that the number of reference points used, what the terrain type is, or how the accuracy values are determined is rarely reported. Ussyshkin et al. (2009) added that accuracy of ALTM systems calculated by manufacturers is determined under certain operational and environmental conditions to

minimize the impact of scanning geometry (i.e., determine accuracy when the scan angle is small).

Due to ALTM manufacturers determining accuracies under optimal conditions and claims by independent users of these values being enthusiastic, accuracy studies undertaken by private, academic, and governmental investigators should yield more realistic real world measures.

ALTM Vertical Accuracies from Independent Studies

Depending on the focus of the researcher, some accuracy results came from simple comparisons of ALTM-derived elevations to reference elevations.

Accuracies for other studies were more complex as investigators noted changes as factors such as scan and flying height changed. Others examined system accuracy under varying land cover. Other studies compared the accuracy of one manufacturer's system against another. Thus, ALTM vertical accuracy has been observed under numerous and diverse scenarios. However, reported system accuracies are still uncertain due to study methods and unclear reporting:

The reference data in each study used as a basis for comparison have their own set of errors and levels of accuracy and precision. Some technologies and methods used are more accurate. For instance, reference points established using a total station (also known as a tachymeter) would be far more accurate than those established via stadia methods. The forthcoming section, Reference

Data Errors, Accuracies, and Precisions will present comparisons and limitations of each method.

Additionally, errors can be absolute or relative. Comparison between two ALTM elevations obtained from different parts of the same mapping swath would provide a relative error. Many researchers reported absolute accuracies, whereby, they made direct comparisons between ALTM-derived elevations and reference point elevations, similar to the Airborne 1 Corporation study shown in Table 2. Unfortunately, numerous studies did not indicate whether their observed errors were absolute or relative.

Furthermore, some researchers reported accuracies after removing bias. For example, the mean of differences between all ALTM and reference elevations represents a systematic bias. Removal of this bias minimizes the difference between the ALTM and reference values (Bethel et al., 2006). This mean value defines the bias for both the ALTM system and the reference data. In some studies, the ALTM-derived elevations were adjusted by subtraction (or addition) of this mean value. This correction is the equivalent of creating a block in statistical analysis. Kraus and Pfeifer (1998) observed a significant improvement in accuracy after removing this bias. Bowen and Waltermire (2002) stated that without the block correction, RMSE of ALTM vertical error would have been 30 percent greater. In Daniels (2001) study, 75 laser strikes on flat terrain were within 0.5 m of a reference point. Twenty six percent of these were within the stated elevation accuracy of the ALTM system. By removing the systematic bias,

83 percent then met the ALTM manufacturer's quoted accuracy. In the same study: 30 percent of 524 strikes within 2.5 m (also on flat terrain) of reference points, met manufacturer's quoted accuracy. This accuracy increased to 84 percent after bias removal. In other studies, it was not apparent if a block correction was made.

Lastly, many authors did not state whether they subtracted the reference point elevations from the ALTM-derived elevations or vice versa. Therefore, it was unknown if the ALTM system generated consistently high or low data.

Via the use of inaccurate techniques to establish reference data, or not reporting the type of reference data, to not specifying bias removal, whether errors were relative or absolute, or not reporting how comparisons were made, led to some level of confusion about accuracy results.

From the studies with enough clarity, the majority of the findings are comparable to Airborne 1 Corporation's (2001) survey and Flood's (2001) findings in that, absolute vertical accuracy is typically 0.15 m or less. However, this accuracy is below of some of the manufacturers, as given in Table 1. In fairness, a direct comparison between the results of some of the studies and the quoted accuracies in Table 1 cannot be made since the latter represents the latest technology. Most of the studies predate this equipment. Although, Baltsavias (1999b), Airborne 1 Corporation (2001), Flood (2001), Adams and Chandler (2002), and T. James, Murray, Barrand, and Barr (2006) did observe disparities

between their results and quoted accuracies of the time. Bowen and Waltermire (2002) indicated they found errors that were twice as large as found in typical ALTM accuracy specifications. They asserted that the optimistic manufacturer accuracies could only be achieved on mapping sorties over flat terrain and confining criteria such as a low flying height.

From these statements, researchers indicated that ALTM system accuracy is highest on flat terrain and degrades on sloping ground.

Accuracies, Errors and Causes for Error on Sloping Terrain

ALTM Vertical Accuracies on Sloping Terrain

From Goulden (2009), terrain slope is regarded as one of the largest sources of error in ALTM laser strike positions and it is not typically included as part of the error budget. He did find a decrease in both accuracy and precision on higher slopes.

The consensus from material published on the topic is that vertical error increases on sloping terrain. While some studies were unable to make a strong correlation between slope and increased elevation error, most did observe a direct relationship. Hodgson et al. (2005) named several factors responsible for increasing error: degree of terrain slope, size of the laser footprint, and misclassification of ALTM laser strikes as ground points (this thesis also investigated the latter two factors, which appear in forthcoming sections).

As part of their findings, Huising and Gomes Pereira (1998) stated that terrain geometry strongly affects ALTM-derived elevations. Similarly, Kraus and Pfeifer (1998) showed that the larger the slope angle, the lower the accuracy of ALTM-derived ground heights. Yu et al. (2005) showed that accuracy generally deteriorates when slope angle increases to more than fifteen degrees. Baltasvias (1999a) indicated that as slopes increase, elevation error increases, approaching or even exceeding the planimetric error.

As for trends, H. Hyyppä et al. (2005) found that ALTM elevation accuracy deteriorates gradually with increasing slope and that elevation errors in test sites under tree cover increase more dramatically for slopes greater than fifteen degrees, based on a comparison of ALTM-derived DTMs to gridded reference points. Spaete et al. (2011) found that slope has a significant effect on mean RMSE values in that, strikes on slopes greater than ten degrees have errors roughly twice that for strikes on slopes less than ten degrees. Hodgson and Bresnahan (2004), based on a study of sloping terrain of 1.7 degrees to 4.8 degrees, predicted that observable elevation errors on slopes greater than 25 degrees should be twice as those on slopes of less than four degrees.

Xhardé et al. (2006) studied vertical error on slopes ranging from zero degrees to greater than 55 degrees and found the relationship to be linear:

$$\text{Vertical RMSE} = 0.10 + (0.0079 \cdot \text{Slope}) \quad \text{Eq. (1)}$$

From their work, the constant (0.10) in the equation defines ALTM systematic vertical error and slope coefficient (0.0079) is a function of terrain slope and ALTM systematic horizontal error.

Xhardé et al. (2006) also examined Kraus and Pfeifer's (1998) data and determined that they also exhibit a linear relationship:

$$\text{Vertical RMSE} = 0.0253 + (0.0267 \cdot \text{Slope}) \quad \text{Eq. (2)}$$

Terrain slope in the Kraus and Pfeifer work ranged from three degrees to 31 degrees. Estornell et al. (2011) also found the relationship between RMSE and slope to be linear. Although, in another part of their study, the RMSE value for ground strikes on 21.8 degree (40%) terrain was similar to those strikes on level ground.

Goulden (2009) did not observe a strong trend but did find a decrease in accuracy and precision on steeper slopes. Additionally, Adams and Chandler (2002) found that as terrain slope increases, ALTM elevation data increasingly underestimate the ground elevation. Unfortunately, they could not offer a definitive conclusion as the tussocky grass cover in their study area created a large variety of local slopes and aspects that invalidated general slope values.

Not all studies found a direct correlation between increasing terrain slope and an increase in elevation error: Haneberg (2008) did not find any strong relationships

between slope and absolute vertical error. The correlation was statistically significant but he considered the relationship weak. Su and Bork (2006) found that signed vertical error did not increase proportionately to slope but absolute vertical error and RMSE did. They also noted that the largest error was on intermediate slopes of two to five degrees. Reutebuch, McGaughey, Andersen, and Carson (2003), in their analysis comparing an ALTM-derived DTM to total station data, did not find any relationship between elevation accuracy and slope on sloping terrain ranging from zero degrees to 40 degrees (mean slope: 11°). Stewart et al. (2009) found minimal elevation bias when comparing an ALTM-derived DTM to total station-derived elevations on steeply sloping terrain (~40°).

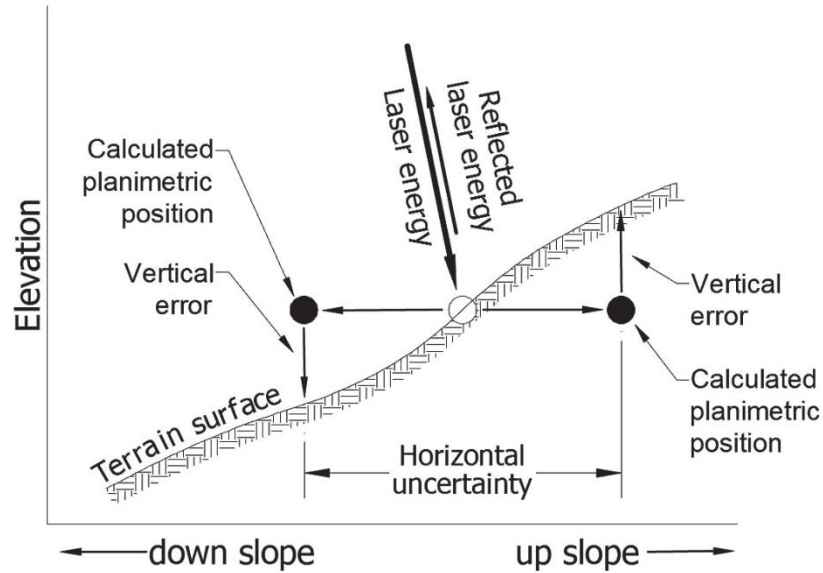
Some of these investigations focused only on ALTM vertical accuracies while most examined slope in addition to other influences. Overall, their work found vertical error does increase as slope increases. Of interest, the vertical accuracies on flat terrain in these studies are similar to those findings of other studies that limited observations to fairly level terrain.

Nonetheless, even these studies are limited, as the authors point out: Most of the evaluations were on slopes of about twenty degrees or less. Only a few of the studies appraised steeper slopes but the findings were speculative due to small sample numbers. Only two studies had relatively large samples on steep terrain (Goulden, 2009 and Estornell et al., 2012). As stated by the authors, another limitation of some of the studies was inadequate DTMs. A forthcoming

section (see: Limitations of Digital Terrain Model Errors on ALTM Accuracy) explores the weaknesses of using DTMs for evaluation purposes on steep slopes.

Effect of Horizontal Error on Vertical Error

Some of the studies on sloping terrain sought to determine why vertical error is higher on sloping terrain. Aside from deficient DTMs used for evaluation, the most probable reason afforded was geometry-based. As documented by Maling (1989) in his book, *Measurements and Maps: Principles and Methods of Cartometry*, a relationship exists between horizontal error and vertical error on sloping terrain. In Figure 6, the sloping line represents the terrain. A change in the horizontal position of a laser strike results in a change in elevation. As detailed previously, ALTM-derived horizontal coordinates are subject to inaccuracies and imprecisions. Studies have found errors ranging from 0.05-1 m (see the sections: ALTM Horizontal Accuracies and ALTM Accuracies as stated by System Manufacturers). Hence, this horizontal unknown creates vertical error.



-Adapted from Hodgson et al. (2005)
& Hodgson & Bresnahan (2004)

Figure 6. Profile view of change in elevation due to horizontal displacement.

The following formula adapted from Hodgson and Bresnahan (2004) further describes the relationship:

$$\text{Vertical Error} = \text{Tan}(\text{Slope}) \cdot \text{Horizontal Displacement} \quad \text{Eq. (3)}$$

From the figure and formula: the greater the terrain slope or the greater the horizontal error, the greater the vertical error. While the figure indicates a higher than true ALTM-derived elevation, horizontal displacement downslope can result in an ALTM elevation lower than actual.

Schenk (2001), Hodgson and Bresnahan (2004), Hodgson et al. (2005), Su and Bork (2006), and Estornell et al. (2012) cited this relationship as being responsible for at least some of the vertical error on sloping terrain. Spaete et al. (2011) noted that their assumed horizontal error of 0.30 m could potentially

contribute to mean RMSE values for strikes on slopes greater than ten degrees. Su and Bork (2006) observed a mean signed error of 0.02 m (RMSE 0.59)⁵ when comparing a DTM built from ALTM-derived elevations to 256 reference points. They found an RMSE of 0.28 m on slopes greater than ten degrees due to horizontal displacement. They calculated vertical error due to the horizontal error of laser strikes as being 0.13 m (RMSE). Eight centimeters (RMSE) was due to ALTM error and 0.05 m due to horizontal error in their reference data. Bowen and Waltermire (2002) stated that horizontal positioning limitations of one to two meters increases the probability for larger elevation errors in areas with variable terrain and large topographic relief.

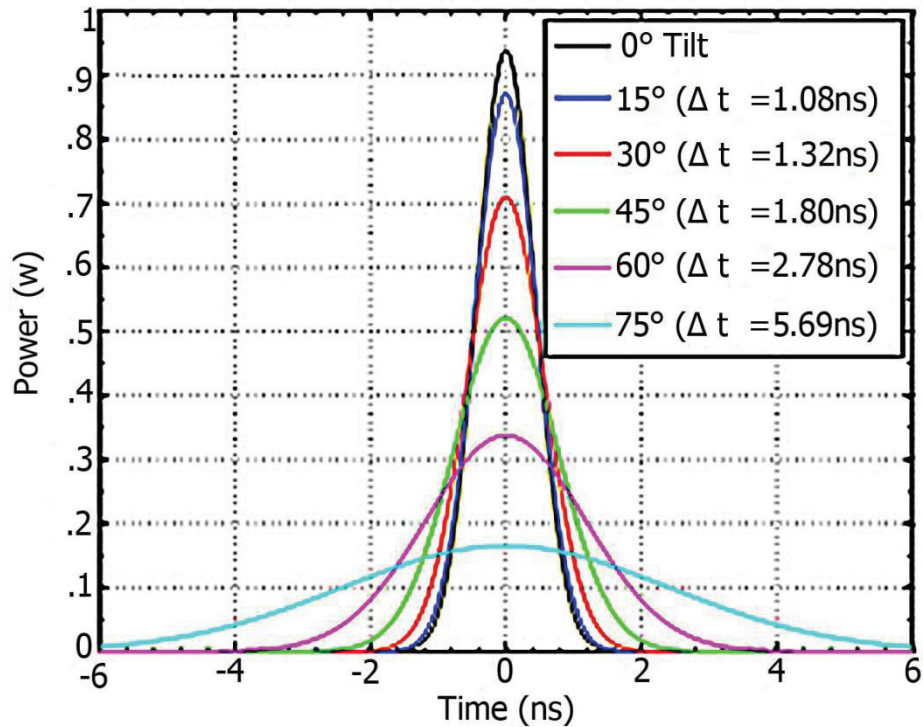
Horizontal displacement may not always affect ALTM elevations: If the horizontal error shifts the point across the slope (i.e., along the contour), then no vertical error occurs. From these scenarios, vertical error due to horizontal error can range from nil to a maximum if the displacement is directly up or down the slope. However, the errors associated with horizontal displacement are random and non-linear (Schenk, 2001) and the direction of the displacement for each laser strike is unknown (Hodgson & Bresnahan, 2004).

As Ussyshkin et al. (2009) expressed, aspects outside of the system components may responsible for the largest percentage of ALTM errors. Horizontal displacement is one of these, as is incidence angle.

⁵ Vertical Error = ALTM-derived Elevation - Reference Point Elevation

Incidence Angle

As introduced in the discussion on signal strength (see the section, LiDAR Unit), Johnson (2009) measured a decrease in pulse power from a tilted reflecting surface. His findings show graphically in Figure 7. Johnson stated that if the range was more than a few kilometers, the laser pulse, striking a tilted surface of approximately 45 degrees or greater, elongates during the reflection process, resulting in an increase in width of the returning signal and a delay in time. From Johnson's figure, this elongation effect does not happen just at 45 degrees, but the loss of the signal's sharp peak begins with at a lower angle and continues on past 45 degrees. This increase in width delays the receiving sensor's ability to recognize the reflected energy resulting in a significant range measurement error. Jutzi and Stilla (2003) had also noted an increased pulse width with a surface slanted at 33 degrees. Ussyshkin et al. (2009) showed a similar result where range measurement errors increase when a laser pulse strikes flat terrain at an angle of 30 degrees. Hence, sloping terrain or an off nadir scan angle can create such a tilted surface and induce range error.



Emitted pulse parameters

$E=1\text{nJ}$ - Energy of pulse (in nanoJoules)

$\Delta t = 1\text{ns}$ - Pulse duration
(Full-width half-maximum)

$\lambda = 1.5\mu\text{m}$ - Wavelength

$W_0=2.5\text{cm}$ - Width of beam at laser aperture

$Z_0 = F_0 = 10\text{k}$ - Range from laser to target

(0° Tilt corresponds to pulse with highest power at Time 0.)

(75° Tilt corresponds to pulse with lowest power at Time 0.)

-Johnson (2009)

Figure 7. Change in pulse duration due to pulse reflection off an inclined surface.

The majority, if not all, mapping scenarios involve the use of a scanning mirror to angle laser pulses and sloping terrain. Both of these angles independently and combined together, create a tilted surface. Given that the scanning mirror directs most laser pulses at some angle other than nadir, or the propensity to map sloping terrain, most laser strikes reflect off tilted surfaces. Furthermore, the

orientation of the slope, that is, slope aspect, also interacts with both of these angles resulting in a higher likelihood of reflecting off a tilted surface.

One way of describing the angle resulting from this geometry is illustrated in Figure 8. This figure shows three scenarios resulting in three different angles. The angle between a vector normal to the terrain surface and the centerline of the laser beam defines the interplay between these three factors. This angle between the two vectors is termed, incidence angle, given as θ in the figure.

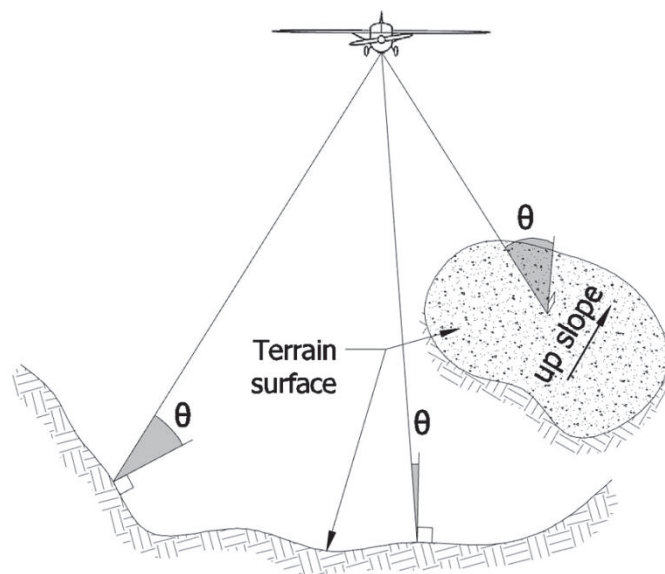


Figure 8. Influence of scan angle, slope angle, and slope aspect on incidence angle.

Schaer et al. (2007) and Stebler et al. (2009) also recognized the loss in accuracy due to this geometry and developed a relative accuracy value for each laser strike. They found that as incidence angle increases, accuracy decreases. Ussyshkin et al. (2009) termed it, angle of incidence, and stated that the geometry of these three angles may result in highly a variable range

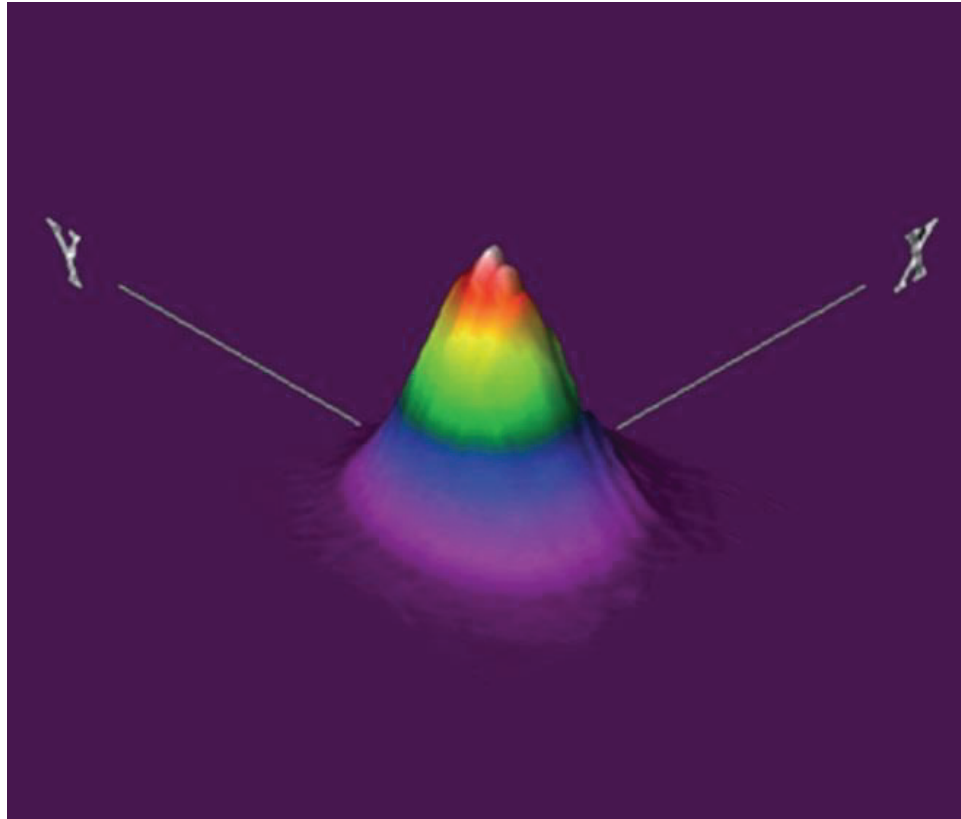
measurement yielding imprecise planimetric coordinates and elevation for a laser strike.

Singling out slope aspect, Peng and Shih (2006) found that the 95th percentile mean absolute error is significantly different between aspect classes ($p < .05$) for a flight with a flying height of 1800 m. They also found a significance difference for a flight at an AGL of 1100 m. However, when the cross flight data were incorporated into this lower flight, the 95th percentile mean absolute error is not significantly different ($p = .607$). Haneberg (2008) found no strong relationship between absolute vertical error and slope aspect. A correlation between the two was statistically significant but weak and had little explanatory power.

Footprint Reflectivity

Where in the footprint the laser signal reflects from, may also result in ALTM elevation errors.

While Adams and Chandler (2002) suggested that the energy of an emitted pulse averages out across the footprint, Glennie (2007) indicated that the ALTM unit records the apparent position of the laser strike along the emitted beam centerline; thus, the center of the footprint on the ground. He and Ussyshkin et al. (2009) put forward that the power dispersal is concentrated about the centerline and approximately follows a Gaussian distribution.



-Adapted from Glennie (2007)

Color spectrum denotes relative amount of power.

Figure 9. Relative power distribution of an emitted laser pulse.

As illustrated in *Figure 9*, the power across the pulse is not uniform and has a definite peak and slopes indicating the greater power near the center of the beam. With the greatest amount of energy striking the ground near the center of the footprint, it was logical that the likelihood of the return signal originates from the center also.

However, Kobler et al. (2007) and Goulden and Hopkinson (2010) stated that laser strike location can be subject to significant errors caused by the edge of the beam footprint making contact with surface features first. Goulden and

Hopkinson continued by stating that breaks in terrain are especially prone to creating vertical error since the edge of the footprint makes first contact and then the remaining energy experiences a time delay prior to contacting the surface.

Baltsavias (1999a) stated that the three-dimensional structure of the terrain within the footprint and the type of reflectivity of the target (diffuse and specular) are important. He offered that the minimum detectable object within the footprint does not depend on the object's size, but primarily on reflectivity. He stated that the object responsible for the laser pulse return could be smaller than the size of the footprint. From this premise, an object with requisite reflective properties could be situated anywhere inside the footprint. He noted that range may be affected by multiple reflecting targets within the footprint. Airborne1, in their 2001 publication, were slightly more definitive by stating that the return signal from a target surface is a function of the integrated energy distribution across the footprint, weighted by the reflectivity profile of the terrain within the footprint.

Schaer et al. (2007) stated though, that the range measurement could lie anywhere within the laser beam's footprint. Wagner et al. (2004), Glennie (2007), and Ussyshkin et al. (2009) also stated that the actual location of the power peak or another threshold point at the pulse front, which will trigger the rangefinder electronics is, generally speaking, unknown.

Regardless of whether reflective material or some other dynamic of the footprint is responsible for range measurement and elevation, a reflection originating from anywhere other than the center of the footprint, can add error. Hence, the further away from the center, the greater the error potential. Therefore, footprint size may be a factor affecting vertical error.

Footprint Size

Numerous elements dictate how large the laser pulse's footprint will be when it intersects the ground. Similar to most light sources, laser light expands as it travels outward.

While the laser beam emitted by the LiDAR system is highly collimated, as stated in the section, LiDAR Unit, it does diverge as it travels downward towards the ground.

Flying height is one of the elements that influences footprint size. As presented previously, a higher AGL results in a larger footprint (Baltsavias 1999a).

Another element is the size of the laser transmit aperture that is part of the LiDAR unit. Most units do have a fixed divergence angle. Within an ALTM manufacturer's range of models, each model typically has a different divergence angle since each unit is designed for a particularly type of mapping (Leica Geosystems, 2012; Optech Incorporated, 2012; RIEGL Laser Measurement Systems GmbH, 2012a). However, some models do offer a user changeable divergence angle (Optech Incorporated, n.d.).

From Goulden and Hopkinson (2010), divergence is the angular spread, in milliradians (mrad), of a circular cross-section of the beam as it propagates. They and Glennie (2007) stated that it is practical to describe the beam footprint as a percentage of the peak power emitted. Footprint size then, is calculated using the equation: $1/e^2$. However, within the ALTM industry, manufacturers and users calculate footprint diameters at the $1/e$ power level (Goulden & Hopkinson, 2010). Detailed earlier, the beam propagates outwards from the LiDAR unit in the form of a cone for most systems.

Goulden (2009) stated that errors increase due to the increase in the spread of energy. When Glennie (2007) compared an ALTM-derived DTM to reference data, he found that divergence angle affects vertical accuracy. Emanating from a unit with a beam divergence of 0.5 mrad, laser strikes had improved vertical accuracies over strikes from a unit with a divergence angle of 2.7 mrad. He reiterated that the variation in accuracy could be the result of the location responsible for range could be situated anywhere in the footprint. The larger footprint due to the wider divergence angle could result in the range measurement based on some point further away from the center.

Larger footprints are the result of other factors besides divergence angle: A propagating laser spreads outward and intersects the ground below in the form of a circle when the beam points towards nadir. When the scanning mirror deflects the laser beam off nadir, the cone intersects the ground at an angle

resulting in the footprint being in the shape of an ellipse and. However, this effect on ALTM elevations differs between studies:

From Baltsavias (1999a) and in part, Glennie (2007), depending on where the reflective material or responsible point for the range measurement is in the footprint, the elevation may be above or below true. If the material is on the nadir side of the footprint, the range value will be less than true, resulting in an elevation higher than actual. Figure 10 (a) illustrates this scenario, whereby three-dimensional coordinates of the laser strike are assigned based on the value of the scanning mirror unit that is oriented to the center of the footprint.

Meanwhile, the range, measured from the reflective material (or elsewhere), is less than the distance from the LiDAR unit to the center of the footprint. The combination of these measurements provides the wrong elevation for the set of planimetric (X and Y) coordinates. Conversely, if the reflective material is on the far side of the footprint, the range is longer and the elevation is lower than they should be ((b) in the figure). To a lesser degree, some inaccuracy in the planimetric coordinates is also incurred due to the range measurement in either case.

A differing view of where the range measurement originates from is held by Kobler et al. (2007) and Goulden and Hopkinson (2010). They indicated that the reflected energy will come from that area of the footprint that receives the transmitted energy first ((a) in the figure) resulting in all range measurements being less than true for flat slanted targets.

The contradiction between these sets of studies is further complicated by Jutzi and Stilla (2003), Johnson (2009), and Ussyshkin et al.'s (2009) work which found that range measurements are longer than actual due to the elongation of the pulse being reflected off a tilted surface (see the section, Incidence Angle).

From all these studies (aside from Johnson), as scan angle increases, footprint size also increases and the reflected energy observed by the LiDAR unit may come from some point even further away from the footprint's center, resulting in the greater elevation error.

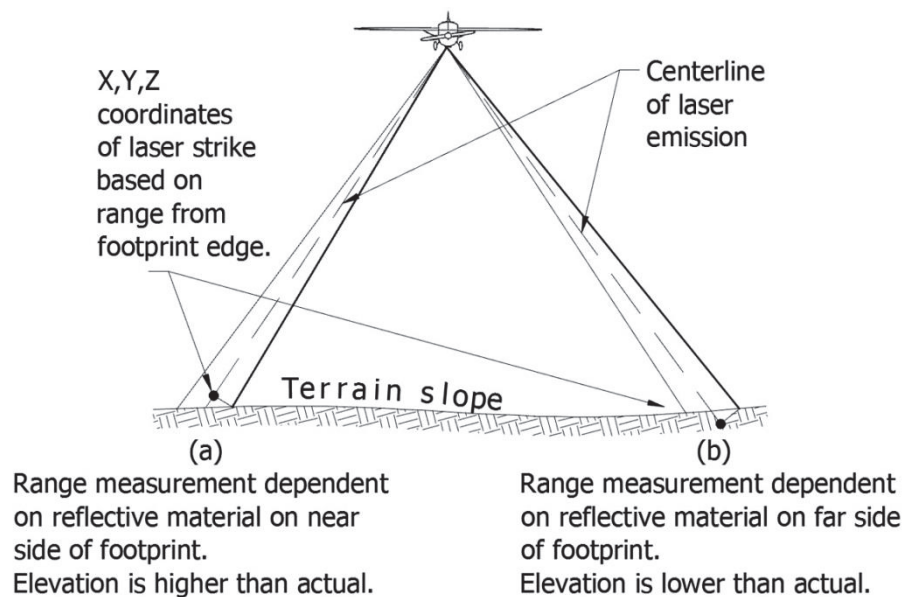


Figure 10. Errors in range measurements due to scan angle.

With a scan angle of zero, sloping terrain can create the same situation since the laser strike's footprint is also in the shape of an ellipse. From Figure 11, if the range measurement is dependent on some element located other than at the

center of the footprint, the result is an inaccurate elevation. Figure 11 (a) depicts an example whereby, the reflection originates at the upper edge of the footprint. The elevation disparity between these two increases as slope steepens (Figure 11 (b)). From Baltasvias (1999a) and Glennie (2007), the reflection may originate on the downhill side of the footprint. Figure 11 (b) shows this. The size of the footprint increasing as slope increases also compounds these disparities.

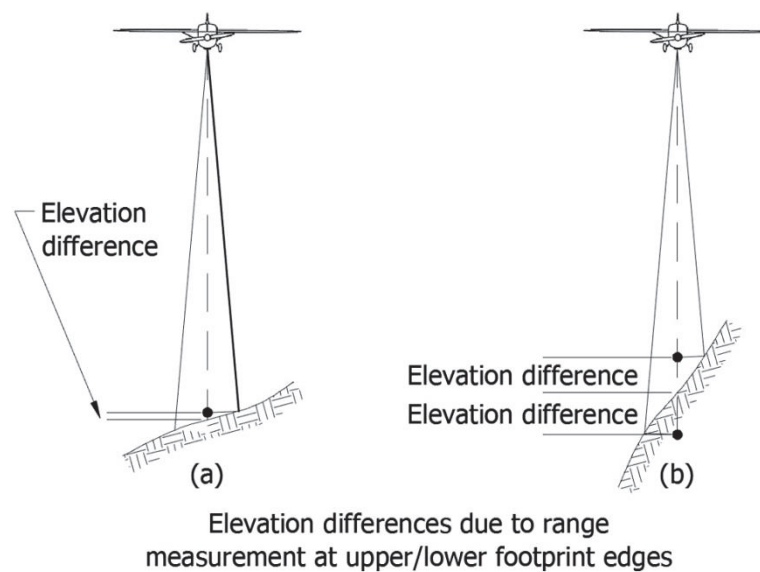


Figure 11. Errors in range measurements due to sloping terrain.

As presented in the section titled, Incidence Angle, the scan angle and slope interact by complementing, diminishing, or negating each other to define the extent of the footprint. Additionally, slope aspect also interplays with these two angles to affect the size (see Figure 8). Thus, all three factors affect footprint size (Schenk, 2001; Skaloud, Schaer, Stebler, & Tomé, 2010). At times, slope aspect can have more influence than either slope angle or scan angle on

affecting footprint size. For example, the emitted laser pulse striking on a slope with the aspect nearly perpendicular to the flight path will result in the light smearing across the terrain creating a considerably large footprint (Goulden, 2009). The outcome will be divergent elevations between the uphill and downhill edges of the footprint.

Footprint size was a concern in this study given the high flying height (4907 m). The footprint size of a laser strike at nadir and on flat terrain is 1.62 m (diameter). This footprint is significantly larger than those found in other accuracy studies where footprints ranged from 0.22 m to 0.79 m. Thus, the potential for greater elevation errors was higher in this study.

Limitations of Digital Terrain Model Errors on ALTM Accuracy

Filtering. In order to replicate the terrain accurately, a dense collection of ground strikes is needed (H. Hyypä et al., 2005). They and other investigators suggested that observed vertical errors might have been unreasonably large due to DTM limitations. Most researchers indicated one of two (some indicated both) reasons why DTMs are deficient:

1) Bao et al. (2008) noted that ground strikes will occur in open areas but few will land under trees. Land cover will intercept strikes reducing the density. J. Hyypä et al. (2000) observed penetration rates ranging from 24 to 29 percent for coniferous forests in Finland. In deciduous forests in summertime, they found that the penetration rate is 22 to 25 percent. They noted that test flights

undertaken by TopoSys, an ALTM data provider, showed that the number of recorded ground strikes decreases with scan angles greater than ten degrees off nadir. With near vertical incidence angles, Ackermann (1999) reported that laser strikes reaching the ground in European forests range from 20 to 40 percent. Hodgson et al. (2003) noted similar results. Yu et al. (2005) found that the lowest penetration rate was through spruce canopies. Cowen et al. (2000) observed that 80 to 90 percent of the laser strikes reach the ground when the terrain consists of vegetation with a canopy closure of 30 to 40 percent. However, when the canopy is 80 to 90 percent closed, only about 10 to 40 percent of the laser strikes are ground strikes. Where the canopy cover is minimal, the DTM derived from the ALTM elevations is within 0.50 m, plus or minus, of the reference data (their study site was along a railroad corridor). They articulated that the relationship between posting density of ground strikes and percent canopy closure is strongly linear.

With fewer ground strikes, the resulting DTM will be a coarse representation of the ground other than for very flat terrain. Raber, Jensen, Schill, and Schuckman (2002), Hodgson et al. (2003), Hodgson and Bresnahan (2004), Guo, Li, Yu, and Alvarez (2010), as well as others in their studies, stated that the amount of ALTM vertical error varied on the spacing between ALTM laser strikes. Olsen, Puetz, and Anderson (2009) found that DTM accuracy drops dramatically as average spacing between ground strikes increased to five meters. Greater spacing results in little loss of accuracy but the DTM already was seriously degraded. Estornell et

al. (2011) found that RMSE values remain constant with point densities from greater than twelve points to eight points per square meter but that RMSE increases as spacing increases to only one point per square meter. Aguilar et al. (2010) noted that DTM information loss grows linearly with rugged terrain (i.e., increasing slope) and forms a non-linear, inverse relationship with ALTM ground sampling density.

Reutebuch et al. (2003) in their use of a DTM under a conifer forest canopy recommended the use of high-density ALTM data to provide eight to ten ground strikes per meter to achieve sub-canopy elevation accuracy comparable to open areas.

2) DTMs are deficient for ALTM accuracy studies for another reason: Misclassified laser strikes. Laser pulses will penetrate the upper canopy and strike non-ground features, such as lower branches and leaves, ground vegetation, rocks, downed logs, etc. (Su & Bork, 2006). The algorithm that separates the laser point cloud into ground points and above ground points can be flawed (Raber et al., 2002). It can miscategorize and commit these laser strikes as ground strikes. In areas of low grass, marsh grass, short vegetation, or sub-canopies, algorithms incorrectly identified some of the ALTM laser strikes that reflected off the vegetation as ground points (Hodgson et al., 2003; Clark et al., 2004; H. Hyyppä et al., 2005; and C. Wang et al., 2009; among others). This misclassification results in ensuing DTMs being too high which overestimate ground elevations. Hollaus et

al. (2006) found errors in a DTM up to approximately fifteen meters in forested areas.

Alternatively, the algorithm can miscategorize and omit legitimate ground strikes, resulting in fewer strikes (i.e., voids in the data) with which to create a DTM.

Sithole and Vosselman (2004) noted difficulties on steep slopes. This misclassification can also occur along ridgelines and changes in terrain slope. Mis-categorizing has been problematic with filtering methods that typically involve moving a window through the ALTM point cloud, searching for the lowest points and comparing the elevation of a laser strike to neighboring ones (Bao et al., 2008). With both low vegetation and sloping terrain, very small separation distances between a dense collection of laser strikes amplifies the difficulty (Lloyd & Atkinson, 2002). Surface roughness also makes classification more difficult as the filtering process deems actual ground strikes too high or too low from neighboring ones, resulting in a model smoother than the actual surface (Huising & Gomes Pereira, 1998; Chou, Liu, & Dezzani, 1999; Bowen & Waltermire, 2002; Raber et al., 2002; Gao, 2007, Guo et al., 2010). Raber et al. (2002) found these DTMs often under-predict terrain elevation.

This omission and commission by algorithms has been a topic that has garnered much research (Gao, 2007). The product of an ALTM mapping project is a point cloud of hundreds of thousands into the hundreds of millions of laser strikes, each with a unique geographic position in three dimensions (Flood, 2001). These strikes are not labeled or otherwise defined. Thus, it is up to the analyst to

decipher these points and determine which data represent the ground, which represent features such as trees, buildings, shrubs, and grass, etc. The sheer abundance of points prohibits processing manually. System manufacturers and researchers have written and refined numerous algorithms to process with as little manual editing as possible. However, these algorithms are limited with misclassification of ground strikes being an ongoing problem (Gao, 2007).

Algorithms and processes continue to evolve as investigators attempt to process point clouds with less manual intervention and of even harsher terrain (Bao et al., 2008).

Interestingly, having a dense set of correctly classified ground strikes does not necessarily improve the accuracy of a DTM. Terrain properties such as slope, derived from such a DTM, may suffer greater inaccuracies due to close proximity of laser strikes. See Goulden (2009) for an excellent discussion of DTM error derived from high-density data (see Goulden's section 3.2).

Interpolation. Many studies used DTMs derived from ALTM data to evaluate vertical accuracy but some studies used other products such as a TIN or a profile. Shan and Toth (2008) indicated these are also common products of ALTM data. In addition to inaccuracies caused by sparse ground strikes, omission of ground strikes and inclusion of non-ground strikes, all three model types have other limitations. Since an ALTM laser strike rarely falls directly on a ground reference point, direct comparisons must be supplemented by other means. These typically involve interpolation to determine elevations. Yu et al. (2005)

observed that as slopes increase, interpolation errors also increase. Their results may indicate that this relationship is the dominant factor influencing the accuracy of an ALTM-derived DTM.

If the model is a TIN, adjacent ground strikes serve as the vertices of triangles whose face has a particular slope and aspect. The model is a mass collection of these faces encompassing all the ground strikes. This type of model is the truest representation of the ALTM data (National Oceanic and Atmospheric Administration [NOAA], 2008). Nevertheless, a comparison of elevations involves interpolating the elevation on a triangle's face corresponding to the planimetric location of the reference point. A linear interpolation assumes the triangle face is a smooth surface between the three ground strikes when the actual terrain most likely, is not.

A gridded DTM may be built from a TIN whereby each grid intersection is interpolated from the TIN surface. This additional interpolation adds more error. Some DTMs build directly off the ground strikes using inverse distance weighting, spline, kriging, binning, and other techniques. Each method has varying effects on the DTM's accuracy, depending on strike density, terrain roughness, etc. (Lloyd & Atkinson, 2002; Chen, Fan, Yue, & Dai, 2012). But again, interpolation is unavoidable (NOAA, 2008; Schmid, et al., 2011; Ding et al., 2011).

Another variable affecting DTM accuracy is cell size. Vosselman (2008), Raber et al. (2007), Leigh et al. (2009), and Schmid et al. (2011) noted that the DTM

accuracy deteriorates with decreasing density. Thus, the cell size selected for an ALTM accuracy study can influence the results. The third model type, a profile, is typically built from a DTM with yet, more interpolation.

The use of TINs, DTMs, and profiles for comparing elevations on relatively flat un-vegetated terrain has been shown to be a valid method since DTMs accurately replicate this terrain (Hodgson et al., 2003; Clark et al., 2004; Vaze et al., 2010). However, on sloping terrain, DTM accuracy degrades (Bolstad & Stowe, 1994;, Cobby et al., 2001; H. Hyypä et al., 2005; Clark et al., 2004; Aguilar et al., 2010; and others).

Liu (2008) provides an excellent overview and issues of point cloud filtering, DTM interpolation, DTM resolution.

Reference Data Errors, Accuracies, and Precisions

One last category of errors pertaining to ALTM vertical error remains: accuracy and precision of the reference data. Since the establishment of the reference points is not without error, most analyses of ALTM error includes reference errors. Unfortunately, some of the studies seen in the literature review did not indicate how reference points were established. Most studies (e.g., J. Hyypä et al., 2000; Reutebuch et al., 2000 and 2003; Adams & Chandler, 2002; Hodgson et al., 2003; Clark et al., 2004; Hodgson et al., 2005; H. Hyypä et al., 2005; Yu et al., 2005; Su & Bork, 2006; Kobler et al., 2007; Raber et al., 2007; Burns et al., 2010; White et al., 2010; Schmid et al., 2011) compared ALTM data to

reference points created predominately using traditional survey methods and equipment (total station, leveling, tachymetry, etc.) while others used terrestrially derived GNSS points as reference data (e.g., Daniels, 2001; Raber et al., 2002; Ahokas, et al., 2003; Hodgson & Bresnahan, 2004; Bethel et al., 2006; Peng & Shih, 2006; Xhardé et al., 2006; Csanyi & Toth, 2007; Lang & McCarty, 2009; Glenn et al., 2010; Goulden & Hopkinson, 2010; Skaloud et al., 2010; Dahlqvist, Rönnholm, Salo, & Vermeer, 2011; Kumari, 2011; Spaete et al., 2011; Chen et al., 2012). Studies varied on where they established reference points: scattered in semi-random placements, following stratified sampling methods, or on transect lines. The errors and limitations of these methods were worthy of examination.

Reference Points Established using Traditional or Real Time Kinematic

Methods

The most accurate of all survey techniques for determining elevations involves a survey-grade level mounted on a tripod. Following proper procedures, an accuracy of 0.012 m per 1000 m traveled is obtainable (Bossler, 1984)⁶.

Unfortunately, using a level is very time consuming and the extra work involved when surveying on sloping terrain makes the process blunder-prone (Ghilani & Wolf, 2010).

⁶ Values based on obtaining FGCC Third Order results. Third Order is least accurate where:

$$\text{Allowable Misclosure} = 12\text{mm} \cdot \sqrt{\text{Total length leveled in kilometers}} \quad \text{Eq. (4)}$$

Other traditional survey equipment, assuming proper methodology is used, are more accurate than others, but not always. Total stations, a fusion of two instruments: theodolite and an Electronic Distance Measurement (EDM) device, can be quite accurate, assuming that the instrument is accurately leveled and that distances from the instrument to the reference points are reasonable. Accuracies of $0.001 \text{ m} + \text{one ppm}^7$ (Topcon Positioning Systems Incorporated, 2012b) are achievable for high-end instruments with $0.005 \text{ m} + \text{one ppm}$ being the typical accuracy of most commonly used instruments (Ghilani & Wolf, 2010). However, as distance between the total station and target increases, pointing error, angular resolution limitations, stability of the instrument setup, and imprecise leveling of the instrument amplify inaccuracies and imprecision. While total stations can be used on steep slopes to determine elevations, angular measurements up or down slope increase error. This error is dependent on the law of cosines, also known as the Abbe error (Ghilani & Wolf, 2010).

Other traditional survey methods such as tachymetry using a stadia rod predate the use of EDMs and horizontal and vertical accuracies are much less. Horizontal distance measurements only have an accuracy of 1:300, typically (Deumlich, 1982). Furthermore, similar to a total station, vertical measurement accuracy and precision is dependent on the severity of the angle up and downslope.

⁷ Accuracy is for measurement made under good conditions, no haze, visibility $\sim 40 \text{ km}$, overcast, and no scintillation. ppm (distance between the instrument and prism, in parts per million).

Additionally, all of the traditional survey techniques suffer from the need for inter-visibility between survey points making them very time consuming to use in vegetated terrain.

The use of Real Time Kinematic (RTK) GNSS to establish reference points is very common as many studies used this technology. With RTK, it is quite easy to establish thousands or tens of thousands of reference points in a short amount of time; considerably more than what can ever be established using traditional survey equipment. By following proper methods, no degradation occurs on steeper slopes. Additionally, accuracy of GNSS technology is the same regardless of terrain. Trimble Navigation, a GNSS receiver manufacturer, states that the vertical accuracy for their GNSS R8 model is 0.015 m + one ppm (RMSE; Trimble Navigation Limited, 2012). Nevertheless, it is not without errors and limitations. While the section, Global Navigation Satellite System Unit identified many of the common error sources, a more in-depth review follows.

The methodology of RTK GNSS surveys, typically only generates one set of coordinates from the measurements made at each geographic location. Consequently, there is no redundancy. When the receiver is briefly stationary at one position to obtain multiple readings, the subsequent measurements may be subject to the same errors such as multipath⁸, affecting the first set. Optimally, re-occupying the point later, after the satellite configuration has changed,

⁸ See the section, Global Navigation Satellite System Unit for an explanation of multipath.

provides the greatest check against errors (Kaplan, 1996). However, no studies followed this procedure other than for control points.

From these elements, elevations of ground reference points obtained using either traditional survey or static GNSS methods are inevitably more accurate than RTK GNSS data due to repeated measurements at the same point allowing for redundancy and mathematical checks, assuming proper methodology is used.

Establishing reference points by static GNSS differs from RTK GNSS by the length of occupation. The receiver remains stationary for a much longer duration and collects many measurements deriving many sets of coordinates for the point's location. The longer observation period and numerous measurements aid in eliminating and minimizing errors and improving precision. Static GNSS is also known as rapid static GNSS, depending on the distance between the base receiver and the roving receiver and occupation times. Similar to RTK GNSS, the base receiver occupies a known control point while the roving receiver remains stationary at the new point whose location is desired. However, the GNSS receiver at the new point may sit for twenty minutes or longer, collecting 120 measurements or more. The combination of multiple measurements and a varying satellite configuration produces a very accurate position: three millimeters +0.5 ppm (RMSE horizontal) and five millimeters +0.5 ppm (RMSE vertical) (Trimble Navigation Limited, 2012).

Clearly, this technology is the most accurate but is very time consuming and not practical for most accuracy assessments where ALTM laser strikes number in the millions.

Reference Points Established using Line Transects

Transects have been and continue to be a common sampling method in the natural resources, as evidenced by their use in numerous studies. Some of the ALTM accuracy studies established reference points using traditional survey or GNSS methods with the points in linear arrangements thus, creating transects. Having reference data all in a line for this type of study is immaterial. Typically, the studies employing transects compared reference transect data to DTMs.

However, several studies based slope calculations on transect data. Hodgson et al. (2003 & 2005) and others determined slope by using rise versus run data between the reference points along each transect line. As Hodgson noted, transects did not always align with the slopes. Some transects ran up/downhill while others were situated across the slope. Thus, the derivative slope values used for comparison purposes do not necessarily match the predominant slope of the terrain. This procedure clouds evaluation of vertical error when arranged by slope.

Proximal to Reference Points

Some studies compared ALTM-derived elevations to reference elevations using more reliable methods than DTM or TIN models.

Given that ALTM laser strikes will rarely fall directly on a reference point, evaluations of elevations have used proximal points. Loosely termed, *proximal point* describes a laser strike in close planimetric proximity to a reference point. Some studies opted to compare elevations of the laser strike closest to each reference point while others assessed the strikes within a certain radius of each reference point. From the literature review, ten studies utilized proximal point comparison:

Webster (2005) used laser strikes within five meters and within three meters of validation points while Hopkinson et al. (2004) and Estornell et al. (2012) limited the radius to 0.5 m. Other studies employed values in between. Csanyi and Toth (2007), as part of their study to develop ALTM-specific ground targets, compared ground strikes on and about fabricated targets two meters in diameter. Dahlqvist et al. (2011) used a GNSS receiver mounted on the roof of a car to create reference points and compared these to the four nearest laser strikes.

One benefit from this methodology is that any misclassification of laser strikes is usually quite evident since several correctly filtered laser strikes about a reference point should have similar elevations.

However, one limitation of proximal point comparison is on sloping terrain. With steep slopes, such as those encountered by Bowen and Waltermire (2002), an ALTM laser strike two to three meters away can have a significantly higher or lower elevation than the reference point.

Peng and Shih (2006) found that mean distance from the reference point to the nearest ground strike was linearly correlated to the elevation error. They also determined that the combination of slope and proximal point spacing influences vertical error. These relationships existed regardless of flight height (AGLs of 1100 m and 1800 m).

Unfortunately, of the ALTM accuracy studies, few used proximal points. Regardless, the technique cannot be used on sloping terrain without incurring inaccuracies.

Reference points Established precisely at Laser Strikes

Aside from methodology used by Csanyi and Toth (2007) outlined in the previous section, by far the best method to assess ALTM elevations is to measure the ground elevation at the actual laser strike. This requires collecting the reference data after the mapping foray. Since laser strikes are not visible on the ground, this process involves navigating to the planimetric coordinates of a laser strike provided by the ALTM system using GNSS, or some other method. Once at that location, the ground elevation is measured using a conventional level, total station or GNSS receiver. This method provides for a direct comparison of ALTM-derived elevation to ground elevation and incurs the least amount of error. This approach eliminates the shortcomings of using DTMs and proximal points. From a review of the literature, only two studies used this procedure to determine vertical accuracies of discrete ALTM systems:

Hodgson and Bresnahan (2004) established control points using rapid static GNSS. From these points, they used a total station to locate 654 ground strikes.

Montané and Torres (2006) used RTK GNSS to navigate to the planimetric coordinates of the ground strikes. At each of the 334 laser strikes in their sample set, they measured reference elevations.

This method of navigating to the planimetric coordinates incurs the least amount of error. However, it has seen little use. This paucity may be due to time commitments needed to navigate under forest cover using either traditional survey equipment or GNSS (see section, Reference Points Established using Traditional or Real Time Kinematic Methods). However, for evaluation of vertical error on sloping terrain, this modus appeared to be the optimal method.

Summary of Errors and Accuracies

While there are many factors that influence ALTM accuracies, for this study, error examination was limited to only those that have a perceptible effect on vertical accuracy on steep slopes.

Errors are due to each of the system components (i.e., GNSS, IMU, Scan Angle unit, and LiDAR unit) independently. Additional errors emanate from the integration of the components. Calibration and proper procedures eliminate many systematic errors. However, some error, including random error, remains. Given this residual error, airborne laser terrain mapping routinely produces elevations plus or minus fifteen centimeters on flat un-vegetated terrain.

Additional factors outside of the main components, such as flying height, terrain slope, incidence angle, footprint size, etc., also affect the accuracy of ALTM data.

Regarding flying height, several studies indicated that as flying height increases, ALTM vertical accuracy decreases. This relationship was a concern with this study as the flying height was significantly higher than every other cited study.

Several studies measured ALTM elevations on gently sloping terrain (less than 20°) and noted diminished accuracies and/or imprecisions compared to level terrain. A few investigations reported a sizeable decline in accuracy on steeper slopes. Several indicated that horizontal imprecision might be responsible for vertical inaccuracy on sloping terrain. Most investigators did note that these were more observations than findings since due to very small sample sizes. Studies conflict regarding the relationship and the amount of error as slope increases.

A few studies investigated incidence angle. These indicated that an increase in incidence angle results in an increase in ALTM error. Range measurements used to calculate laser strike coordinates incur error when striking tilted surfaces.

However, no articles have produced hard data showing the actual effect incidence angle has on vertical error.

Several studies postulated that the size of a laser strike's footprint influences error, although only one study offered data. The range measurement may be due to reflective material or some other element located other than at the center of the footprint. Alternatively, the range may be reflecting off the higher edge of

the footprint. Sloping terrain causes the footprint size to increase. Thus, laser strikes on slopes may result in reflective material or the rising edge to be further away from the footprint center. The distance between the center of the footprint and the location responsible for the laser reflection was a concern in this study since the higher flying height resulted in a footprint size considerably larger than in other studies.

As slope increases, the elevation range across the footprint increases such that the upper and lower reaches of the footprint have increasingly higher and lower elevations than the center. Reflective material or some other element responsible for the range measurement situated off center results in a calculated elevation disparate with the center of the footprint. No studies have determined the impact of disparities in elevation across the footprint on ALTM vertical error.

Investigators found that DTMs built from fewer ground strikes are less accurate than those which had higher densities (i.e., under forest canopy versus open terrain).

Another significant limitation of DTMs is interpolation, which incurs errors and obscures the actual accuracy of ALTM data. Numerous researchers indicated that DTMs do not serve as valid reference data when stringently evaluating ALTM accuracies.

Proximal points methodology negates the use of DTMs as it evaluates elevations of laser strikes in close proximity to reference points. The literature review

uncovered very few studies that employed this method. While superior to DTM use for assessment purposes, this technique is not feasible on sloping terrain.

The optimal method appeared to be navigating to actual laser strike locations on the ground using the planimetric coordinates of the strikes provided by the ALTM system. At each ground strike location, a measurement of the ground elevation provides for a direct comparison to the ALTM-derived elevation. Only two studies had employed this method and neither had done so on steeply sloping terrain.

Lastly, reference data are not without error. Based on the equipment and methods used, inaccuracies and imprecisions vary. Terrestrial-based methods are believed to offer the most accurate and precise results. Traditional equipment tends to be the most accurate but does incur loss in accuracy on sloping terrain and is a time consuming method. More practical is RTK GNSS. While slightly more inaccurate, establishing reference points is quicker with RTK GNSS. However, confidence is limited due to the lack of redundant data. Static GNSS has greater accuracy and guards against larger errors but it significantly more time consuming. Additionally, use of GNSS under vegetative cover is typically slow and arduous.

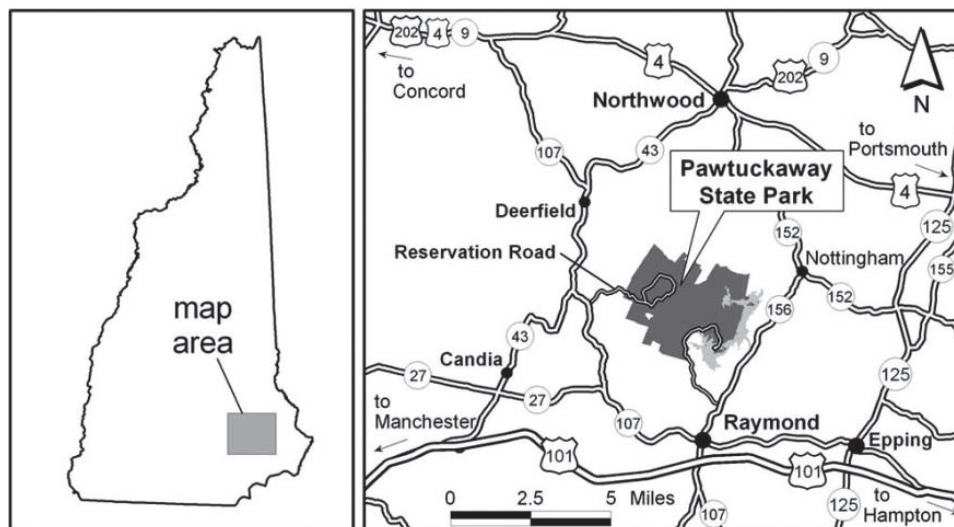
The review of the pertinent errors of the ALTM system emphasized which factors the study should focus on. Similarly, the review of previous studies indicated which methods would be best to establish reference points for definitive comparisons.

Chapter 3

Data and Methodology

Study Site

Pawtuckaway State Park, situated in southeastern New Hampshire (see Figure 12), served as the study site.



-NH Natural Heritage Bureau (2010)

Figure 12. Locus map of Pawtuckaway State Park.

This park is a 2240 hectare preserve (NH Natural Heritage Bureau, 2010), situated in the towns of Northwood and Deerfield, in Rockingham county, approximately 33 kilometers northwest of Portsmouth. Elevations within the park

range from 137 m to 308 m. The steepest terrain in southeastern New Hampshire is located in this park. In addition to Pawtuckaway Pond, the most defining feature of the park is the Pawtuckaway Mountains.

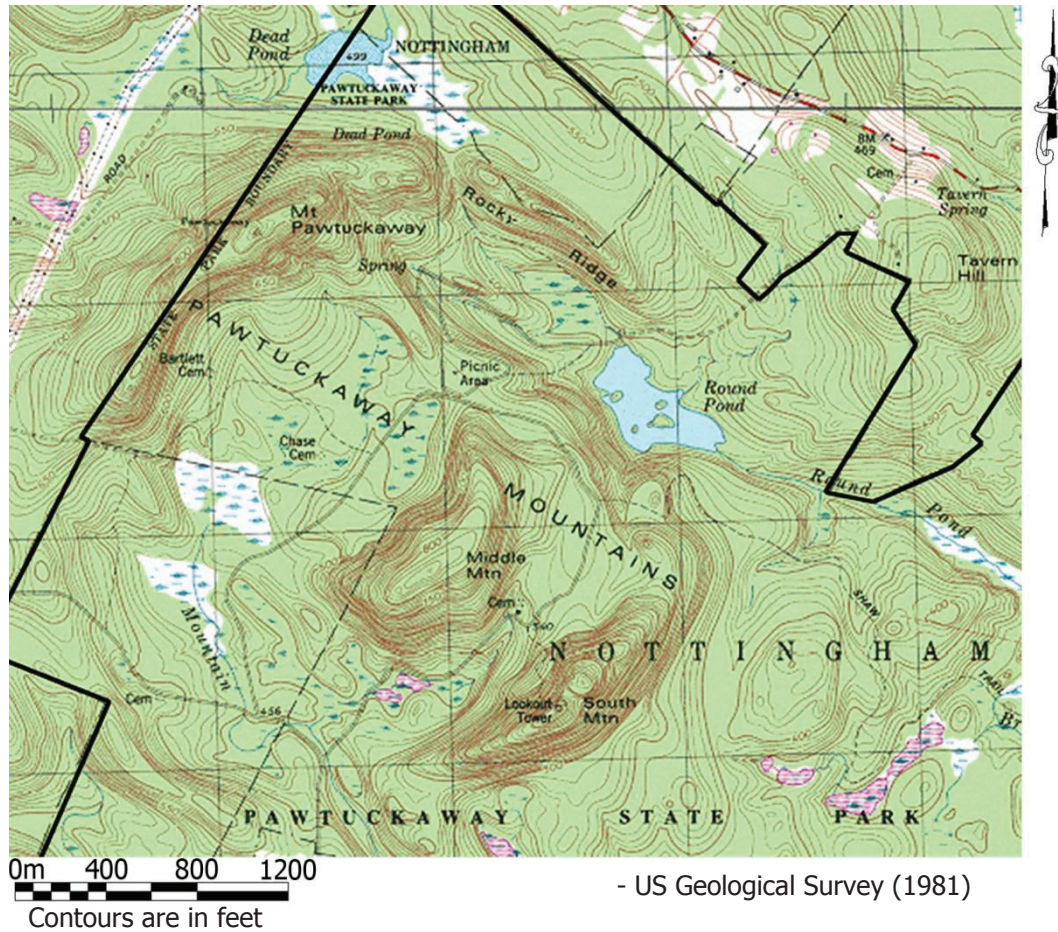


Figure 13. Topographic map showing ring dike of Pawtuckaway Mountains.

These mountains are a fairly rare geologic occurrence known as a ring dike. The mountains are comprised of a dike whereby, intruding magma filled a fissure in the bedrock. The intensity of the magma forced the bedrock upward, crating the mountains. What makes this geologically unique is the dike is in the shape of a circle versus a straight line, thus the name: ring dike. Figures 13 and 14 depict

the circular arrangement of the mountains and ridges. On the topographic map, the heavy black line represents the State Park boundary.

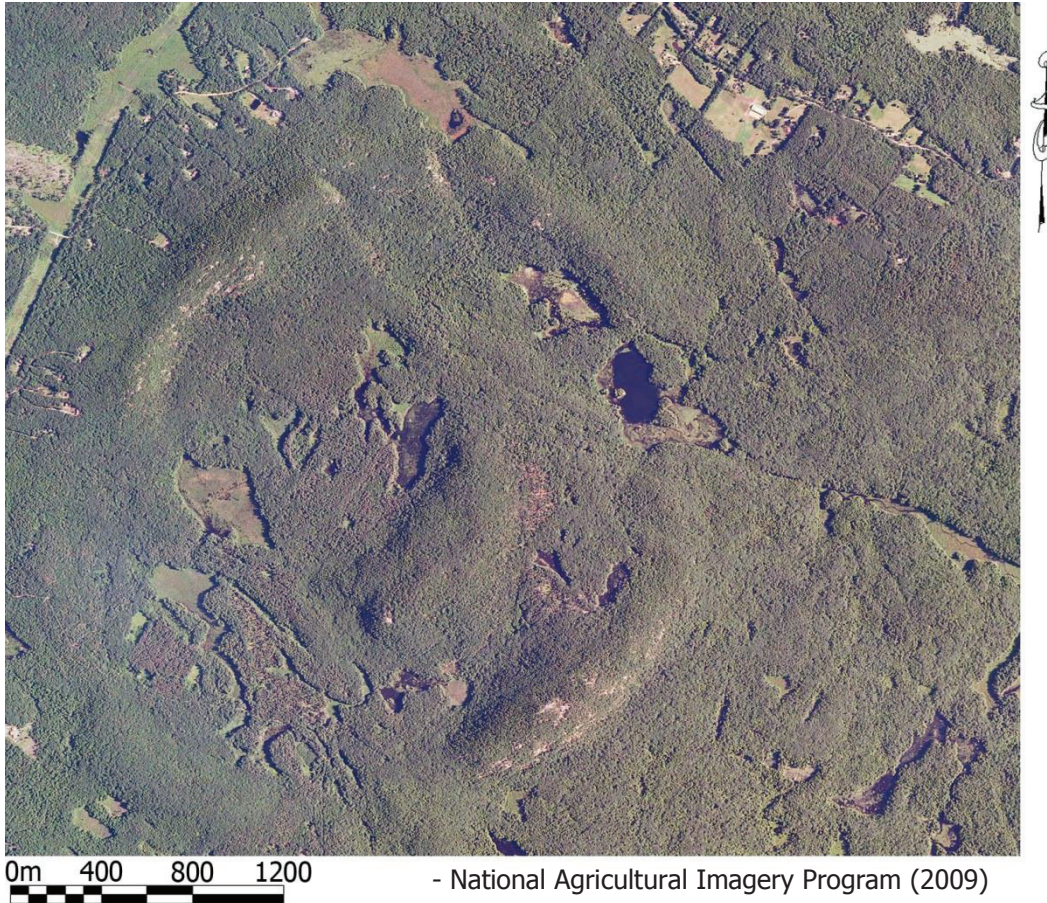


Figure 14. Aerial photograph showing ring dike of Pawtuckaway Mountains.

Within the ring, is a long-dormant volcanic cauldron that has subsided (Freedman, 1950). The ring dike is three quarters complete with Mount Pawtuckaway (also known as North Mountain ~308 m) to the northwest, Rocky Ridge to the northeast and South Mountain (~270 m) to the southeast. The land within the ring dike (i.e., cauldron) is predominately flat which served as an ideal

location to evaluate ALTM elevations on level terrain. Also in the interior, northwest of South Mountain, is Middle Mountain (~255 m).

The flat terrain of the interior changes abruptly to much steeper slopes at the edge of the ring dike with slopes up to and exceeding 90 degrees. The severity of the slopes then gradually eases to the rounded top of the dike, which is the ridgeline of the mountains. While the elevation of the ridgeline varies, in the study area, it is approximately 175 m above the surrounding terrain. The slopes on the outside of the dike are gradual from the ridgeline down onto the gently sloping terrain that is more typical of southeastern New Hampshire.

The park contains a diverse mix of upland and wetland communities. The dominant natural community is primarily Hemlock-Beech-Oak-Pine forest with only a few areas being selectively harvested (NH Natural Heritage Bureau, 2010). This forest type is interspersed with bodies of water and a wide variety of wetland types, including peat lands, herbaceous marshes, and forested swamps. Much of the interior of the ring dike is comprised of these wetlands and swamps. In addition to the topographic map of Figure 13, the aerial photo of Figure 14, Figure 15 displays a representative view of the land cover. In this photograph taken in a southeasterly direction from Rocky Ridge, a forested swamp is visible in the distance with the slope of Middle Mountain to the right-hand side.



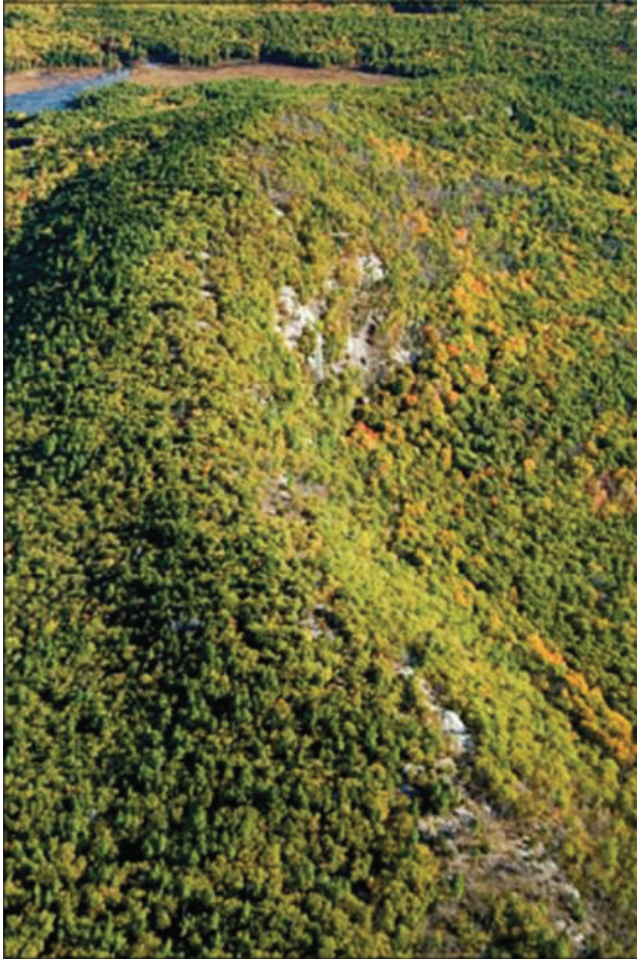
Figure 15. Typical forest cover and terrain of Pawtuckaway State Park.

Given the steep slopes and structure of the ring dike, the mountains have large amounts of exposed bedrock and ledges. Some of steeper slopes and the base of the ring dike are strewn with rocks, boulders, and blocks of various sizes creating a rough surface. In the study site, the terrain is scattered with rocks, fine boulders (0.25-0.5 m in size) and medium boulders (0.5-1.0 m), based on the Blair and MacPherson adaptation of the Udden-Wentworth grain-size scale (Blair & McPherson, 1999). Figure 16 depicts the boulders and rock commonly found on the slopes of the ring dike.



Figure 16. Typical terrain of study area in Pawtuckaway State Park.

This park is easily accessible off state highways and via un-gated gravel roads that extend into the interior. Well-maintained hiking trails along the ridgeline and up to the mountain peaks provide access to the steeply sloping areas. Since a good portion of the steep terrain is exposed bedrock with sparse tree cover, it provided favorable conditions for numerous laser strikes and GNSS field measurements. The ledges and exposed bedrock are visible in an aerial view of Mount Pawtuckaway, looking north (see Figure 17).



-NH Natural Heritage Bureau
(2010)

Figure 17. Oblique view showing exposed bedrock and steep slopes of Mount Pawtuckaway ridgeline.

The study site was limited to the ring dike and its interior. The ring is approximately three kilometers across, and the study area approximately 712 hectares in size. The elevations within this area range from 137 m to 308 m and slopes range from zero degrees to greater than 90 degrees.

ALTM Data

Data Collection

DeLorme of Yarmouth, Maine, traditionally known for their large format paper atlases, mapped this area and offered the data to the University of NH for this project. DeLorme collected ALTM data and digital imagery of Pawtuckaway State Park on June 17, 2003. The weather during the flight was clear, with a relative humidity of 44 to 45 percent and winds of seven to eight knots (see Appendix A, ALTM Flight Conditions. Table A-1, Climatological Data for the ALTM Mapping Period from 15:30 to 15:47 on June 17, 2003). DeLorme used a Leica Geosystems ALS40 airborne laser scanner for the mapping. This LiDAR unit was a predecessor to the current ALS70 unit. Additionally, a Leica Geosystems ADS40 digital camera mounted in the fixed-wing aircraft, captured images of the area. From the manufacturer, the stated vertical accuracy of the ALS40 scanner is consistently 0.15 m with horizontal accuracies well below one meter. Vertical accuracies of 0.06-0.10 m are typical during calibration testing Leica Geosystems (2002). The flight lines for the project were nearly north/south with the flying height approximately 4907 m (16,100 ft.) AGL. From Leica Geosystems, the maximum AGL of this ALS40 system is 6100 m.

Interpolating this height against Leica Geosystems' graphs for the ALS40 (see Figure 4, Variations in horizontal and vertical accuracies due to flying height), the accuracy is 0.38 m vertical (SD=1) and 0.59 m horizontal (Leica Geosystems, 2002). As mentioned, this altitude is atypical when compared to the flying

heights of accuracy studies found in the literature. This flying height allowed for greater coverage that was part of the DeLorme's business model at the time (D. DeLorme, personal communication, September 26, 2003). The ALS40 LiDAR unit measured two returns from each laser pulse. Optimally, these pulses represent the top of the canopy and the ground. The scanning mirror unit swept across the flight line at ten scan lines per second. The limits of the scan were 32 degrees off nadir, making the Field Of View (FOV) 64 degrees. The width of the mapped swath was approximately 6132 m. The aircraft made three parallel flight lines over the park with the swaths overlapping by fifteen percent. These flights resulted in mapping 10,836 hectares of the park and surrounding environs.

The pulse rate of the laser was 20,000 Hz. The pulse rate combined with the AGL, scan rate, and aircraft speed of 270 knots, resulted in a laser strike posting of approximately 8.3 m across the flight line (i.e., along the scan line) and 5.5 m approximately, between scan lines, for a total of 6,978,339 laser strikes collected for the 10,386 hectare area.

On board Applanix hardware supplied the Position and Orientation System (POS) data which included the RTK GNSS unit that provided real time horizontal coordinates and elevation, and the IMU that measured the roll, pitch, and heading of the LiDAR unit (Applanix, 2012).

DeLorme used Applanix and Leica Geosystems software to combine the POS and LiDAR unit data to assign unique geographic coordinates to each of the laser

strikes. The post processing also combined the laser strikes from all three flight lines into one point cloud.

A typical issue with ALTM data is the mismatch of data along the edges of overlapping swathes. Several investigators have noted that errors between overlapping swaths are common and require rectification as part of the post processing (e.g., Huising & Gomes Pereira, 1998; Maas, 2002; Morin, 2002; Davenport et al., 2004; Schaer et al., 2007; Csanyi & Toth, 2007; Leigh et al., 2009; Skaloud et al., 2010). They postulated several sources for this error: horizontal displacement, scan angle encoder error, alignment errors between the ALTM components, etc., with IMU drift being the predominate source. Many of these errors are systematic and eliminated or reduced by various methods, such as rectification using redundant data from overlapping swaths and a flight across the flight lines which also provides redundant data. The study site is not near a swath edge and one flight line mapped the site in its entirety. Based on the study site's location within the flight line, the relative elevations and errors between laser points in the study area were believed to have minimal or no impact from any corrections undertaken by DeLorme for swath misalignment.

Since this is a mountainous area, gravity anomalies may have been influential on the IMU (see section, Inertial Measurement Unit). Gravimetric information can be found in Appendix A, ALTM Flight Conditions: Figure A-1, Aeromagnetic map of study area. It was unknown what corrective measures were taken.

Given the rather small size of the site compared to swath width, most of these errors, including IMU drift, most likely had little impact on the relative locations between sample points.

Subsequent to combining the swaths, a proprietary algorithm created by DeLorme classified the laser strikes in the point cloud. The type (e.g., morphological, slope-based) or the specifics of the filtering algorithm used by DeLorme were not known. The algorithm removed erroneous values higher than the highest elevation in the area (Pawtuckaway Mountain) and points from the cloud that were below the minimum expected elevation. These types of points result from the laser beam scattering and reflecting off secondary objects before returning to the optical sensor. This delay results in lower than actual elevations assigned to the laser strikes (Kobler et al., 2007; Goulden & Hopkinson, 2010). Nine points were higher than Pawtuckaway Mountain and 171,844 strikes were below ground level and stripped out of the data set. DeLorme's algorithm then classified laser strikes into ground strikes. This processing categorized 4,631,063 strikes or 66 percent of all laser strikes as ground strikes.

The data provided by DeLorme were the planimetric coordinates of the ground strikes referenced the Universal Transverse Mercator (UTM) North coordinate system, Zone 19 (72° west to 66° west). The elevations were Heights Above the Ellipsoid (HAE) referenced to the WGS84 ellipsoid.

ALTM Data Assembly

The data provided by DeLorme were cropped to the study area, reducing the amount of data and the number of ALTM ground strikes from 4,631,063 to 31,333, which provided for easier management in subsequent software. These ground strikes are displayed in Figure 18. The near vertical line depicts the flight line over the study area where the flight flew south.

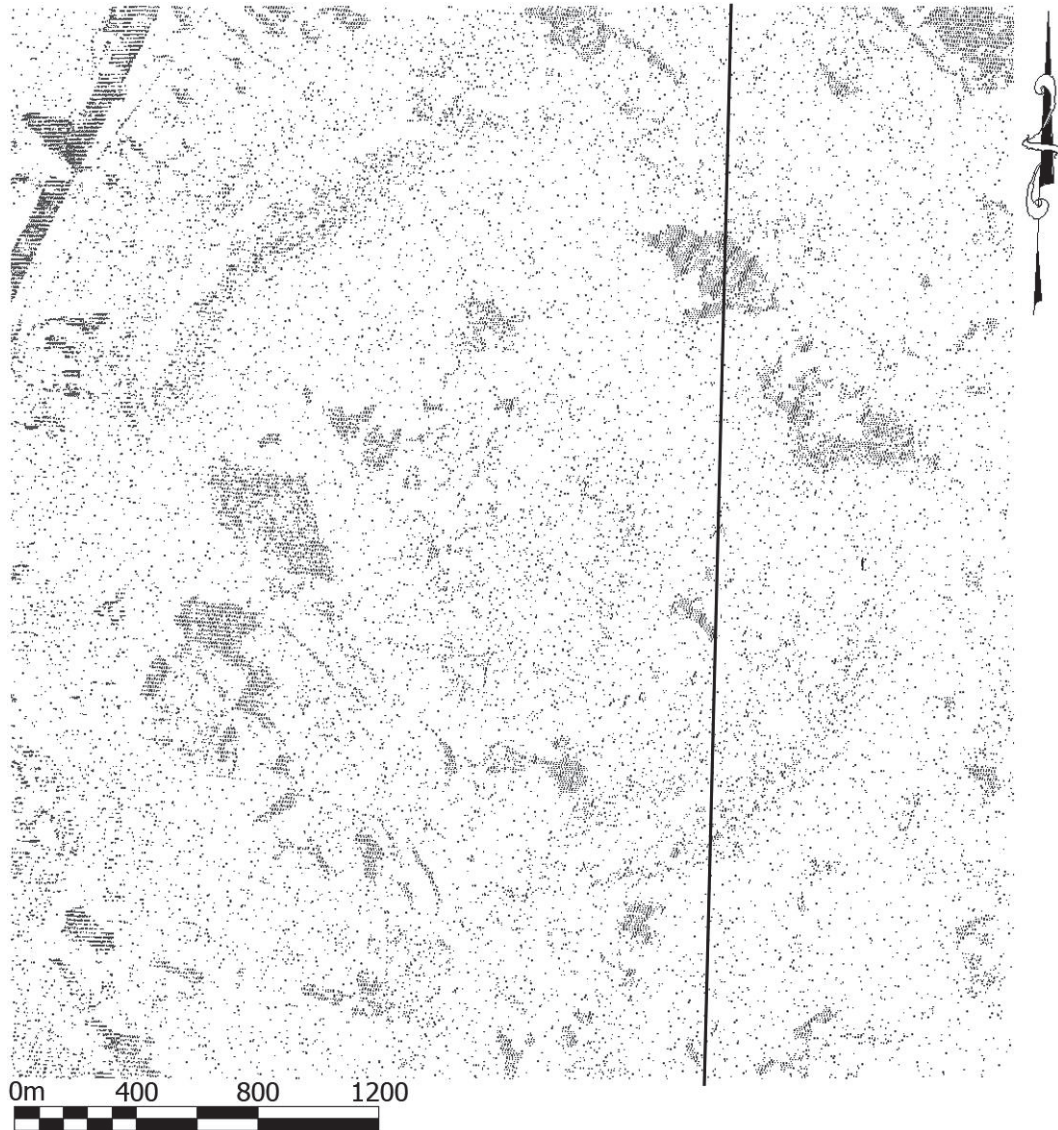


Figure 18. Plan view of ALTM ground strikes in study area with vertical line representing flight line.

The spacing of ground strikes across the study site is highly inconsistent due to the variety of canopy cover such that, a mean point density value was impractical to calculate. While densities are high in open areas, distances of 65 m between ground strikes are common under canopies of dense hemlock and other conifers. Figure 18 displays several areas of dense ground strikes while ground

strikes for much of the study area are sparse. The areas of greatest density are water bodies, open fields outside the park and a power line situated northwest of the study area. Aside from these, the areas with the next highest density are open ledges and bedrock that were free from vegetation. These coincide with the steeper slopes of the ridgelines and mountains. The density of ground strikes in these areas depicts the ring dike in this figure.

In preparation for the fieldwork, a calculation determined the size of a ground strike's footprint at nadir and on flat terrain. As discussed previously in Footprint Size, the size of the laser's footprint directly relates to AGL and laser beam divergence. For the Leica Geosystems ALS40 laser scanner, the beam divergence is 0.33 milli-radians (mrad) measured at the $1/e$ point. The following formula, supplied by Baltsavias (1999a), determined the footprint size for the AGL of 4907 m to be 1.62 m. Graphical representation of the geometry and formula is illustrated in Figure 19.

$$\text{Laser footprint diameter} = 2 \cdot \text{AGL} \cdot \tan(\text{Laser beam divergence}/2) \quad \text{Eq. (5)}$$

Where:

laser beam divergence is in radians

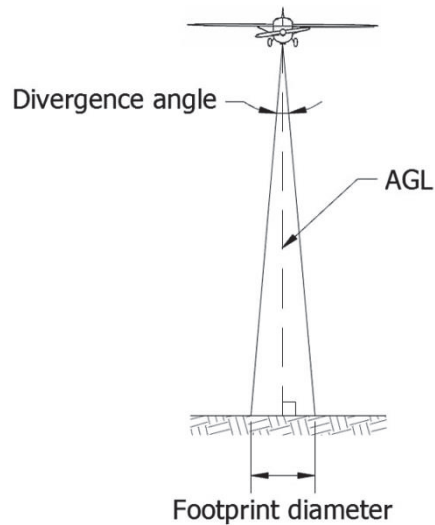


Figure 19. Geometry of ALTM laser beam which defined footprint size.

Determination of Terrain Slope

A US Geological Survey 7-1/2 minute quadrangle topographic map (US Geological Survey, 1981) and a TIN created from the ALTM ground strikes, assisted in deriving slope categories in the study area. Creating the TIN was via Carlson Survey 2011 software; a land surveying and civil engineering AutoCAD-based program (Carlson Software, 2010). Further editing of the data with this software changed the rectangular bounding box of the ALTM data (see Figure 18) to a more rounded one that conformed to the natural form of the ring dike (see Figure 20). This step reduced the number of ground strikes to 17,318. Hence, the extent of the study area was 7,009,750 m² or 701 hectares, being nearly circular with a diameter of approximately 3000 meters.

In Figure 20, the triangular faces of the TIN are visible. Each of the 34,557 faces is coded using a gray scale to indicate severity of slope.

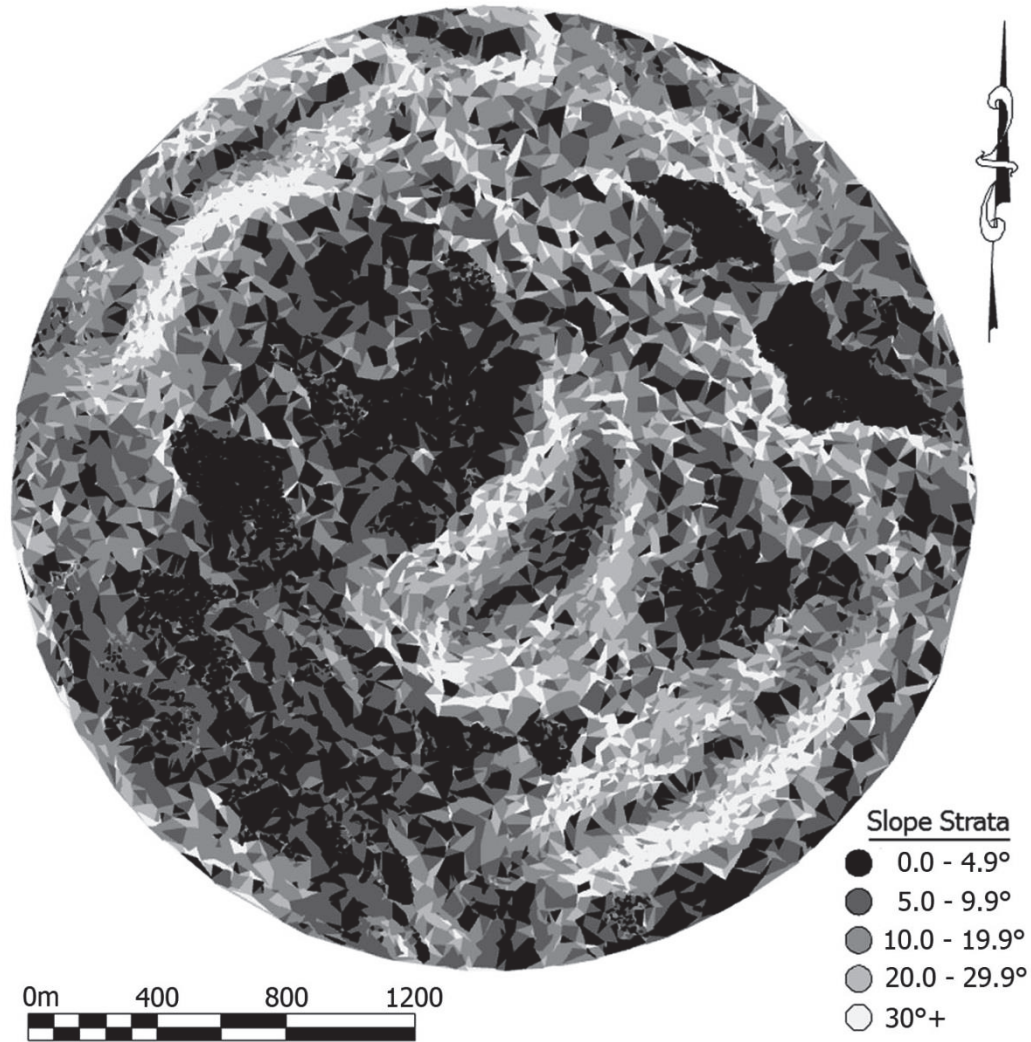


Figure 20. Degree of slopes from ALTM-derived TIN in study area.

The steepest terrain, shown in white, corresponds to the slopes on the side of the three main peaks and ridges: Mount Pawtuckaway in the northeast, Middle Mountain, and South Mountain in the southeast. Since the apexes of the summits and ridges are rounded, moderate and even level terrain exist on the ridge tops

and are shown in darker shades in between the whiteness of the steep slopes. Based on this processing and an attempt to match slope categories used in previous studies, the slope strata were established for this study as:

- 0.0-4.9 degrees (28.2% of the study site area)
- 5.0-9.9 degrees (25.5%)
- 10.0-19.9 degrees (26.4%)
- 20.0-29.9 degrees (11.6%)
- 30 degrees and greater (8.3%)

GNSS used to establish Reference Data

As presented earlier, survey-grade RTK GNSS equipment determined reference point elevations. Accuracy and precision of GNSS technology is the same regardless of terrain. There is, however, greater error under canopy cover unless stringent methods are followed.

GNSS, more In-Depth

GNSS is a satellite-based positioning system in which a GNSS receiver observes microwave signals (L-band) broadcast continuously by orbiting satellites specifically built for this system. By receiving and measuring the signal data, the software in the receiver uses the signal travel time to calculate its distance from each satellite. The receiver performs these measurements with several satellites simultaneously, using the data to triangulate its location. Interactive software in most GNSS receivers provides the user with: 1) the geographic coordinates,

including elevation, of the user's current location, 2) the ability to store the coordinates of the user's location and, 3) navigate to any set of coordinates corresponding to other positions.

As alluded to in the sections, Global Navigation Satellite System Unit and Reference Points Established using Traditional or Real Time Kinematic Methods, accurate positioning requires two GNSS receivers: a base receiver situated over a control point with known coordinates and a roving receiver used to determine the coordinates of new points. Both receivers independently triangulate their own positions. However, the base station, with its known coordinates entered into the software, assesses the difference between the calculated and known three-dimensional coordinates. Software in the base receiver then refines the calculated distances between it and the satellites. Subsequently applying these refinements to the roving receiver's measurements, results in considerably more accurate and precise coordinates. The transfer of these corrective data occurs in one of two ways: After the fieldwork is completed, the data are downloaded from the base receiver and integrated into the roving receiver's measurements during post processing. Alternatively, the corrective data are transferred in real time: As part of the base receiver, a radio transmitter operating at 902 to 928 MHz broadcast these corrections at a rate of one, five, ten, or twenty Hertz (user defined). A separate antenna on the user's GNSS receiver receives these signals (Topcon Positioning Systems Incorporated, 2004) and onboard software incorporates these corrections providing accurate, real time coordinates. For

navigation, the heading and distance between the receiver and the destination is also more precise.

In order to obtain the stated level of accuracy for GNSS receivers, appropriate procedures and methods must be met. As highlighted in Global Navigation Satellite System Unit, the location of satellites relative to one another and the GNSS receiver is critical. With the receiver at the vertex, satellites should be at, or close to, 90 degrees to one another, with another overhead to maximize vertical accuracy. Since measured distances and calculated angles are used to provide the receiver's location, geometry has a predominate influence on accuracy. Subject to the laws of cosines, the triangles and figures formed between the satellites and the receiver can be relatively strong or weak, the latter being less accurate. A receiver can calculate its position with a minimum of four satellites but a fifth satellite provides redundant data. Use of additional satellites also adds redundancy and increases accuracy (Topcon Positioning Systems Incorporated, 2004). The user can check satellite numbers in the field as the receiver provides satellite statistics in real time. A unit-less measure termed Position Dilution Of Precision (PDOP) rates the strength of figure resulting from the distribution of the satellites about the sky. The lower the PDOP value, the better the geometry, and thus, accuracy. Since the satellites are in continuous motion and orbit the earth twice a day (Kaplan, 1996), PDOP is constantly changing and requires continuous monitoring while measurements are being made. Given the numerous GNSS-specific satellites available, ideal PDOP is

not a difficult specification to meet. The multitude of satellites is due to two GNSSs readily available: GPS and GLONASS. While the term *GPS* is commonly used to describe satellite navigation and surveying, it is the name of the United States-based satellite positioning system (Global Positioning System).

GLObal'naya NAVigatsionnaya Sputnikovaya Sistema (GLONASS) is the Russian equivalent. Many receivers are able to use both satellite systems that provides for longer periods with optimum PDOP.

Accuracy is also dependent on satellite signal integrity. Several atmospheric elements (e.g., water vapor, charged particles) delay satellite signals. Similar to a LiDAR unit, time measurement is an integral and crucial part of the determining GNSS receiver position, hence, correcting these delays is necessary. To moderate these errors, models of the ionosphere and troposphere are used. Additionally, employing the corrective data calculated by the base receiver also diminishes atmospheric effects (Topcon Positioning Systems Incorporated, 2004). High-end receivers also utilize two different signals from each satellite. Sampling signals on two different frequencies aids immensely in negating atmospheric effects. Typically, accuracies are higher with dual frequency receivers, even in forested conditions (Næsset, 2001).

As mentioned in the section, Global Navigation Satellite System Unit, there is a trade-off between satellite geometry and signal strength: the best geometry is when the satellites are at the horizon but atmospheric effects severely delay the signal since the signals must pass through more of the atmosphere. In practice,

the receiver is set to disregard satellites situated from zero to ten or fifteen degrees off the horizon since these delays significantly outweigh the benefits of the stronger geometry.

GNSS receivers have a major shortcoming when used under forest canopy: The satellite signals are inherently weak and are prone to loss and interruption by solid objects such as branches, leaves, and tree trunks (Hasegawa & Yoshimura, 2003). Typically, fewer satellite signals are able to penetrate through the forest to the GNSS receiver, especially those emanating from satellites near the horizon. The result is poorer satellite geometry and/or signal to noise ratio and thus, less than desirable accuracy. In these conditions, mapping-grade and survey-grade receivers are further handicapped since they require largely uninterrupted satellite signals for the duration of the observation. Regularly, the signal is lost when a satellite transits behind a tree or dense foliage. Losses and long interruptions many times require the measurement process to begin anew. Consequently, most high accuracy GNSS work is limited to areas with open views of the sky (Van Sickle, 1996).

Forests and other vegetative areas add another complexity: an increase in risk of multipath. All GNSS receivers can suffer from errors when a satellite signal reflects off an object prior to reaching the receiver. This delay results in a significant range error that results in a false location (Rodríguez-Pérez et al., 2007). In open areas, assessing the potential for multipath is by observing the nearby few hard surfaces are nearby and taking steps to mitigate it. In forested

conditions, tree stems serve as signal reflectors, so recognizing and alleviating multipath is difficult. In addition, with vegetative cover, water droplets on leaves and branches cause signal delay and multipath. The effect is such that many times a GNSS receiver cannot calculate a position at all when vegetation is wet. These can be detrimental to any GNSS receiver, not just survey-grade units (Rodríguez-Pérez et al., 2007; Van Sickle, 1996).

Thus, to obtain the highest accuracy, high PDOP values, low signal to noise ratios are important, as are other factors: being cognizant of multipath-prone areas, both receivers being stable and stationary when measuring, and redundant checks of receiver antenna height.

For this study, survey-grade GNSS receivers were used for several reasons:

Foremost, they are the most accurate when compared to lesser GNSS products⁹. Additionally, these types of receivers have greater antenna sensitivity to satellite signals and sophisticated software and firmware that have greater success in detecting and correcting multipath.

Testing and Accuracy of GNSS Equipment and Procedures

The Civil Technology program of the Thompson School of Applied Science at the University of NH provided the GNSS equipment used for this study. The two units were survey-grade geodetic Topcon Positioning Systems HiPer Lite Plus models,

⁹ Topcon Positioning Systems, states that the accuracy for their survey-grade HiPer Lite Plus system can be estimated as 10 mm + 1 mm ppm (horizontal) and 15 mm + 1 ppm (vertical) when using RTK techniques. Topcon does not provide confidence limits (Topcon, 2004).

which are 40-channel dual-frequency receivers capable of receiving signals from GPS and GLONASS satellites.

This study site was atypical for a high accuracy GNSS survey in that, the majority of the site was in dense woods with a high percentage of canopy cover. The concerns outlined in the last section and minimal documentation of high accuracy GNSS surveys in forested conditions lead to investigation of the efficacy and accuracy of survey-grade receivers for this project prior to the field work.

A portion of this investigation involved using a GNSS test course established by the USDA Forest Service in Durham, NH. This course is a collection of ten points positioned in hardwood and softwood forests with varying canopy cover. Each point is a survey disk set in ledge or concrete. All points have accurate planimetric coordinates and most have accurate elevations.

To replicate field conditions of the study site in Pawtuckaway State Park, the base station was set at a control point with an open view of the sky, approximately two kilometers away from the test course. This distance is comparable from the center of the ring dike to any point in the study area. The roving receiver, while receiving the correction signals from the base station, collected positioning data at each of the monuments in the test course, during leaf-on conditions. The points were re-visited at different times of the day since results may vary as satellite geometry changes. Elsewhere, other points under

varying canopy cover were established and re-occupied on varying days and times.

Several issues arose from the testing: The roving receiver was only able to receive satellite signals from one or two satellites under heavy forest cover and moderate hemlock cover. The signals were weak and intermittent resulting in the receiver unable to determine its position under these covers. In addition, an obvious difference was the length of time needed to acquire enough satellite signals to begin calculating a position between open areas and under forest cover. In open areas, the time to acquire is characteristically only 20-30 seconds. Under forest canopy, two to five minutes was typical. Furthermore, the receiver lost satellite signals frequently while calculating positions. However, the receiver did calculate accurate three-dimensional coordinates at most points.

As highlighted in the section, Reference Points Established using Traditional or Real Time Kinematic Methods, RTK GNSS surveys typically calculate and average one to three sets of measurements per position. If the receiver is constantly moving, then only one measurement can be made at each position. If two or more measurements are preferred, the receiver must stop temporarily to collect these multiple measurements at each position. The user sets the number of measurements; one, five, or ten seconds are typical (The Topcon Positioning Systems software allows the measurement interval to range from one second to 24 hours). While a quick interval between measurements reduces field time, a longer interval allows for a minor change in satellite geometry and may allow for

recognition and correction of multipath errors. This type of error is less likely to happen if the measurements are made in quick succession.

Based on the work on the US Forest Service test course and elsewhere under varying canopy cover, for this receiver, 40 sets of measurements at each position, one second apart, afforded a high accuracy elevation and allowed for a long enough observation period to safeguard against errant positioning by multipath.

Certainly, with such longer observation periods, multipath or change in PDOP due to loss of signal can arise during the measurement phase. However, the user has the ability to monitor these occurrences and terminate data collection if serious degradation occurs. However, the receiver typically produces more accurate and precise data when the observation period is longer.

For the ensuing field work, Topcon Positioning Systems' mission planning software, which predicts the GNSS satellite configuration and PDOP values for future dates and times, was used to determine the best times of the day for GNSS work.

In addition to collecting data during optimal PDOP, the software identified times of the day when VDOP (Vertical Dilution Of Precision) was best. VDOP is similar to PDOP where, PDOP indicates the quality of the satellite configuration for overall three-dimensional positioning; VDOP is an indicator as to when geometry is ideal for elevation measurements. As with PDOP, lower VDOP values are best

and are highly correlated to when a satellite is directly overhead. While PDOP values can be very good for several hours at a time, optimal VDOP is more intermittent with satellites near zenith constantly changing position.

Since it is an integral part of the ALTM system, conditions also need to be favorable for GNSS when mapping. When this study site was mapped, the PDOP was 2.1 at the beginning of the flight line, dropping to 2.0 at the end and VDOP was 1.8 at the beginning of the flight line, dropping to 1.7 (see Appendix A, ALTM Flight Conditions: Figure A-2, Chart of GPS satellite geometry at the time of the ALTM flight June 17, 2003.). These PDOP and VDOP values indicate optimal satellite geometry during the mapping foray.

Eight satellites were above the horizon and available for the ALTM GPS unit to receiver signals from. In 2003, the GLONASS system was not yet functioning and eight visible satellites were considered ideal. Thus, positioning conditions were optimum.

With an understanding of the limitations of these particular terrestrial GNSS receivers, preliminary fieldwork began.

Establishment of GNSS Control Points for Reference Data

Establishment of five control points about the study area, provided for close proximity to all portions of the study area. The key criteria for control point locations were clear views of the sky, remote locations since the GNSS units would operate unattended, and be in close proximity to the study area due to

range limitation of the base receiver's transmitter that broadcasts the corrective data (see Figure 21 for the siting of one of the GNSS control points). For the Topcon Positioning Systems HiPer Lite Plus system, maximum broadcast distance of the corrective signal is 2.5 km (Topcon Positioning Systems Incorporated, 2004). However, was considerably less in the forested environment due to interception of the signal by trees, leaves, and branches.



Figure 21. Photograph of GNSS receiver stationed at control point named MJD.

When establishing highly accurate positions, occupation times of 30 minutes at each new control point are required, as per manufacturer recommendations (Topcon Positioning Systems Incorporated, 2004). As mentioned, longer occupation times customarily result in greater accuracies. Given the distance of the study site to existing control points, observation periods were, minimally, four hours for each point.

Post processing incorporated corrective data from established base stations to determine the three-dimensional coordinates of these points. This data came from three National Geodetic Survey sanctioned permanent base stations that provide free data. Access and use of this information was straightforward as the National Geodetic Survey offers the ability to collect base station data and post process the measurements online. This service is the Online Positioning User Service (OPUS) (National Geodetic Survey, 2012b). After uploading the GNSS observations for the new control points in the study area, OPUS automatically gathered corrective data from established base stations in close proximity. While corrective data from one base station is sufficient, OPUS uses data from three base stations for redundancy against blunders and increases the accuracy of the coordinates via least squares processing.

Surprisingly, for the first two new control points, the online software rejected large portions of the data. For these control points, named RGM and RGC, OPUS used only 72 and 56 percent of the total observations, respectively. The criterion OPUS uses to reject data was unknown. However, post processing software

typically excludes data when the signal to noise ratio is too low, a satellite's signal is repeatedly blocked, or a satellite's signal is only received by one of the receivers (Kaplan, 1996; Van Sickle, 1996; Topcon Positioning Systems Incorporated, 2012a; National Geodetic Survey, 2012a). Processing of the same data using OPUS but at a later date, tested these initial solutions. Interestingly, for the second iteration, OPUS selected different base stations and provided three-dimensional positions quite different from the first set. For point RGM, 0.104 m represented the elevation difference between the two solutions even though the RMSE for both iterations was circa 0.030 m. Since OPUS used base stations that were rather distant from the study site, the long baselines may be responsible for the discrepancies. See Appendix B, GNSS Postprocessing with OPUS: Table B-1, Varied Results with OPUS Processing of GNSS Data. Given the disparities, Topcon Tools, a proprietary software package, calculated an additional set of coordinates. This software allows for more user control. Instead of the distant base stations used by OPUS, post processing incorporated data from the base station NHUN, operated by the University of NH. NHUN is the closest base station to the study site at only nineteen kilometers away. Using this base station, the vertical RMSE for the two control points RGM and RGC, were 0.018 m and 0.013 m, respectively. The measurement data of the two new points were then processed again using a different base station 30.1 km away. The results were elevations within ten millimeters of those computed from the NHUN data for both stations RGM and RGC. These accuracies were comparable

to *a-priori* estimates. The solutions produced by the Topcon Tools software served as the coordinates of the new control points based on the lower RMSE values, the ability to choose the base station, and acceptance of a larger majority of the measurements by the software. Three-dimensional position values for RGM and RGC via OPUS and Topcon Tools using the different base stations can be seen in Appendix B, GNSS Postprocessing with OPUS: Table B-2, Comparison of Results Using Different GNSS Processing Software and Base Stations.

Processing of the measurements for the remaining control points was via Topcon Tools, using NHUN base station data.

With control points established in the study area, one last check was needed prior to sampling.

Validation of ALTM Planimetric Coordinates

The ALTM planimetric coordinate system and the ground control coordinate system were in registration needed to be confirmed. Even though both were referenced to the UTM coordinate system, one or both sets of coordinates could be inaccurate. If the systems were not in alignment, navigating to a laser strike's coordinates in the field would have resulted in sampling a position away from the actual laser strike location. One example why these systems could be mis-registered is if the distance between the study site and the base station for the ALTM mapping foray was significantly greater than that for the terrestrial survey. From the section, Global Navigation Satellite System Unit, inaccuracy increases as this distance increases. The base station(s) used for processing of the ALTM

data was unknown and hence, this distance was undetermined. The use of different base station control points between the aerial and terrestrial work could also result in mis-registration.

To check for mis-registration, routines in Topcon Tools overlaid the ALTM laser strikes on top of an aerial image captured of the study site during the flight by the onboard Leica Geosystems ADS40 digital camera. Using this image assumed accurate registration between the aerial digital camera and the ALTM system. ALTM-derived planimetric coordinates for ten identifiable laser strikes on the photo were navigated to in the field using GNSS. Comparisons between field features and visible features in the aerial photo confirmed that the photo and field points were the same. Unfortunately, no strikes were at definitive locations such as sign posts, utility poles, painted lines on pavement, etc. that were readily identifiable in the field. As such, strikes near road intersections had to serve as the checkpoints. However, the visual comparison did provide confidence that the ALTM laser strikes and ground control were in registration and met the needs of this study. Figure 22 shows a GNSS receiver precisely measuring one of the ten laser strike positions.



Figure 22. GNSS receiver establishing a horizontal position for orientation of reference points to ALTM ground strikes.

Confidence in the registration increased during the actual sampling of laser strikes that did not end up on unlikely places. Many times during navigation, when approaching the laser strike, the location was obvious as it would be under the only opening in the forest canopy.

Thus, no transformation was required between the ALTM and terrestrial coordinate systems.

Field Test

Before the onset of the actual sampling, testing of the developed procedures occurred via a field trial. Twelve ALTM laser strikes with varying canopy cover and slopes provided for a representative sample of the study area. For the test, a GNSS receiver stationed at one of the new control points served as the base station and broadcasted correctional data. Performance of the GNSS equipment was similar to that on the US Forest Service test course.

During post processing, the vertical RMSE indicating accuracy for each sampled strike was, on average, 0.005 m. These results under the varying conditions, confirmed that the 40-second observation period appeared ideal.

Unexpectedly, the broadcast signal from the base station receiver was limited to only 500 m, approximately, in dense woods. The range of the signal was significantly less than the range of 2.5 km specified in the manufacturer's literature. (Topcon Positioning Systems Incorporated, 2004). It is possible that the manufacturer's value is for predominately open terrain. During the test run, the base receiver and transmitting antenna were approximately two meters above ground level. Subsequent testing showed that mounting the base receiver and transmitter atop a telescoping prism pole extending 4.69 m high allowed the correction signal to propagate much further. Figure 23 depicts the latter arrangement of the GNSS base receiver at a control point. This increase in height resulted in no broadcast issues and this configuration served as the norm during the subsequent fieldwork.



Figure 23. Typical configuration of GNSS base receiver stationed at a control point.

Determination of Sample Size

Originally, the 17,318 ALTM laser strikes were to be stratified by degree of slope and randomly sampled. Once the fieldwork commenced, it became obvious that random sampling was not viable due to rover receiver's inability to observe satellite signals under dense canopies. Much of the study area has heavy canopy cover, which reduced sampling sites to limited areas having minimal and moderate cover. These areas included unpaved roads, recently harvested forests,

wet areas, and ledges. Figure 15, Typical forest cover and terrain of Pawtuckaway State Park and Figure 17, Oblique view showing exposed bedrock and steep slopes of Mount Pawtuckaway ridgeline are photographs of typical forest cover in the study site. This heavy cover reduced the number of potential laser strikes samples down to only several hundred. The most feasible sites were the open ledges of the ridgelines. The ridgeline of Mount Pawtuckaway in the northwest was most conducive to sampling due to the expansiveness of open areas. Rather than randomly sample the several hundred, yielding a small sample set, sampling was of most of the laser strikes with minimal canopy cover. While the limitation significantly reduced sampling areas, it did not diminish the full range of slopes.

The fieldwork resulted in visiting 924 ALTM laser strikes. Of these, limitations resulted in the rejection of 495 samples, leaving 429 samples remaining. Some of the rejections were due to poor satellite reception or signal loss, neither allowing for sampling. Lack of a satellite signal from overhead resulted in the rejection of others. At these locations, real time PDOP values were ideal but VDOP values were not. Weak VDOP would have compromised the vertical accuracy of the reference data. Laser strikes in close proximity to one another ($< \sim 5$ m) resulted in further exclusion. Many sites were eliminated since the strikes were on top of boulders, rocks, tree stumps or some feature other than the ground. Similarly, terrain around other strikes was not uniform. Some were close to slope breaks or among boulder fields. For inclusion, the area about the strike location had to be

homogenous and unvarying three meters in all directions. A typical field day saw 48 laser strike locations visited with only 22 viable ALTM laser strikes sampled.

The relative location of the ALTM laser strikes to the base receiver determined the sampling pattern. In each open area or area of minimal canopy cover, the GNSS receiver moved from one sample to the next based on proximity, regardless of slope category. Thus, opportunistic sampling best describes the sampling technique.

Field Work

For each sampled laser strike, the GNSS receiver was used to navigate to within 0.11 m (i.e., ≤ 0.08 m north/south and 0.08 m east/west) of the ALTM coordinates. Navigating any closer was exceedingly time consuming since the GNSS receiver frequently lost satellite reception when repositioned. Given the size of the footprint (~ 1.62 m), navigation to within 0.11 m was more than sufficient. Subsequent processing indicated that the distance between the GNSS receiver location (where elevation measurements occurred) and the actual ALTM horizontal coordinates averaged 0.048 m.

Onboard software provided horizontal and vertical accuracies in real time, but these are only estimates (Topcon Positioning Systems Incorporated, 2004). Early investigations indicated these values were conservative. Subsequently, they guided some measurements by extending observation periods until vertical accuracy estimates dropped to acceptable values. Post processing of all 429

sampled laser strikes resulted in precisions of 0.003 m RMSE horizontally and 0.005 m (RMSE) vertically.

The multiple measurements at each strike location aided in detecting multipath when it occurred. Again, multipath is not readily apparent: At the onset of an observation, the software provided approximate coordinates and accuracy in real time. With multipath, the software could only maintain erroneous coordinates for a few seconds before it stopped the measurement process. Sometimes the multipath event would last several minutes. When conditions allowed for positioning again, the new geographic coordinates provided by the software were wildly different, being several meters away from those given when data collection began. The interruption occurred five to twenty seconds after the beginning of data collection. With RTK GNSS, measurement periods of one to five seconds would not have allowed the software to determine that the incoming signals were reflections.

During the course of the fieldwork, several checks confirmed the accuracy of the GNSS data. Resampling of several laser strikes took place on different days and at different times. Navigating to laser strikes a second time led to the same location as the first observations. Elevation measurements for these checks were well within manufacturer's quoted accuracies.

The most common user error in GNSS surveying is incorrect measurement of GNSS antenna height (Van Sickle, 1996). Using a prism pole with a set height of

two meters negated this type of error. This prism pole is visible in Figure 22. The receiver was atop either the prism pole or a surveyor's four meter, three-section leveling rod. Typical use of this type of level rod is with none, one, or both sections extended. While the height of the level rod is infinitely adjustable, its use was limited to being only one of the three fixed heights. The ability to raise or lower the GNSS receiver proved particularly beneficial in order to place the receiver among openings in the forest canopy for improved satellite signal reception. In many instances, signals were available at only one of the three heights. In areas with ledge or large boulders, extending level rod to maximum height, when possible, aided in minimizing multipath errors.

Elimination of other errors including using a bull's eye levels on both the leveling rod and prism pole kept the receiver precisely over the point during measurements. Fabrication of a small footpad for the prism pole (visible in Figure 22) kept the pole from sinking into the ground and thus, maintaining the correct antenna height.

Review of the field data revealed that six of the sampled strikes had high planimetric errors even though the real time software in the field indicated otherwise. Further scrutiny resulted in removal of an additional three strikes since they were within five meters of other sampled laser strikes. Possibly due to multipath, one sampled point fell more than two meters away from the actual laser strike. A search of the remainder of the data for evidence of erroneous antenna heights, cover type errors, etc., revealed no other errors.

During an initial comparison between ALTM-derived and field-derived elevations, numerous sets had exceedingly large disparities. The largest elevation range being 7.783 m. Sixty-six (15.8%) laser strikes had elevations too high to have been ground strikes. Revisiting twelve of these laser strikes proved this true. Vegetation at heights corresponding to the ALTM-derived elevations implied that these strikes occurred in the canopy. These non-ground strikes were most likely the result of misclassification by the algorithm that processed the ALTM point cloud. During the early stages of the fieldwork, the ALTM elevations were purposely not available in the field. Not having this data during the fieldwork avoided any sampling bias relative to elevation disparities. However, uncovering of these 66 misclassified strikes, resulted in bringing the ALTM-derived elevations into the field to compare with field elevations prior to data collection to guard against future misclassified strikes. Gross disparities with ALTM-derived elevation being sizably higher than the GNSS elevation, resulted in assessment of obstructions overhead. Large branches or an array of leaves corresponding to the ALTM elevation strikes resulted in rejection of strikes.

These analyses of sampled strikes resulted in a reduction in the number of samples from 429 to 353.

After completion of the fieldwork, minor transformations eliminated the last of the systematic error of the reference data. As stated previously, navigation to the laser strikes was not exact. The difference planimetrically between the laser strike coordinates and the field location averaged 0.048 m. A transformation for

each field position shifted planimetric coordinates to coincide with the exact ALTM coordinates. These shifts also adjusted the elevations based on the slope and slope aspect of each position. The vast majority of the adjustments resulted in very minor elevation changes with the mean being -0.001 m (RMSE 0.008). While this change appeared minor and the transformations overkill, the purpose was to increase the accuracy of field position elevations on very steep slopes. A review of the transformations indicated that the maximum elevation shift for one position was 0.048 m.

From the testing of the Topcon Positioning Systems GNSS and elimination of systematic errors, the mean vertical accuracy of the GNSS-derived elevations was 0.010 m (RMSE).

Additional Data Collected in the Field

Thorough comparison of reference elevations to laser strike elevations required additional field data.

At each strike location, a digital carpenter's level, mounted on a wooden dowel 1.62 m long, aided in measuring the terrain slope (see Figure 24).

The length of the dowel equaled the diameter of the footprint of a laser strike on flat terrain at nadir, calculated previously (see the section, ALTM Data Assembly). The dowel also afforded a long base for the digital level allowing it to lay parallel to the terrain unaffected by local ground roughness. Slope angle measurements were to the nearest 0.1 degree.



Figure 24. Digital carpenter's level attached to 1.62 m long wooden dowel.

Figure 25 shows the level in use, indicating the slope. The level rod is vertical with its white base visible positioned at a laser strike.



Figure 25. Digital level in use measuring terrain slope.

The digital level was checked for accuracy prior to its use in the field, again half-way through the field work, and a third time once all the fieldwork was complete.

The sampled laser strike slopes ranged from 0.5 degrees to 62.1¹⁰ degrees (see Figures 26 and 27). In Figure 27, a climbing rope is visible that was used for safety purposes.



Figure 26. ALTM ground strike location on moderately sloping terrain.

¹⁰ n=429. For the analysis, sample size was 353 in which the maximum slope angle is 50.6°.



Figure 27. ALTM ground strike location on steeply sloping terrain.

An azimuthal compass, interpretable to the nearest degree, determined slope aspects for each sampled laser strike. Each azimuth described the heading of an imaginary line from the laser strike running upslope. Compass readings were cognizant of the influences of metal objects, electronics, and bedrock outcroppings.

Chapter 4

Results and Discussion

Comparison of the ALTM-derived elevations to the GNSS-derived elevations used the following formulas:

$$Elevation_{Error} = Elevation_{ALTM} - Elevation_{Reference} \quad Eq. (6)$$

$$RMSE_{Elevation} = \sqrt{\frac{\Sigma(Elevation_{ALTM} - Elevation_{Reference})^2}{n}} \quad Eq. (7)$$

$$Standard\ deviation = \sqrt{\frac{\Sigma(x - \bar{x})^2}{(n - 1)}} \quad Eq. (8)$$

Normality of the ALTM-derived Elevations

Several studies showed that ALTM-derived elevation errors do not follow a normal distribution. Zandbergen, in 2008 and 2011, stated that the occurrence of non-normal distributions in high-resolution elevation data is widely recognized. He referred to the American Society for Photogrammetry and Remote Sensing guidelines for vertical accuracy reporting of ALTM data and the National Digital Elevation Program's guidelines for handling elevation data, which also acknowledge that data may not be normally distributed. Zandbergen indicated

that using RMSE to report error is not valid. Errors, even though few in number, that are major outliers heavily influence RMSE values. He endorsed the use of two commonly used techniques when data were non-normal: Report the RMSE based on the 95th percentile or trim the data to remove the outliers prior to performing statistical routines, which are dependent on normally distributed data. Oksanen and Sarjakoski (2006) and Zandbergen revealed that the non-normality of the errors is the result of using DTMs for comparisons. Although, Zandbergen implicated other factors, such as land cover and slope.

Misclassification of laser strikes can also lead to non-normality.

In this study, inclusion of the 66 misclassified laser strikes would have resulted in numerous outliers and a non-normal distribution. Descriptive statistics for 419 samples, including these 66, results in a maximum error of 7.783 m., a skewness of 3.48 and a kurtosis value of 22.5. Several tests of normality indicated significant non-normality with this dataset. Manual data trimming eliminated these 66 since ALTM elevations that were significantly higher than ground elevations. The trimming of data was subjective with the goal of removing the largest of the disparities.

Initial statistical analysis of ALTM elevation accuracy included the 353 sampled laser strikes. In subsequent exploration, two of the strikes served as undesirable leverage points and inhibited regression modeling. Rather than having some of the analyses with 353 strikes and some with 351, removal of these two points

made for direct comparisons among the results without the stipulation of different sample sizes.

Returning to the topic of non-normality of ALTM data, a histogram of the 351 sample points (see Figure 28), qualitatively shows the errors following a normal distribution. The errors resulting from subtracting the reference elevation from the ALTM-derived elevation for each sampled strike ranges from -0.618 m to 1.355 m. The frequency of error amounts, allotted into to 0.1 m bins, appears in the histogram whereby, the 0.1 to 0.2 m bin has the highest frequency. While the mean was not zero, the data still followed a typical normal distribution. Comparing the histogram to the normal curve in the figure, one bin is somewhat higher than the curve but overall, the rest of the bins are slightly above or below the normal curve. And, as per a normal distribution, the extreme differences in error had the lowest frequencies.

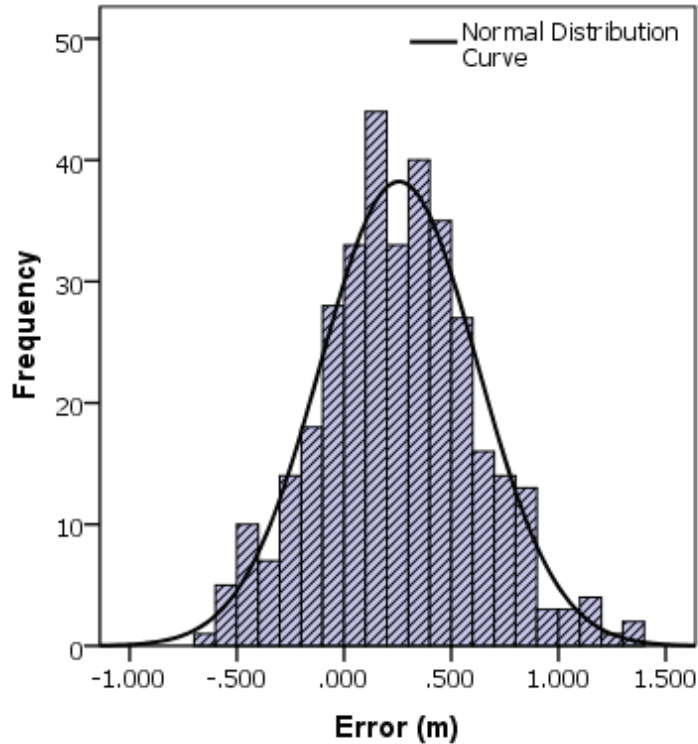


Figure 28. Histogram of the sampled ALTM ground strike vertical errors (n=351).

A box plot of the elevation differences also indicated normalcy (see Figure 29). The horizontal line in the middle of the shaded box, representing the median (0.247 m) of the data, is centered between the top of the box, representing the upper quartile (0.484 m), and the bottom of the box representing the lower quartile (0.009 m). This centering indicated a lack of skewness. Similarly, the box centered between the whiskers showed symmetry and not skewness. The relative location of the whiskers further indicated a lack of kurtosis. Similar to the histogram, the center of the boxplot aligns with an error greater than 0.000 m. The three circles above the top whisker in the boxplot indicated sampled strikes where the difference in elevations are greater than 1.5 but less than three times

the interquartile range (0.475 m). While typically deemed outliers when appearing outside the whiskers, evaluation of these strikes, coupled with subjective evaluation using the interquartile method maintained that these strikes are valid.

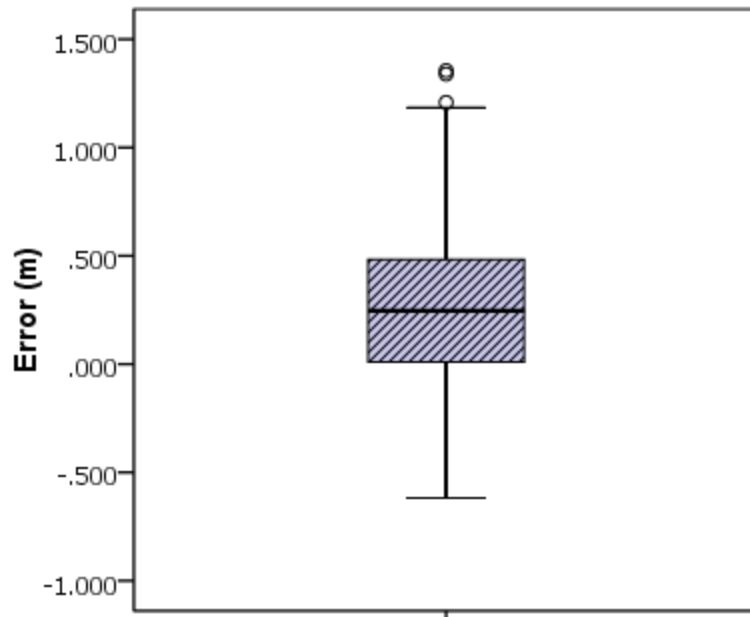


Figure 29. Boxplot of the sampled ALTM ground strike vertical errors (n=351).

Comparing numerical values, the closeness of the median to the mean of the dataset also supported that the data followed a normal distribution with little skewness (\bar{x} =0.257 m, median=0.247 m). The skewness value 0.152 (standard error 0.130) was low and close to 0.000 but indicated a slight positive skew. The calculated skewness z-score of 1.17 is less than 1.96, which indicated the result is not significant at the 95 percent confidence level. With negligible skewness,

calculations produced a kurtosis value of 0.094¹¹ (standard error 0.260). The kurtosis z-score of 0.362 is well below 1.96 and hence, not significant either. From these indicators, both skewness and kurtosis values appeared to signify normalcy and approximately symmetrical data.

The quantiles of observed errors of the sampled laser strikes, when plotted against quantiles of expected errors, show as circles in the Quantile-Quantile plot (see Figure 30). The arrangement of these circles to one another forms a fairly straight line. An imaginary line through these circles coincides with the line in the figure representing a very strong correlation between observed and expected and thus, normalcy. The lowest and highest quantiles of the error distribution deviate from what was expected. A positive skew typically has the lowest and highest quantiles on the right-hand side (or below) of the line and quantiles in the middle being to the left (or above) the line. The lowest and highest quantiles follow this pattern and may show the skewness mentioned earlier. However, the middle quantiles do not. It may be that the large number of sampled laser strikes occluded this portion of the skew being visible in the graph. Alternatively, it may be that those sampled strikes with the greatest error (both where ALTM elevations are higher than and lower than reference elevations) appear as outliers. Regardless, interpretation of the plot deemed the deviations as minor.

¹¹ For the statistical software used (Statistical Package for the Social Sciences 19 (SPSS) and GraphPad Prism 5), the kurtosis value of a Gaussian distribution is zero.

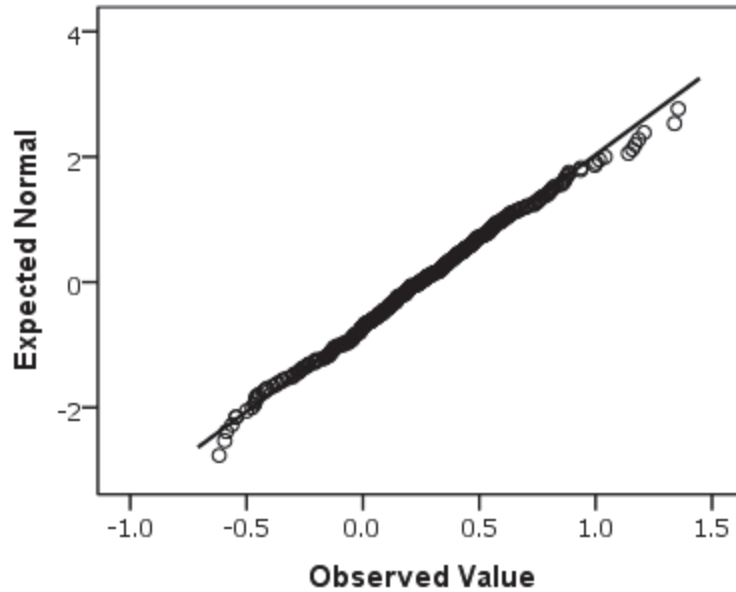


Figure 30. Quantile-Quantile plot of the sampled ALTM ground strike vertical errors (n=351).

Quantitative tests also demonstrated normalcy of the data. The D’Agostino – Pearson K2 test for normality, which assesses both skewness and kurtosis simultaneously, is not significant ($p = .446$). While substantiating the previous assessments, the result was unexpected as this test is subject to Type 1 errors. A Shapiro – Wilk test, another omnibus test, also indicated the data to be normally distributed ($p = .288$). This result was encouraging since this test is sensitive to minor outliers in large sample sizes. Lastly, the Jarque – Bera LM test, which typically has the lowest Type 1 error rate of the three with larger sample sizes indicated no significance ($p = .489$). It also tests for both skewness and kurtosis.

From these qualitative and quantitative evaluations, it appeared that the elimination of vegetative laser strikes, misclassified as ground strikes and the

avoidance of DTMs for comparative purposes results in a normal distribution of the ALTM-derived elevation errors.

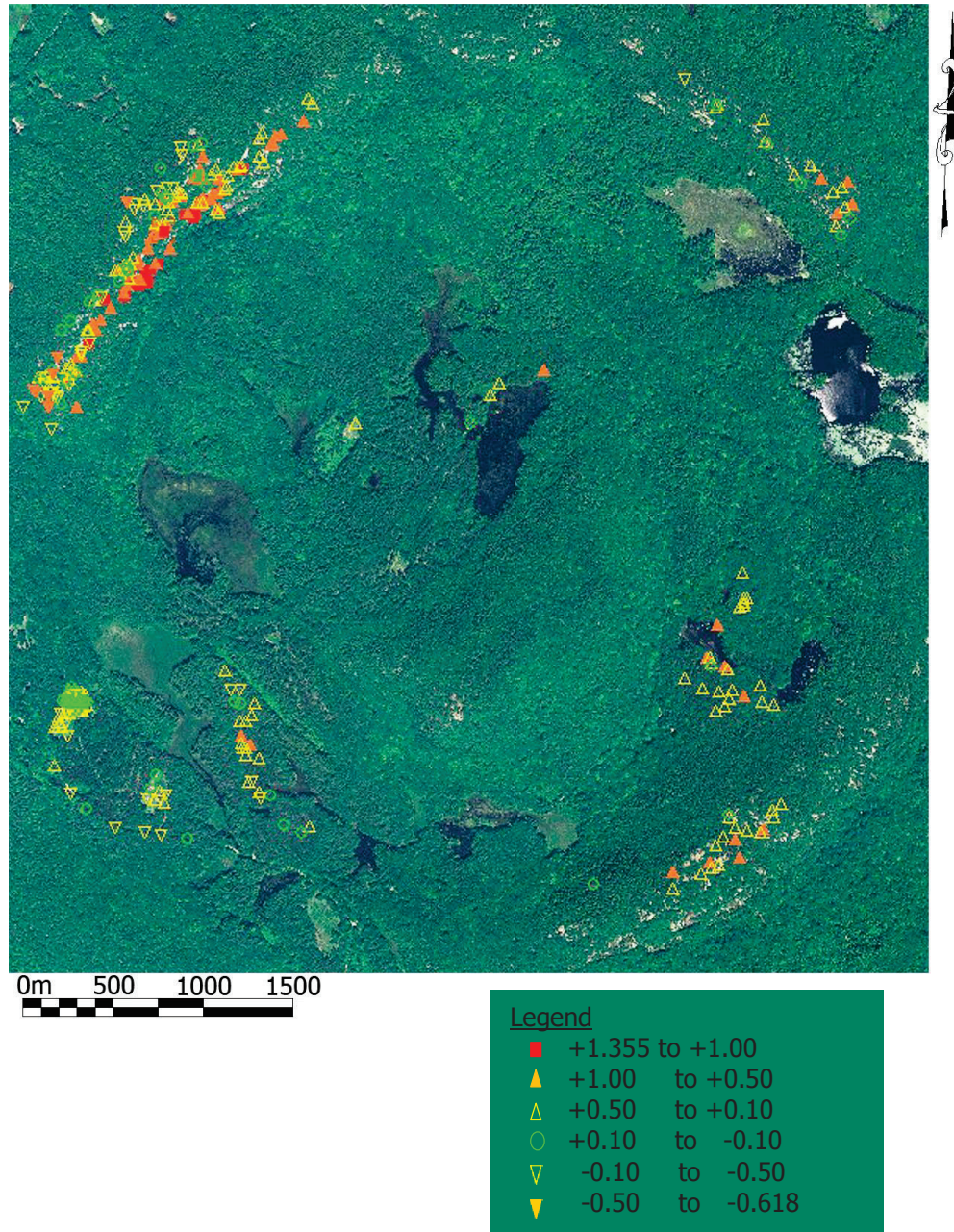


Figure 31. Plan view of the sampled ALTM ground strike locations with vertical errors coded by magnitude (n=351).

Figure 31 displays the 351 sampled strikes overlaid on an aerial photo and coded by the relative amount of error. From this figure, the magnitude of the errors are equally scattered about the four quadrants of the study site although, no occurrences of ALTM elevations less than reference elevations appear on or near South Mountain, in the southeast quadrant.

From Figure 31, it appeared that sampling occurred in only a few locales in the study area. As described in the section, Determination of Sample Size, sampling was limited to locations with open canopy for GNSS observations and no ground cover.

Since the mean error of all sampled elevations is positive ($\bar{x} = 0.256$ m, RMSE 0.446), the ALTM-derived elevations are on average, higher than the reference elevations. Indeed, 268 of the 351 sampled laser strikes are above reference elevations. For this dataset, the 95 percent confidence interval for the true mean ranges from 0.218 to 0.294 m (± 0.038 m). This mean error indicated that a bias exists in the ALTM system such that it overestimates elevations.

Flat Terrain ALTM Vertical Errors and Block Correction

Based other accuracy assessment studies, ALTM elevation quality can be determined by comparing ALTM and reference elevations on relatively flat terrain.

In this study, 85 ALTM laser strikes are on slopes less than five degrees. The mean elevation error of these 85 strikes is 0.158 m with a 95 percent confidence interval from 0.094 to 0.222 m (± 0.064 m, RMSE 0.336). While this mean is lower than the mean for all the sampled strikes, the confidence interval is larger. This larger interval could be due the difference between sample sizes (85 versus 351). For strikes on slopes less than five degrees error ranges from -0.563 m to 0.871 m.

This mean value of 0.158 m with the likely range of 0.094 to 0.222 m represents the inherent errors in both the ALTM system and the Topcon Positioning Systems HiPer Lite Plus GNSS used to develop reference elevations. From previous discussions, systematic error and biases exist in ALTM elevations due to accuracy losses in each component of the system: GNSS, IMU, LiDAR, oscillating mirror, boresight alignment, etc. Correspondingly, the Topcon Positioning Systems GNSS has errors due to satellite configurations, limitations in atmospheric modeling, etc. This error value is comparable to the findings on level terrain of others. Figure 32 displays the histogram for each of the 85 laser strikes on slopes less than five degrees in which the bins are again 0.01 m wide and where the frequency of error is centered about 0.158 m.

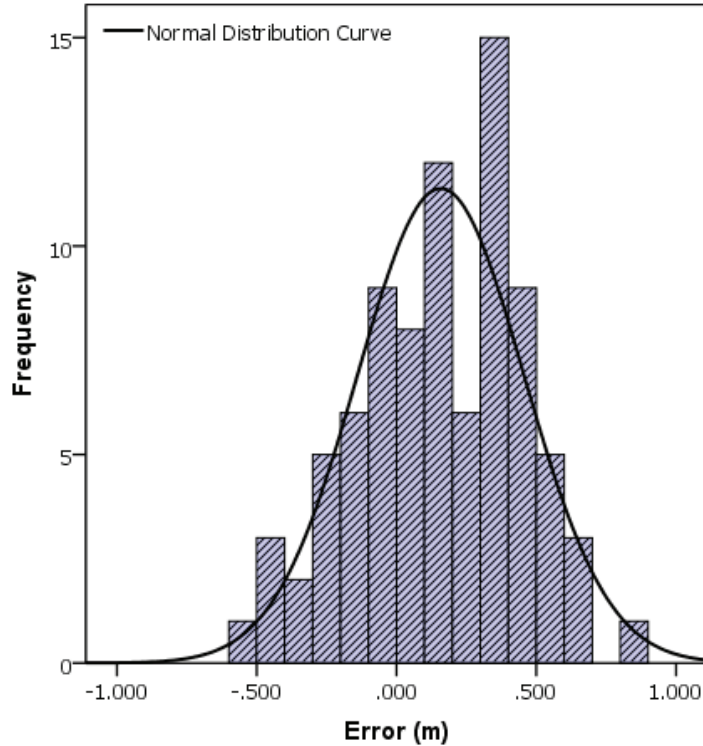


Figure 32. Histogram of the sampled ALTM ground strike vertical errors for slopes less than 5° (n=85).

The second column in Table 3 lists the descriptive statistics for these laser strikes on level terrain. While the mean error of 0.158 m is comparable to other studies, the standard deviation for these 85 points (0.298) is larger than others including Goulden (2009), who observed a standard deviation of 0.111 m for 65 strikes in a flat parking lot. These results were surprising given the rather small scan angles of this study: The 85 scan angles averaged 12°12'48" with a range of 0°12'09" to 21°24'53"¹². The rather low scan angles should have curtailed

¹² Scan angle calculations were based on the assumption that the aircraft flew along a straight path at a constant height of 4907 m over the study site.

imprecisions compared to other studies with higher scan angles. This reasoning came from studies such as Baltsavias (1999a), Airborne 1 (2001), Ahokas et al. (2003), Schaer et al. (2007), and Ussyshkin et al. (2009) who found larger elevation errors as scan angle increases (see the section, Scanning Mirror Unit). Possibly other factors, such as large range values and/or the considerably higher flying height of this study, is responsible. As presented in the section, Flying Height Influence on ALTM Errors, the laser signal is subject to degradation by temperature and aging with higher AGLs.

Table 3
Descriptive Statistics of the Sampled ALTM Ground Strike Vertical Errors for Slopes less than 5°

| | Uncorrected | After Block Correction |
|----------------------------------------------------|----------------|------------------------|
| No. of Samples | 85 | 85 |
| Mean Signed Error (m) | 0.158 | 0.000 |
| Confidence Limits (95%) for signed mean error | 0.094 to 0.222 | -0.064 to 0.064 |
| Median Error | 0.148 | -0.010 |
| RMSE | 0.336 | 0.296 |
| Standard deviation | 0.298 | 0.298 |
| Max. ALTM elevation below Reference elevation | -0.563 | -0.721 |
| Max. ALTM elevation above Reference elevation | 0.871 | 0.712 |
| Count: ALTM elevation below Reference elevation | 26 | 44 |
| Count: ALTM elevation above Reference elevation | 59 | 41 |
| Mean Absolute Error | 0.278 | 0.243 |
| Confidence Limits (95%) for mean absolute error | 0.237 to 0.319 | 0.207 to 0.280 |
| Minimum Absolute Error | 0.000 | 0.003 |

As noted by others (see the section, ALTM Vertical Accuracies on Sloping Terrain), the relationship between increasing slopes and increasing vertical error is not visible on low angle slopes. This study concurs with these findings as seen in Figure 33 which shows only strikes on slopes less than five degrees. Although a contrarian discovery appeared in the form of a slightly downward linear trend as slope increase from zero to five degrees. However, a linear regression model could not be developed for this relationship as the coefficient of determination was quite low ($R^2=0.0021$) and the model was not found to be significant ($p = .677$).

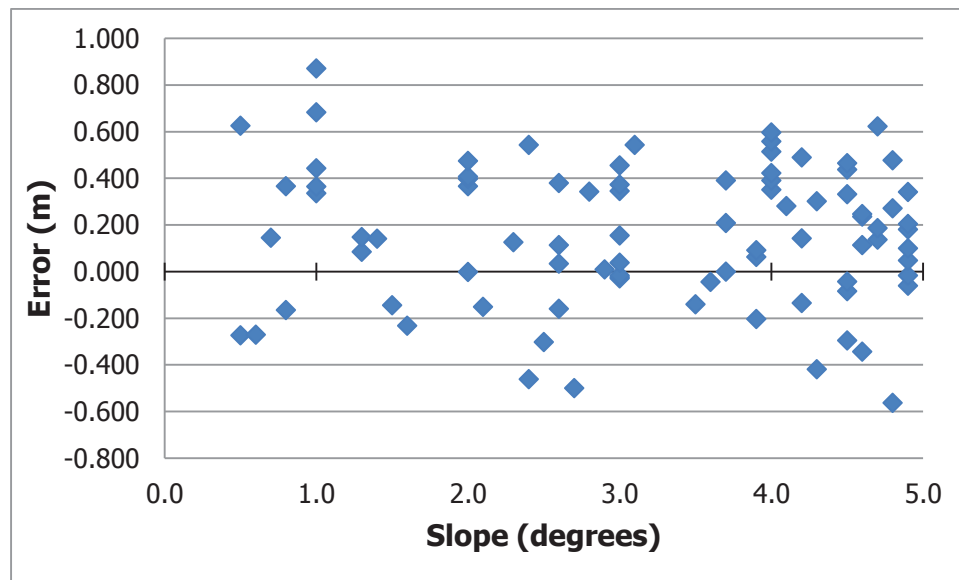


Figure 33. Scatterplot of the sampled ALTM ground strike vertical errors for slopes less than 5° prior to block correction ($n=85$).

Returning to bias, Bowen and Waltermire (2002), Montané and Torres (2006), Stewart et al. (2009), Goulden (2009), and others examined ALTM system bias

and developed error constants by using the mean elevation difference between ALTM-derived elevations and reference data on relatively flat terrain. Employing their methods, the mean error of 0.158 m was subtracted from all of the ALTM-derived elevations.

By removing this bias, the elevations of the 85 ALTM laser strikes on slopes less than five degrees then ranged from -0.721 m to 0.712 m. The RMSE lessened to from 0.336 m to 0.296 m as shown in the third column of Table 3. Table 4 lists the statistics for all 351 sampled strikes both before and after the correction. The mean elevation error then became 0.098 m with the 95 percent confidence interval ranging from 0.060 m to 0.136 m. The RMSE dropped to 0.379 (from 0.446), the maximum error where the ALTM-derived elevation was below the reference elevation became -0.776 m, and the maximum error where the ALTM-derived elevation was above the reference elevation changed to 1.197 m. The number of laser strikes with elevations higher than reference elevations then dropped to 206 out of 351 (down from 268).

Table 4
Descriptive Statistics of the Sampled ALTM Ground Strike Vertical Errors (n=351)

| | Uncorrected | After Block Correction |
|----------------------------------------------------|----------------|------------------------|
| No. of Samples | 351 | 351 |
| Mean Signed Error (m) | 0.256 | 0.098 |
| Confidence Limits (95%) for signed mean error | 0.218 to 0.294 | 0.060 to 0.136 |
| Upper Quartile | 0.484 | 0.326 |
| Median Error | 0.247 | 0.089 |
| Lower Quartile | 0.010 | -0.148 |
| RMSE | 0.446 | 0.379 |
| Standard deviation | 0.366 | 0.366 |
| Max. ALTM elevation below Reference elevation | -0.618 | -0.776 |
| Max. ALTM elevation above Reference elevation | 1.355 | 1.197 |
| Count: ALTM elevation below Reference elevation | 83 | 145 |
| Count: ALTM elevation above Reference elevation | 268 | 206 |
| Mean Absolute Error | 0.355 | 0.297 |
| Confidence Limits (95%) for absolute mean error | 0.327 to 0.384 | 0.272 to 0.322 |
| Mean Absolute Deviation | 0.290 | 0.290 |
| Minimum Absolute Error | 0.000 | 0.002 |

While these statistical values in Table 4 were interesting, they have little merit as they summarize the sampled data as a whole, regardless of degree of slope. Thus, averaging of all elevation errors is not particularly meaningful.

Influence of Sloping Terrain on ALTM-derived Elevations

Table 5 shows the results of allocating the vertical error in slope strata:.

Table 5

Descriptive Statistics of the Sampled ALTM Ground Strike Vertical Errors by Slope Strata

| | Slope Category | | | | |
|-------------------------------------------------------|--------------------|--------------------|--------------------|-------------------|-------------------|
| | 0.0-4.9° | 5.0-9.9° | 10.0-19.9° | 20.0-29.9° | 30+° |
| No. of Samples | 85 | 91 | 91 | 48 | 36 |
| Mean Signed Error (m) | 0.000 | 0.000 | 0.019 | 0.275 | 0.540 |
| Confidence Limits (95%) for signed mean | -0.064 to 0.064 | -0.051 to 0.050 | -0.047 to 0.085 | 0.149 to 0.402 | 0.407 to 0.674 |
| RMSE | 0.296 | 0.241 | 0.316 | 0.511 | 0.666 |
| Standard deviation | 0.298 | 0.243 | 0.317 | 0.435 | 0.394 |
| Max. ALTM elevation below Reference elevation | -0.721 | -0.634 | -0.745 | -0.776 | -0.285 |
| Max. ALTM elevation above Reference elevation | 0.712 | 0.499 | 0.603 | 0.883 | 1.196 |
| Count: ALTM elevation below Reference elevation | 44 | 43 | 41 | 13 | 4 |
| Count: ALTM elevation above Reference elevation | 41 | 48 | 50 | 35 | 32 |
| Sign. From 0.000 ($p < 0.05$) | 1.000 | 0.988 | 0.566 | 0.000 | 0.000 |
| Mean Absolute Error | 0.243 | 0.195 | 0.252 | 0.451 | 0.590 |
| Confidence Limits (95%) for mean absolute error | 0.207 to 0.280 | 0.165 to 0.225 | 0.212 to 0.292 | 0.381 to 0.522 | 0.484 to 0.696 |
| Minimum Absolute Error | 0.003 | 0.012 | 0.002 | 0.012 | 0.043 |

Note. These values are subsequent to the block correction.

The second column of Table 5 is identical to the third column of Table 3 for the 85 sample strikes on terrain slopes less than five degrees. The RMSE of this slope class (0.296) is less than for all 351 sampled strikes (0.379). This lower RMSE was expected since most of the pertinent literature indicated greater error

with higher slopes. Of interest though, was that the mean error of the next slope class (5.0 to 9.9 degrees) is also 0.000 m and has both smaller confidence interval and RMSE values. Compared to the less than five degrees slope stratum, the confidence range shrank by 21 percent while the RMSE is nineteen percent smaller. This decrease in RMSE is contrary to the findings of several other studies (e.g., Hodgson et al., 2003; Hodgson et al., 2005; Hollaus et al., 2006; Xhardé et al., 2006) which noted greater error as slope increases from zero to ten degrees. Hodgson et al., in 2003, noted RMSE essentially doubles as slopes of zero to two degrees increases to eight to ten degrees. In 2005, Hodgson et al. again found error significantly increases as slope increases for terrain covered by low grass. Xhardé et al. (2006) found that a linear correlation exists between RMSE and terrain slope.

With regards to accuracy only, H. Hyypä et al. (2005) commented that ALTM elevation accuracy deteriorates gradually with increasing slope. Peng and Shih (2006) remarked that a linear correlation between vertical error and slope. Both studies found that ALTM-derived elevations were higher than actual. Su and Bork (2006) found that signed error does not increase proportionately to slope but absolute vertical errors and RMSE do. Hodgson et al. (2003) described the relationship between absolute error and slope as a consistent monotonic relationship. From Table 5, the mean absolute error values in this study, do not increase and appear to have decreased slightly.

Comparison between the other slope strata found: mean error, absolute mean error, and RMSE increase as slope increases (see Table 5). The RMSE value increases 31 percent, between the 5.0 to 9.9 degree and the 10.0 to 19.9 degree strata, then by 61 percent between the 10.0 to 19.9 degree and the 20.0 to 29.9 degree strata. The change between the 20.0 to 29.9 degree and 30-degree and above strata is 30 percent. Error increases as slope increases are similar to findings by Lemmens (1997), Huising and Gomes Pereira (1998), and Kraus and Pfeiffer (1998) where vertical error is strongly related to slope. These studies also found that ALTM overestimated elevations. Interestingly, Reutebuch et al. (2003), in their analysis comparing an ALTM-derived DTM to total station reference data, did not find any correlation between elevation error and slopes ranging from zero to 40 degrees.

Goulden (2009), the only other significant study with largish sample numbers on steep slopes, found mean vertical errors of -0.13 m (SD 0.27, $n < 165$) on one of his sites with slopes greater than fifteen degrees. This data was also block corrected. Goulden found laser strikes under reporting elevations, which is contrary to the other studies mentioned in the preceding paragraphs (i.e., H. Hyypä et al. 2005; Peng & Shih, 2006; Lemmens, 1997; Huising & Gomes Pereira, 1998; Kraus & Pfeiffer, 1998).

In this study, mean error for slopes greater than fifteen degrees is 0.448 m (RMSE 0.627, $n = 118$) prior to any correction. Bias correcting using the mean signed error for all 351 strikes ($\bar{x} = 0.256$ m) yielded a mean error of 0.192 m

(RMSE 0.479) for slopes greater than fifteen degrees. Standard deviation remains unchanged, regardless of bias correction (SD 0.441). Comparing this study to Goulden's, the mean signed error in this study was higher, but more significant was that the standard deviation was nearly double that of Goulden's.

Goulden had a second site where slopes were twenty degrees and greater.¹³ Here, he observed a vertical error of 0.26 m (SD 0.24, n=61). The mean error for slopes greater than twenty degrees in this study is 0.547 m (RMSE 0.698, n=84) prior to any correction for bias. After subtracting the mean error of 0.256 m from the ALTM-derived elevations for all 351 strikes, the mean error on slopes twenty degrees and greater became 0.291 m. After the correction, RMSE drops to 0.522 m, while the standard deviation remains the same at 0.436 m.

Compared to Goulden's second study site, the vertical error was essentially identical while again, the standard deviation was nearly double. The precisions of Goulden's findings are much higher than in this study. Possibly, due to the higher flying height of this study and longer range values, the errors are greater.

Investigation of these factors appears in forthcoming sections.

In this study, further testing between slope strata included an independent samples *t*-test to determine if the mean error of each stratum was statistically different from 0.000 m. Clearly, the first two slope categories are not. Nor is the

¹³ Slope values of fifteen and twenty degrees were derived by scaling off scatterplots in Goulden's report.

10.0 to 19.9 degree category ($p = .566$). The confidence limits also indicated no significant difference as the range between the limits encompasses 0.000 m. This finding was enlightening since many studies found or predicted greater error on slopes steeper than ten degrees (e.g., Clark et al., 2004; Xhardé et al., 2006).

An ANalysis Of VAriance (ANOVA) tested the homogeneity between strata by comparing mean values for equality. First, Levine's test evaluated homogeneity between variances of the strata. This test indicated that variances (i.e., the standard deviations) between the slope strata are not that similar, and significantly so ($p = .000$). The 5.0 to 9.9 degree slope stratum has the lowest standard deviation (0.243) and the 20.0 to 29.9 degree stratum has the highest (0.435). This difference amounts to the latter stratum having more than three times the variation of the lower slope stratum. Similar variances between strata are a requirement for an ANOVA. However, a significant result of Levine's test does not negate the use of an ANOVA as the latter is robust to some non-normalities but it can cast doubt on the ANOVA's outcome. As an alternative, this analysis used Welch F and Brown-Forsythe F tests. Both of these tests are more robust than Levine's test when groups are unequal in size. These tests provide a substitute to calculate the requisite F-ratio typically found using an ANOVA. Both of these tests (along with the ANOVA), indicated a significant difference between the slope strata ($p = .000$ for all three tests). A post hoc test (Games-Howell¹⁴)

¹⁴ Games-Howell was used since the variances between the slope strata were not equal.

identified the significant differences between strata. Shown in Table 6, the mean error on slopes greater than 30.0 degrees is significantly different from all other slope categories. The same held true for the 20.0 to 29.9 degree category. No significant differences exist between the strata for slopes less than 20.0 degrees.

Table 6
Significance Levels for the Sampled ALTM Ground Strike Vertical Errors Between Slope Strata

| | Slope Category | | | |
|------------|----------------|----------|------------|------------|
| | 0.0-4.9° | 5.0-9.9° | 10.0-19.9° | 20.0-29.9° |
| 5.0-9.9° | 1.000 | | | |
| 10.0-19.9° | 0.994 | 0.990 | | |
| 20.0-29.9° | 0.002 | 0.001 | 0.005 | |
| 30.0°+ | 0.000 | 0.000 | 0.000 | 0.036 |

H. Hyypä et al. (2005) stated that inaccuracy increases gradually as slope increases from zero degrees, then increases more dramatically for slopes greater than fifteen degrees. This study appeared to confirm this relationship. However, as presented previously, elevation inaccuracy does not increase until slopes reach ten degrees or more, based on the slope strata.

Interestingly, Hodgson and Bresnahan (2004) predicted that inaccuracies on slopes greater than 25 degrees are two times greater than on slopes less than four degrees. In this study, inaccuracy on slopes zero to four degrees is 0.139 m (RMSE 0.330; before block correction) while inaccuracy on slopes greater than 25 degrees is 0.647 m (RMSE 0.761). This increase between the two slope strata

is nearly five-fold; significantly greater than the factor of two estimated by Hodgson and Bresnahan.

Lastly, from Table 5, as slopes increase beyond ten degrees, values describing error spread (e.g., standard deviation, maximum, and minimum values) tend to increase as slope increases. An increase in error spread indicates a loss in precision. This change is similar to Su and Bork (2006) who observed an increase in variability as slope increases. However, similar to RMSE, there is less variation in the 5.0 to 9.9 degree stratum compared to the 0.0 to 4.9 degree stratum (SD 0.298 versus 0.243, respectively). This represents an eighteen percent drop. Additionally, a nine percent drop occurs between the 20.0 to 29.9 degree and the 30-degree and above strata (SD 0.435 and 0.394, respectively). The lower value in the 30-degree and above stratum may be the result of fewer sample numbers. However, the true reasons for these are unknown.

Temporarily ignoring the slope strata, a scatterplot of vertical error against slope showed a positive relationship between the two (see Figure 34). The correlation coefficient is 0.467 (r).

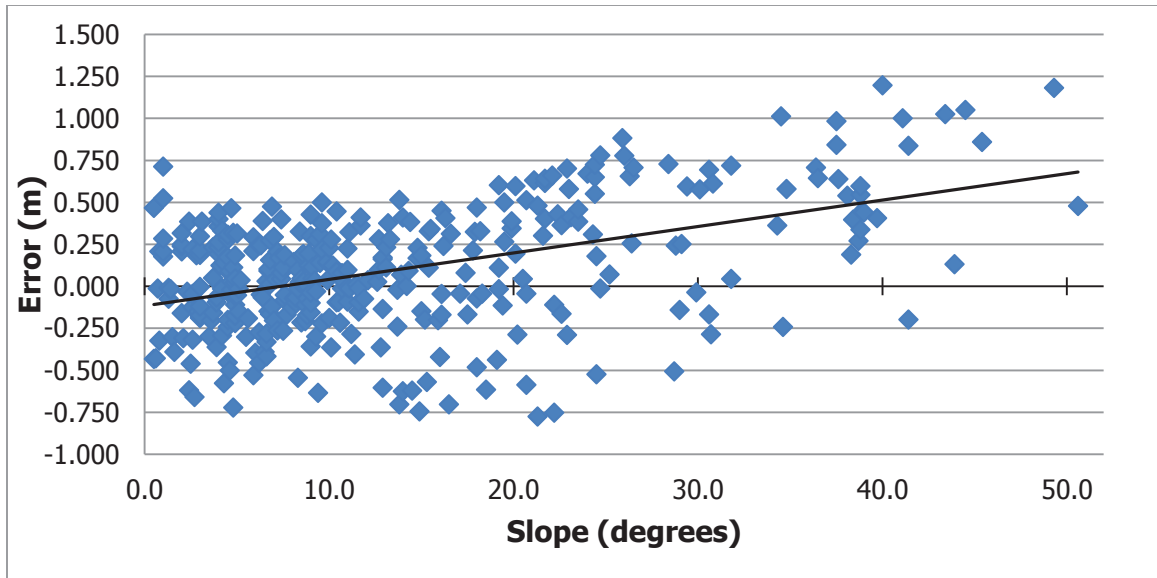


Figure 34. Scatterplot of the sampled ALTM ground strike vertical errors for all slopes (n=351).

Using inferential statistics to plot a linear line through the 351 sampled laser strikes via a least squares fit, yielded:

$$\text{Vertical error} = 0.016 \cdot \text{Slope} - 0.117 \quad \text{Eq. (9)}$$

The ANOVA for this model indicated that the line significantly fit the data and the t -test of the slope coefficient indicated that the slope is significantly different from 0.000 ($p = .000$ for both). However, by evaluating the line in Figure 34 qualitatively, it was apparent that the line did not truly represent the relationship. The proportion of common variation (i.e., strength) typically described by the coefficient of determination value for the line is rather low ($R^2 = 0.218$), meaning that only 21.8 percent of the error can be explained by slope. The standard error of the estimate was quite high at 0.324. This latter statistic represents the

variability between the observed vertical error and the value predicted by the model (the line) for each observed slope value. This statistic is the equivalent of RMSE for regression modeling.

While the ANOVA indicated this model is highly significant, it only stipulates that the model is an improvement over using a line with no slope and a y-intercept of 0.098 (mean of all sample strikes). Baltasvias (1999a) indicated that the relationship between increasing error and slope is not linear and in this study, this relationship appeared to hold true.

Fitting a curvilinear line to the data provided for a slightly better fit with an R^2 value of 0.238. The ANOVA associated with this curve also indicated that the model resulted in a significantly better prediction than if only the mean value was used ($p = .000$). The coefficient of x^2 term, where x^2 represents slope squared, also had a significant t -test value ($p = .000$). The quadratic equation for this line is:

$$\text{Vertical error} = 0.0004 \cdot \text{Slope}^2 + 0.0005 \cdot \text{Slope} - 0.024 \quad \text{Eq. (10)}$$

Figure 35 depicts this curve, where the plot of laser strikes is the second-order polynomial line has replaced the linear regression line of Figure 34. The improvement by using a quadratic formula model amounts to a slight increase in the coefficient of determination of nine percent. However, a Ramsey REgression Specific Error Test (RESET) used to compare the two models, indicated that predictor variables of the quadratic equation (i.e., slope and slope squared)

significantly provides for a better model than the single predictor (i.e., slope) of the linear model.

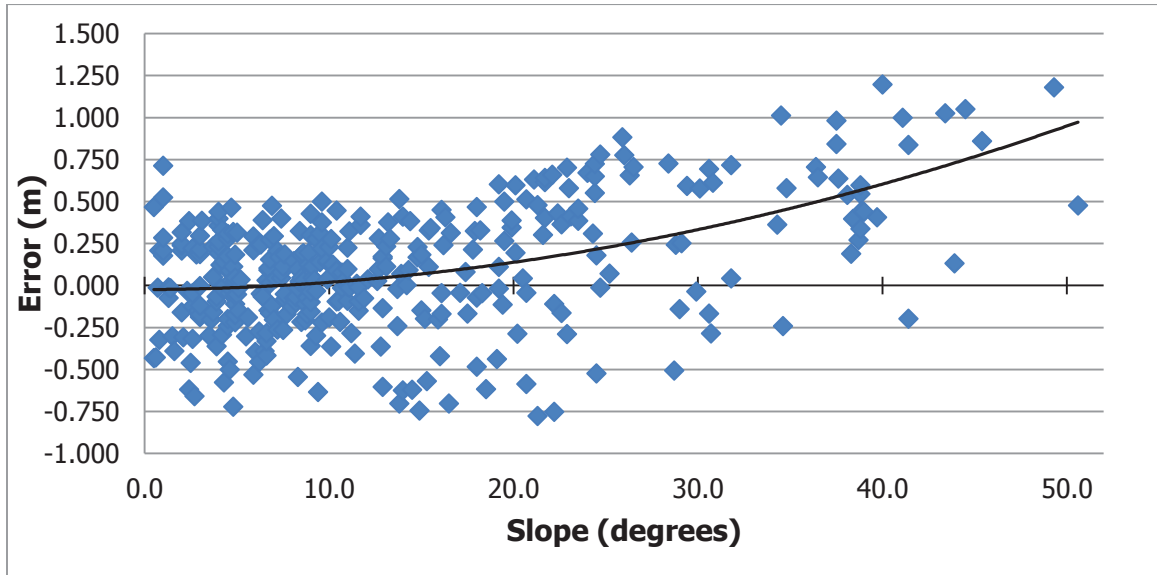


Figure 35. Scatterplot of the sampled ALTM ground strike vertical errors for all slopes fitted with curvilinear line (n=351).

Again, this finding was contrary to Peng and Shih (2006) who observed a linear correlation. Xhardé et al. (2006) also found the relationship to be linear although, they had created a model using RMSE values.

While the fit of a curvilinear model is slightly improved, the relationship is loose as there are many sampled strikes away from the line. The standard error of the estimate is 0.321; an insignificant improvement over the linear model (0.324). The R^2 value of 0.238 indicates slope only accounts for 23.8 percent of the error. From the high standard error of the estimate and the low R^2 value, this model lacks the ability to use slope values to predict ALTM elevation error.

Further examination of the relationship between ALTM elevations and slope used a scatterplot of absolute error. Absolute errors can be beneficial in identifying trends. In this study, an upward trend between absolute error and slope was readily apparent (see Figure 36).

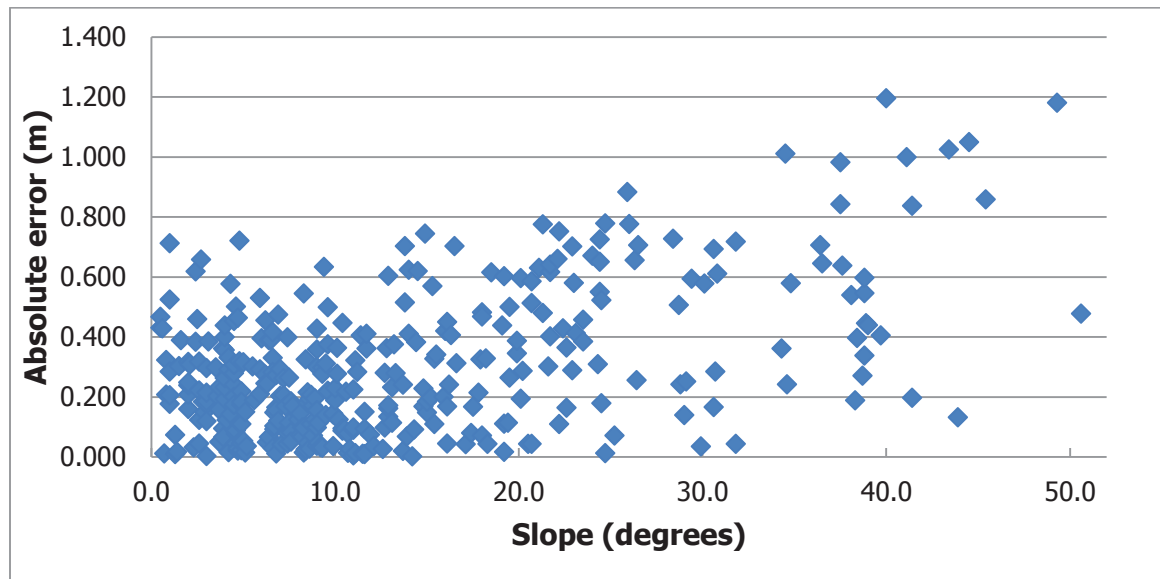


Figure 36. Scatterplot of the sampled ALTM ground strike absolute vertical errors for all slopes (n=351).

These results do agree with Su and Bork (2006), who found absolute vertical errors and RMSE increases proportionately to slope, and with Clark et al. (2004) where very steep slopes have the largest overestimation of error.

The findings did not fully concur with other studies such as Hollaus et al. (2006), who indicated that RMSE increases rapidly as steepness of terrain increases. In this study, signed error RMSE does increase as slope increases, but not

dramatically so, as visible in Figure 35 and Table 5. However, RMSE does increase more substantially with absolute errors as evidenced in Figure 36.

The findings also appeared to concur with those of Kobler et al. (2007) and Goulden and Hopkinson (2010) whereby, the rising side of the footprint is responsible for the range measurement and hence, elevation. This relationship is also evident by the counts where larger numbers of strikes had positive vertical errors (see Table 5). This observation then, disagreed with findings of Baltsavias (1999a), Glennie (2007), and Ussyshkin et al. (2009) where the reflective material or other element responsible for the range measurement may be situated anywhere in the footprint. Similarly, it appeared to disagree with Jutzi and Stilla (2003), Johnson (2009), and Ussyshkin et al.'s (2009) work that sloping terrain would result in a delay of the laser signal, resulting in a longer than actual range measurement and lower than actual elevation.

While this information provided some definitive information on the relationship of elevation errors to increasing slope, several other factors that affect and interplay with slope needed examination.

Influence of Scan Angle on ALTM-derived Elevations

As highlighted previously, Airborne 1 Corporation (2001), Schaer et al. (2007), Ussyshkin et al. (2009), and Goulden and Hopkinson (2010) found a direct relationship between ALTM-derived elevations and scan angle. As scan angle increases, so does vertical error. Ahokas et al. (2003) stated that random errors

generally increase as scan angle increases, although their own findings were contrary to this assertion.

Interestingly, Su and Bork (2006) found evidence to the contrary where elevation errors are greater with the laser pointed within three degrees of nadir.

In this study, an inspection of the sampled strikes plotted against scan angle indicated no obvious relationship (see Figure 37). What was apparent from the figure is the clustering of laser strikes. This grouping is due to the limited locations of open canopy needed for the field GNSS work. Apart from the groupings, the only other pattern observed may be a higher dispersion in error with scan angles greater than fifteen degrees. Scan angles for all the sampled laser strikes range from $0^{\circ}01'21''$ to $22^{\circ}15'57''$ ($n=351$)¹⁵.

¹⁵ Scan angles were calculated based on assumption that the aircraft flew along a straight path at a constant height of 4907 m over the study site.

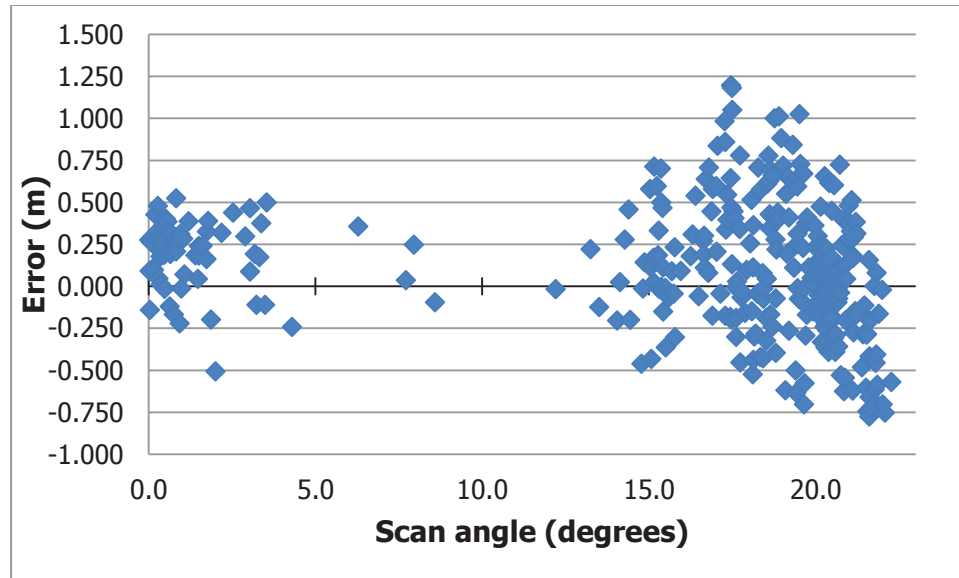


Figure 37. Scatterplot of the sampled ALTM ground strike vertical errors for all scan angles (n=351).

Due to finding a relationship between slope and error, slope was removed from further scan angle analysis by using only samples with slopes less than ten degrees. One form of comparison was the scatterplot displayed in Figure 38. This figure appeared to be essentially Figure 37 but with fewer samples.

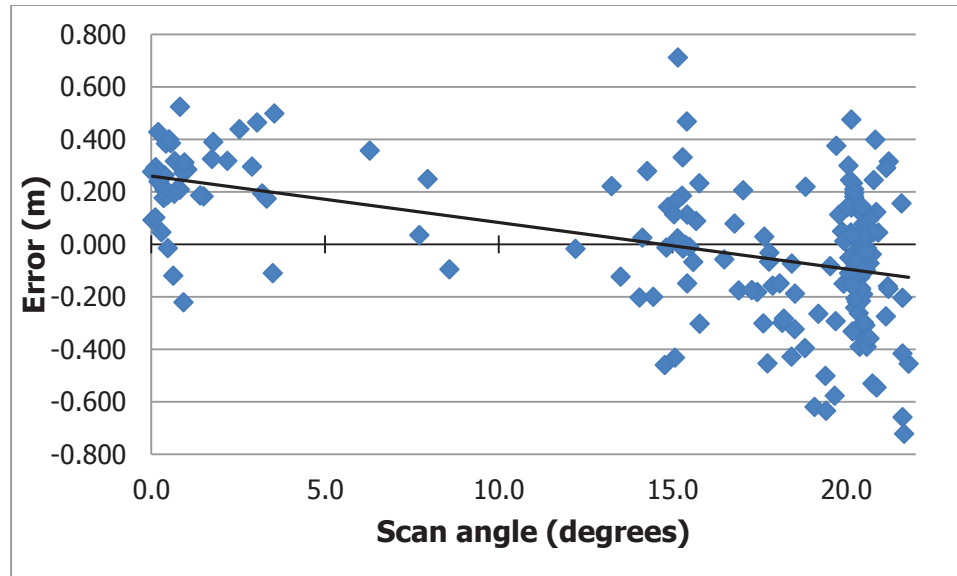


Figure 38. Scatterplot of the sampled ALTM ground strike vertical errors for all scan angles on slopes less than 10° (n=176).

From this figure, the laser strikes near nadir have higher signed vertical error than those laser strikes with scan angles of fifteen degrees or more. In this instance, signed error indicates the directionality of errors. The linear regression line developed to model this is shown in the figure and is an improvement over using the mean based on an ANOVA ($p = .000$). The t -test of the coefficient is also significant ($p = .000$).

$$\text{Vertical error} = -0.018 \cdot \text{Scan angle} + 0.261 \quad \text{Eq. (11)}$$

However, the model is not a particularly good fit ($R^2=0.258$, standard error of the estimate=0.366).

The line aided though, in seeing that the signed mean of strikes with low scan angles is greater than the signed mean error of the strikes with scan angles

greater than twenty degrees. The x-intercept of the line is approximately 14.5 degrees.

The signed mean error of strikes with scan angles less than five degrees (on slopes less than ten degrees) is 0.239 (RMSE 0.289, n=39). This mean indicated that the ALTM-derived elevations for most of these strikes are higher than the reference elevations. By comparison, the signed mean error for those strikes with scan angles greater than eighteen degrees is -0.104 m (RMSE 0.274, n=94).

This finding agreed with Jutzi and Stilla (2003), Johnson (2009), and Ussyshkin et al.'s (2009) work whereby, a tilted surface lengthens the received signal at the LiDAR unit, delaying recognition of signal resulting in a longer range. This observation, in turn, contradicts Kobler et al. (2007) and Goulden and Hopkinson (2010) who noted that the rising or leading edge of the footprint is responsible for a shorter than actual range and thus, a higher than actual elevation. The propensity of negative error values as scan angle increases is indicative of range values being longer than what they should be.

A scatterplot of absolute errors (see Figure 39) showed similar results. The absolute mean error of the strikes with scan angles less than five degrees is 0.263 (RMSE 0.289, n=39). The absolute mean error for those strikes with scan angles greater than eighteen degrees is 0.217 m (RMSE 0.274, n=94).

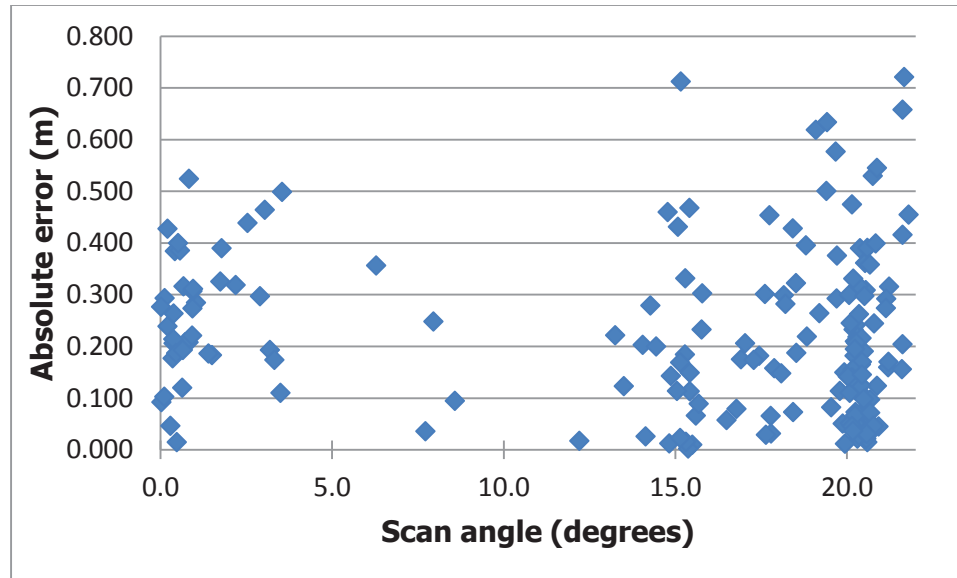


Figure 39. Scatterplot of the sampled ALTM ground strike vertical absolute errors for all scan angles on slopes less than 10° ($n=176$).

Su and Bork reasoned that a higher error value at nadir was due to extreme errors caused by outliers, as the top five errors near nadir were 23 times larger than their overall errors. In this study, extreme outliers had been removed previously. One possible reason may be the disparity between the numbers of sampled laser strikes. Specifically, the low number for scan angles less than five degrees. It may be that a larger number of samples would result in mean values similar to strikes with higher scan angles. Another reason may be that laser beam, when directed at nadir, may have a higher incidence of striking ground vegetation since flat deciduous leaves are normal to the laser beam with more surface area, increasing the probability of intercepting the beam. When the beam is pointed off-nadir, it may have a larger likelihood of angling underneath leaves and striking the ground. Ni-Meister, Jupp, and Dubayah (2001) as part of their

study on forest profiling using waveform LiDAR, found that leaf orientation and shape influence accuracy. Similarly, branches of evergreen trees may act the same way to intercept the laser beam when it originates overhead. In this study however, the reason for higher elevation error at nadir was unknown, as careful evaluation of laser strike locations eliminated any sampling where ground cover could have been a factor.

Revisiting the block correction performed earlier to eliminate the systematic bias, the most appropriate sampled laser strikes to use should have been those on flat to gently sloping terrain (slopes $<5^\circ$) and with low scan angles. In this study, due to the unexpected higher errors associated with low scan angles, this would have been problematic. The mean error for this grouping is 0.248 m (RMSE 0.290, $n=25$). This value is 0.090 m higher than the block correction based on slope alone (0.158 m). More so, the sample size is rather small ($n=25$). This diminutive sample set, coupled with the contradictory findings of scan angle errors, resulted in using only the slope angle criterion to determine system bias.

Influence of Flying Height on ALTM-derived Elevations

Compared to the AGLs of other studies, the AGL of 4907 m of this study is higher than most. Flying heights of other studies from the literature review ranged from 70 m (Huisling & Gomes Pereira, 1998) to 2400 m (Hodgson et al., 2003). Only one other study has an AGL above 2400 (3657 m. Hodgson et al. (2005)). As presented in the section, Flying Height Influence on ALTM Errors, the high AGL

used in this study would appear to incur relatively more error than other studies. Summarizing, Goulden (2010) found that errors and impreciseness of angular measurements (e.g., IMU, scan angle) result in increases in planimetric and vertical error. Glennie (2007) also documented that angular errors increase proportionally to an increase in AGL. Ahokas et al. (2003) found that the higher the altitude, the larger the error in ALTM-derived elevations. Triglav-Čekada et al. (2009) found a range difference of six centimeters between measurements made at sea level and those at 2000 m.

Since this study area was mapped only once, there is no additional ground elevation data from a different AGL. Therefore, no comparisons could be made between ALTM-derived elevations and different flying heights. Nevertheless, because AGL influences other factors, studying these other factors provided insight in the effects of a high AGL.

Influence of Horizontal Inaccuracy on ALTM-derived Elevations

A higher flying height results in greater planimetric error that, in turn, can produce greater elevation error on sloping terrain. Previous explanation of these linkages can be found the sections, Flying Height Influence on ALTM Errors, ALTM Horizontal Accuracies, and Effect of Horizontal Error on Vertical Error.

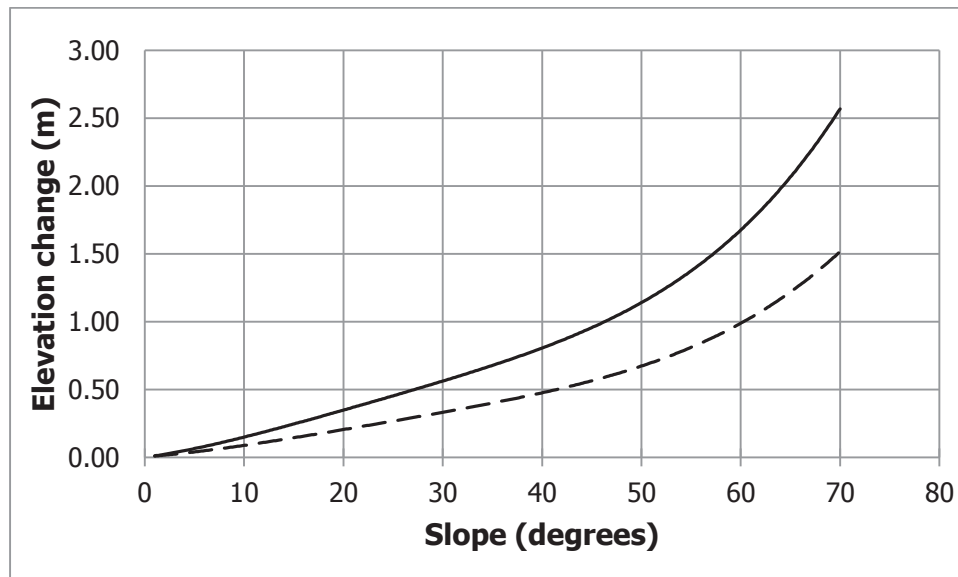
As depicted in *Figure 6*, Profile view of change in elevation due to horizontal displacement and the accompanying formula (see equation (3)), the greater the

error in planimetric location, the greater the elevation error. Likewise, the steeper the slope, the greater the elevation error can be.

Of interest in this study, was whether horizontal inaccuracy could explain the trend between increase in vertical error and increasing slopes (see the section, Influence of Sloping Terrain on ALTM-derived Elevations and Figure 35). While it appeared the rising edge of the footprint is responsible for the shorter than actual range measurement and the higher than actual elevation, an answer was sought as to whether horizontal displacement of the laser strike account for all the observed vertical error.

For purposes of determining the affect of horizontal error on vertical error for steeply sloping terrain, the optimal solution would be to measure the amount of horizontal displacement. However, observing the amount of shift was not possible. The lack of definitive ground features (e.g., buildings, pavement edges, walkways, other improvements) in the study area excluded any measurements of horizontal error. The next best solution would have been to use horizontal error results from a comparable study. Unfortunately, relatively few studies definitively determined horizontal accuracy. Furthermore, these studies had rather low AGLs compared to the AGL of this study. Again, a higher AGL results in greater horizontal error. These facts lead to reframing the question: Given a horizontal displacement one meter in the up slope direction, can such a displacement account for the observed vertical error?

The findings of Flood (2001) and others served as the basis for using one meter as a base error. He and others indicated that this was an expected amount of horizontal error for a typical mapping project. Interpreting the graph for the ALTM system used to map the study site yielded a horizontal error value of only 0.59 m for the given AGL (see *Figure 4*, Variations in horizontal and vertical accuracies due to flying height). However, numerous studies indicated that manufacturer’s accuracy quotes tended to be overly optimistic. Hence, the horizontal error value of one meter prevailed.



Upper solid line: 1 m displacement.
 Lower dashed line: 0.59 m displacement.

Figure 40. Change in vertical error due to slope angle increase from horizontal displacement.

Calculating the error for numerous slope angles holding horizontal displacement constant at one meter and using equation (3), yielded the upper solid line in

Figure 40. Also in the figure, is a dashed line representing the effect on error if the horizontal displacement is 0.59 m indicating the variation between the two.

This figure indicates the amount of vertical error for a worst-case scenario created by the horizontal displacement occurring directly up the slope. Since this relationship is quadratic, a one-meter horizontal shift results in a greater increase in elevation error on higher slopes.

Conversely, the maximum elevation change can result in a negative change if the horizontal displacement is down the slope. No change in elevation will result if the horizontal shift is across the slope (i.e., along the contour). However, the true amount or direction of displacement is unknown since errors are random and nonlinear (Wagner et al., 2004; Glennie, 2007; Schenk, 2001; Hodgson & Bresnahan, 2004; Ussyshkin et al., 2009).

For this examination, a new elevation was calculated for each ALTM-derived elevation based on a horizontal displacement one-meter upslope for strikes where the ALTM elevation is lower than the reference elevation. The purpose was to determine if a one-meter horizontal shift can account for the observed vertical error. Stated graphically via Figure 41(a), the horizontal shift of one meter in the upslope direction will amount to a change in elevation. Would the change in elevation be equal to or greater than the observed vertical error? If so, a one-meter horizontal error could then account for the observed elevation difference between the ALTM-derived and reference elevations. Figure 41(b)

depicts the scenario where the reference elevation is still higher than the adjusted ALTM elevation, meaning that the one-meter horizontal shift cannot account for all of the observed error.

For ALTM-derived elevations that are higher than reference elevations, the horizontal displacement was downslope. Similarly, this examination compared these new elevations to reference elevations.

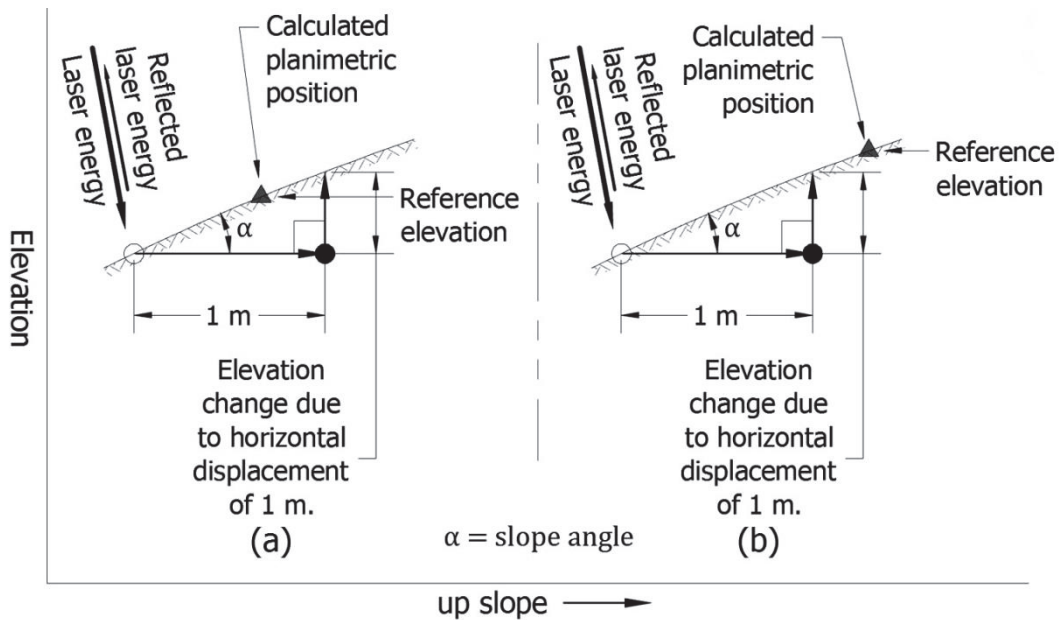


Figure 41. Change in elevation due to horizontal displacement of one meter.

Given the ground slopes for the sampled laser strikes range from 0.5 degrees to 50.6 degrees, the change in elevations due to a one-meter horizontal displacement varies from 0.009 m to 1.217 m, respectively. The mean displacement is then 0.256 m (SD 0.227).

Of the 351 sampled strikes, horizontal displacement can optimally account for 152 (or 43.3 percent) of the strikes' vertical error. Stated another way, even with the horizontal one meter shift upslope (or downslope), towards the direction of the reference elevation, the ALTM-based elevation is still below (or above) that of the reference elevation for 56.7 percent of the strikes. Of the 199 laser strikes with elevations that still fall short of the reference elevations, the disparity is, on average, 0.191 m (SD 0.137).

Table 7
Descriptive Statistics of the Sampled ALTM Ground Strike Vertical Errors Remaining After Vertical Adjustment Based on Horizontal Displacement

| | Slope Category | | | | | Overall |
|----------------------------------------------------------------------------|----------------|--------------|----------------|----------------|-------|---------|
| | 0.0- 4.9° | 5.0- 9.9° | 10.0- 19.9° | 20.0- 29.9° | 30°+ | |
| Max. adjusted ALTM elevation below Reference elevation (m) | -0.637 | -0.469 | -0.479 | -0.386 | None | -0.637 |
| Max. adjusted ALTM elevation above Reference elevation | 0.695 | 0.354 | 0.270 | 0.398 | 0.357 | 0.695 |
| Mean Absolute Error | 0.237 | 0.160 | 0.165 | 0.196 | 0.135 | 0.191 |
| RMSE | 0.284 | 0.198 | 0.209 | 0.224 | 0.174 | 0.343 |
| No. of strikes where adjustment cannot account for observed vertical error | 69 | 51 | 41 | 27 | 11 | 199 |
| No. of strikes where adjustment accounts for observed vertical error | 16 | 40 | 50 | 21 | 25 | 152 |
| Percentage of strikes where adjustment accounts for vertical error | 18.8% | 44.0 | 54.9 | 43.8 | 69.4 | 43.3 |

Maximum disparities between the new ALTM elevations and reference elevations are -0.637 m and 0.695 m. These are listed in the last column of Table 7. The

maximum vertical errors observed without adjustment for horizontal displacement are -0.776 m and 1.197 m (see Table 4). For those laser strikes where a horizontal shift of one meter could not account for the observed vertical error, Table 7 gives a breakdown of vertical error that remains after the adjustment.

In the table, *ALTM elevation below Reference elevation-Maximum* indicates the largest of the vertical errors where the adjusted ALTM-derived elevation is still lower than the reference elevation. *ALTM elevation above Reference elevation-Maximum* indicates the largest error remaining between the reference elevation and the ALTM elevation that is still higher than the reference elevation. The mean of the remaining vertical error between the adjusted ALTM-derived and reference elevations has been calculated using absolute values (see *Mean Absolute Error* in the table). These and similar remaining error values pertain to the 199 laser strikes only.

From the table, the adjustment accounted for very little of the error in the 0.0 to 4.9 degree slope category (18.8 percent). This minor change was understandable since a horizontal shift results in a smaller change in elevation on lesser slopes than on steeper ones (see Figure 40). The one-meter shift in horizontal location on a slope of five degrees amounts to a maximum elevation change of only plus or minus 0.087 m. For a ten-degree slope, the maximum elevation change will be plus or minus 0.176 m. From this relationship, the greatest elevation changes due to horizontal displacement, are on steeper

slopes, as evidenced by the success rate in the 30-degree and above slope stratum (69.4%). In this stratum, vertical adjustments range from 0.577 (30°) to 1.217 m (50.6°). This relationship is illustrated in Figure 42, where the vertical errors of the 351 sampled strikes are plotted against slope.

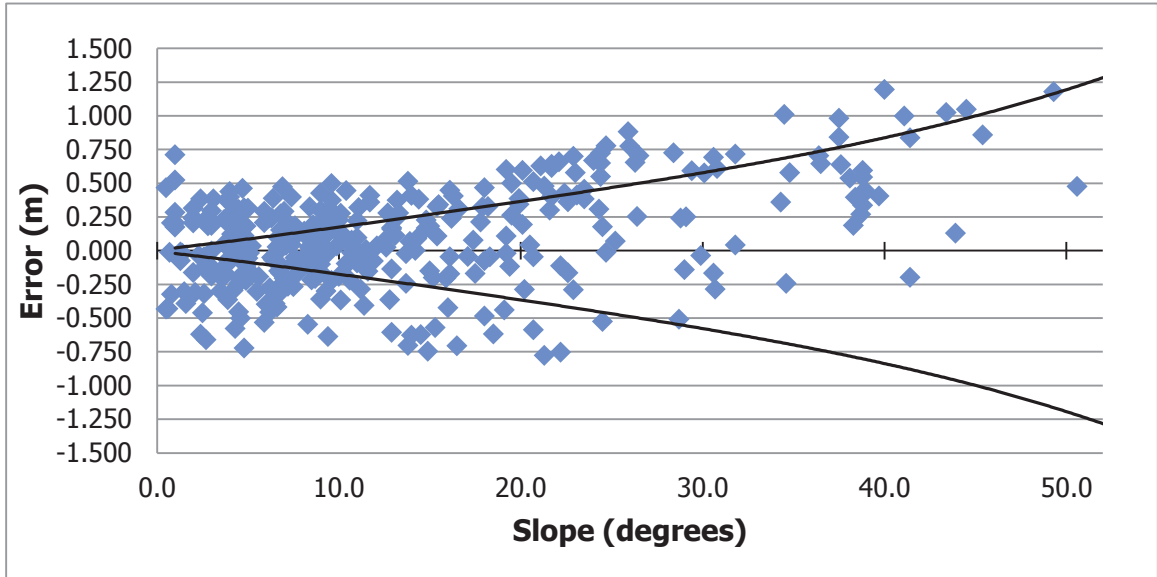


Figure 42. Scatterplot of the sampled ALTM ground strike vertical errors for all slopes with lines representing change in vertical error due to slope angle increase from horizontal displacement of one meter (n=351).

Again, the top line represents the amount of error incurred for a one-meter shift in horizontal position upslope for any given slope. This line is the same as the solid line shown in Figure 40. The bottom line is similar, representing the same one-meter shift downslope. Sampled laser strikes between the two lines indicate that a horizontal shift of one meter can account for all of the strike’s observed error between the ALTM-derived elevation and the reference elevation. Again, this one-meter shift could account for the observable error for 152 of the strikes.

Other strikes situated above the top line or below the bottom line have more error than what the horizontal displacement can account for (n=199).

From Figure 42, the range of error accounted for by horizontal shift increases markedly as slope increases and that many of the sampled strike errors on higher slopes are within the two lines. Conversely, very little of the error on flat and gently sloping terrain can be accounted for by this displacement.

Interestingly, the percentages of success (last row of Table 7) do not consecutively increase as slope increases. The absolute RMSE values remain high, which was logical, given the disparity that remains among those strikes not accounted for by the displacement. These values are understandably lower than values prior to the adjustment (see Table 5).

Comparing the horizontal displacement's affect on vertical error using the Leica Geosystems horizontal accuracy value (0.59 m), only 93 (26.5%) of the strikes' error can be accounted for. The percentages are lower in each slope strata: 0.0 to 4.9 degrees: 9.4 percent; 5.0 to 9.9 degrees: 24.2 percent; 10.0 to 19.9 degrees: 38.5 percent; 20.0 to 29.9 degrees: 27.1 percent; above 30 degrees: 41.6 percent. All values of mean absolute error and RMSE are also higher.

For the horizontal displacement to be responsible for 95 percent of the observed elevation error, the displacement would need to be 8.5 m. This much shift is an unreasonable amount of error; more than four times greater than the manufacturer's quoted accuracy (0.59 m). To account for 95 percent of the error

for strikes only on slopes greater than twenty degrees, the displacement would need to be 1.67 m. Again, this is an error amount considerably higher than that found by others. In fact, it was not expected for horizontal displacement to account for all or most error on relatively flat terrain. This error is most likely due to the system components and other factors affecting imprecision. Some of which were presented in the section, ALTM Errors, Accuracies, and Precisions.

In comparison to others, Su and Bork (2006) calculated a vertical RMSE of 0.28 m on slopes greater than ten degrees due to horizontal displacement. They calculated vertical error due to the horizontal inaccuracy of laser strikes as being 0.08 m (RMSE 0.13). In this study, for laser strike vertical error not accounted for by horizontal displacement, the RMSE is 0.212 (for slopes greater than ten degrees, $n=77$).

Horizontal displacement accounting for errors for only a relatively small number of strikes, lead to the examination of other factors.

Influence of Laser's Footprint Size on ALTM-derived Elevations

Given the low percentage of error explained by horizontal displacement, the study investigated the effect of footprint size. As presented previously, the size of the laser strike footprint may influence the increase in vertical error as slope increases.

In the section, Footprint Reflectivity, Kobler et al. (2007) and Goulden and Hopkinson (2010) theorized that the rising side of the footprint is responsible for range measurement. Similarly, Baltsavias (1999a) believed that highly reflective objects, wherever they are located in the footprint, determine the range measurement of the laser strike. If this material is not at the center of the footprint, the range and thus, the elevation are in error. As footprint size increases, it was logical to assume vertical error increases. Glennie (2007) did compare two different laser beam divergence angles resulting in differing footprint sizes. He did find a correlation between the two.

Based on Kobler et al. and Baltsavias' postulations, reflective material could be further away from the center with larger footprints. The influence of this offset on vertical error may be exacerbated in this study due to the larger than typical footprint size.

In addition to AGL, the size of the footprint is due to divergence angle, slope angle, slope aspect, and scan angle. The interplay of these variables creates a different sized footprint for each laser strike. As presented previously, the laser energy radiates outward from the transmitter in the shape of a cone (for the ALTM used in this study). Given a slope facing the flight line, if the scan and slope angles are equal, the footprint on the ground is circular in shape. This is similar to a laser strike at nadir on level ground (i.e., both angles are 0°). For any other combination of scan and slope angles, the footprint is in the shape of an ellipse.

This study calculated footprint sizes for all the sampled laser strikes. For each strike, a plane surface represents the terrain based on field-measured slope angle and slope aspect (see the \hat{t} - \hat{s} plane in Figure 43). Two vectors \hat{t} and \hat{s} define each plane¹⁶. The laser strike, labeled **O**, serves as the initial points of both vectors. The direction of vector \hat{t} runs up the slope. The direction of vector \hat{s} is 90 degrees to vector \hat{t} and hence, across the slope.

If the slope aspect faces the flight path, the major axis of the elliptical footprint is parallel with the slope. If the slope has any other orientation, the major axis of the ellipse no longer aligns up and down the slope. In these instances, the orientation of the major axis aligns with an imaginary line running from the ground strike to a point on the \hat{t} - \hat{s} plane closest to the aircraft (i.e., nadir on the \hat{t} - \hat{s} plane).

Calculating the orientation of the major axis for each footprint involved several steps. Figure 43 illustrates a typical footprint, axes, and requisite vectors needed to calculate footprint size.

¹⁶ Vectors with the hat symbol ($\hat{}$) are unit vectors meaning, the magnitude of the vector is one.

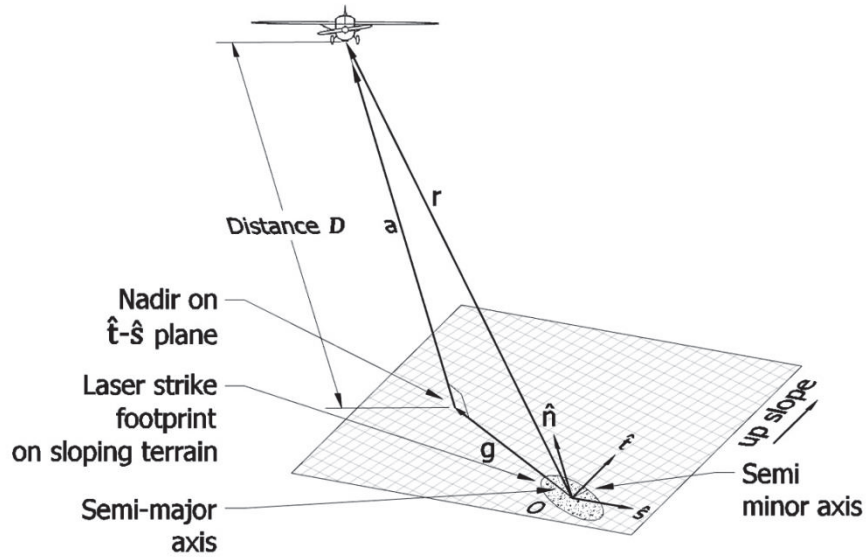


Figure 43. Influence of scan angle, slope angle and slope aspect on footprint size.

The vector \mathbf{r} represents the vector with its initial point at laser strike \mathbf{O} and its direction is towards the LiDAR system (i.e., the opposite direction that the laser beam traveled). This vector is derived from the azimuth of the flight path, flying height, scan angle, and elevation of each laser strike.

Vector $\hat{\mathbf{n}}$ describes a vector normal to the terrain (i.e., $\hat{\mathbf{t}}\text{-}\hat{\mathbf{s}}$ plane) and is derived using the following formula:

$$\mathbf{S} \times \mathbf{T} = |\hat{\mathbf{s}}| \cdot |\hat{\mathbf{t}}| \cdot \sin(90^\circ) \quad \text{Eq. (12)}$$

Where:

$\mathbf{S} \times \mathbf{T}$ = cross product of vectors $\hat{\mathbf{s}}$ and $\hat{\mathbf{t}}$ (i.e., vector $\hat{\mathbf{n}}$).

$|\hat{\mathbf{s}}|, |\hat{\mathbf{t}}|$ = magnitudes of vectors $\hat{\mathbf{s}}$ and $\hat{\mathbf{t}}$, respectively.

90° = angle between vectors $\hat{\mathbf{s}}$ and $\hat{\mathbf{t}}$.

Vector \mathbf{a} describes the vector from the aircraft's nadir point on the $\hat{\mathbf{t}}\text{-}\hat{\mathbf{s}}$ plane to the aircraft. This vector \mathbf{a} , is normal to the $\hat{\mathbf{t}}\text{-}\hat{\mathbf{s}}$ plane and thus, co-linear with vector $\hat{\mathbf{n}}$.

The components of vector \mathbf{a} were found by multiplying the components of vector $\hat{\mathbf{n}}$ by the distance D . This value represents the distance from the aircraft to the nadir point on the $\hat{\mathbf{t}}\text{-}\hat{\mathbf{s}}$ plane. By multiplying the corresponding components of vectors $\hat{\mathbf{n}}$ and \mathbf{r} and summing these results generates distance D :

$$D = \hat{n}_x \cdot r_x + \hat{n}_y \cdot r_y + \hat{n}_z \cdot r_z \quad \text{Eq. (13)}$$

Where:

$$D = \text{Distance from aircraft to nadir on } \hat{\mathbf{t}}\text{-}\hat{\mathbf{s}} \text{ plane.}$$

The direction of vector \mathbf{a} was reversed (i.e., the signs of the components were changed to have the initial point of the vector at the LiDAR system and directed to nadir) as required for vector addition. Then vector \mathbf{a} was added to vector \mathbf{r} to develop vector \mathbf{g} . The initial point of vector \mathbf{g} is the laser strike and its direction points to the aircraft's nadir point on the $\hat{\mathbf{t}}\text{-}\hat{\mathbf{s}}$ plane. The major axis of the footprint aligns with vector \mathbf{g} .

The length of the semi-major axis of the footprint was calculated via law of sines and knowing distance D , the divergence angle of the LiDAR unit (0.00033 mrad),

and the angle between vectors \mathbf{r} and \mathbf{g} . This latter angle was determined using the following formula:

$$\theta = \cos^{-1} \left(\frac{\mathbf{r} \cdot \mathbf{g}}{|\mathbf{r}| |\mathbf{g}|} \right) \quad Eq. (14)$$

Where:

θ = angle between two vectors.

$\mathbf{r} \cdot \mathbf{g}$ = dot product of the vector \mathbf{r} and vector \mathbf{g} .

$|\mathbf{r}| |\mathbf{g}|$ = magnitudes of vectors \mathbf{r} and \mathbf{g} , respectively.

Since the semi-minor axis of the footprint is at a right angle to vector \mathbf{r} , the following formula derives the length of the semi-minor axis:

$$\text{Length of semi-minor axis} = \tan(\text{Divergence angle}) \cdot \text{Range} \quad Eq. (15)$$

With the lengths of the axes known, the size of the footprint for each laser strike was derived from:

$$\text{Area of footprint} = \pi \cdot a \cdot b \quad Eq. (16)$$

Where:

a = length of the semi-major axis of the footprint.

b = length of the semi-minor axis of the footprint.

These footprint sizes are not absolute. As presented earlier in the section, Footprint Size, divergence angle, a component of these footprint calculations, is described as a percentage of the total energy emitted: The energy in the beam

(i.e., pulse) is concentrated about the center of the beam (see Figure 9), but this power follows a Gaussian curve in that energy trails off in every direction. Manufacturers define divergence angle as the angular spread (in mrad) of the beam at the $1/e$ level. At the $1/e$ level, the power equates to approximately 84 percent of the total energy emitted. Hence, given a specific mrad value and calculating footprint size, as employed here, accounts for only 84 percent of the total energy emitted. Based on the principles of normal distribution, the footprint can be much larger and theoretically, extend to infinity. See Goulden and Hopkinson (2010) and references therein for more information. Even though footprint sizes in this study (and others) are based on only a percentage of the total energy, the relative sizes of footprints between laser strikes provided some insight into relationships between ALTM factors and vertical error.

Apportioning the footprint sizes into the slope strata (see Table 8) confirmed that footprint size increases as slope increases.

Table 8
Descriptive Statistics of the Sampled ALTM Ground Strike Footprint Sizes by Slope Strata

| | Slope Category | | | | | Overall |
|------------------------|----------------|----------|------------|------------|-------|---------|
| | 0-4.9° | 5.0-9.9° | 10.0-19.9° | 20.0-29.9° | 30°+ | |
| Mean (m ²) | 2.259 | 2.359 | 2.394 | 2.445 | 2.782 | 2.399 |
| Standard Deviation | 0.159 | 0.153 | 0.217 | 0.260 | 0.322 | 0.253 |
| Minimum | 1.980 | 1.986 | 2.020 | 2.119 | 2.319 | 1.980 |
| Maximum | 2.583 | 2.618 | 2.978 | 3.096 | 3.532 | 3.532 |

From the data in this table, the minimum footprint size was 1.980 m², which was smaller than the 2.059 m² value for a footprint on flat terrain at nadir (i.e., with a footprint diameter of 1.62 m). This lower value represents laser strikes, where scan angle and slope angle are nearly equal (e.g., scan angle and slope angle $\approx 0^\circ$), but at higher elevations. The increase in footprint size as slope increased is also evident in Figure 44. A relationship between the two was calculated.

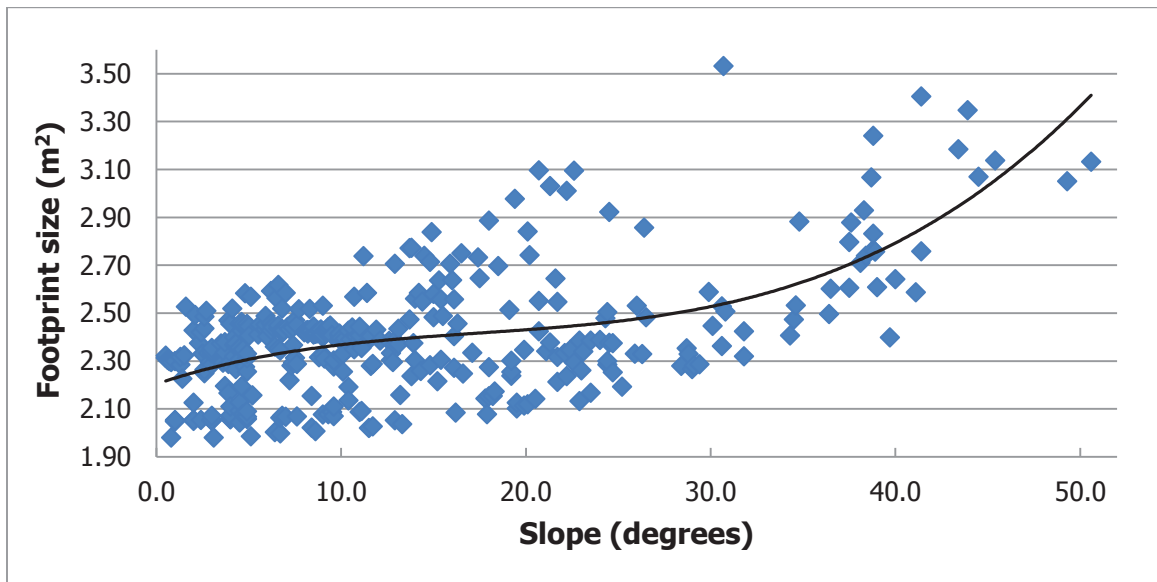


Figure 44. Scatterplot of the sampled ALTM ground strike footprint sizes relative to slopes (n=351).

A polynomial line plotted through this data has the following values:

$$\text{Footprint size} = 0.0000226 \cdot x^3 - 0.001 \cdot x^2 + 0.026 \cdot x + 2.204 \quad \text{Eq. (17)}$$

This model proved to be significant when compared to a quadratic or linear model and the R² value (0.355) is slightly higher than the R² values of the latter two (0.330 and 0.306, respectively). The standard error of the estimate is 0.204.

Ramsey's RESET indicates that the cubic value predictor coefficient of the model is significant and that the quadratic and linear models are mis-specified. Thus, the coefficients of the latter two models are not adequate. The somewhat low R^2 value of 0.355 and standard error of the estimate acknowledge the pattern in *Figure 44* whereby, many strikes are not clustered tightly about the line. There is tight clustering of sampled strikes for slopes of zero to twelve degrees. However, on slopes from twelve to 23 degrees, numerous strikes above the line display more variation. This deviation was also evident via the standard deviation values in Table 8.

Describing the relationship on steeper slopes was limited with only 36 sampled strikes having slopes 30 degrees and above. However, the larger footprints (>2.6 m^2) predominately come from sampled strikes on slopes greater than 30 degrees ($n=24$). Larger footprints (>2.6 m^2) also occur on lesser slopes where nine strikes are on slopes 20.0 to 29.9 degrees and sixteen strikes on 10.0 to 19.9 degree slopes. Interestingly, the largest footprint is not for the laser strike on the highest sampled slope (50.6°), but on a slope of 30.7 degrees. Thus, scan angle and slope aspect have more influence with this strike as is the case with other strikes located above and below the line in *Figure 44*.

A direct comparison of vertical error to footprint size is displayed in the scatterplot of *Figure 45*:

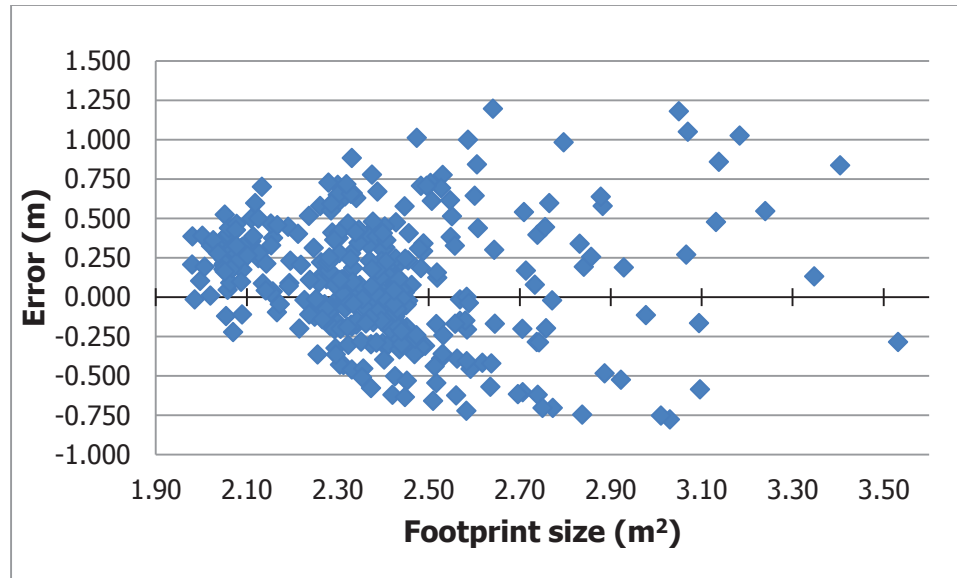


Figure 45. Scatterplot of the sampled ALTM ground strike vertical errors for all footprint sizes (n=351).

From this plot, the dispersion of error is relatively minimal for the smallest of footprints. For footprints greater than 2.2 m², the dispersion increases as footprint sizes increases. Vertical error associated with footprint sizes greater than 2.6 m² appeared to follow a similar pattern but this observation required qualification due to the limited number of sampled strikes with large footprints. However, this dispersion appeared to indicate that laser strikes may originate from reflective material or some other element located elsewhere in the footprint, as presented by Baltasvias (1999a), Glennie (2007), and Ussyshkin et al. (2009). This observation would contradict Kobler et al. (2007) and Goulden and Hopkinson (2010) who indicated that the upper reach of the footprint is responsible for a shorter than actual range measurement and a higher than

actual elevation. For their assertion to be true, a trend between signed vertical error and footprint size would be evident.

From Figure 45, no upward trend is apparent between increasing footprint size and an increase in signed error. A linear regression model was found to be not significant ($p = .074$), but only slightly so. Interestingly, some of the larger footprints had less error.

With closer inspection, a slight downward trend exists for sampled strikes with footprint sizes from 2.0 to 2.5 m². Further investigation first curtailed the influence of slope: From the section, Influence of Sloping Terrain on ALTM-derived Elevations, specifically Table 5, the three lowest slope strata have vertical errors of 0.00 m, 0.00m, and 0.019 m, respectively. These strata encompass slopes from 0.0 to 19.9 degrees. Using only strikes from these strata, a scatterplot of footprint sizes better shows this downward trend (see Figure 46). The smallest footprints have positive errors indicating that ALTM-derived elevations are above reference elevations. The mean error for footprints smaller than 2.1 m² is 0.231 m (RMSE 0.277, n=46).

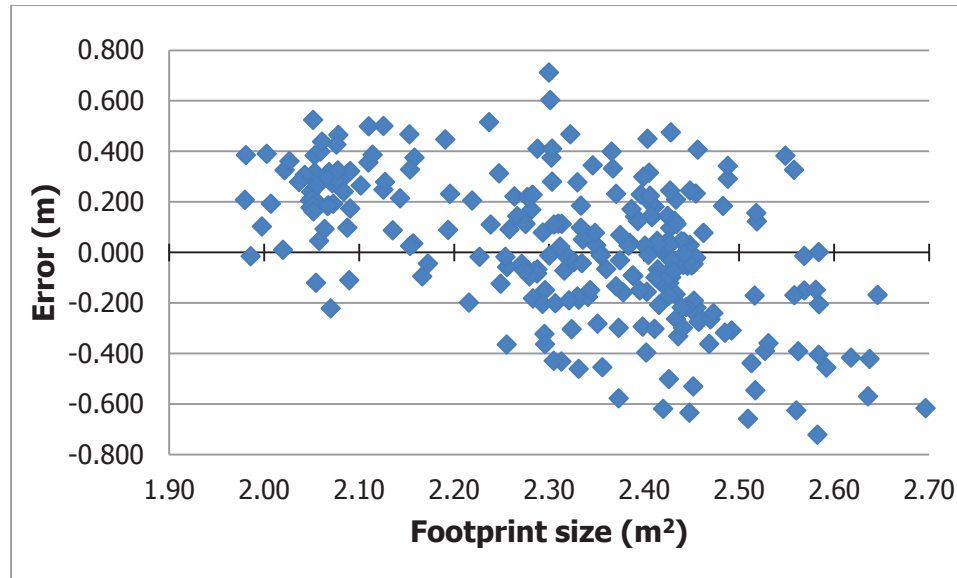


Figure 46. Scatterplot of the sampled ALTM ground strike vertical errors for footprint sizes on slopes less than 20.0° ($n=267$).

This pattern is the same when using only the data for slope strata of 0.0 to 4.9 degrees ($n=85$) and when using only 5.0 to 9.9 degrees ($n=91$).

Concerning dispersion, Figure 46 shows an increase in dispersion as footprint size increases. First, footprint size can vary in size, even on flat terrain due to scan angle and ground elevation: A higher scan angle or lower elevation would result in a larger footprint. However, the true reason for this dispersion is unknown since the footprints are on level terrain, hence, there is no rising side of the footprint. Similarly, reflective material or some other element situated elsewhere in the footprint could not impart enough error in the range measurement to account for the vertical errors observed here.

From the scatterplot of absolute vertical errors against footprint size shown in Figure 47, an upward trend in error as footprint size increases was somewhat visible.

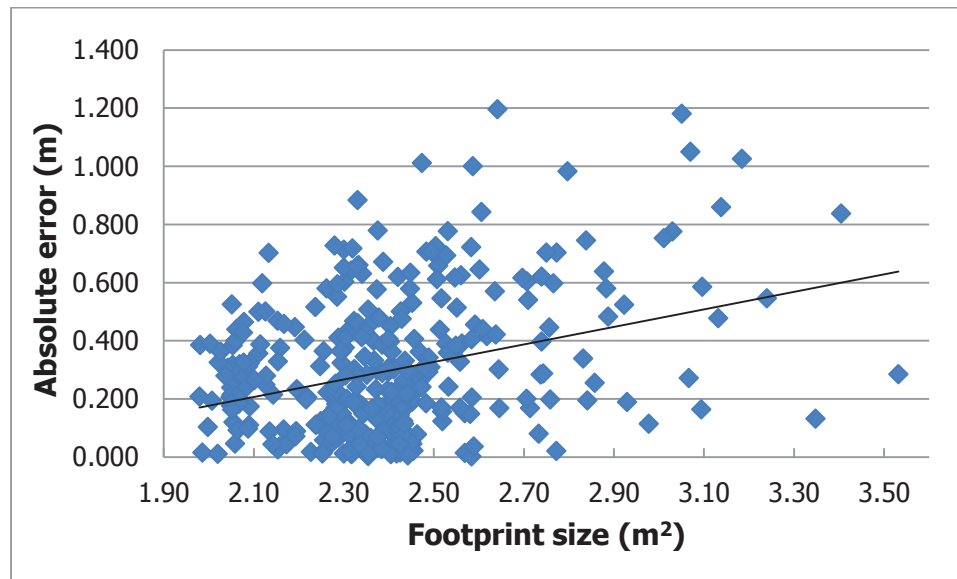


Figure 47. Scatterplot of the sampled ALTM ground strike absolute vertical errors for all footprint sizes (n=351).

However, the correlation coefficient for a least squares model is very low ($R^2=0.106$). The model is significant (ANOVA and t -test for significance of slope coefficient: $p = .000$). But again, the F-test of the ANOVA only indicates that the model is an improvement over using only the mean error value to describe the relationship. The rather small number of laser strikes with small ($<2.2 \text{ m}^2$, $n=69$) and large ($>2.6 \text{ m}^2$, $n=49$) footprints may have prohibited visualizing or developing a relationship.

Since footprint size is also dependent on slope aspect, scan angle, AGL, and laser range (a variable dependent on the last two factors), comparisons made between footprint size and these other factors. However, no obvious results were discernable patterns except for the comparison to scan angle:

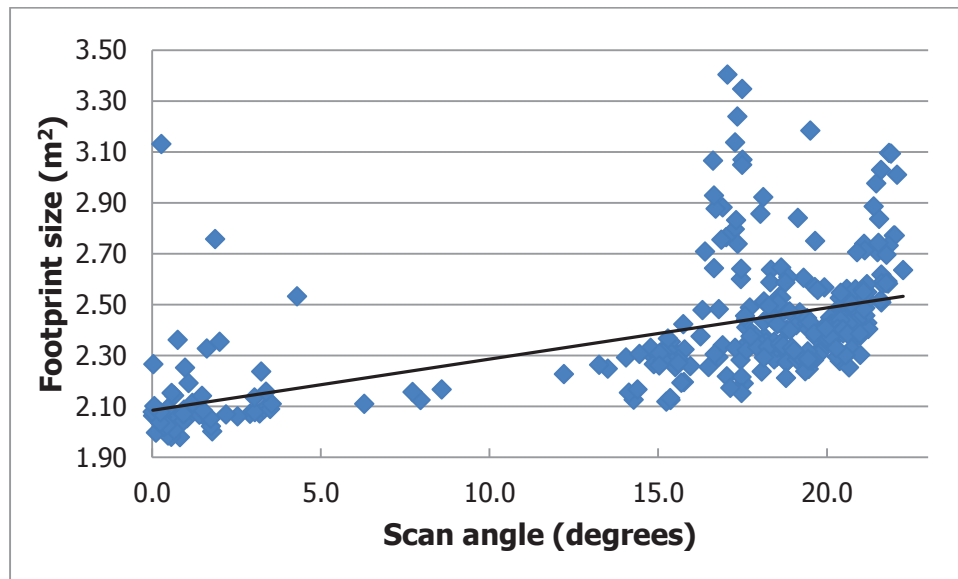


Figure 48. Scatterplot of the sampled ALTM ground strike footprint sizes relative to scan angles (n=351).

In Figure 48, the laser strikes with the smallest footprints have the lowest scan angle. More so, the smallest footprints have scan angles between zero and two degrees. The scatterplot showed that as scan angle increases, footprint size does the same. This association was most evident when focusing on only the smallest footprints at all scan angles.

A least squares line added to this plot to yielded a low coefficient of determination ($R^2=0.325$) and a minimal slope for this line where, for every one degree increase in scan angle, the footprint size only increases 0.020 m²:

$$\text{Footprint size} = 0.020 \cdot \text{Scan angle} + 2.085 \quad \text{Eq. (18)}$$

The ANOVA and t -tests confirming the validity of the model and the equation's coefficients indicated that both are significant ($p = .000$). However, given the R^2 value and a standard error of the estimate of 0.208, the relationship is weak.

This weakness is due to the multiple strikes with large footprints situated well above the line. These strikes are most likely sites where slope has more influence on footprint size than scan angle. Comparing the influence of slope to scan angle on footprint size, the standard error of the estimate (0.204 and 0.208, respectively) and coefficient of determination (0.355 and 0.325, respectively) are very similar, indicating that both factors contribute equally to footprint size. AGL also has some influence but much less so.

This examination of footprint size showed no strong trend between footprint size and either signed or absolute error. The only trend found was an observable downward trend in signed error but the reason for this was not entirely clear. Both signed and absolute error did suggest dispersion as footprint size increased indicating a loss in precision. However, the relatively small number of laser strikes with footprints greater than 2.6 m² tempers this observation.

Subsequently, the study expanded to compare elevations within the footprints to the reference elevations. As per Baltasvias (1999a), Glennie (2007), Kobler et al. (2007), Ussyshkin et al. (2009), and Goulden and Hopkinson's (2010) theories, reflective material or other elements situated anywhere in footprint could be responsible for the return of the laser pulse and affect range and elevation. Therefore, greater elevation disparity could be responsible for the larger observable error on steep slopes.

Exploration of Varying Elevations within Laser's Footprint due to Sloping Terrain

A scenario was created to determine if the change in elevation between the center of the footprint and the reflective material could account for the observed vertical error. Since the location of the reflective material or other element responsible for the range measurement was unknown, the elevations at the upper and lower edges of each laser strike's footprint were calculated. These elevations were then compared to reference elevations. If the reference elevation fell between the elevations of the upper and lower edges of the footprint, then, reflective material could be responsible for the observed vertical error.

As with footprint size, the elevations of the upper and lower reaches of the footprint are due to divergence angle, slope angle, slope aspect, AGL, and scan angle. The interplay of these variables not only creates a different sized footprint

for each laser strike but a different orientation on the terrain. The size and orientation on the slope delineates these elevations.

The upslope and downslope elevations at edges of each laser strike's footprint were calculated based vector algebra and ellipse formulas. Calculations began with defining the angle between vector $\hat{\mathbf{t}}$ and vector \mathbf{g} for each footprint. Refer to the previous section, Influence of Laser's Footprint Size on ALTM-derived Elevations, where these vectors were determined. From that section and Figure 43, Vector $\hat{\mathbf{t}}$ has its initial point at the laser strike and its direction is up the slope. Vector \mathbf{g} also has its initial point at the laser strike and its direction is towards the aircraft's nadir point on the $\hat{\mathbf{t}}\text{-}\hat{\mathbf{s}}$ plane. Vector \mathbf{g} coincides with the major axis of the footprint. Equation (14) produces the angle between vector $\hat{\mathbf{t}}$ and \mathbf{g} . (vector $\hat{\mathbf{t}}$ replaces vector \mathbf{r} in the equation). This angle yields the orientation of the footprint relative to the slope, specifically: the angle between an imaginary line running upslope and the semi-major axis of the footprint.

Computing the elevation of the uppermost reach of a footprint employed a line running across the slope, parallel to vector $\hat{\mathbf{s}}$, and tangent to uppermost edge of the ellipse representing the footprint. For clarity between formulas, nontraditional terms were used to define the line:

$$t = m \cdot s + c \tag{Eq. (19)}$$

Where:

- t = t coordinate in the \hat{t} - \hat{s} Cartesian coordinate system
- m = slope of the line
- s = s coordinate in the \hat{t} - \hat{s} Cartesian coordinate system
- c = \hat{t} axis intercept

In the \hat{t} - \hat{s} plane, this line has a slope of zero and hence, $t = c$ (see Figure 49(a)). From this construction, the \hat{t} -intercept of this line represents the upper reach of the footprint numerically.

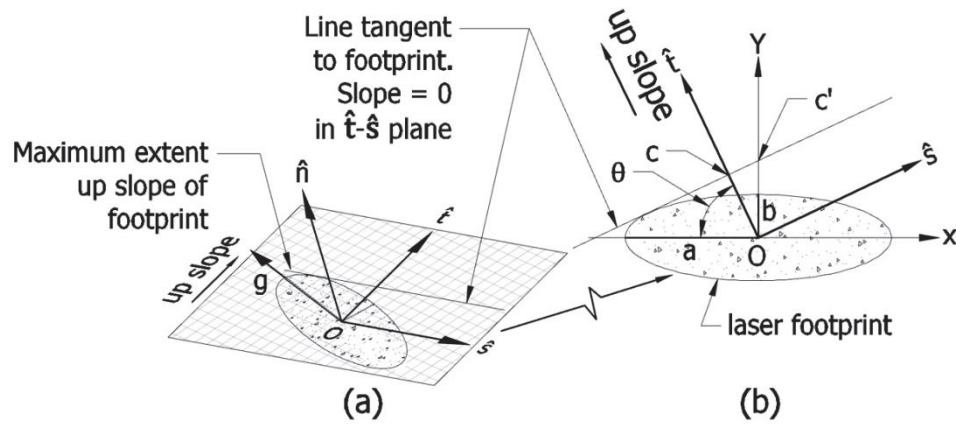


Figure 49. Calculation of the slope of the line tangent to the footprint at the point furthest uphill.

The following formula, known as the tangency condition, is a derivation of the formulas for a line and an ellipse and is used to calculate the value of the Y -intercept:

$$c'^2 = a^2 \cdot m^2 + b^2 \quad \text{Eq. (20)}$$

Where:

c' = Y-intercept in an X-Y Cartesian coordinate system

a = semi-major axis length of footprint

m = slope of the line

b = semi-minor axis length of the footprint

While the slope of the line in the $\hat{\mathbf{t}}\text{-}\hat{\mathbf{s}}$ plane ($m = 0$) is known, it must be calculated relative to the axes of the ellipse (a and b) using:

$$m = \tan(90 - \theta) \quad \text{Eq. (21)}$$

Where:

θ = the angle between vectors $\hat{\mathbf{t}}$ and \mathbf{g} .

Thus, c' represents the Y-intercept of the ellipses' X-Y coordinate system (i.e., $a - b$ plane) and is not the same as c representing the $\hat{\mathbf{t}}$ -intercept of the $\hat{\mathbf{t}}\text{-}\hat{\mathbf{s}}$ plane. Figure 49 (b) depicts the differences between the Y-intercept and the $\hat{\mathbf{t}}$ -intercept.

Once c' was calculated, c was determined using:

$$c = \text{Sin}\theta \cdot c' \quad \text{Eq. (22)}$$

Again, c represents the upper reach of the footprint on the slope. The change in elevation from the center of the laser strike to the upper most edge of the footprint was then calculated:

$$\text{Change in elevation} = \sin(\text{slope angle}) \cdot c \quad \text{Eq. (23)}$$

Note in equation (20) c' can be positive or negative. The sign of this value carries through the subsequent calculations such that the change in elevation value can be both positive and negative. Thus, adding this value to the ALTM-derived elevation produced the uppermost elevation of the footprint and subtracting this value produced the lowermost elevation of the footprint.

Table 9
Descriptive Statistics of the Sample ALTM Ground Strike Elevation Spreads Across the Footprint by Slope Strata

| | Slope Category | | | | | Overall |
|----------|----------------|----------|------------|------------|-------|---------|
| | 0.0-4.9° | 5.0-9.9° | 10.0-19.9° | 20.0-29.9° | 30°+ | |
| Mean (m) | 0.095 | 0.233 | 0.435 | 0.734 | 1.270 | 0.427 |
| RMSE | 0.103 | 0.236 | 0.446 | 0.740 | 1.295 | 0.562 |
| Minimum | 0.015 | 0.142 | 0.295 | 0.565 | 0.897 | 0.015 |
| Maximum | 0.160 | 0.303 | 0.734 | 0.944 | 1.939 | 1.939 |

The difference or spread, between the uppermost and lowermost elevations for all the footprints are listed in Table 9, arranged by slope strata. Again, these are not definitive values as they are the result of calculations based on a laser beam divergence angle that theoretically, only accounts for 84 percent of the laser

pulse's energy (see the section, Influence of Laser's Footprint Size on ALTM-derived Elevations).

As expected, the difference between the elevation of the high point and the low point of a footprint on sloping terrain increases as slope increases. On flat terrain, the elevation difference is minimal with a mean of only 0.095 m.

Reinforcing this negligible effect is that the minimum elevation spread for one sampled laser strike is 0.015 m and the maximum spread in this stratum being only 0.160 m. Of note is the largest spread: 1.939 m. This value alone is significant in that, it showed how much variability could exist across a footprint.

A scatterplot of difference in elevations across the footprint versus slope angle showed a very strong relationship between the two (see Figure 50).

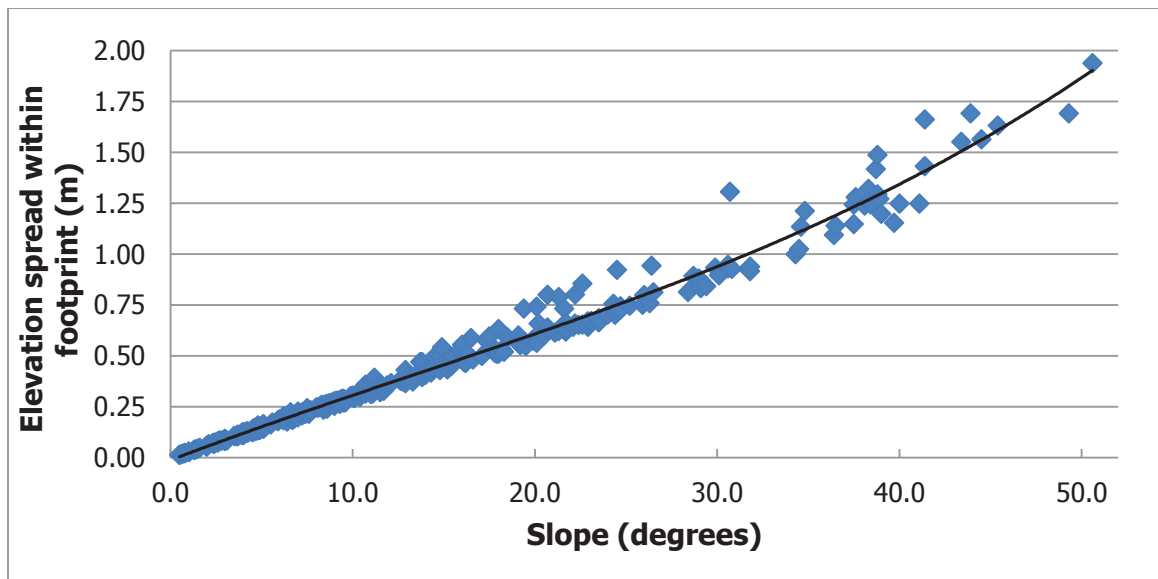


Figure 50. Scatterplot of the sampled ALTM ground strike elevation spread within footprints relative to slopes (n=351).

A cubic equation describes this relationship:

$$\text{Elevation spread} = 0.000008 \cdot x^3 - 0.0003 \cdot x^2 + 0.034 \cdot x - 0.012 \quad \text{Eq. (24)}$$

The coefficient of determination for this model is 0.984 (R^2). The ANOVA and t -tests for the model are significant ($p = .000$) and the standard error of the estimate is low: 0.046. The Ramsey RESET indicates that this is the best model when compared to quadratic and linear models.

The descriptive statistics of the elevation spread across the footprint given in Table 9 are similar to those of footprint size. However, it was meaningful to view a scatterplot of these two products. From Figure 51, the very high correlation initially perceived between the two was not a correct assumption. The correlation coefficient is 0.411 (r), which is considered moderate. From the figure, much variability exists between the two.

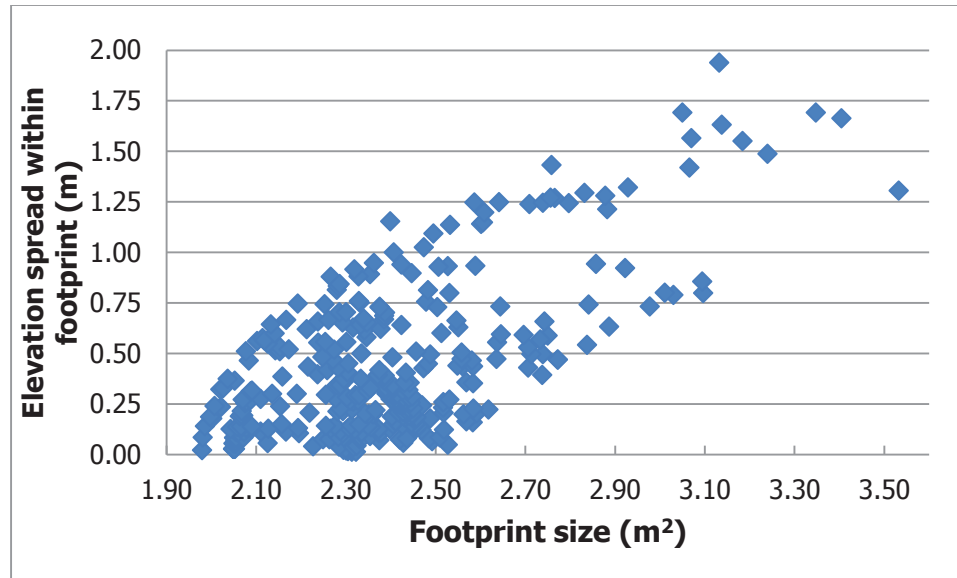


Figure 51. Scatterplot of the sampled ALTM ground strike elevation spread within footprints relative to footprint sizes (n=351).

In general, as footprint size increases, the elevation spread across the footprint also increases. However, variability exists, possibly due to scan angle more so than slope aspect, such that larger footprints regularly occur on lesser slopes. Meaning, larger footprints can have small elevation spreads. This observation is shown graphically by laser strikes on the bottom edge of Figure 51, along the X-axis where footprints have negligible elevation spreads. Similarly, there is a wide range in footprint sizes for any given elevation spread.

Due to concerns of causality between elevation spread across the footprint and footprint size, no model of this relationship was developed.

A change of focus to vertical error compared the elevation spread between the upper and lowermost reaches of each footprint to corresponding reference

elevations. The reference elevations fall within the elevation spread for 129, or 36.8 percent, of the of the sample strikes (n=351). Hence, 222 laser strikes have reference elevations higher than the uppermost elevation of footprint or lower than the lowest elevation of the footprint. Figure 52 shows the possible relationships between the reference elevation and the footprint spread.

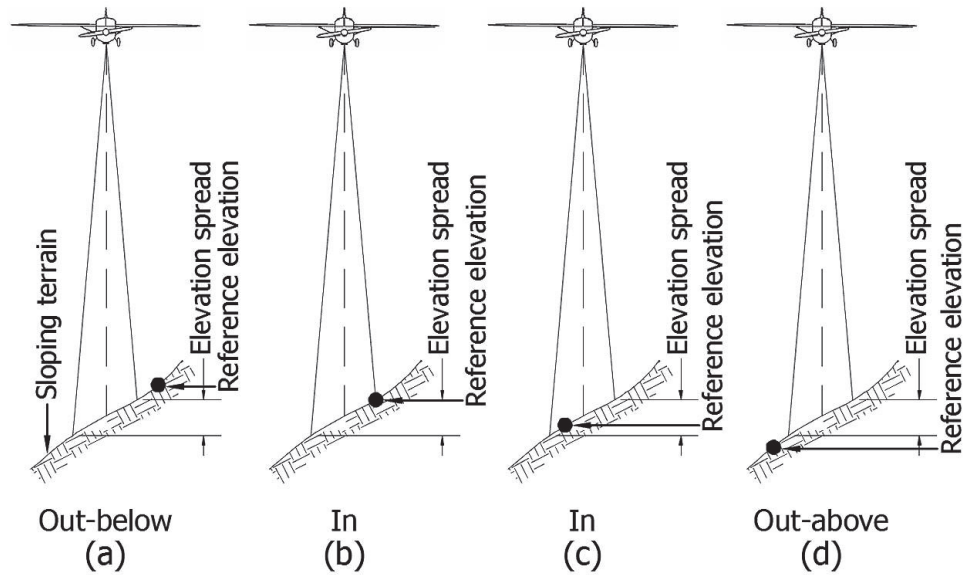


Figure 52. Elevation of laser strike footprint relative to reference elevation.

If the reference elevation fell within the elevation spread from the uppermost edge of the footprint to the lowermost edge ((b) or (c) in the figure), the elevation spread can conceivably be responsible for the observed elevation error. Qualifying this statement, the reflective material situated in the footprint would have to be at a specific location to correspond to the observed ALTM elevation. Figure 52 (a) and (d) depicts when reference elevations fall outside of the footprint elevations. In this study, reference elevations were either higher or

lower than footprint elevations for 222 laser strikes. Of these, 135 of the laser strikes are higher than the reference elevation (d), while the remaining 87 strikes had elevations of the upper edge of the footprint still below the reference elevations (a). This discovery coincides with initial findings where the majority of the ALTM elevations are above reference elevations. Table 10 shows the breakdown of vertical error remaining between the elevation at the edge of the footprint and the reference elevation for the 222 laser strikes.

Table 10
Descriptive Statistics of the Sampled ALTM Ground Strike Vertical Errors Remaining After Comparing Reference Elevation to Uppermost and Lowermost Footprint Elevations

| | Slope Category | | | | | Overall |
|---------------------------------------------------------------------------|----------------|--------------|----------------|----------------|-------|---------|
| | 0.0- 4.9° | 5.0- 9.9° | 10.0- 19.9° | 20.0- 29.9° | 30°+ | |
| Max. adjusted ALTM elevation below Reference elevation (m) | -0.641 | -0.489 | -0.473 | -0.38 | none | -0.641 |
| Max. adjusted ALTM elevation above Reference elevation | 0.698 | 0.339 | 0.325 | 0.507 | 0.572 | 0.698 |
| Mean Absolute Error | 0.233 | 0.164 | 0.182 | 0.246 | 0.249 | 0.208 |
| RMSE | 0.282 | 0.203 | 0.221 | 0.276 | 0.291 | 0.252 |
| No. of strikes where footprint cannot account for observed vertical error | 73 | 56 | 46 | 31 | 16 | 222 |
| No. of strikes where footprint accounts for observed vertical error | 12 | 35 | 45 | 17 | 20 | 129 |
| Percentage of strikes where footprint accounts for vertical error | 14.1% | 38.5 | 49.5 | 35.4 | 55.6 | 36.8 |

ALTM elevation below Reference elevation-Maximum indicates the largest of the vertical errors remaining between the reference elevation and the elevation at

the uppermost edge of the footprint (see Figure 52 (a)). *ALTM elevation above Reference elevation-Maximum* indicates the largest error remaining where the ALTM elevation at the lowermost edge of the footprint is still higher than the reference elevation (d). The *Mean Absolute Error* in the table summarizes vertical error between the reference elevation and the footprint edge elevation closest to the reference elevation for these 222 laser strikes.

Data in Table 10 indicated that the 30-degree and above slope class has the highest percentage of sample strikes where the reference elevation falls within the footprint's elevation spread (55.6 percent), while the lowest slopes has the fewest reference elevations falling within the spread (14.1 percent). This was logical since the higher slopes have the larger elevation spreads between high and low footprint elevations. This relationship follows the reasoning for horizontal displacement's affect on sloping terrain (see the section, Influence of Horizontal Inaccuracy on ALTM-derived Elevations). Footprints on relatively flat terrain have rather small elevation differences. From Table 9 again, the mean elevation spread in the 0.0 to 4.9 degrees slope class is only 0.095 m. And, as highlighted previously, the imprecisions observed on lower slopes are most likely due to the other factors that comprise the ALTM system.

Of interest, was that the elevation range across the footprint can possibly explain the elevation errors observed in 129 or 36.8 percent of the laser strikes. Previous work indicated that horizontal displacement of one meter explains 152 or 43.3 percent of the strikes' vertical error. Comparing the data in tables for each (see

Table 7 and Table 10), most all of the values for mean absolute error, RMSE, maximums, etc. which describe error remaining after the adjustment are similar or less for the horizontal displacement adjustment. This observation appeared to indicate that horizontal error has more affect on vertical error than footprint size and spread. However, this statement was moderated by not knowing actual horizontal errors and effects were based on a subjective horizontal displacement of one meter.

A scatterplot of vertical error based on the spread of elevation within the footprint provided insight (see Figure 53). In this plot, an upward trend in signed error is evident although the statistical relationship is weak.

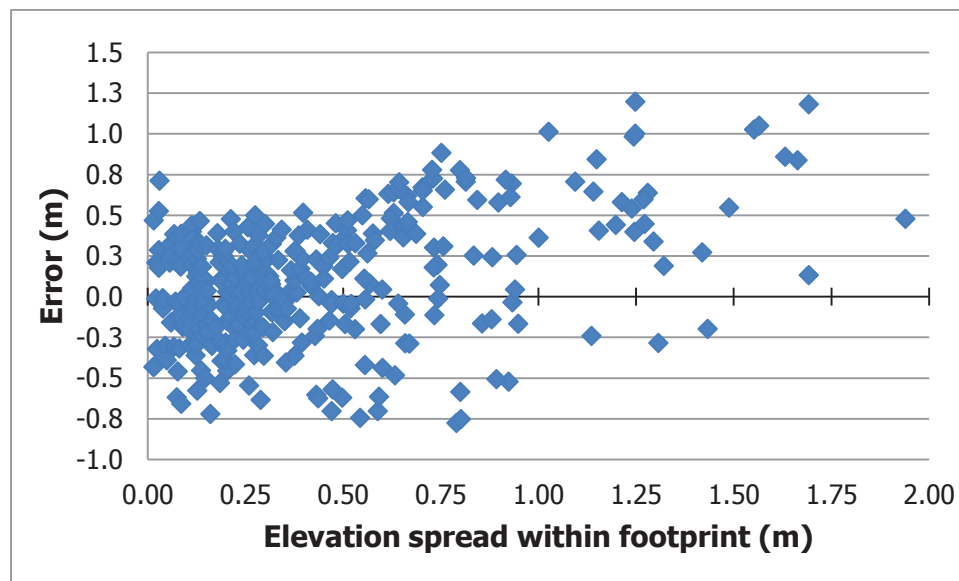


Figure 53. Scatterplot of the sampled ALTM ground strike vertical errors for all elevation spreads within footprints (n=351).

This trend may correspond with the findings of Kobler et al. (2007) and Goulden and Hopkinson (2010) in that, the uphill side of the footprint is responsible for the range measurement resulting in higher than actual elevations. This discovery may then conflict with Jutzi and Stilla (2003), Johnson (2009), and Ussyshkin et al. (2009) where the trend should be negative due to longer range measurement resulting in a lower than actual elevation. This effect also appears to contradict Baltsavias (1999a) and others who stated the reflected energy can come from elsewhere in the footprint, and not just the rising side. Interestingly, the signed error appeared capped at 0.5 m until the elevation disparity in the footprint increases to greater than 0.5 m.

Horizontal Displacement combined with Elevation Spread across the Footprint on Sloping Terrain

The next examination combined the horizontal displacement of one meter and elevations of the uppermost and lowermost edges of the footprint. Since neither can account for the majority of the observed vertical error alone, could the union of both explain all of the error?

For each laser strike where the reference elevation is higher than the ALTM-derived elevation, the change in elevation due to a horizontal shift of one-meter upslope was added to the elevation of the uppermost reach of the footprint. If this new elevation is higher than the reference, then both of these methods combined could account for the observed error. Similarly, subtracting the

elevation change due to horizontal shift from the lower edge of the footprint resulted in a new elevation for those laser strikes where the ALTM elevation was higher than the reference. This merging of elevations and displacements obviously created a best-case scenario. Table 11 provides the results of this combining.

Table 11
Descriptive Statistics of the Sampled ALTM Ground Strike Vertical Errors Remaining After Vertical Adjustment Using Uppermost and Lowermost Footprint Elevations and Horizontal Displacement

| | Slope Category | | | | | Overall |
|-----------------------------------------------------------------------------|----------------|--------------|----------------|----------------|------|---------|
| | 0.0- 4.9° | 5.0- 9.9° | 10.0- 19.9° | 20.0- 29.9° | 30°+ | |
| Adjusted ALTM elevation below Reference elevation-Maximum (m) | -0.568 | -0.334 | -0.221 | 0.022 | ---- | -0.568 |
| Max. adjusted ALTM elevation above Reference elevation | 0.68 | 0.248 | 0.114 | 0.022 | ---- | 0.68 |
| Mean Absolute Error | 0.209 | 0.121 | 0.109 | 0.022 | ---- | 0.171 |
| RMSE | 0.260 | 0.153 | 0.126 | ---- | ---- | 0.270 |
| No. of strikes where adjustments cannot account for observed vertical error | 64 | 31 | 12 | 1 | 0 | 108 |
| No. of strikes where adjustments account for observed vertical error | 21 | 60 | 79 | 47 | 36 | 243 |
| Percentage of strikes where adjustments account for vertical error | 24.7% | 65.9 | 86.8 | 97.9 | 100 | 69.2 |

ALTM elevation below Reference elevation-Maximum indicates the largest of the vertical errors where the reference elevation is still higher than the uppermost edge of the footprint (see Figure 52 (a)), after adjustment for the horizontal displacement upslope. *ALTM elevation above Reference elevation-Maximum*

describes the opposite where the ALTM-derived elevation at the lowermost edge of the footprint is still higher than the reference elevation ((d) in Figure 52). The *Mean Absolute Error* in the table summarizes vertical error between the reference elevation and the elevation at the footprint edge closest to it. Again, the data in this table are only for laser strikes not encompassed by the ALTM elevations.

As expected, the wider elevation spreads created by combining the imprecision due to planimetric displacement and elevations at the edges of the footprint led to better results. A larger percentage of reference elevations are within these extreme ALTM elevations. The number of reference elevations falling within the broadened ALTM elevation spread increases from 152 for the horizontal displacement adjustment alone to 243 or 69.2 percent (Using only the elevation spread within the footprint alone, 129 reference elevations fall within the uppermost and lowermost reaches). While the combination of the horizontal adjustment and elevation spread is better than each used individually, the expanded elevation range still cannot account for the observed error of 108 strikes (30.8%).

Combination of the two resulted in improvements across all slope strata. The mean absolute error, RMSE, and maximum values across all strata are less than each method used singly. As slope increases, the broadening of the elevation range results in a higher success rate between successive strata. Most notable was that the combination of these two adjustments can explain all of the error in

the 30-degree and above strata. These two techniques provide such an expansive elevation spread for each of the strikes in the 30-degree and above strata that the reference elevation are well within the ALTM adjusted elevation extremes. Similarly, for all other strata other than the 0.0 to 4.9 degree stratum, the success rate was impressive.

The combined adjustment can only explain a portion of the disparity on the lowest of slopes. In the 0.0 to 4.9 degree category, the combination of these two models can only account for 24.7 percent. As previously discussed, elevation change, as the result of planimetric displacement or disparity across the footprint, on flat and low sloping terrain is negligible compared to the observed ALTM vertical error. As presented previously, the error in this stratum may be the result of ALTM system imprecision that may be equally present in all other strata.

Completion of the investigations pertaining to footprint, focus was then on other factors.

Influence of Incidence Angle on ALTM-derived Elevations

Highlighted previously, Johnson (2009) measured a decrease in pulse power off a tilted reflecting surface. His findings are graphically illustrated in Figure 7. This decrease in pulse power results in an increase in imprecision in the range. Jutzi and Stilla (2003) and Ussyshkin et al. (2009) showed a similar outcome when a laser pulse struck flat terrain at an angle of 33 and 30 degrees, respectively.

Schaer et al. (2007) and Stebler et al. (2009) also recognized a loss in accuracy

due to the angle at which the pulse intersects the ground. They surmised that as incidence angle, the angle between the vector normal to the terrain and the laser beam (see Figure 8) increases, ALTM accuracy decreases. An angle of zero degrees indicates that the terrain is perpendicular to the laser beam's path and thus, the vector normal to the terrain is pointed directly at the LiDAR system. The literature review did not find any studies with specific vertical error data relative to incidence angle.

For this study, the incidence angle was determined for each laser strike. Again, incidence angle is the angle between a vector normal to the terrain (vector \hat{n}) and the centerline of the laser beam (vector \mathbf{r}). Both of these vectors were derived in a previous section (see Influence of Laser's Footprint Size on ALTM-derived Elevations). Equation (14) provided the incidence angle between the two vectors.

Summarizing the results, the mean incidence angle of the sampled strikes is $18^{\circ}37'18''$ (SD $10^{\circ}43'31''$). The high standard deviation indicates that the incidence angle is, as was expected, highly variable and not truly centered about mean value. Allotting the incidence angles into slope strata assisted in detecting patterns. These observations are shown numerically in Table 12:

Table 12

Descriptive Statistics of the Sampled ALTM Ground Strike Incidence Angles by Slope Strata

| | Slope Category | | | | | Overall |
|--------------------|----------------|-----------|------------|------------|-----------|-----------|
| | 0.0-4.9° | 5.0-9.9° | 10.0-19.9° | 20.0-29.9° | 30°+ | |
| Mean | 12°32'25" | 14°35'14" | 18°47'12" | 23°27'19" | 36°19'04" | 18°37'18" |
| Standard deviation | 6°52'27" | 5°10'17" | 9°53'25" | 10°17'38" | 9°22'46" | 10°43'31" |
| Minimum | 0°02'39" | 5°23'22" | 1°52'14" | 4°55'40" | 13°57'27" | 0°02'39" |
| Maximum | 26°25'18" | 28°09'51" | 40°10'52" | 42°02'55" | 50°43'24" | 50°43'24" |

The range of incidence angles is from 0°02'39" to 50°43'24". By comparing the means of each slope stratum, incidence angle increases as slope increases. This relationship was logical since slope factored highly into calculating the vector normal to the terrain. The standard deviation values for each slope category indicate that there is variation in each stratum. Again, these departures are due to slope aspect and scan angle combining to create a large (or small) incidence angle, even on flat terrain. Interestingly, relatively small incidence angles, seen in the Minimum row in Table 12, occur on slopes up into the 20.0° to 29.9° stratum. These occurrences are possible since the largest scan angle of the sampled strikes is 22°15'57" and high scan angle values can negate similarly high slope angles. However, for this to occur, a strike would also have to be situated on slope parallel to the flight line and on the correct side of the flight line so that the scan and slope angles diminish each other versus complementing each other. It was thought that these four variables combining to create a small incidence angle on steep slopes would have a low probability given the relatively small number of sampled strikes (n=351). Nevertheless, as evidenced, many

small incidence angles occurred on steeper slopes. The relationship and the influence of slope angle on incidence angle are best illustrated in Figure 54, where an easily observable upward trend in incidence angle due to slope exists. The unexpected interplay between scan angle and slope aspect producing low incidence angles is also visible in the figure. These are centered about 18 degrees.

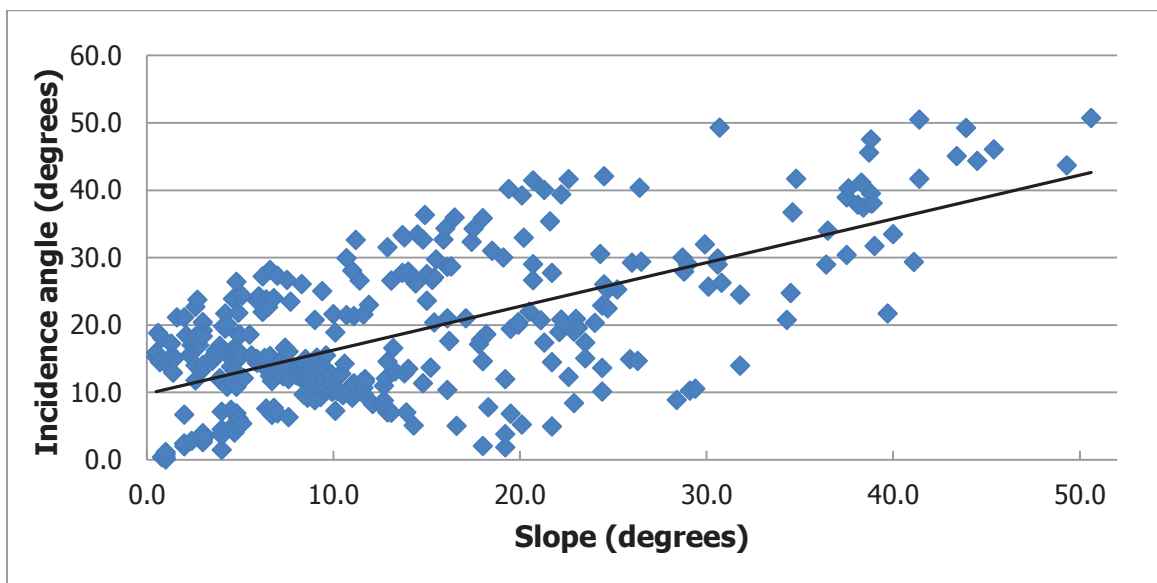


Figure 54. Scatterplot of the sampled ALTM ground strike incidence angles relative to slopes (n=351).

The correlation coefficient describing the relationship between slope and incidence angle is 0.659 (r). A linear model where the variation in incidence angle explained by slope has a coefficient of determination of 0.434 (R^2) and is significant as is the t -test for the slope coefficient ($p = .000$ for both):

$$\text{Incidence angle} = 0.650 \cdot \text{Slope angle} + 9.765 \quad \text{Eq. (25)}$$

The standard error of the estimate is 8.083.

Initial expectations had footprint size and incidence angle wholly correlated.

However, from Figure 55, while the correlation is strong ($r=.810$), variation

exists:

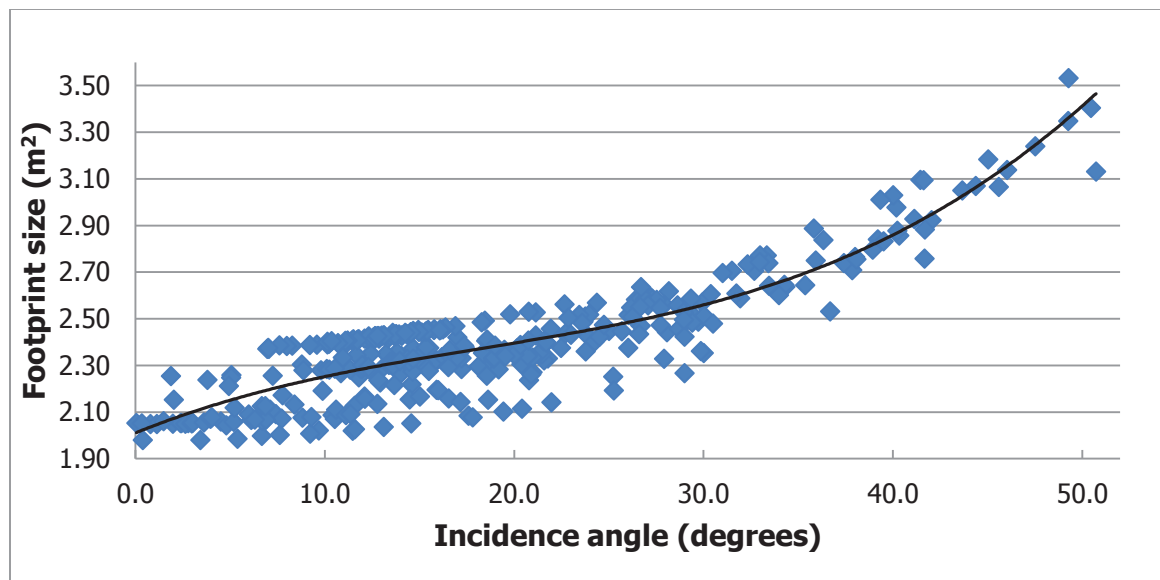


Figure 55. Scatterplot of the sampled ALTM ground strike footprint sizes relative to incidence angles ($n=351$).

The deviations are the result of the differing elevations of strikes. When two strikes have similar scan angles, slope angles, and slope aspect and thus, incidence angles, differing elevations result in dissimilar ranges and footprint sizes. A third-order polynomial line best fit the data:

$$\text{Footprint size} = 0.00002 \cdot x^3 - 0.0011 \cdot x^2 + 0.033 \cdot x + 2.011 \quad \text{Eq. (26)}$$

The ANOVA of the model and t -tests testing the significance of the predictor coefficients found all to be significant ($p = .000$). The coefficient of determination is also high ($R^2=0.810$). The standard error of the estimate is 0.111 m. A Ramsey RESET indicates that the addition of the x^3 term provided for a better model than linear or quadratic.

Plotting the incidence angle versus vertical error for each sampled strike, yielded an obvious pattern (see Figure 56). With low incidence angles, less variation in vertical error occurs. As incidence angle increases, the range of error also increases to a maximum spread when the incidence angle is circa 40 degrees. Any visual pattern with higher incidence angles was not obvious, possibly due to the limited number of sampled points above 40 degrees ($n=20$).

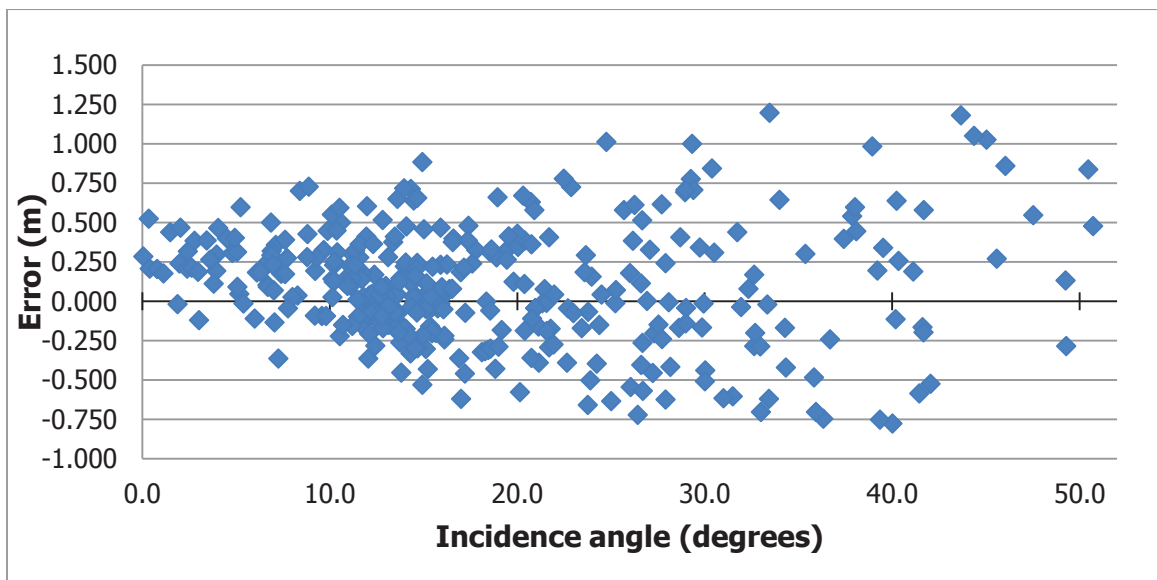


Figure 56. Scatterplot of the sampled ALTM ground strike vertical errors for all incidence angles ($n=351$).

The dispersion pattern of vertical error is evident where the dispersion increases as incidence angle increases. This scattering was also evident using absolute vertical error values (see Figure 57). This observation was interpreted to mean: precision decreases as incidence angle increases. This dispersion may be based on Baltsavias' (1999a) and others' beliefs that the reflected signal may come from anywhere in the footprint. Horizontal inaccuracy may also be responsible for some of the dispersion on higher slopes, similar to vertical error on sloping terrain. These data confirm some of the findings of Schaer et al. (2007) and Stebler et al. (2009): the spread of error increases as incidence angle increases. These authors did not investigate the relationship between elevation error and incidence angle any further as their focus was on assigning a quality indicator on each laser strike.

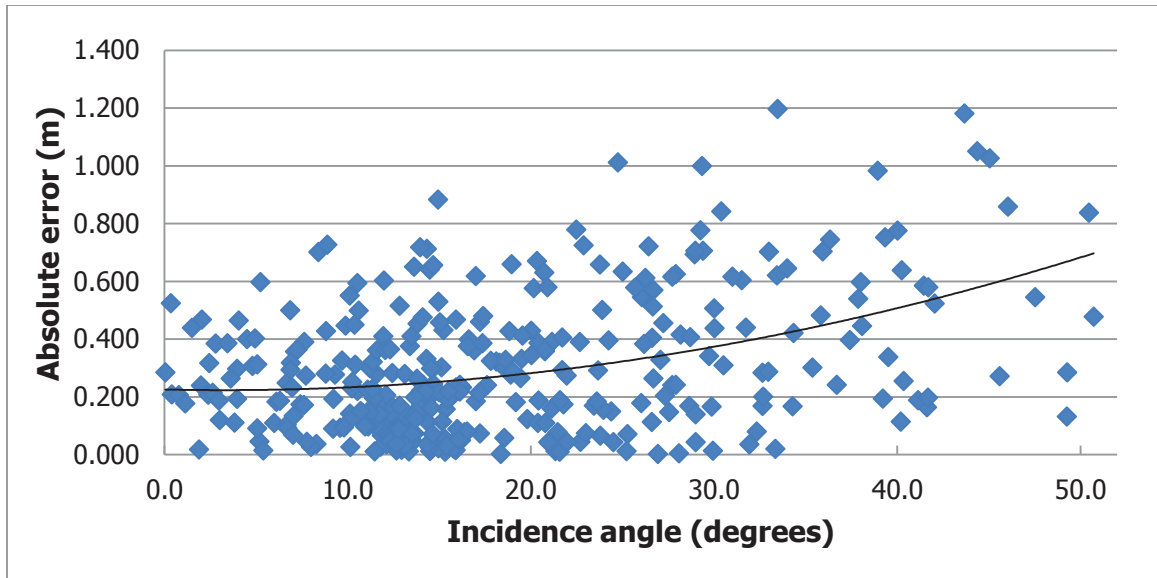


Figure 57. Scatterplot of the sampled ALTM ground strike absolute vertical errors for all incidence angles (n=351).

As for trends, no strong trend was evident using either signed or absolute errors. This absence appeared to contradict the findings of Kobler et al. (2007) and Goulden and Hopkinson (2010) whereby, signed error should have increased as incidence angle increases if the rising portion of the footprint is responsible for the reflection of the pulse and range measurement. Under scrutiny, a slight downward trend is somewhat visible in the scatterplot of signed errors (Figure 56). This trend may exist for incidence angles between zero and fifteen degrees, possibly extending out to 30 degrees. Sampled strikes with low incidence angles ($<10^\circ$), tend to have positive (signed) errors. Thus, strikes with lower incidence angles have higher elevations than the reference elevations. As incidence angle increases, the sign of the errors follows a downward trend until circa 30 degrees, where the vertical error centers about zero meters. This negative trend would

agree with the findings of Jutzi and Stilla (2003), Johnson (2009), and Ussyshkin et al. (2009), who found that lengthening of the return pulse, due to tilting of the target surface increases range error, which, in turn, results in a lower than actual elevation. Since the vertical error shown in this plot is the difference when the reference elevation is subtracted from the ALTM-derived elevation, the trend of an increasing negative error indicates a lower than actual ALTM elevation. However, the trend is as not readily visible as was expected based on the definitive findings of their works. The calculation of a least squares linear model fitted to signed error results in a line with almost no slope, an extremely low coefficient of determination ($R^2=0.002$) and being not statistically significant ($p = .464$). A quadratic curve yielded a significant model ($p = .000$) but also has a low coefficient of determination ($R^2=0.059$).

The lack of a clear link was notable given the relationship between incidence angle and slope angle and the association between slope angle and signed error. The pattern is similar to scan angle versus vertical error (see Figure 38). It may be that with low incidence angles, the influence of scan angle on vertical error is predominating but no linkage was evident between the two. Alternatively, this pattern may be due to the rather small number of sampled strikes with incidence angles less than ten degrees ($n=61$). Similarly, another reason may be that laser strikes on level terrain but with high scan angles will register as having high incidence angles. Since 267 of 351 samples were on slope less than twenty degrees (176 samples were on slopes $<10^\circ$), not many samples remained on

higher slopes with which to evaluate. A scatterplot and statistical analysis of these remaining 84 strikes yielded similar results to the above data.

Modeling the relationship between absolute vertical errors and incidence angle yielded the following:

$$\text{Absolute vertical error} = 0.0002 \cdot \text{Incidence}^2 + 0.226 \quad \text{Eq. (27)}$$

The ANOVA for this model indicates significance ($p = .000$) as does the t -test for the incidence angle squared coefficient ($p = .010$). There is no incidence angle coefficient in the model as the t -test for this coefficient is not significant ($p = .772$). The Ramsey RESET indicates that a linear model is misstated and thus, the quadratic model above is a better fit. The coefficient of determination for the quadratic model is still low: 0.158 (R^2) and the standard error of the estimate high (0.216) such that, the model is rather weak. Nevertheless, it aided in visualizing that absolute vertical error increases as incidence angle increases.

From this portion of the study, no strong trend between incidence angle and signed or absolute error was evident. However, as incidence angles increases the dispersion of both signed error and absolute error increases, which indicated that precision decreases.

Comparing incidence angle to scan angle and slope aspect generated less convincing relationships.

Influence of Slope Aspect on ALTM-derived Elevations

As evidenced previously, slope aspect, in conjunction with slope and scan angle, impart some influence on incidence angle, footprint size, and vertical error.

Figure 58 shows vertical error plotted against aspect for each sampled ground strike.

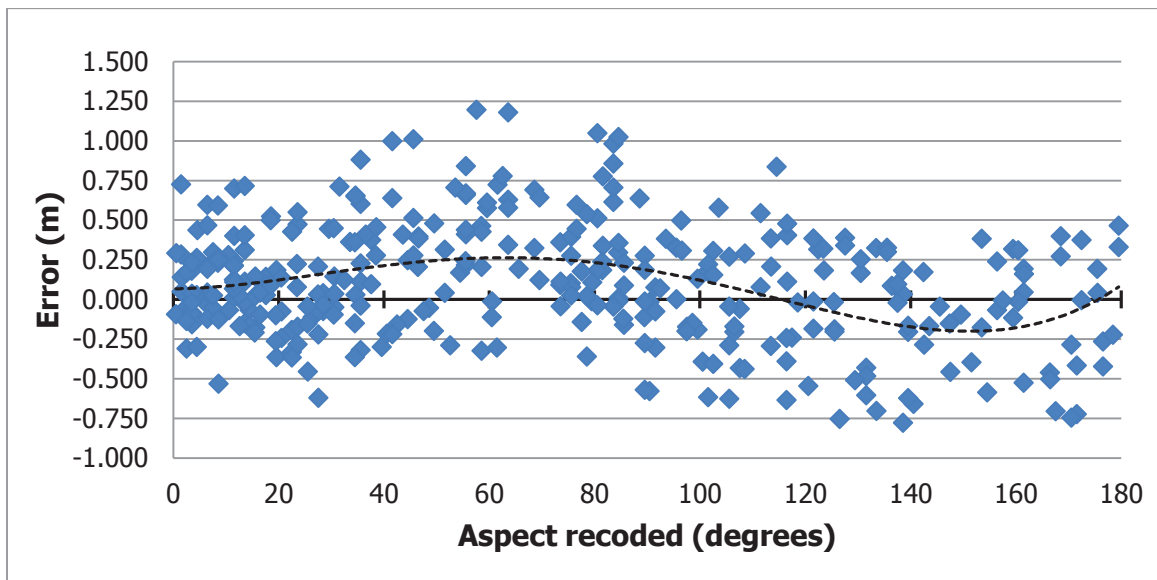


Figure 58. Scatterplot of the sampled ALTM ground strike vertical errors for all recorded slope aspects (n=351).

In the figure, the aspect range extends from zero to only 180 degrees. All of the azimuths were recoded for two reasons: Since azimuths typically range from zero degrees to 360 degrees, an inherent problem exists. A slope with an azimuth of 359 degrees is quite similar to a slope with an azimuth of one degree. However, statistical analyses and visual aids, such as scatterplots, often make no connection between zero degrees and 360 degrees. They typically depict these

two values as opposite ends of a scale. In addition, for this study the absolute azimuth of the slope was of less value than knowing the orientation of the slope relative to the flight line. As discussed in the section, Influence of Laser's Footprint Size on ALTM-derived Elevations, the laser beam intersecting a slope parallel to the scan line creates a much larger footprint and typically, a greater incidence angle than a beam intersecting a slope facing the flight line. Thus, the orientation of the slopes of the sampled strikes were recoded such that a slope facing the flight line (i.e., perpendicular) was assigned the value of 0 degrees (see (a) in Figure 59). A slope facing the direction of flight (i.e., parallel to the scan line) was assigned a value of 90 degrees. A slope perpendicular to the flight path but facing away has a new value of 180 degrees (see (b) in Figure 59).

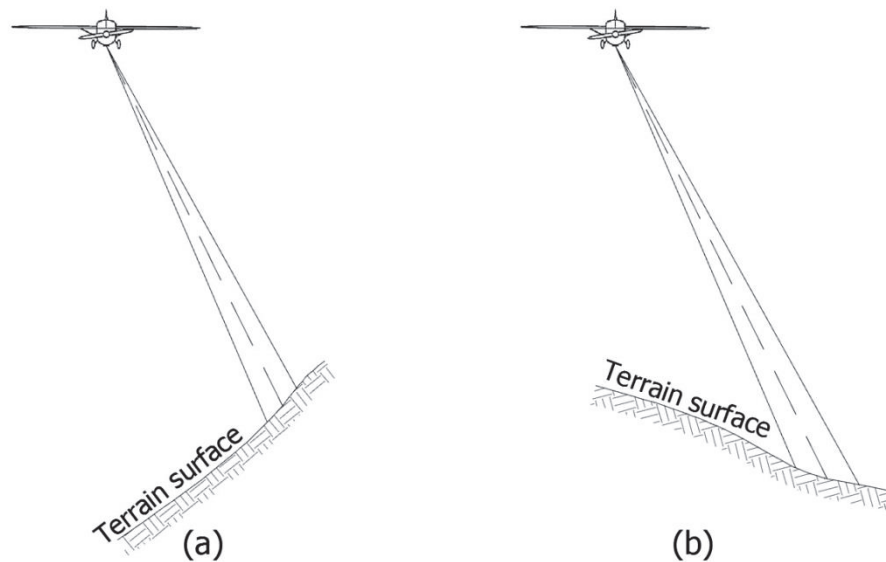



Figure 59. Orientation of slope to the flight Line.

Recoding resulted in a slope facing the direction from where the flight had originated having the same value as a slope facing the direction of the flight: both were coded $91^{\circ}27'14''^{17}$. Similarly, there was no distinction between laser strikes located on opposite sides of the flight line. Since the swath of one flight line mapped the entire study, complications due to numerous flight lines were not issues.

Comparing aspect to elevation error, one unexpected pattern appeared. From Figure 58, the mean signed vertical error appeared to increase from zero degrees to approximately 70 degrees. Beyond 70 degrees, the signed error decreases until approximately 150 degrees. From 150 degrees to 180 degrees, signed error increases again. The dashed line added to the figure aided in visualizing this pattern. Based on Kobler et al. (2007) and Goulden and Hopkinson (2010), the rising side of the footprint responsible for the range measurement should have resulted in a trend resembling a moustache () with the apex centered at 90 degrees. Based on Jutzi and Stilla (2003), Johnson (2009), and Ussyshkin et al. (2009), the expectation was for no trend at all as sloping terrain and/or scan angles would be responsible for the tilted surfaces resulting in longer range measurements and vertical error making slope aspect irrelevant.

The pattern observed may not be the result of a direct relationship between error and aspect; it may be due to the influence of slope angle on error but

¹⁷ Azimuth of the flight line was $181^{\circ}27'14''$.

not as Jutzi and Stilla, Johnson, and Ussyshkin et al. postulated. As presented previously, vertical error increases as slope increases (see section, Influence of Sloping Terrain on ALTM-derived Elevations). The signed error of laser strikes with aspects of zero and 180 degrees center about 0.000 m in Figure 58. From Figure 60, these aspects tend to be on flat and gently sloping terrain.

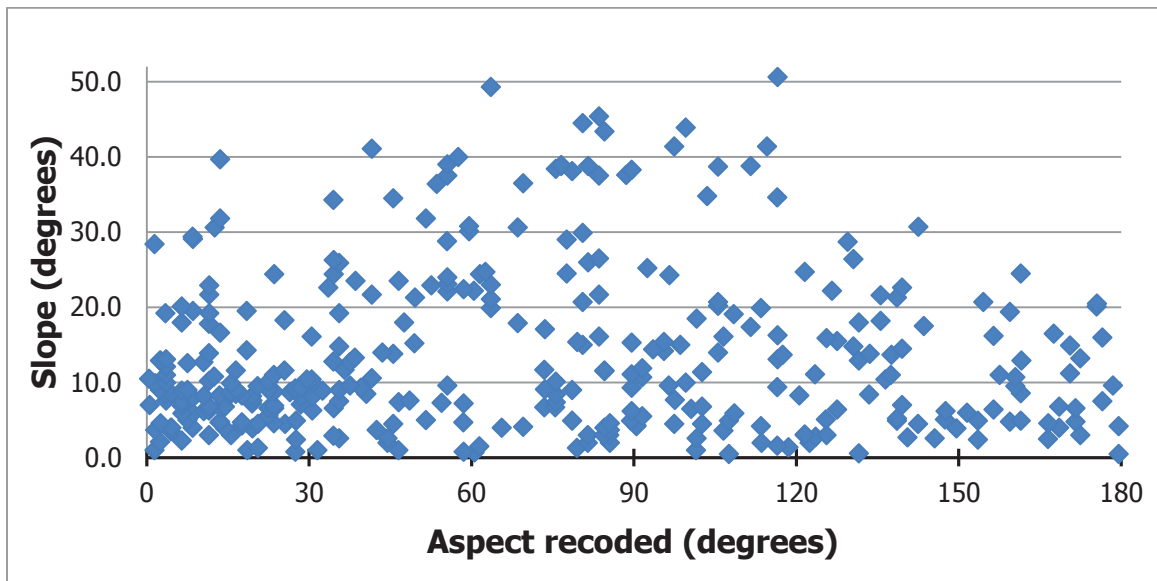


Figure 60. Scatterplot of the sampled ALTM ground strike slopes relative to recorded slope aspects (n=351).

A scatterplot with only strikes on slopes greater than twenty degrees (n=84) yielded a similar result but with more pronounced curves. However, the reason for the fluctuation in signed error between these two extremes is not entirely known.

Concerning Kobler et al. and Goulden and Hopkinson's theories, expectations were for greater positive signed errors with recorded aspects of 90 degrees. A

laser beam striking a slope nearly parallel to the scan should result in large footprints due to a smearing of the light across the terrain. Greater footprint sizes at these aspects should have resulted in higher signed errors due to the larger and higher rising side of the footprint. Goulden (2009) had also noted this association should result in an error increase. This observation would also correspond to previous findings in this study which show a linkage between vertical error and increasing slope (see Influence of Sloping Terrain on ALTM-derived Elevations). The amount of positive vertical error would then decrease as footprints became smaller due to slope aspect changing from 90 to 180 degrees. From Figure 58, this relationship was not evident. This outcome lead to creation of a scatterplot comparing aspect against footprint size (see Figure 61).

In this figure, footprint sizes do not follow the expected pattern of being small with low recoded aspects, becoming greater for recoded aspects of 90 degrees, and then reducing in size again for aspects approaching 180 degrees.

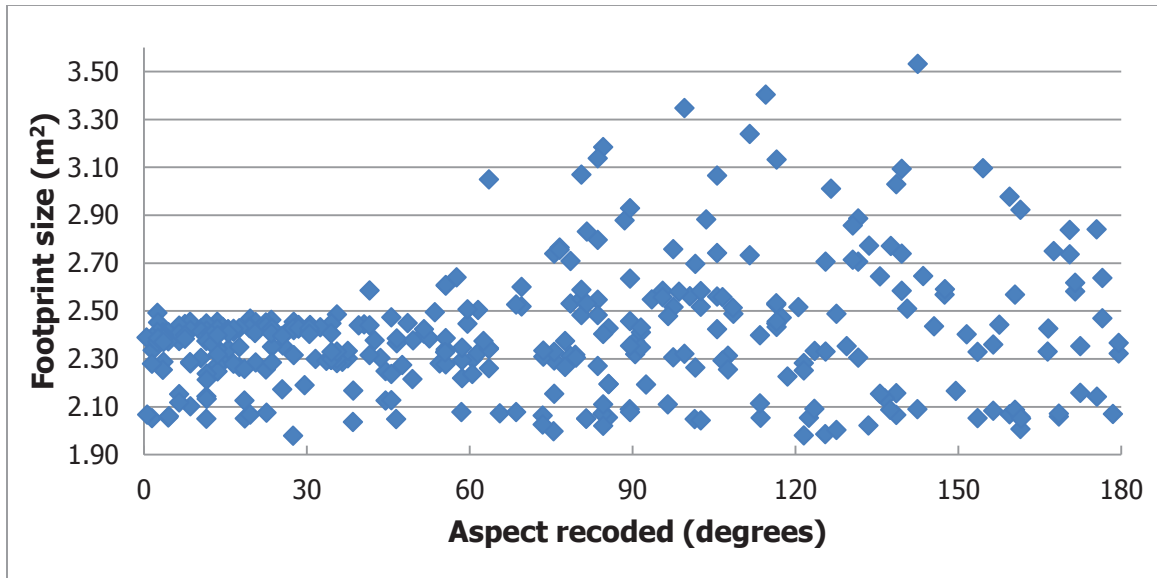


Figure 61. Scatterplot of the sampled ALTM ground strike footprint sizes relative to recorded slope aspects (n=351).

Figure 61 added more perplexity with footprint size capped at 2.50 m² for aspects below 54 degrees and dispersion continuing to increase as aspect increases beyond 90 degrees. The reasons for these observations are also unknown.

Of note, was that dispersion of vertical error remains fairly uniform regardless of recorded aspect (see Figure 58). From this and other observations, slope and scan angle may be more influential than aspect, especially given the high flying height of this study.

Influence on Ground Elevation on ALTM-derived Elevations

By qualitative evaluation of the data in Figure 62, two relationships between elevations of laser ground strikes and vertical error seemed apparent. First, the distribution of elevations is in three groups: the first cluster is centered about the elevation of 120 m (height above the ellipsoid) and the second is around 150 m. The third grouping of sampled strikes, have elevations between 210 and 265 m.

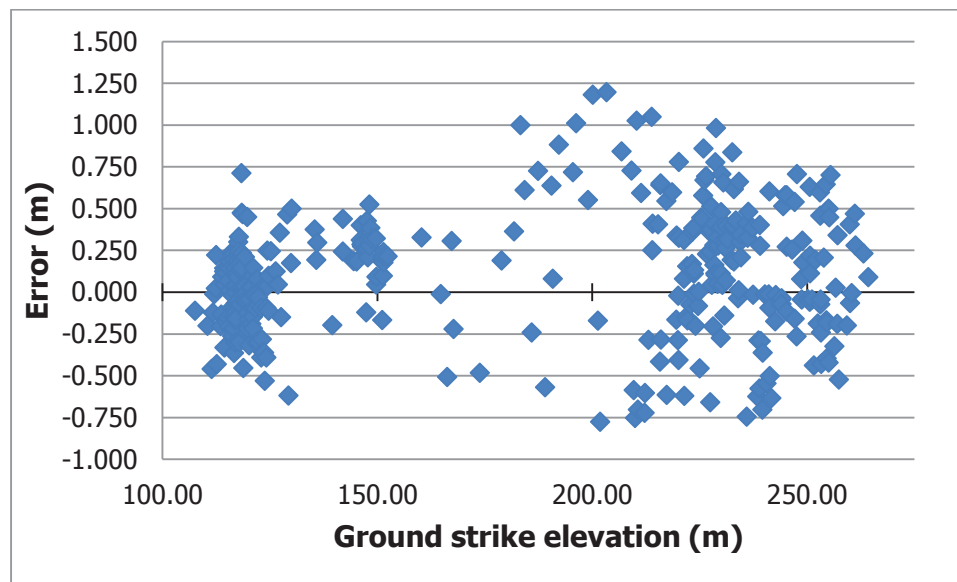


Figure 62. Scatterplot of the sampled ALTM ground strike vertical errors for all ALTM-derived elevations (n=351).

These groupings are the result of sample locations in the study area. The first cluster of strikes is on relatively level terrain within the ring dike. The strikes with elevations of 150 m are from a different locale located between Middle Mountain and South Mountain in the southeast quadrant of the study area (see Figure 13, Topographic map showing ring dike of Pawtuckaway Mountains and Figure 31,

Plan view of the sampled ALTM ground strike locations with vertical errors coded by magnitude (n=351)). Here, the floor between these two peaks is higher than that of the ring dike floor but the samples are also on predominately level terrain. This clustering is the result of opportunistic sampling of open areas. The higher strikes (210+ m) are on the slopes of Mount Pawtuckaway and South Mountain.

The second relationship visible in Figure 62, are differences in error dispersion between these groupings. The least amount of spread is in the 150 m grouping, while the 118 m group also has little dispersion. These spreads are the result of greater influence by the other factors previously discussed, such as slope, rather than substantial influence by ground strike elevations.

Comparisons were made of strike elevations to factors influencing vertical error (e.g., slope, scan angle). Because the majority of sampled laser strikes at the 118 m elevation are in close proximity to one another, they all have similar slopes ($<15^\circ$), incidence angles, (5° to 20°), footprint sizes ($\sim 2.4 \text{ m}^2$) and recoded slope aspects ($<30^\circ$). The laser strikes in the 150 m grouping are also in close proximity to one another and showed similar relationships to other factors: Slopes ($<10^\circ$), incidence angles ($<10^\circ$), footprint sizes ($\sim 2.0 \text{ m}^2$) and recoded slope aspects ($<30^\circ$).

From the scatterplot of vertical errors against strike elevations shown in Figure 62, no strong linear (or curvilinear) correlation was evident. A least squares line was plotted which has only a very slight rise:

$$\text{Vertical Error} = 0.001 \cdot \text{Ground Elevation} - 0.085 \quad \text{Eq. (28)}$$

While the model and coefficient are valid ($p = .005$ for both), the coefficient of determination is very low ($R^2 = 0.022$). The standard error of the estimate is 0.363. A similarly weak relationship exists between ground strike elevations and absolute errors: Defined best by a quadratic relationship, the coefficient of determination is 0.092 (R^2) and the standard error of the estimate is 0.210. This model and its coefficients are significant ($p = .000$ for all). Both of these models indicated that as ground elevation increases, vertical error increases. While weak, this observation is contrary to most studies where the closer the LiDAR unit is to the ground (i.e., the shorter the range), the more accurate the ALTM-derived elevations (see Flying Height Influence on ALTM Errors). Haneberg (2008) was one of the few studies that investigated the relationship between elevation and vertical error but also found that higher elevations resulted in less error.

Since the lower two clusters (elevation-wise) are on flat terrain, it may be the slope has more influence over vertical error dispersion than ground elevation. The lower two clusters again, are the result of opportunistic sampling, and may

be misleading the findings. While the relationship between absolute error and elevation was statistically significant, it was weak with no explanatory power.

Influence of Laser Range on ALTM-derived Elevations

Given the contrarian findings of ground elevation in regards to vertical error in the last section, the next logical investigation was between vertical error and range. From previous studies, the expectation was for less accurate elevations and precision as range increased (see the section, Flying Height Influence on ALTM Errors). The relationship found in this study is shown graphically in Figure 63.

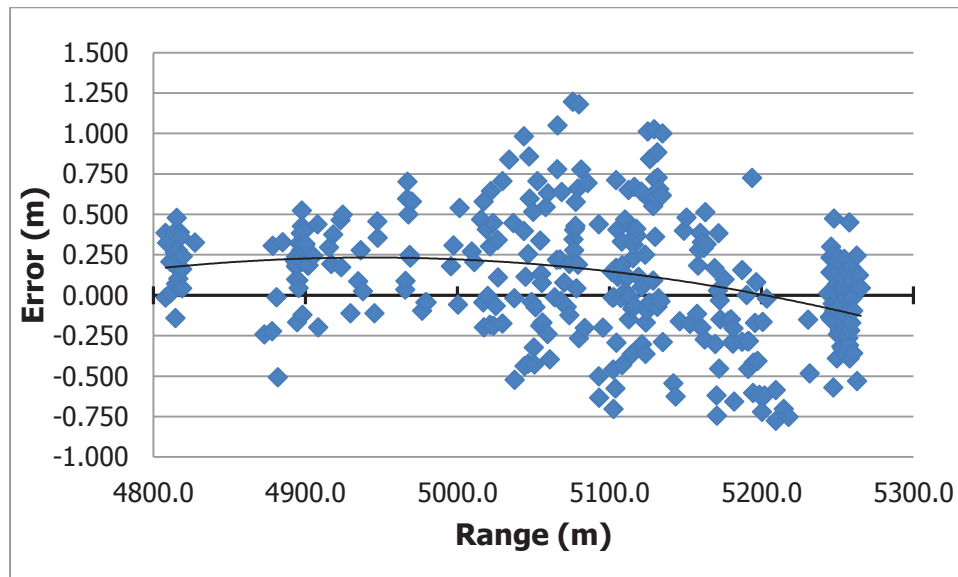


Figure 63. Scatterplot of the sampled ALTM ground strike vertical errors for all laser pulse ranges (n=351).

A quadratic equation describes this relationship further:

$$\text{Vertical error} = -0.0000035 \cdot \text{Range}^2 + 0.034 \cdot \text{Range} - 84.178 \quad \text{Eq. (29)}$$

This model is more representative than a linear model based on the results of a Ramsey RESET. The model and coefficients are all significant ($p = .000$ for the model, $p = .001$ for Range^2 and $p = .002$ for Range). The coefficient of determination (R^2) is quite low though, at 0.110 with the standard error of the estimate high, at 0.346. These values indicated a weak link between range and error. By viewing the scatterplot and examining the equation, the relationship seemed anomalous: signed error increases, then decreases as range increases. Similar to the relationship of ground elevation on vertical error, this relationship may skew from opportunistic sampling.

From Figure 63, two clusters of sampled strikes are evident. These two groupings have average ranges of 4810 m and 5250 m. These clusters correspond to the same ground elevation groupings seen in Figure 62 (see section, Influence on Ground Elevation on ALTM-derived Elevations). The cluster about the range of 4810 m is the same set of strikes with an elevation of 150 m. The second cluster with a range averaging 5250 m corresponds to those strikes with elevations of 118 m. This correlation initially seemed incongruent since the shortest ranges should correspond to the highest elevations (Note in Figure 62 that the highest elevations are greater than 250 m). However, scan angle also dictates range, and in this study, more so than elevation. The grouping of strikes about the range of 5250 m is associated with the higher scan angles.

In Figure 63, ignoring these two clusters (about 4810 m and 5250 m), vertical error appeared to increase as range increases. However, a direct linkage between increasing error and range still was not evident.

As alluded to, a strong relationship between range and scan angle exists, as evidenced by the scatterplot in Figure 64.

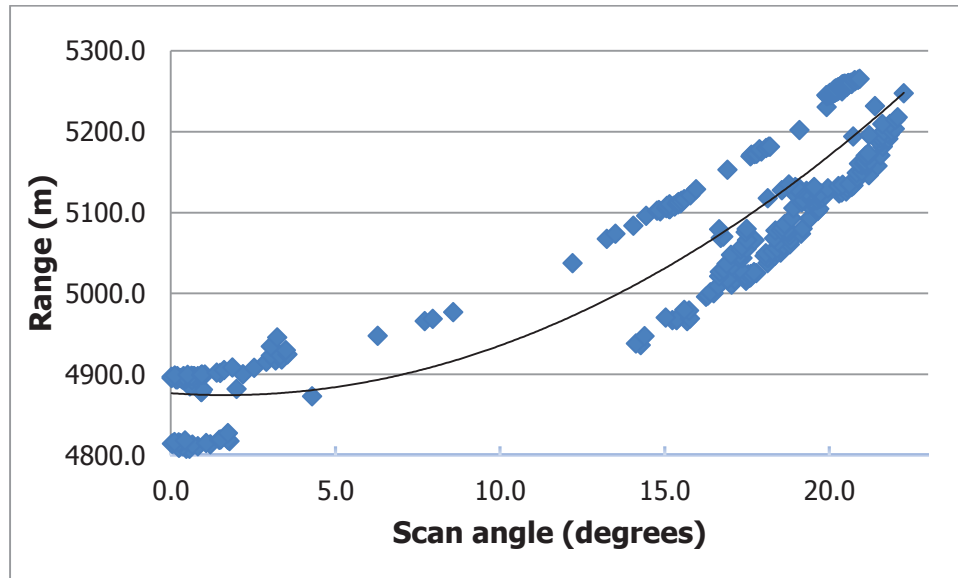


Figure 64. Scatterplot of the sampled ALTM ground strike laser pulse ranges to scan angles (n=351).

From the figure, as scan angle increases, range increases quadratically. This correlation is the result of the geometry of the scan angle and flying height and, as evidenced, to a lesser degree, ground elevation.

One of two noticeable artifacts in the figure is the gap between sample strikes with scan angles of three and thirteen degrees, approximately. This break between the samples is also the result of the opportunistic sampling method,

which limited sample sites in the study area. This gap is also visible in Figure 38, Scatterplot of the sampled ALTM ground strike vertical errors for all scan angles on slopes less than 10° (n=176), Figure 39, Scatterplot of the sampled ALTM ground strike vertical absolute errors for all scan angles on slopes less than 10° (n=176), and Figure 48, Scatterplot of the sampled ALTM ground strike footprint sizes relative to scan angles (n=351).

Also visible in Figure 64, is the gap in the data with respect to range. Two separate groupings of laser strikes were apparent. Moreover, two distinct curved lines appeared to represent the data: one curve could begin with a range of 4800 m and the other 4900 m. This separation of laser strikes into two groups is also the result of the terrain and sampling methods. Open areas for sampling at nadir are on the floor of the ring-dike (represented by data with a range of 4900 m) or on the ridgeline of South Mountain (ranges of 4800 m). Similarly, sample locations with higher scan angles are on the ring-dike floor or on the ridgeline of Mount Pawtuckaway. However, the data were treated as a whole as they were for other portions of the study.

The coefficient of determination (R^2) for the relationship between range and scan angle is 0.808, indicating a strong association. The best-fit model is described by:

$$\text{Range} = 0.879 \cdot \text{Scan angle}^2 + 4876.7 \quad \text{Eq. (30)}$$

The ANOVA and t -test for the scan angle square coefficient are significant ($p = .000$), while the t -test for the scan angle coefficient is not ($p = .185$). The Ramsey RESET found the coefficient of the linear model to be misstated, resulting in the quadratic model being a better fit. However, given the distinct separation between the data (the strikes above the line versus the strikes below the line in the figure), the standard error of the estimate is quite large (57.602 m).

Scatterplots of laser range showed no relationships with other factors except for footprint size. Footprint size increases as range increases (see *Figure 65*). This association was logical since the laser beam diverges and expands as it travels away from the emitter.

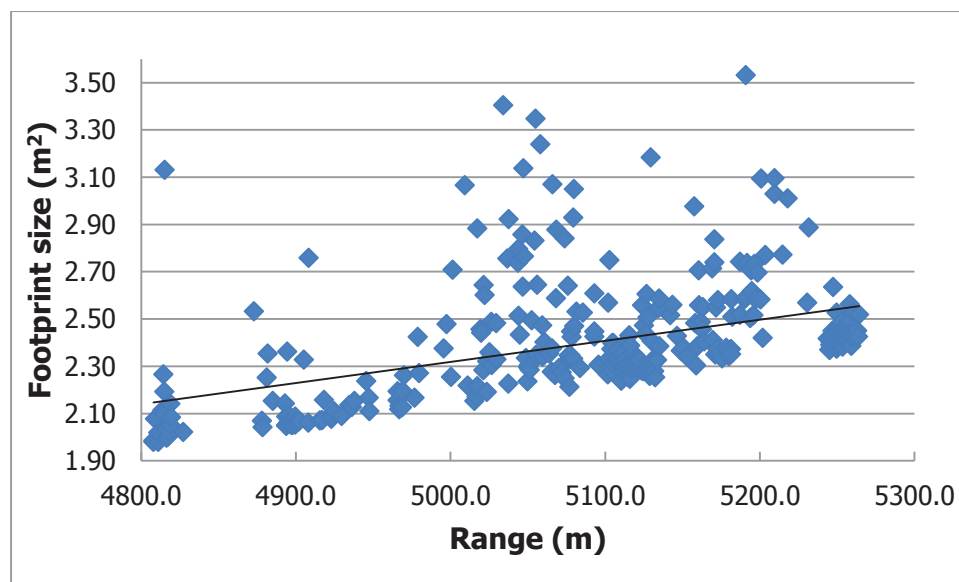


Figure 65. Scatterplot of the sampled ALTM ground strike footprint sizes relative to laser pulse ranges (n=351).

The coefficient of determination for this relationship is 0.212 (R^2). The ANOVA to test the model and the t -test of the slope coefficient are both significant ($p = .000$). The standard error of the estimate is 0.225. The linear equation best described this relationship:

$$\text{Footprint size} = 0.001 \cdot \text{Range} - 2.13 \quad \text{Eq. (31)}$$

A curvilinear model fit slightly better based on the coefficient of determination and the comparative Ramsey RESET test. However, the laser strikes with ranges from approximately 5010 m to 5080 m having larger footprints unduly influenced the model.

Similar to scan angle and ground elevation, the limitation of laser strike sampling to the relatively few areas of the study site constrained interpretations from the range data. A trend between range and signed error was weak and contradictory and no clear relationship between range and dispersion was observed in this study.

Determination of Most Influential Factors on ALTM-derived Elevations

After investigating the effects each factor (e.g., slope, scan angle, slope aspect) had on vertical error individually, the examination then focused on the interplay between the factors.

Using inferential statistics, the best analyses proved to be stepwise linear regression. This technique specifically allows inspection of the affect each factor has on error with the other factors present. This type of regression also provides some clues about the interplay between factors and identifying dominate factors.

The nine factors for each laser strike used in the regression models were:

- Terrain slope angle
- Slope aspect angle-recoded
- Scan angle
- Incidence angle
- Footprint size
- Difference in elevation across footprint
- ALTM-derived elevation
- Laser range
- Terrain slope angle squared

The outcome variable was signed vertical error (subtracting reference elevations from ALTM-derived elevations).

Terrain slope angle and slope aspect angle came from field data while the remaining factors derived from subsequent calculations, as explained in prior sections.

As derived previously, a quadratic equation best describes the relationship between vertical error and slope (see the section, Influence of Sloping Terrain on ALTM-derived Elevations and Equation (10). In order to include this relationship

in a linear regression where all other predictors were linear, the values for slope were squared, creating a new predictor.

The result of these analyses is the following regression model:

Vertical error =

$$0.001 \cdot Slope^2 - 0.024 \cdot Incidence\ angle + 0.001 \cdot Elevation \quad Eq. (32)$$

Expounding this formula:

- As terrain slope is squared and increases by one degree, vertical error should increase 0.001 meters.
- As incidence angle increases by one degree, vertical error should decrease by 0.024 meters.
- As ground elevation of the laser strike increases by one meter, vertical error should increase by 0.001 meters.

Examination of the model's components yielded some not so logical findings: Of interest was the inclusion of incidence angle in the model, specifically, an inverse relationship whereby, as incidence angle increases, signed vertical error decreases. Also noteworthy was another contrarian relationship between laser strike ground elevations and vertical error whereby, as the higher the elevation, the greater the vertical error.

For this analysis, one of the governing elements of stepwise regression, the *F-to-enter* statistic, was set at .05. Meaning, only those predictors with probabilities less than .05 (significant at the 95% confidence level) could be used in the

model. The *F-to remove* criteria for predictors already in the model was set to .10 meaning, predictors with probabilities greater than .10 (at the 95% confidence level) were removed from the model (SPSS, version 19).

While there is much criticism of stepwise regression (Whittingham, Stephens, Bradbury, & Freckleton, 2006; Mundry & Nunn, 2009; Hegyi & Garamszegi, 2011), one of its beneficial uses is in narrowing down the influential predictors and combinations thereof when the combinations are many. In this study with nine predictors, there were nearly 363,000 possible combinations.

While the software automated the process, correct use requires much hands-on work reviewing each model's residual errors for homogeneity, outliers, inspection for cases of multi-collinearity, and omission of legitimate predictors.

The statistical software allows for several different types of stepwise regressions processes, including forward regression. This process produced identical models to those created using the stepwise process. Additionally, manual multiple regressing using varying predictors confirmed these results. Evaluation between models used in part, the Akaike Information Criterion (AIC). Normally but not always, the model with the lowest AIC indicates the best model, after assessment of validity of the predictors, proper inferences, etc. (Mazerolle, 2006). The model given in equation (32) had an AIC value of -933.172.

During model development, other predictors were included. Due to the lack of clear linear relationships between factors and vertical error, other factors such as

incidence angle squared and range squared were also included in some of the iterations.

Focusing on the results of the stepwise regression process, the inclusion of slope squared was logical due to the strong relationship seen previously between vertical error and slope (see the section, Influence of Sloping Terrain on ALTM-derived Elevations). Other stages in the investigation also implied dominance of slope over other factors (e.g., aspect, ground elevation).

Somewhat perplexing was inclusion of incidence angle due to the lack of a distinctive trend between this factor and signed vertical error (see Figure 56, Scatterplot of the sampled ALTM ground strike vertical errors for all incidence angles (n=351)). Incidence angle had a very low coefficient of determination ($R^2=0.002$) with signed error for all angles. A model of the relationship is not significant either ($p = .464$). The stepwise process may have detected the possible negative trend alluded to in that section, between zero and fifteen degrees, possibly extending out to 30 degrees, seen in the figure. This negative trend seemed contradictory since Schaer et al. (2007) and Stebler et al. (2009) implied a loss in vertical accuracy as incidence angle increases, and Kobler et al. (2007) and Goulden and Hopkinson (2010) indicated that the rising side of the footprint is responsible for the range measurement which results in higher than actual elevations. However, Jutzi and Stilla (2003), Johnson (2009), and Ussyshkin et al. (2009) found that a tilting of the target surface results in lengthening of the return pulse and a lengthening of the range. This range error

would then result in lower than actual elevations, visible as negative signed errors. Hence, this relationship may have some validity. Also noteworthy was the strong link between incidence angle and slope exist ($r=0.659$) and slope and vertical error, but no clear relationship between incidence angle and error.

The third predictor added to the model by the stepwise procedure was ground strike elevation. This factor did not have much influence when assessed separately in this study. Nor has it received much attention in other studies. In these studies, the error analysis was of flying height or range, which is a derivative product of flying height and elevation. From the section, Influence on Ground Elevation on ALTM-derived Elevations, in which ground elevation was assessed individually, the change in ground elevation is akin to other studies where AGL was changed. However, the simple regression model of ground elevation alone and the multiple regression model both indicate that vertical error increases as ground elevation increases. This relationship is contrary to the findings of others and common belief. As presented in this section, a weak relationship between signed vertical error and ground elevations was found with the coefficient of determination very low ($R^2=0.022$). However, the model is significant ($p = .005$).

Standardized coefficients (beta) provide for the relative effect each predictor has on singed vertical error:

- Slope squared: .896
- Incidence angle: -.700
- Ground elevation: .157

These values indicate, for example: a one standard deviation increase in slope squared should result in a 0.896 standard deviation increase in vertical error.

A comparison of these standardized coefficients, indicated that slope (slope squared, specifically) had the most influence as it had the largest absolute value. Incidence had 22 percent less effect than slope squared and ground elevation had 82 percent less.

While the model is valid, based on statistical criteria and the proofing explained previously, the inclusion of incidence angle and ground elevation, with contrarian signs of coefficients, created doubts. While numerous stepwise and forward regression procedures produced similar results, backward regressing produced models with different predictors:

Vertical error =

$$0.001 \cdot Slope^2 + 0.018 \cdot Scan\ angle - 0.023 \cdot Incidence\ angle - 0.001 \cdot Range + 5.768 \quad Eq. (33)$$

All three models (i.e., stepwise, forward, and backward) include slope squared and incidence angle as predictors with similar coefficients.

However, in the backward regression model, range appears as a predictor and the sign of the coefficient indicates that as range decreases, vertical error increases. Again, this result is contrary to common expectations. The reason may be skewness of the data due to opportunistic sampling (see the section, Influence of Laser Range on ALTM-derived Elevations).

The backward model also includes scan angle as a predictor. Accompanied by a positively signed coefficient that indicates as scan increases, vertical error increases. This observation corresponded to the findings of others (Baltsavias, 1999a; Ahokas et al., 2003; Schaer et al., 2007, Ussyshkin et al., 2009. See the section, Scanning Mirror Unit). However, it was contrary to the results derived earlier in this study where signed vertical error decreases as scan angle increases (see Influence of Scan Angle on ALTM-derived Elevations and Equation 11).

For this model, the standardized coefficient (beta) values were:

- Slope squared: .867
- Scan angle: .350
- Incidence angle: -.686
- Range: -.402

As with the stepwise regression model, slope squared has the most impact on vertical error then, incidence angle (21% less than slope squared). Range has 54 percent less bearing on error than slope squared and scan angle has 60 percent less. Of interest was scan angle being the second predictor entered into the

model by the regression process even though incidence angle has more influence on vertical error.

Having stepwise and backward regressing producing different models was problematic. Optimally, all three regressing techniques, stepwise, forward, and backward should have created similar models. This inconsistency however, is not an uncommon situation (Draper & Smith, 1998). Some degree of multi-collinearity may have been present. It was statistically apparent, that slope squared and incidence angle did have worthwhile influences on signed error. For the remainder of the predictors, it may be that the relationship between range and ground elevation, even though weak, resulted in one or the other being included in models. Both of these predictors have the least impact on signed error, given their lower standardized coefficient values and being the last predictor added into their respective models. These results may indicate that their effect has been over-valued.

Further comparison of the two models focused on AIC values. The backward regression model has an AIC of -939.262. The difference between the stepwise and backward regression models is 6.09 (Δ_i). Using AIC alone to determine the best model, a change value (Δ_i) between three and seven indicated that the stepwise regression model has considerably less support as being best meaning, the backward model is the best model, statistically (Mazerolle, 2006).

Another worthwhile comparison was of the simple regression models against the multiple ones using AIC:

Table 13

Akaike Information Criterion for least squares linear regression models

| Factor | AIC | Δ_i |
|----------------------------------------|----------|------------|
| Slope only | -788.438 | 150.824 |
| Slope squared only | -795.560 | 143.702 |
| Incidence angle only | -702.613 | 236.649 |
| Footprint size only | -705.278 | 233.984 |
| Elevation spread across footprint only | -774.253 | 165.009 |
| Aspect recoded only | -712.056 | 227.206 |
| Ground elevation only | -709.973 | 229.289 |
| Range only | -732.547 | 206.715 |
| Multiple (Stepwise) | -933.172 | 6.09 |
| Multiple (Backward) | -939.262 | ----- |

As evidenced in the table, the change in AIC values ($AIC_i - AIC_{Backward}$) are all substantial, other than possibly between the two multiple regression models. From Mazerolle (2006), models with change values (Δ_i) greater than ten (above the lowest model) indicate that the model is very unlikely. In addition to statistical results, other considerations included the validity of including scan angle and range as predictors in the model versus ground elevation.

For the data in this study, it appeared that the backward regression model (Equation 33) is the best model for describing which factors most influenced signed vertical error. However, it was believed that the predominate factors were slope and incidence angle and that the other factors play a lesser role. This

principle was based inclusion of these as predictors in the backward regressing only, beta values, and analysis of the factors individually.

Of interest, another multiple regression model with only slope squared and incidence angle as predictors has an AIC of -921.955. Compared to the backward regression model, the change in AIC (Δ_i) is 17.307.

Since absolute values are sometimes useful to identify trends (Su & Bork, 2006), all three multiple regression techniques were used with absolute error as the outcome. Similarly, manual multiple regressions and checks were part of the process to validate the resulting models.

With absolute value, the stepwise and forward regressing converged on the same models with only two predictors: slope squared and ground elevation. Again, models included a positive relationship between ground elevation and vertical error: as laser strike ground elevation increases, absolute error increases:

$$\text{Absolute error} = 0.0002 \cdot \text{Slope}^2 + 0.001 \cdot \text{Elevation} + 0.112 \quad \text{Eq. (34)}$$

The backward regression model had several factors:

Absolute error =

$$\begin{aligned} &0.0005 \cdot \textit{Slope}^2 + 3.076 \cdot \textit{Footprint size} - 0.028 \cdot \textit{Incidence angle} \\ &\quad + 1.82 \cdot \textit{Slope} - 0.002 \cdot \textit{Range} \\ &- 6.478 \cdot \textit{Elevation spread across footprint} + 5.808 \end{aligned} \quad \textit{Eq. (35)}$$

This model provided some troubling results: absolute error increases as incidence angle, range, and elevation spread across the footprint decrease. These are contrary to expectations and some of the previous findings of this study. The beta values of the coefficients are:

- Slope squared: 0.969
- Footprint size: 3.316
- Incidence angle: -1.292
- Slope: 8.413
- Range: -1.340
- Elevation spread
across footprint: -10.080

From these values, elevation spread has the most influence on absolute error followed by slope.

The backward regression model has the lowest AIC value and the change in AIC (Δ) between this and the stepwise model is 44.707. Comparisons could not be made using AIC values between these models and the first multiple regression models since the outcome variables were different. Simple regression models with absolute value as an outcome have similar AIC values to that of the backward regression model.

Returning to signed vertical error, from analyses of the models with multiple factors, it appeared that slope and incidence angle have the most influential effect. However, this observation is problematic: It indicates that vertical error increases as slope angle increases, possibly due the rising side of the footprint being responsible for the range and elevation measurements (Kobler et al., 2007; Goulden & Hopkinson, 2010). The model also states that vertical error decreases as incidence angle increases. Using Kobler et al.'s theory, vertical error should increase as incidence angle increases. Hence, part of the model concurs with Kobler et al.'s comments while another does not. Concerning incidence angle, the relationship appeared to follow Jutzi and Stilla (2003), Johnson's (2009), and Ussyshkin et al.'s (2009) beliefs that a delay in the returning signal due to being reflected off a tilted surface results in a longer range measurement and lower than actual elevation. As presented repeatedly, the two theories contradict one another and the inclusion of both in a model was perplexing.

Chapter 5

Summary of Results

This study of ALTM elevation error was distinctive for several reasons including the collection of reference data and precise measurement of slope at actual laser strike locations. Previously, very little work examined vertical errors on steeply sloping terrain. In addition to slope, the specific effects on vertical error by other factors, such as displacement of laser strike due to horizontal error, slope aspect, incidence angle, footprint size, and footprint orientation on sloping terrain were investigated for the first time.

Reference elevations were measured using survey-grade GNSS receivers with exceptionally rigorous methodology to obtain data with minimal error. In all, field visits were to 920 laser strikes. Of which, only 351 were sampled after having met stringent criteria to insure accurate results. Interestingly, misclassification of ground strikes occurred 15.8 percent of the time. The overall error between ALTM-derived and reference elevations is 0.256 m (RMSE 0.446), regardless of slope. The 95 percent confidence interval for the true mean ranged from 0.218 to 0.294 m. The combined systematic error for the ALTM system and the GNSS receivers used to establish the reference elevations is 0.158 m. Subsequent to the correction; mean vertical error is 0.098 m with a confidence interval of 0.060

m to 0.136 m (RMSE 0.379). The ALTM-derived elevations are on average, higher than the reference elevations (206 of 351 after correction).

Concerning slope, this study found as others had: vertical error increases as slope increases. A quadratic model best describes the relationship. This upward trend appeared to indicate that the rising edge of the footprint is responsible for the reflection of the laser pulse and thus, the range and elevation, as Kobler et al. (2007), and Goulden and Hopkinson (2010) had surmised.

When allocated in strata, mean error is essentially non-existent on slopes below twenty degrees. This finding was contrary to other studies where error increases, or is predicted to increase, on slopes greater than ten degrees.

This study found a positive relationship between dispersion of vertical error and sloping terrain. Interestingly, the 5.0 to 9.9 degree stratum has an eighteen percent lower standard deviation than the 0.0 to 4.9 degree stratum. In addition, the 30-degree and above stratum has a nine percent lower standard deviation than the 20.0 to 29.9 degree stratum. This result may be due to the low sample size in the 30-degree and above stratum ($n=36$). However, the true reasons for these findings are unknown. Regardless, the overall increase in the scatter of vertical error as slope increases could be explained by both the horizontal inaccuracy of the laser strikes and the elevation disparity across the footprint.

The effect of scan angle on vertical error was dissimilar to most all other studies reviewed. With others, as scan angle increases vertical error also increases. In

this study, scan angles of zero degrees (nadir) have higher signed errors that decrease as scan angle increases. However, this outcome concurs with Jutzi and Stilla (2003), Johnson (2009), and Ussyshkin et al.'s (2009) work whereby, angled reflecting surfaces produce erroneous larger range values, resulting in lower than actual elevations.

Relatively few other investigations had explored incidence angle, the angle between the laser beam and a vector normal to the terrain. This study, calculated the incidence angles for all sampled strikes. Scatterplots showed a weak negative trend among low incidence angles and signed error: Low angles have positive signed errors that decrease as incidence angle increases to approximately 30 degrees. If this trend does exist, it would also confer Jutzi and Stilla (2003), Johnson (2009), and Ussyshkin et al.'s (2009) findings in that the elongated returning range signal results in a delay, which creates a longer than actual range value and a lower than actual elevation value. A positive but weak, trend was found between incidence angle and absolute errors.

Continuing with incidence angle, dispersion (i.e., standard deviation, range, larger maximum and minimum values, etc.) of error increases as incidence angle increases. This dispersion may be due to horizontal inaccuracy affecting vertical accuracy on sloping terrain.

This study also calculated the footprint size for each sampled laser strike.

Footprint size is dependent on scan angle, laser beam divergence, range, slope,

and slope aspect. Modeled using ellipse formulas, sizes range from 1.980 m² to 3.532 m². Other studies computed footprint size and alluded to its impact on vertical error but did not analyze this relationship. From this study, dispersion of error increases as footprint size increases. This outcome aligns with the postulation of Baltsavias (1999a) whereby, reflective material regardless of where it is located in the footprint is responsible for the range measurement and thus, elevation. Similarly, Glennie (2007) and Ussyshkin et al. (2009) stated that the range measurement could come from anywhere in the footprint. Aside from this, no clear trend existed whereby error increases (or decreases) as footprint size increases. Similar to scan and incidence angles, a possible, slight downward trend occurred between the signed vertical error and footprint size for the footprints between 2.0 and approximately 2.5 m². The reason for this correlation was not entirely clear. The strong relationship between incidence angles and footprint sizes may be influencing this connection. No trend existed between absolute errors and footprint size.

The theories that some position other than the center of the footprint, is responsible for the range measurement made by the LiDAR system, led to the examination of elevations within the footprint. Calculations produced elevations of the upper and lowermost reaches of the footprint on sloping terrain for each sampled strike. The same factors that influence footprint size also influence disparity between these two elevations. The maximum difference between upper and lowermost elevations within a footprint is 1.939 m. No strong relationship

exists between footprint size and elevation spread across the footprint. While both size and spread have strong relationships with slope, the latter relationship is stronger while footprint size has a stronger relationship with scan angle. A positive but weak trend appeared between signed vertical error and elevation spread across the footprint. This finding would indicate that the range measurement comes from the rising side of the footprint as deduced by Kobler et al. (2007) and Goulden and Hopkinson (2010). Comparing reference elevations to the range between the upper and lower most elevations, reference elevations fell within the range only 36.8 percent of the time. This statement is dampened by the low success rate on flat terrain. Higher success rates occurred on steeper slopes. The errors observed on flat terrain may be attributable to imprecision in the other components and factors of ALTM. These statements pertaining to footprint sizes are qualified since calculations of sizes and elevations were based on only theoretically, 84 percent of the laser's emitted energy.

Horizontal inaccuracy also has an effect on vertical error. In this study, the amount and direction of horizontal error was unknown. A common error estimate of one meter was used to shift laser strikes upslope and downslope producing alternate elevations. Comparison of reference elevations to these new elevations indicated that horizontal error could account for 43.3 percent of the observed vertical error. This value is also depressed by the low success rates on relatively flat terrain. On slopes greater than twenty degrees, the success rate is 54.8 percent. The changes in elevation due to the horizontal displacement were

combined with the upper and lower elevations of each footprint. The rationale was to determine if the observable vertical error could be explained by the combination of horizontal inaccuracy and the elevation measurement based on some element within the upper and lower reaches of the footprint. The combination of these two variables could explain 69.2 percent of all observed vertical error and 98.8 percent of the error on slopes greater than twenty degrees.

This was only the second study to investigate the effect of slope aspect on error. In this study, an *S*-curve described the signed errors when aspects ranged from facing the flight line, to facing the direction of the flight, to facing away from the flight line. The reason for this curve was not entirely clear. It may be a symptom of other factors influencing error, such as slope. The expected greater dispersion of error on slopes facing the direction of the flight (parallel to the scan line) due to larger footprints was not evident. This lack of a clear relationship may be the result of the high flying height that can diminish or negate the effects of slope aspect on errors.

Others had found that, in general, vertical error increases as ground elevations of laser strikes decrease. This relationship is more a function of the distance between the ALTM unit and the terrain (i.e., range). Nevertheless, this study showed a contradictory relationship whereby signed error increases as laser strike elevations increase. However, the relationship was weak and may the

result of the opportunistic sampling methods employed or it may be that scan angle has a greater influence and obscured results.

The association between laser range and vertical error was also problematic as an increase in range results in an increase in signed error followed by a decrease in signed error with higher ranges. Opportunistic sampling of laser strikes and the greater influence of scan angle also may have biased this finding.

Following investigations of these factors alone (e.g., slope, scan angle, incidence angle, footprint size), multiple regression sought to determine which had the most influence on vertical error. Employing all factors as predictors, slope and incidence angle demonstrated the strongest effect. The inclusion of laser strike ground elevation and its contrarian relationship with error was problematic. Additionally, muddled results were due to stepwise and backward regression not converging on similar models. Backward regression models also included predictors with contrarian trends. While revealing that many factors result in dispersion of vertical error, no clear trends could be shown between any of these factors and error other than with slope and incidence angle. However, vertical error decreases as incidence angle increases. This result contradicted the perception that error would decrease as incidence angle decreases.

What was perplexing from the investigations are the contrarian results. From the literature review, two different schools of thought exist on what determines range and thus, elevation measurements. Two studies (Kobler et al., 2007;

Goulden & Hopkinson, 2010) postulate that the rising side of a laser strike's footprint is responsible for the range (and elevation) measurement. This would result in elevations higher than actual. Other studies offer that the range measurement is based randomly in the footprint (Baltsavias, 1999a; Glennie, 2007; Ussyshkin et al., 2009). Hence, the recorded elevation can be the same, higher, or lower than actual. In this study, no clear-cut evidence was found to support either hypothesis. Investigation of some factors affecting vertical error (e.g., slope, incidence angle) supported one theory while other factors supported the other. Complicating this, several studies (Jutzi & Stilla, 2003; Johnson, 2009; Ussyshkin et al., 2009) noted that a laser pulse striking a tilted surface elongates the returning range signal resulting in a time delay which causes a lower than actual elevation. Specifically, the decrease in signed vertical error as scan angle increases opposes all other studies but one. However, this relationship can be explained via Jutzi and Stilla and others where a tilted surface elongates the returning range signal resulting in a time delay which causes a lower than actual elevation. Yet, this statement appeared to conflict and contradict with the reasoning for greater vertical error on increasing slopes: The rising side of the footprint is responsible for the range measurement (Kobler et al.; Goulden & Hopkinson). Similarly, the weak trend observed between error and incidence angle could be explained by Jutzi and Stilla and others theories but again, is in direct conflict with the clearly seen increase in error on sloping terrain supported by Kobler and others. The contradiction extended to the increase in vertical error

as elevation spread within the footprint increased. The reasoning for this observation supported the claims of Kobler and others, contradicting Jutzi and Stilla and others.

Elsewhere, the reason for increase in error dispersion as incidence angle increased conflicted with that for the increase in error on increasing slope. The range measurement repeatedly reflecting off the rising side of the footprint could be responsible for the latter. However, the dispersion with both positive and negative signed errors associated with incidence angle indicated that the range measurement would reflect off varying locales in the footprint, both on the uphill and downhill sides of the footprint (Baltsavias, 1999a; Glennie, 2007; Ussyshkin et al., 2009).

Similar contradictions occurred between the explanations for observations of other error influencing factors.

One possible explanation could be: While Jutzi and Stilla (2003), Johnson (2009), and Ussyshkin et al. (2009) showed laser pulse elongation and range measurement error when the laser pulse reflects off a tilted surface, their data could not be transferred to this study and hence, specific error values or the magnitude of this error remains unknown. However, if this error is minimal, a new reason is needed to explain the trends observed for scan angle and incidence angle. And, contradictions remain between the reasons for other

observations: range measurement due to the rising side of the footprint only or due to reflective material located anywhere in the footprint.

From the literature review, others offered five reasons for observed errors on sloping terrain. As presented, some of these contradict with others while some can supplement each other to explain observed errors. To aid in applying these reasons to observed results, the following was used: Table C-1, Appraisal of Origins for Observed Vertical Errors in Appendix C, Breakdown of Conflicting Reasons for Range Measurement Error on Sloping Terrain.

As evidenced, separating out and developing relationships between vertical error and other factors was not simple and straightforward as was originally thought. The interactions and relationships between factors made it difficult to interpret results.

Chapter 6

Conclusions

This study produced several new findings regarding ALTM elevation errors. These discoveries were possible due to direct comparison of very accurate reference data collected at actual laser strike locations. From these comparisons, misclassification of ground strikes occurred 15.8 percent of the time (n=420) in a pine-beech-oak forest where slopes range from zero to 62.1 degrees.

Furthermore, direct comparison determined definitively that ALTM elevations are higher 58.7 percent of the time after correcting for bias given the same forest type and slopes. These findings provide well-founded estimates of what ALTM data users can expect on similar terrain and can compensate for accordingly. The bias of 0.158 m describes combined error of both the reference data collection methods and the ALTM system. This bias is typical of other ALTM accuracy studies (e.g., Daniels, 2001; Adams & Chandler, 2002; Clark et al., 2004; Csayni & Toth, 2005; Hodgson et al., 2005; Lang & McCarty, 2009) but was unexpectedly low considering the flying height of this study. Other users of high altitude data can have confidence that a high flying height does not seriously diminish accuracy and precision.

Concerning slopes, this study provided clear evidence of a trend between increasing vertical error and increasing slope but only on steeper slopes. This trend is not linear as others (e.g., Xhardé et al., 2006), had postulated but quadratic. When allocated in slope strata, mean error is essentially non-existent on slopes below twenty degrees. This finding was also contrary to most other studies where error increases, or was predicted to increase, on slopes greater than ten degrees. The direct comparison method of this study most likely avoided errors incurred by other studies using DTMs and misclassified laser strikes. Also from this study, ALTM elevations become less precise as slope increases, although ALTM system errors appear responsible for some imprecision regardless of slope.

Additional factors, not previously explored, provided additional insight into ALTM errors. For example: A laser strike on sloping terrain has an elevation disparity between the upper and lower reaches of the footprint. It was shown that elevation differences within a laser strike's footprint can account for observable ALTM elevation error 44.0 percent of the time for slopes greater than twenty degrees, less so on lower slopes (33.2%) where the ALTM system appear to be the predominate error source.

The investigation of horizontal error's effect on elevation error found that a horizontal displacement of one meter can account for observed vertical error 54.8 percent on slopes greater than twenty degrees (38.3% on lower slopes).

The combination of elevation difference within the footprint and horizontal

displacement can account for the observed vertical error 98.8 percent of the time on slopes greater than twenty degrees and 69.2 percent of the time, regardless of slope. When these two factors are combined, success rates continually increase as slope increases. These results are beneficial since few studies provided data indicating what factors are responsible for the observed increase in ALTM elevation errors on sloping terrain. Now, more is known about the effect of horizontal error on vertical error and elements located in the footprint, but off center, that are responsible for the range and elevation measurements.

This study also found that signed vertical error decreases as scan angle increases. This discovery is contrary to almost all other studies (e.g., Baltasvias, 1999a & 1999b; Airborne 1, 2001; Schaer et al., 2007; Ussyshkin et al., 2009). Given the direct comparison of ALTM to reference elevations, further investigation of this relationship appears warranted.

In addition to elevation differences within the footprint and horizontal displacement, other ALTM factors such as footprint size, incidence angle, and slope aspect, which affect ALTM elevation, were definitively examined for the first time.

Both incidence angle and footprint size affect elevation precision. As either factor increases, ALTM elevations become less precise. A similar link appears between elevation differences within the footprint and elevation. Trends between vertical error and incidence angle, footprint size, and elevation differences within the

footprint were weak. Hence, the increase in the size of a laser strike's footprint degrades precision but not necessarily accuracy. Multiple regression models were created to determine the influence of all the factors (i.e., slope, scan angle, footprint size, elevation disparity within the footprint, incidence angle, slope aspect, ground elevation, and laser range) on ALTM vertical error. The results of the modeling were problematic. However, the outcomes were interpreted to reveal that slope has the greatest effect—and may have the only effect—on elevation accuracy.

Uses for this Study

Bowen and Waltermire (2002) stated:

If ground GPS data at precise X and Y locations from the LiDAR survey were not available and no correction were applied, the RMSEs would have been 30 percent larger. This finding highlights the importance of collecting at least a minimal set of ground survey validation data as part of a LiDAR projects.

This study found that 15.8 percent of the ground strikes had been misclassified and observed a systematic bias of 0.158 m. An increase in accuracy resulted from removal of this bias. This accuracy increase will hopefully, encourage users of ALTM data to remove this bias and be cognizant that not all laser strikes will be accurately classified.

This study confirmed that ALTM elevation accuracy decreases as slope increases. More so, it found that slope has no real impact on ALTM elevations on terrain less than twenty degrees. Additionally, the study provides a relationship between vertical error and terrain slopes up to 50 degrees.

This study also sought to differentiate between inaccuracy and imprecision. ALTM elevations degrade in accuracy and precision as slope increases. Users of ALTM data also now know that footprint size, footprint orientation on sloping terrain, and incidence angle affect elevation precision: As any of these increase, imprecision increases. Greater imprecisions can also occur on level terrain since large scan angles typically result in larger footprints and incidence angles. Furthermore, only slope has an effect on ALTM elevation accuracy.

From this study, horizontal error and elevation disparity across the footprint alone and combined, may explain large percentages of the observed vertical imprecision on steeper slopes. Not so, on flat and nearly level terrain, though where ALTM system errors appear to be predominate.

For planners of ALTM missions, the reduction in footprint size appeared to be one of the main criteria in minimizing vertical error dispersion. A smaller footprint equates to low elevation spread across the footprint. Footprint size is dependent on flying height, ground elevations, slope, slope aspect, and scan angle (assuming divergence angle is fixed). Flight line planning ahead of time should identify which areas to be mapped are most crucial for the end user of the data.

Then, flights in these areas should be made with slopes facing the flight line (i.e., flight line parallel to the contours) and giving thought to the relief. Current practice includes planning flight lines parallel to the contours for the majority of the terrain. But now, more is known about the elevation imprecisions in those areas not facing the flight line. The awareness of how incidence angle and footprint size affect precision could lead to refining the mapping process.

For future investigators, the numerous relations shown between ALTM factors (e.g., slope), especially those not previously examined (e.g., footprint size, incidence angle) will hopefully, prove useful.

Limitations of this Study

As with a study such as this, a larger number of sampled laser strikes would have solidified relationships between some factors and vertical error, hopefully. Unfortunately, for some factors connections to vertical error were weak or could not be made. The opportunistic sampling method employed also limited defining some relationships. With more data, clarity about the relationships between vertical error and incidence angle, footprint size, and elevation disparity across the footprint is possible. However, given the millions of data points, sample size will undoubtedly always be an issue.

One trend that emerged but could not be explained is the relationship between vertical error and slope aspect. It may be that slope angle and a high flying

height have influenced what was observed. This study is the first to provide some evidence of the effect of slope aspect and may prove to be intriguing. Previously published reasons for vertical error, when applied to the results, proved contradictory. One hypothesis states that the rising side of the laser strike's footprint is responsible for the range (and elevation) measurement (Kobler et al., 2007; Goulden & Hopkinson, 2010). Another theory states that the range measurement can originate from anywhere inside the footprint (Baltsavias, 1999a; Glennie, 2007; Ussyshkin et al., 2009). Neither theory could account for all of the observed results. Applications of these hypotheses were further impeded by a third theory put forth by others where a laser reflecting off a tilted surface results in an elongated signal and a range measurement longer than actual (Jutzi & Stilla, 2003; Johnson, 2009; Ussyshkin et al., 2009). However, all of these theories could explain some of the results observed which may further clarify reasons for observed elevation errors.

Lastly, newer ALTM systems may have less error than the one used in this study. Leica Geosystems has introduced three successive versions of this system since these data were collected (Leica Geosystems, 2012).

Future Investigations

In order to improve on this study, a few additional steps should improve the results tremendously:

A similar study on sloping terrain with accurate reference elevations at laser strike locations but with a substantially larger number of samples would prove useful.

Furthermore, the AGL of the flight should be closer to the range of AGLs commonly used for mapping projects.

A study site with little surface roughness and no canopy or vegetation cover will eliminate some issues and allow for readily identifying misclassified strikes.

Lastly, clarification is needed between the conflicting trends of slope angle and incidence angle and elevation spread across the footprint. Additionally, resolution between the reasons for them would aid greatly in further understanding ALTM system accuracy and precision.

Appendix

Appendix A

ALTM Flight Conditions

Table A-1
Climatological Data for the ALTM Mapping Period from 15:30 to 15:47 on June 17, 2003

U.S. Department of Commerce
National Oceanic & Atmospheric Administration

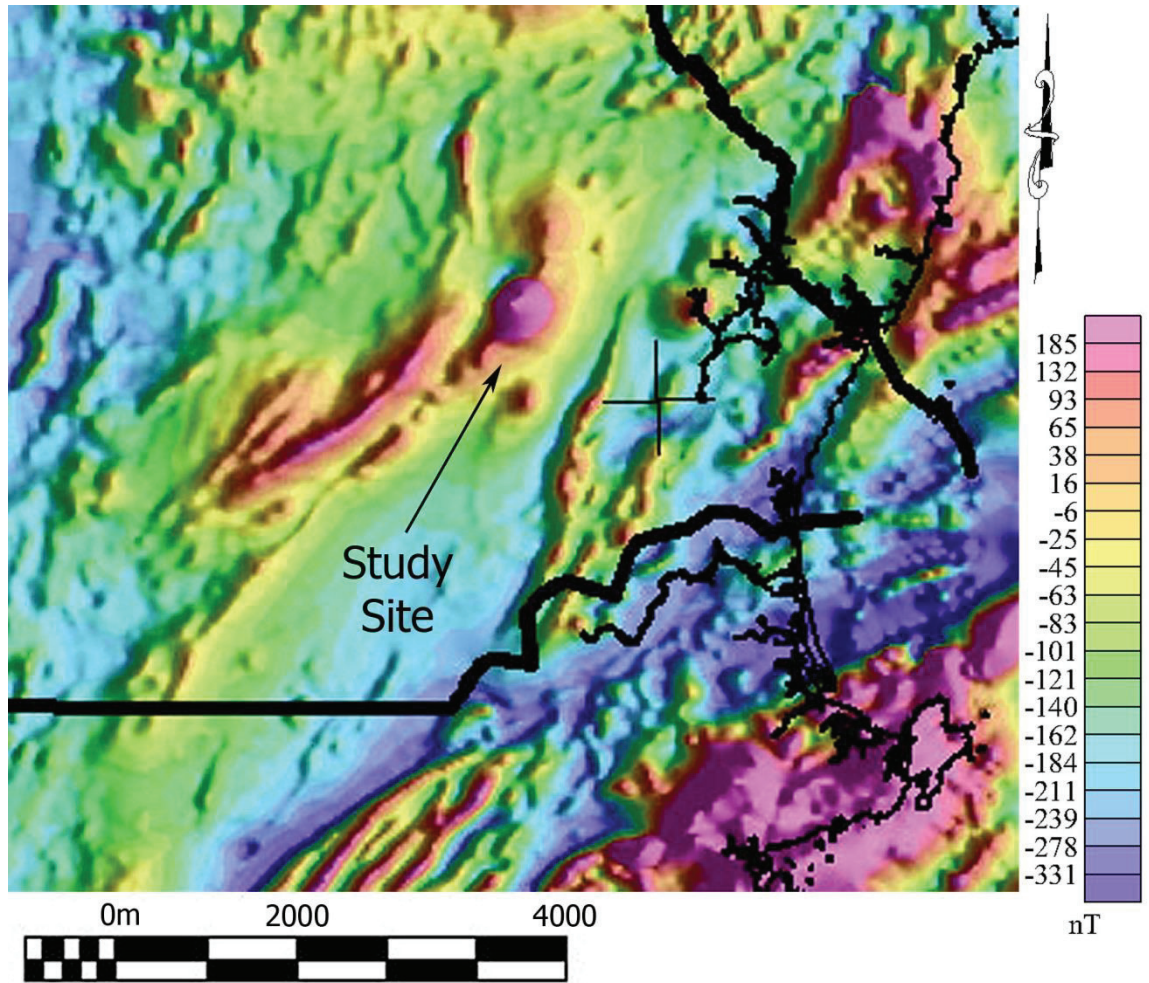
**UNEDITED LOCAL
CLIMATOLOGICAL DATA
HOURLY OBSERVATIONS TABLE
CONCORD MUNICIPAL AIRPORT (CON)
CONCORD, NH
(06/2003)**

National Climatic Data Center
Federal Building
151 Patton Avenue
Asheville, North Carolina 28801

Elevation: 340 ft. above sea level
Latitude: 43°11'N
Longitude: 71°30'W

| Date | Time | Station Type | Maint Indic | Sky Conditions | Visibility | Weather Type | Dry Bulb Temp | | Wet Bulb Temp | | Dew Point Temp | | Rel Humd % | Wind Speed (KT) | Wind Dir | Wind Char. Gusts (KT) | Val. for Wind Char. | Station Pressure | Press Tend | Sea Level Pressure | Report Type | Precip. Total |
|------|------|--------------|-------------|----------------|------------|--------------|---------------|------|---------------|------|----------------|------|------------|-----------------|----------|-----------------------|---------------------|------------------|------------|--------------------|-------------|---------------|
| | | | | | | | (F) | (C) | (F) | (C) | (F) | (C) | | | | | | | | | | |
| 17 | 0051 | AO2 | - | CLR | 10SM | - | 47 | 8.3 | 47 | 8.1 | 46 | 7.8 | 97 | 0 | 000 | - | 0 | 29.93 | 1 | 263 | AA | - |
| 17 | 0151 | AO2 | - | CLR | 10SM | - | 46 | 7.8 | 46 | 7.8 | 46 | 7.8 | 100 | 0 | 000 | - | 0 | 29.93 | - | 260 | AA | - |
| 17 | 0251 | AO2 | - | CLR | 10SM | - | 45 | 7.2 | 45 | 7.0 | 44 | 6.7 | 97 | 0 | 000 | - | 0 | 29.92 | - | 257 | AA | - |
| 17 | 0351 | AO2 | - | CLR | 10SM | - | 42 | 5.6 | 42 | 5.6 | 42 | 5.6 | 100 | 0 | 000 | - | 0 | 29.92 | 5 | 258 | AA | - |
| 17 | 0451 | AO2 | - | CLR | 9SM | - | 42 | 5.6 | 42 | 5.6 | 42 | 5.6 | 100 | 0 | 000 | - | 0 | 29.92 | - | 259 | AA | - |
| 17 | 0551 | AO2 | - | CLR | 10SM | - | 47 | 8.3 | 47 | 8.1 | 46 | 7.8 | 97 | 0 | 000 | - | 0 | 29.93 | - | 260 | AA | - |
| 17 | 0651 | AO2 | - | CLR | 10SM | - | 52 | 11.1 | 50 | 10.2 | 49 | 9.4 | 89 | 0 | 000 | - | 0 | 29.92 | 0 | 259 | AA | - |
| 17 | 0751 | AO2 | - | CLR | 10SM | - | 58 | 14.4 | 54 | 12.1 | 50 | 10.0 | 75 | 3 | VRB | - | 0 | 29.92 | - | 257 | AA | - |
| 17 | 0851 | AO2 | - | CLR | 10SM | - | 62 | 16.7 | 56 | 13.6 | 52 | 11.1 | 70 | 4 | 240 | - | 0 | 29.89 | - | 249 | AA | - |
| 17 | 0951 | AO2 | - | CLR | 10SM | - | 68 | 20.0 | 60 | 15.5 | 54 | 12.2 | 61 | 3 | VRB | - | 0 | 29.87 | 8 | 241 | AA | - |
| 17 | 1051 | AO2 | - | CLR | 10SM | - | 70 | 21.1 | 59 | 15.2 | 51 | 10.6 | 51 | 5 | 280 | - | 0 | 29.85 | - | 234 | AA | - |
| 17 | 1151 | AO2 | - | CLR | 10SM | - | 73 | 22.8 | 60 | 15.3 | 49 | 9.4 | 43 | 4 | VRB | - | 0 | 29.83 | - | 226 | AA | - |
| 17 | 1251 | AO2 | - | CLR | 10SM | - | 75 | 23.9 | 61 | 16.2 | 51 | 10.6 | 43 | 10 | 240 | - | 0 | 29.80 | 8 | 219 | AA | - |
| 17 | 1351 | AO2 | - | CLR | 10SM | - | 76 | 24.4 | 63 | 17.2 | 54 | 12.2 | 47 | 12 | 190 | G | 15 | 29.78 | - | 211 | AA | - |
| 17 | 1451 | AO2 | - | CLR | 10SM | - | 76 | 24.4 | 63 | 16.9 | 53 | 11.7 | 45 | 7 | 200 | - | 0 | 29.77 | - | 206 | AA | - |
| 17 | 1551 | AO2 | - | CLR | 10SM | - | 77 | 25.0 | 63 | 17.2 | 53 | 11.7 | 44 | 8 | 180 | - | 0 | 29.75 | 6 | 199 | AA | - |
| 17 | 1651 | AO2 | - | CLR | 10SM | - | 75 | 23.9 | 62 | 16.8 | 53 | 11.7 | 46 | 8 | 170 | - | 0 | 29.73 | - | 193 | AA | - |
| 17 | 1751 | AO2 | - | CLR | 10SM | - | 74 | 23.3 | 61 | 16.2 | 52 | 11.1 | 46 | 11 | 180 | - | 0 | 29.72 | - | 189 | AA | - |
| 17 | 1851 | AO2 | - | CLR | 10SM | - | 71 | 21.7 | 58 | 14.6 | 48 | 8.9 | 44 | 6 | 200 | - | 0 | 29.72 | 6 | 188 | AA | - |
| 17 | 1951 | AO2 | - | CLR | 10SM | - | 65 | 18.3 | 57 | 13.7 | 50 | 10.0 | 59 | 5 | 170 | - | 0 | 29.72 | - | 189 | AA | - |
| 17 | 2051 | AO2 | - | CLR | 10SM | - | 62 | 16.7 | 55 | 12.8 | 49 | 9.4 | 62 | 7 | 200 | - | 0 | 29.73 | - | 194 | AA | - |
| 17 | 2151 | AO2 | - | CLR | 10SM | - | 61 | 16.1 | 55 | 12.8 | 50 | 10.0 | 67 | 6 | 180 | - | 0 | 29.73 | 0 | 191 | AA | - |
| 17 | 2251 | AO2 | - | CLR | 10SM | - | 58 | 14.4 | 54 | 12.4 | 51 | 10.6 | 78 | 3 | 180 | - | 0 | 29.73 | - | 191 | AA | - |
| 17 | 2351 | AO2 | - | CLR | 10SM | - | 57 | 13.9 | 53 | 11.8 | 50 | 10.0 | 78 | 6 | 200 | - | 0 | 29.71 | - | 187 | AA | - |

Figure A-1. Aeromagnetic map of study area.



-Aeromagnetic map of New England States and the Gulf of Maine by David E. Daniels
US Geological Survey

Figure A-2. Chart of GPS satellite geometry at the time of the ALTM flight June 17, 2003.

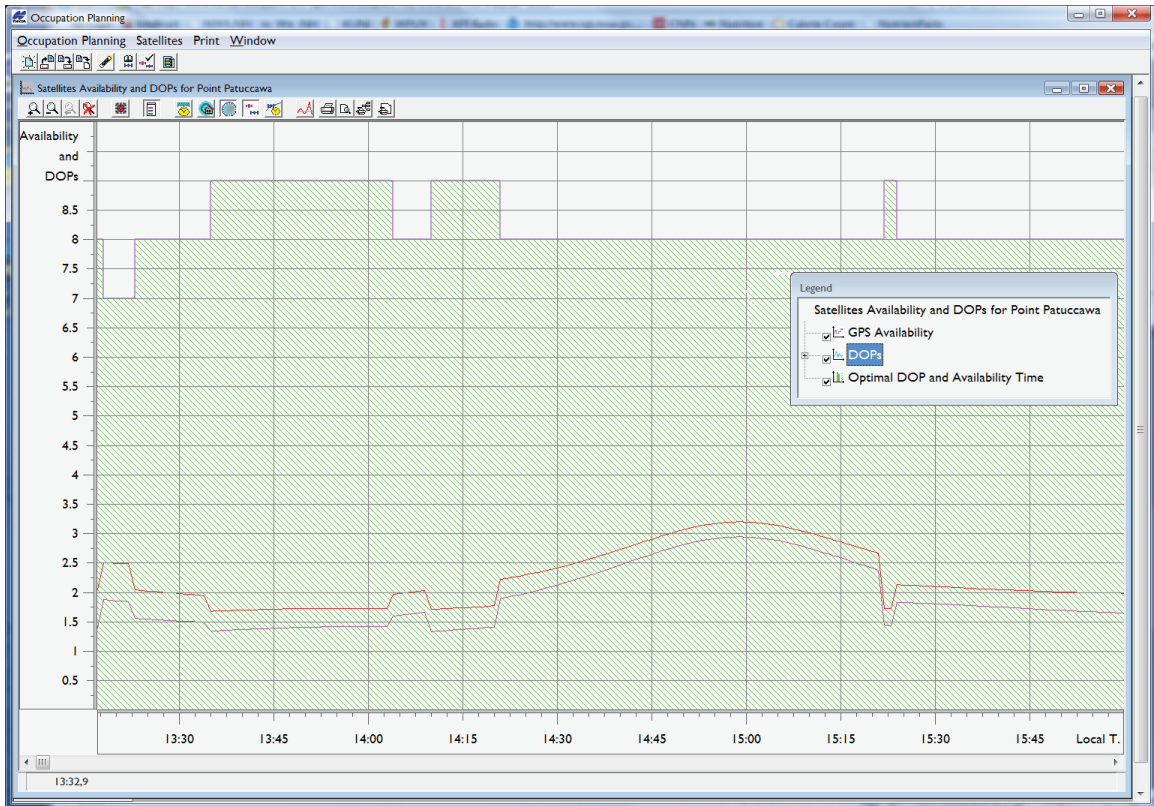


Chart shows the PDOP and VDOP values for the corresponding to the time period when the Mount Pawtuckaway area was mapped with ALTM. The data specific to this project were collected between 15:30 and 15:47 on June 17, 2003.

Red line (upper line): PDOP
 Magenta line (lower line): VDOP
 Green shaded area: Number of GNSS satellites available.
 Software: Topcon Positioning System's Mission Planning

Appendix B

GNSS Postprocessing with OPUS

Table B-1
Varied Results with OPUS Processing of GNSS Data

| | Control Point being established | | | |
|--------------------------------------------|-------------------------------------------------------------------------------------------------------------------|--------------------------------------------------------------------------------------------|--------------------------------------------------------------------------------------------|----------------------------------------------------------------------------------------------------------------|
| | New Control Point RGM | | New Control Point RGC | |
| | OPUS Solution No.1 | OPUS Solution No.2 | OPUS Solution No.1 | OPUS Solution No.2 |
| Iteration | | | | |
| Date | July 17, 2010 | July 5, 2011 | July 17, 2010 | July 5, 2011 |
| Observations Used | 5448 of 7567 (72%) | 5346 of 7383 (72%) | 5296 of 9443 (56%) | 5254 of 9543 (55%) |
| Calculated Northing (m) ^a | 4775501.805 | 4775502.058 | 4774961.770 | 4774961.707 |
| Calculated Easting ^a | 321572.354 | 321572.617 | 322478.083 | 322478.134 |
| Calculated Elevation ² | 147.295 | 147.402 | 174.878 | 174.952 |
| RMSE ^c | 0.029 | 0.030 | 0.024 | 0.025 |
| Base Stations Used | ZBW1 (Boston WAAS1) FMST (Maine Technical Service- Framingham) NHUN (University of NH) | ZBW1 (Boston WAAS1) P776 (Gunstock MRNH 2008) NHUN (University of NH) | ZBW1 (Boston WAAS1) P776 (Gunstock MRNH 2008) NHUN (University of NH) | ZBW1 (Boston WAAS1) NHCO (NH Dept. of Transportation- Concord) NHUN (University of NH) |

^a Northing and Easting values are Universal Transverse Mercator North coordinates-Zone 19.

^b Elevation values are Orthometric Heights.

^c In three dimensions.

Table B-2

Comparison of Results Using Different GNSS Processing Software and Base Stations

| Processing | Northing ^a | Easting ^a | Elevation ^b | RMSE ^c |
|----------------------------|-----------------------|----------------------|------------------------|-------------------|
| New Control Point RGM | | | | |
| OPUS No. 1 | 4775501.805 m | 321572.354 m | 147.295 m | 0.029 m |
| OPUS No. 2 | 4775502.058 | 321572.617 | 147.402 | 0.030 |
| Topcon Tools using NHUN | 4775502.982 | 321572.389 | 147.409 | 0.009 |
| Topcon Tools using NHCO | 4775502.982 | 321572.389 | 147.428 | 0.013 |
| New Control Point RGC | | | | |
| OPUS No. 1 | 4774961.770 | 322478.083 | 174.878 | 0.024 |
| OPUS No. 2 | 4774961.707 | 322478.134 | 174.952 | 0.025 |
| Topcon Tools using NHUN | 4774961.767 | 322478.043 | 175.182 | 0.009 |
| Topcon Tools using NHCO | 4774961.766 | 322478.052 | 175.202 | 0.013 |

^a Northing and Easting values are Universal Transverse Mercator North coordinates- Zone 19.

^b Elevation values are Orthometric Heights.

^c In three dimensions.

Appendix C

Breakdown of Conflicting Reasons for Range Measurement Error on Sloping Terrain

Table C-1

Appraisal of Origins for Observed Vertical Errors

| | Rising edge of footprint | Anywhere in footprint | Elongated range | Horizontal displacement |
|--------------------------|--------------------------|--------------------------|--------------------------|--------------------------|
| Rising edge of footprint | --- | Conflict | 1 | Can combine ² |
| Anywhere in footprint | Conflict | --- | Can combine ³ | Can combine ⁴ |
| Elongated range | 1 | Can combine ³ | --- | Can combine ³ |
| Horizontal displacement | Can combine ² | Can combine ⁴ | Can combine ³ | --- |

Rising edge of footprint. The rising edge of a laser strike's footprint is responsible for the reflection of the laser pulse. This relationship results in a shorter than actual range measurement which adversely affects the laser strike's elevation by making it higher than actual (Kobler et al., 2007; Goulden & Hopkinson, 2010).

This premise describes inaccuracy or a trend in vertical error.

Anywhere in the footprint. Reflective material responsible for the laser pulse can be situated anywhere in the footprint. This scenario results in a shorter or longer than actual range measurement, depending on whether the reflective material is up slope or downslope from the center of the footprint. The laser strike's elevation is adversely affected by making it higher or lower than actual (Baltsavias, 1999a). The element responsible for the range measurement can be situated anywhere in the footprint (Glennie, 2007; Ussyshkin et al., 2009).

This premise describes dispersion or imprecision in vertical error.

Elongated range. A laser pulse reflected off a tilted surface is elongated resulting in a delay before the receiving sensor detects the pulse, resulting in a longer than actual range measurement. The laser strike's elevation is adversely affected by making it lower than actual (Jutzi & Stilla, 2003; Johnson, 2009; Ussyshkin et al., 2009).

This premise describes inaccuracy or a trend in vertical error.

Horizontal displacement. Inaccuracy in horizontal location results in incorrect planimetric (X and Y) coordinates of laser strike. A correct elevation is then coupled with these incorrect coordinates. The distance and direction between the incorrect coordinates and the actual location of the laser strike is unknown and believed to be random. (Maling, 1989; Schenk, 2001; Hodgson & Bresnahan, 2004; Hodgson et al., 2005; Su & Bork, 2006). In this and other studies, the planimetric coordinates were assumed correct and the elevation error was

observed.

This premise describes dispersion or imprecision in vertical error.

- Conflict. Reasons conflict with one another and for purposes of this study, only one of them should be correct.
- Can combine. Reasons do not conflict with one another and one or both (or several) may be responsible for the observed error.

¹ These two reasons may conflict or combine. Based on rising edge of footprint, observed vertical errors should show a rising trend. Elongated range should show a downward trend. The magnitude of elongated range on error is unknown. If it is substantial, these two reasons conflict. If it is minimal, they still conflict but the effect of rising edge of footprint dominates. Hence, an upward trend. If the magnitude of elongated range is great, it dominates, resulting in a downward trend.

² Expectation is an upward trend and an increase in dispersion.

³ Expectation is a downward trend and an increase in dispersion.

⁴ Expectation is an increase in dispersion.

An increase in footprint size and an increase in elevation spread across the footprint can also interact with the above reasons.

A fifth reason for observed error was given in the thesis: Errors associated with DTMs. This degradation in accuracy was a not a concern in this study.

List of References

- Ackermann, F. (1999). Airborne laser scanning - Present status and future expectations. *ISPRS Journal of Photogrammetry and Remote Sensing*, 54(2-3), 64-67.
- Adams, J., & Chandler, J. (2002). Evaluation of LiDAR and medium scale photogrammetry for detecting soft-cliff coastal change. *Photogrammetric Record*, 17(99), 405-418.
- Aguilar, F., & Mills, J. (2008). Accuracy assessment of LiDAR-derived digital elevation models. *The Photogrammetric Record*, 23(122), 148-169.
- Aguilar, F., Mills, J., Delgado, J., Aguilar, M., Negreiros, J., & Pérez, J. (2010). Modelling vertical error in LiDAR-derived digital elevation models. *ISPRS Journal of Photogrammetry & Remote Sensing*, 65(1), 103-110.
- Ahokas, E., Kaartinen, H., & Hyyppä, J. (2003). A quality assessment of airborne laser scanner data. *Proceedings of the ISPRS Working Group III/3 Workshop*, Dresden, Germany. , XXXIV(PART 3/W13).
- Airborne 1 Corporation. (2001). *LiDAR accuracy, an Airborne 1 perspective* [Brochure]. El Segundo, CA.
- Applanix. (2012). *POS AV specifications* [Data Sheet]. Richmond hill, ON.
- Baltsavias, E. (1999a). Airborne laser scanning: Basic relations and formulas. *ISPRS Journal of Photogrammetry and Remote Sensing*, 54(2-3), 199-214.
- Baltsavias, E. (1999b). A comparison between photogrammetry and laser scanning. *ISPRS Journal of Photogrammetry and Remote Sensing*, 54(2-3), 83-94.
- Bao, Y., Cao, C., Zhang, H., Chen, E., He, Q., Huang, H., . . . Gong, P. (2008). Synchronous estimation of DTM and fractional vegetation cover in forested area from airborne LiDAR height and intensity data. *Science in China, Series E: Technological Sciences*, 51, 176-187.
- Baruch, A., & Filin, S. (2011). Detection of gullies in roughly textured terrain using airborne laser scanning data. *ISPRS Journal of Photogrammetry and Remote Sensing*, 66(5), 564-578.
- Bartels, M. (2012). [graphic illustration]. *Remote Sensing: Segmentation and Classification of LIDAR Data*. Retrieved March 25, 2012, from <http://www.cvg.rdg.ac.uk/projects/LIDAR/index.html>.
- Bethel, J., van Gelder, B., Cetin, A. F., & Sampath, A. (2006). *Corridor mapping using aerial technique*. (Final Report No. FWHA/INDOT/JTRP-2006/23). August, 2006: Purdue University.

- Blair, T., & McPherson, J. (1999). Grain-size and textural classification of coarse sedimentary particles. *Journal of Sedimentary Research, Section A: Sedimentary Petrology and Processes*, 69(1), 6-19.
- Bolstad, P., & Stowe, T. (1994). An evaluation of DEM accuracy: Elevation, slope, and aspect. *Photogrammetric Engineering & Remote Sensing*, 60(11), 1327-1332.
- Bossler, J. (1984). *Standards and specifications for geodetic control networks*. Rockville, MD: Federal Geodetic Control Committee (FGCC).
- Bowen, Z., & Waltermire, R. (2002). Evaluation of light detection and ranging (LiDAR) for measuring river corridor topography. *Journal of the American Water Resources Association*, 38(1), 33-41.
- Buccianti, R., Cibien, M., Mari, L., & Rebaglia, B. (2009). Accuracy, trueness, and precision: considerations based on the International Vocabulary of Metrology (VIM, 3rd Ed.) and related standards. Presented at the XIX IMEKO World Congress Fundamental and Applied Metrology, September 6-11, 2009, Lisbon, Portugal. [PowerPoint slides] Retrieved January 7, 2013, from Proceedings webpage at <http://www.imeko.org/>.
- Burns, W., Coe, J., Kaya, B., & Ma, L. (2010). Analysis of elevation changes detected from multi-temporal LiDAR surveys in forested landslide terrain in western Oregon. *Environmental & Engineering Geoscience*, 16(4), 315-341.
- Carlson Software. (2010). *Carlson Survey/Civil/Mining/Takeoff for CAD*. Maysville, KY: Developer.
- Chen, C., Fan, Z., Yue, T., & Dai, H. (2012). A robust estimator for the accuracy assessment of remote-sensing-derived DEMs. *International Journal of Remote Sensing*, 33(8), 2482-2497.
- Chou, Y., Liu, P., & Dezzani, R. (1999). Terrain complexity and reduction of topographic data. *Journal of Geographical Systems*, 1(2), 179-198.
- Clark, M., Clark, D., & Roberts, D. (2004). Small-footprint LiDAR estimation of sub-canopy elevation and tree height in a tropical rain forest landscape. *Remote Sensing of Environment*, 91(1), 68-89.
- Cobby, D., Mason, D., & Davenport, I. (2001). Image processing of airborne scanning laser altimetry data for improved river flood modelling. *ISPRS Journal of Photogrammetry and Remote Sensing*, 56(2), 121-138.
- Corns, A., & Shaw, R. (2009). High resolution 3-dimensional documentation of archaeological monuments & landscapes using airborne LiDAR. *Journal of Cultural Heritage*, 10(December Supplement 1), 72-77.

- Cowen, D., Jensen, J., Hendrix, C., Hodgson, M., & Schili, S. (2000). A GIS-Assisted rail construction econometric model that Incorporates LiDAR data. *Photogrammetric Engineering and Remote Sensing*, 66(11), 1323-1328.
- Csanyi, N., & Toth, C. (2007). Improvement of LiDAR data accuracy using LiDAR-specific ground targets. *Photogrammetric Engineering & Remote Sensing*, 73(4), 385-396.
- Dahlqvist, S., Rönholm, P., Salo, P., & Vermeer, M. (2011). Evaluating the correctness of airborne laser scanning data heights using vehicle-based RTK and VRS GPS observations. *Remote Sensing*, 3, 1902-1913.
- Daniels, R. (2001). Datum conversion issues with LiDAR spot elevation data. *Photogrammetric Engineering and Remote Sensing*, 67(6), 735-740.
- Davenport, I., Holden, N., & Gurney, R. (2004). Characterizing errors in airborne laser altimetry data to extract soil roughness. *IEEE Transactions on Geoscience & Remote Sensing*, 42(10), 2130-2141.
- Deumlich, F. (1982). *Surveying instruments* [Instrumentenkunde der vermessungstechnik] (W. Faig Trans.). Berlin; New York: Walter De Gruyter Inc.
- Ding, Q., Chen, W., King, B., & Liu, Y. (2011). Comparison of LiDAR's characteristics at different flying height. *SPIE. International Symposium on LiDAR and Radar Mapping: Technologies and Application. 26-29 May, 2011*, Nanjing, China, 8286.
- Draper, N., & Smith, H. (1998). *Applied regression analysis* (3rd ed.) Wiley.
- Ene, L., Næsset, E., & Gobakken, T. (2012). Single tree detection in heterogeneous boreal forests using airborne laser scanning and area-based stem number estimates. *International Journal of Remote Sensing*, 33(16), 5171-5193.
- Estornell, J., Ruiz, L., Velázquez-Martí, B., & Hermosilla, T. (2011). Analysis of the factors affecting LiDAR DTM accuracy in a steep shrub area. *International Journal of Digital Earth*, 4(6), 521-538.
- Ferraz, A., Gonçalves, G., Soares, P., Tomé, M., Mallet, C., Jacquemoud, S., ... Pereira, L. (2012). Comparing small-footprint LiDAR and forest inventory data for single strata biomass estimation-A case study over a multi-layered Mediterranean forest. Paper presented at *Geoscience and Remote Sensing Symposium (IGARSS)*, IEEE International, Munich, Germany, 6384-6387.

- Flood, M. (2001). Laser altimetry: From science to commercial LiDAR mapping. *Photogrammetric Engineering & Remote Sensing*, 67(11), 1209-1217.
- Flood, M. (2004). *The "Skinny" on airborne laser mapping*. <http://www.airbornelasermapping.com/ALMSkinny.html>.
- Foote K., & Huebner, D. (1995). Error, Accuracy, and Precision. *The Geographer's Craft Project*, Department of Geography, The University of Colorado at Boulder. <http://www.colorado.edu/geography/gcraft/notes/error/error.html>.
- Fornaciai, A., Pareschi, M., & Mazzarini, F. (2010). The distal segment of Etna's 2001 basaltic lava flow. *Bulletin of Volcanology*, 72(1), 119-127.
- Freedman, J. (1950). Stratigraphy and structure of the Mt. Pawtuckaway quadrangle, southeastern New Hampshire. *Bulletin of the Geological Society of America*, 61, 449-492.
- Gao, J. (2007). Towards accurate determination of surface height using modern geoinformatic methods: Possibilities and limitations. *Progress in Physical Geography*, 31(6), 591-605.
- Ghilani, C., & Wolf, P. (2010). *Elementary surveying: An introduction to geomatics*. (13th ed.). Upper Saddle River, NJ: Prentice Hall.
- Glenn, N., Spaete, L., Sankey, T., Derryberry, D., Hardegree, S., & Mitchell, J. (2010). Errors in LiDAR-derived shrub height and crown area on sloped terrain. *Journal of Arid Environments*, 75(4), 377-382.
- Glennie, C. (2007). Rigorous 3D error analysis of kinematic scanning LiDAR systems. *Journal of Applied Geodesy*, 1, 147-157.
- Goodwin, N., Coops, N., & Culvenor, D. (2006). Assessment of forest structure with airborne LiDAR and the effects of platform altitude. *Remote Sensing of Environment*, 103(2), 140-152.
- Goulden, T. (2009). *Prediction of error due to terrain slope in LiDAR observations* [M.Sc.E. Thesis]. (Technical Report No. 265). Fredericton, NB: University of New Brunswick, Geodesy and Geomatics Engineering, Fredericton, NB.
- Goulden, T., & Hopkinson, C. (2010). The forward propagation of integrated system component errors within airborne LiDAR data. *Photogrammetric Engineering and Remote Sensing*, 76(5), 589-601.
- Guo, Q., Li, W., Yu, H., & Alvarez, O. (2010). Effects of topographic variability and LiDAR sampling density on several DEM interpolation methods. *Photogrammetric Engineering and Remote Sensing*, 76(6), 701-712.

- Habib, A., Bang, K., Kersting, A., & Lee, D. (2009). Error budget of LiDAR systems and quality control of the derived data. *Photogrammetric Engineering & Remote Sensing*, 75(9), 1093-1108.
- Haneberg, W. (2008). Elevation errors in a LiDAR digital elevation model of West Seattle and their effects on slope-stability calculations. *Reviews in Engineering Geology*, 20, 55-65.
- Hasegawa, H., & Yoshimura, T. (2003). Application of dual-frequency GPS receivers for static surveying under tree canopies. *Journal of Forest Research*, 8(2), 103-110.
- Hegy, G., & Garamszegi, L. (2011). Using information theory as a substitute for stepwise regression in ecology and behavior. *Behavioral Ecology and Sociobiology*, 65, 69-76.
- Hodgson, M., & Bresnahan, P. (2004). Accuracy of airborne LiDAR-derived elevation: Empirical assessment and error budget. *Photogrammetric Engineering and Remote Sensing*, 70(3), 331-339.
- Hodgson, M., Jensen, J., Schmidt, L., Schill, S., & Davis, B. (2003). An evaluation of LiDAR- and IFSAR-derived digital elevation models in leaf-on conditions with USGS Level 1 and Level 2 DEMs. *Remote Sensing of Environment*, 84(2), 295-308.
- Hodgson, M., Jensen, J., Raber, G., Tullis, J., Davis, B., Thompson, G., & Schuckman, K. (2005). An evaluation of LiDAR-derived elevation and terrain slope in leaf-off conditions. *Photogrammetric Engineering & Remote Sensing*, 71(7), 817-823.
- Hollaus, M., Dorigo, W., Wagner, W., Schadauer, K., Höfle, B., & Maier, B. (2009). Operational wide-area stem volume estimation based on airborne laser scanning and national forest inventory data. *International Journal of Remote Sensing*, 30(19), 5159-5175.
- Hollaus, M., Wagner, W., Eberhöfer, C., & Karel, W. (2006). Accuracy of large-scale canopy heights derived from LiDAR data under operational constraints in a complex alpine environment. *ISPRS Journal of Photogrammetry and Remote Sensing*, 60(5), 323-338.
- Hongchao, M., & Jianwei, W. (2012). Analysis of Positioning Errors Caused by Platform Vibration of Airborne LiDAR System. Paper presented at the *Proceedings of the 2012 8th IEEE International Symposium on Instrumentation and Control Technology (ISICT 2012)*, London, United Kingdom., 257-261.

- Hopkinson, C., Chasmer, L., Zsigovics, G., Creed, I., Sitar, M., Treitz, P., & Maher, R. (2004). Errors in LiDAR ground elevation and wetland vegetation height estimates. Paper presented at the *Proceedings of the ISPRS Working Group VIII/2*, Freiburg, Germany., XXXVI(PART 8/W2) 108-113.
- Hopkinson, C., Crasto, N., Marsh, P., Forbes, D., & Lesack, L. (2011). Investigating the spatial distribution of water levels in the Mackenzie Delta using airborne LiDAR. *Hydrological Processes*, 25(19), 2995-3011.
- Hudak, A., Evans, J., & Stuart Smith, A. (2009). LiDAR utility for natural resource managers. *Remote Sensing*, 1(4), 934-951.
- Huising, E., & Gomes Pereira, L. (1998). Errors and accuracy estimates of laser data acquired by various laser scanning systems for topographic applications. *ISPRS Journal of Photogrammetry and Remote Sensing*, 53(5), 245-261.
- Hyypä, H., Yu, X., Hyypä, J., Kaartinen, H., Kaasalainen, S., Honkavaara, E., & Rönnholm, P. (2005). Factors affecting the quality of DTM generation in forest areas. *Laser Scanning 2005, WG III/3, III/4, V/3*, Enschede, the Netherlands. , XXXVI(PART 3/W19) 85-90.
- Hyypä, J., Pyysalo, U., Hyypä, H., Haggrén, H., & Ruppert, G. (2000). Accuracy of laser scanning for DTM generation in forested areas. Paper presented at the *Laser Radar Technology and Applications V*, Orlando, FL, USA., 4035 119-130.
- James, T., Murray, T., Barrand, N., & Barr, S. (2006). Extracting photogrammetric ground control from LiDAR DEMs for change detection. *The Photogrammetric Record*, 21(116), 312-328.
- James, L., Watson, D., & Hansen, W. (2007). Using LiDAR data to map gullies and headwater streams under forest canopy: South Carolina, USA [Article in Press]. *Catena*, 71(1), 132-144.
- Johnson, S. E. (2009). Effect of target surface orientation on the range precision of laser detection and ranging systems. *Journal of Applied Remote Sensing*, 3(1)
- Joint Committee for Guides in Metrology. (2008). *International vocabulary of metrology — Basic and general concepts and associated terms (VIM)*. 3rd edition. (JCGM 200:2008) Working Group 2 of the Joint Committee for Guides in Metrology (JCGM/WG 2).

- Jutzi, B., & Stilla, U. (2003). Analysis of laser pulses for gaining surface features of urban objects. Paper presented at the *Data Fusion and Remote Sensing Over Urban Areas, 2nd GRSS/ISPRS Joint Workshop*, 13-17.
- Kaplan, E. (1996). *Understanding GPS principles and applications*. Norwood, MA: Artech House Publishers.
- Kato, A., Moskal, L., Schiess, P., Swanson, M., Calhoun, D., Stuetzle, W. (2009), Capturing tree crown formation through implicit surface reconstruction using airborne LiDAR data. *Remote Sensing of Environment*, 113(6), 1148-1162.
- Kim, S., McGaughey, R., Andersen, H., & Schreuder, G. (2009). Tree species differentiation using intensity data derived from leaf-on and leaf-off airborne laser scanner data. *Remote Sensing of Environment*, 113, 1575-1586.
- Kobler, A., Pfeifer, N., Ogrinc, P., Todorovski, L., Oštir, K., & Džeroski, S. (2007). Repetitive interpolation: A robust algorithm for DTM generation from aerial laser scanner data in forested terrain. *Remote Sensing of Environment*, 108(1), 9-23.
- Kraus, K., & Pfeifer, N. (1998). Determination of terrain models in wooded areas with airborne laser scanner data. *ISPRS Journal of Photogrammetry and Remote Sensing*, 53(4), 193-203.
- Kumari, P. (2011). *A curvature based model for systematic errors adjustment in airborne laser scanning data* [PhD. Dissertation]. (Unpublished Doctor of Philosophy). University of Florida, Gainesville, FL.
- Lang, M., & McCarty, G. (2009). LiDAR intensity for improved detection of inundation below the forest canopy. *Wetlands*, 29(4), 1166-1178.
- Lasaponara, R., & Masini, N. (2011). On the Processing of Aerial LiDAR Data for Supporting Enhancement, Interpretation and Mapping of Archaeological Features. *Lecture Notes in Computer Science*, 6783, 392-406.
- Leica Geosystems. (2002). *ALS40 airborne laser scanner* [Brochure]. Atlanta, GA.
- Leica Geosystems. (2011). *Leica ALS70 airborne laser scanners, performance for diverse applications* [Brochure]. Heerbrugg, Switzerland.
- Leica Geosystems. (2012). *Airborne LiDAR*. http://www.leica-geosystems.com/en/Airborne-LIDAR_86814.htm.
- Leigh, C., Thomas, M., & Kidner, D. (2009). The use of LiDAR in digital surface modelling: Issues and errors. *Transactions in GIS*, 13(4), 345-361.

- Lemmens, M. (1997). Accurate height information from airborne laser-altimetry. *IGARSS '97. Remote Sensing - A Scientific Vision for Sustainable Development., 1997 IEEE International, 1* 423-426.
- Lemmens, M. (2007). Airborne LiDAR scanners. *GIM International, 21*, 24-27.
- Liu, X. (2008). Airborne LiDAR for DEM generation: Some critical issues. *Progress in Physical Geography, 32*(1), 31-49.
- Liu, X. (2011). Accuracy assessment of LiDAR elevation data using survey marks. *Survey Review, 43*(319), 80-93.
- Lloyd, C., & Atkinson, P. (2002). Deriving DSMs from LiDAR data with kriging. *International Journal of Remote Sensing, 23*(12), 2519-2524.
- Maas, H. (2002). Methods for measuring height and planimetry discrepancies in airborne laserscanner data. *Photogrammetric Engineering and Remote Sensing, 68*(9), 933-940.
- Maling, D. (1989). *Measurements from maps: Principles and methods of cartometry*. Oxford, UK: Pergamon Press.
- Marshall, J., Schenewerk, M., Snay, R., & Gutman, S. (2001). The effect of the MAPS weather model on GPS-determined ellipsoidal heights. *GPS Solutions, 5*(1), 1-14.
- Maxwell, A. (2010). *Analysis of LiDAR point data and derived elevation models for mapping and characterizing bouldery landforms* [M.S. Thesis]. (Masters, West Virginia University). *Masters Abstracts International, 49*(02), 1-148.
- Mazerolle, M. (2006). Improving data analysis in herpetology: Using Akaike's Information Criterion (AIC) to assess the strength of biological hypotheses. *Amphibia-Reptilia, 27*, 169-180.
- Montané, J., & Torres, R. (2006). Accuracy assessment of LiDAR saltmarsh topographic data using RTK GPS. *Photogrammetric Engineering and Remote Sensing, 72*(8), 961-967.
- Morin, K. (2002). *Calibration of airborne laser scanners* [M.S. Thesis]. (University of Calgary, Geomatics Engineering No. 20179). Calgary, AB: University of Calgary.
- Mundry, R., & Nunn, C. (2009). Stepwise model fitting and statistical inference: Turning noise into signal pollution. *American Naturalist, 171*(1), 119-123.

- Næsset, E. (2001). Effects of differential single- and dual-frequency GPS and GLONASS observations on point accuracy under forest canopies. *Photogrammetric Engineering & Remote Sensing*, 67(9), 1021-1026.
- Næsset, E. (2009). Effects of different sensors, flying altitudes, and pulse repetition frequencies on forest canopy metrics and biophysical stand properties derived from small-footprint airborne laser data. *Remote Sensing of Environment*, 113(1), 148-159.
- National Agricultural Imagery Program. (2009). *2009 NAIP imagery, 1:40,000* [Digital Ortho Quarter Quad]. (NAIP Imagery ed.). Salt Lake City, UT: US Department of Agriculture, Farm Service Agency, Aerial Photography Field Office. <http://www.granit.unh.edu>.
- National Geodetic Survey. (2012a). *OPUS: Online Positioning User Service*. Retrieved December 12, 2010, from <https://www.ngs.noaa.gov/OPUS/>.
- National Geodetic Survey. (2012b). *Survey mark datasheets. station designation: Patuccawa*. http://www.ngs.noaa.gov/cgi-bin/ds_desig.prl.
- National Oceanic and Atmospheric Administration. (2008). *LiDAR 101: An introduction LiDAR technology, data, and applications*. Charleston, SC: NOAA, Coastal Services Center.
- NDT Educational Resource Center. (2013). *Accuracy, error, precision, and uncertainty*. The Collaboration for NDT Education, Iowa State University. <http://www.ndt-ed.org/GeneralResources/ErrorAnalysis/UncertaintyTerms.htm>.
- NH Natural Heritage Bureau. (2010). *North Mountain at Pawtuckaway State Park* [Brochure]. Concord, NH: NH Department of Forest & Lands.
- Ni-Meister, W., Jupp, D., & Dubayah, R. (2001). Modeling LiDAR waveforms in heterogeneous and discrete canopies. *IEEE Transactions on Geoscience and Remote Sensing*, 39(9), 1943-1958.
- Olsen, R., Puetz, A., & Anderson, B. (2009). Effects of LiDAR point density on bare earth extraction and DEM creation. *ASPRS Annual Conference, Baltimore, MD, March 9-13, 2009*.
- Oksanen, J., & Sarjakoski, T. (2006). Uncovering the statistical and spatial characteristics of fine toposcale DEM error. *International Journal of Geographical Information Science*, 20(4), 345-369.
- Optech Incorporated. (2012). *Main page*. <http://www.optech.ca/>.
- Optech Incorporated. (n.d.). *Complete solutions for airborne mapping* [Brochure]. Vaughan, ON.

- Peng, M., & Shih, T. (2006). Error assessment in two LiDAR-derived TIN datasets. *Photogrammetric Engineering and Remote Sensing*, 72(8), 933-947.
- Petzold, B., Reiss, P., & Stössel, W. (1999). Laser scanning—surveying and mapping agencies are using a new technique for the derivation of digital terrain models. *ISPRS Journal of Photogrammetry and Remote Sensing*, 54(2-3), 95-104.
- Raber, G., Jensen, J., Hodgson, M., Tullis, J., Davis, B., & Berglund, J. (2007). Impact of LiDAR nominal post-spacing on DEM accuracy and flood zone delineation. *Photogrammetric Engineering and Remote Sensing*, 73(7), 793-804.
- Raber, G., Jensen, J., Schill, S., & Schuckman, K. (2002). Creation of digital terrain models using an adaptive LiDAR vegetation point removal process. *Photogrammetric Engineering and Remote Sensing*, 68(12), 1307-1315.
- Renslow, M., Greenfield, P., & Guay, T. (2000). *Evaluation of multi-return LiDAR for forestry applications*. (Liason and Special Reports No. RSAC-2060/4810-LSP-0001-RPT1). Salt Lake City, UT: US Department of Agriculture, Forest Service - Engineering. . (Project Report)
- Reutebuch, S., Ahmed, K., Curtis, T., Petermann, D., Wellander, M., & Froslie, M. (2000). A test of airborne laser mapping under varying forest canopy. *American Society of Photogrammetry & Remote Sensing 2000 Annual Conference, 22–26 may 2000*, Washington, DC.
- Reutebuch, S., McGaughey, R., Andersen, H., & Carson, W. (2003). Accuracy of a high-resolution LiDAR terrain model under a conifer forest canopy. *Canadian Journal of Remote Sensing*, 29(5), 527-535.
- RIEGL Laser Measurement Systems GmbH. (2012a). *Airborne laser scanning*. <http://www.riegl.com/nc/products/airborne-scanning/>.
- RIEGL Laser Measurement Systems GmbH. (2012b). *Full waveform analysis airborne laser scanner for high operating altitudes, LMS-Q780. Preliminary data sheet [Brochure]*. Horn, Austria.
- Rodríguez-Pérez, J., Alvarez, M., & Sanz-Ablanedo, E. (2007). Assessment of low-cost GPS receiver accuracy and precision in forest environments. *Journal of Surveying Engineering*, 133(4), 159-167.
- Royal Society of Chemistry (2003). *Terminology - the key to understanding analytical science. Part 1: Accuracy, precision and uncertainty*. (AMC technical brief No. 13), Analytical Methods Committee.

- Sapeta, K. (2000). Have you seen the light? LiDAR technology is creating believers. *Geoworld*, 13(10), 32-35.
- Schaer, P., Skaloud, J., Landtwing, S., & Legat, K. (2007). Accuracy estimation for laser point cloud including scanning geometry. *5th International Symposium on Mobile Mapping Technology*, Padova, Italy. , *Mobile Mapping Symposium 2007*.
- Schenk, T. (2001). *Modeling and analyzing systematic errors in airborne laser scanners*. (Technical Notes in Photogrammetry No. 19). Columbus, OH: Ohio State University.
- Schmid, K., Hadley, B., & Wijekoon, N. (2011). Vertical accuracy and use of topographic LiDAR data in coastal marshes. *Journal of Coastal Research*, 27(6A (Supplement)), 116-132.
- Seeber, G. (2003). *Satellite Geodesy* (2nd ed.). New York: Walter de Gruyter.
- Shan, J., & Toth, C. (Eds.). (2008). *Topographic laser ranging and scanning* (1st Ed. ed.) CRC Press.
- Siegman, A. (1986). *Lasers*. Sausalito, California. University Science Books.
- Sithole, G., & Vosselman, G. (2004). Experimental comparison of filter algorithms for bare-Earth extraction from airborne laser scanning point clouds. *ISPRS Journal of Photogrammetry & Remote Sensing*, 59(1), 85-101.
- Skaloud, J., Schaer, P., Stebler, Y., & Tomé, P. (2010). Real-time registration of airborne laser data with sub-decimeter accuracy. *ISPRS Journal of Photogrammetry & Remote Sensing*, 65(2), 208-217.
- Spaete, L., Glenn, N., Derryberry, D., Sankey, T., Mitchell, J., & Hardegree, S. (2011). Vegetation and slope effects on accuracy of a LiDAR-derived DEM in the sagebrush steppe. *Remote Sensing Letters*, 2(4), 317-326.
- Stebler, Y., Stengele, R., Tomé, P., Schaer, P., & Skaloud, J. (2009). Airborne LiDAR: In-flight accuracy estimation. *GPS World*, 20/8, 37-41.
- Stewart, J., Hu, J., Kayen, R., Lembo Jr., A., Collins, B., Davis, C., & O'Rourke, T. (2009). Use of airborne and terrestrial LiDAR to detect ground displacement hazards to water systems. *Journal of Surveying Engineering*, 135(3), 113-124.
- Su, J., & Bork, E. (2006). Influence of vegetation, slope, and LiDAR sampling angle on DEM accuracy. *Photogrammetric Engineering and Remote Sensing*, 72(11), 1265-1274.

- Thoma, D., Gupta, S., Bauer, M., & Kirchoff, C. (2005). Airborne laser scanning for riverbank erosion assessment. *Remote Sensing of Environment*, 95(4), 493-501.
- Topcon Positioning Systems Incorporated. (2004). *HiPerLite and HiPerLite+ operator's manual*. US.
- Topcon Positioning Systems Incorporated. (2012a). *GPS*. <http://www.topconpositioning.com/products/gps>.
- Topcon Positioning Systems Incorporated. (2012b). *MS series total stations*. <http://www.topconpositioning.com/products/total-stations/robotic/ms-series>.
- Töyrä, J., Pietroniro, A., Hopkinson, C., & Kalbfleisch, W. (2003). Assessment of airborne scanning laser altimetry (LiDAR) in a deltaic wetland environment. *Canadian Journal of Remote Sensing*, 29(6), 718-728.
- Treitz, P. (2012). [graphic illustration]. *Evaluation and Development of LiDAR Data Acquisition Standards for Forest Inventory Applications and Predictive Forest Ecosite Classification*. <http://www.geog.queensu.ca/larsees/research.htm>.
- Triglav-Čekada, M., Crosilla, F., & Kosmatin-Fras, M. (2009). A simplified analytical model for a-priori LiDAR point-positioning error estimation and a review of LiDAR error sources. *Photogrammetric Engineering and Remote Sensing*, 75(12), 1425-1439.
- Trimble Navigation Limited. (2012). *Trimble R8 GNSS receiver* [Datasheet] (04/2012 ed.). Dayton, OH.
- US Geological Survey. (1981). *Mt. Pawtuckaway quadrangle, New Hampshire-Rockingham Co. Photorevised 1988*. [Topographic Map]. (7.5 Minute Quadrangle Series ed.). Reston, VA: United States Department of Interior, USGS.
- Ussyshkin, R., Ravi, R., Ilnicki, M., & Pokorny, M. (2009). Mitigating the impact of the laser footprint size on airborne LiDAR data accuracy. *ASPRS Annual Conference, Baltimore, MD, March 9-13, 2009*.
- Van Leeuwen, M., Coops, N., & Wulder, M. (2010). Canopy surface reconstruction from a LiDAR point cloud using Hough transform. *Remote Sensing Letters*, 1(3), 125-137.
- Van Sickle, J. (1996). *GPS for land surveyors*, Ann Arbor Press.

- Vaughn, C., Bufton, J., Krabill, W., & Rabine, D. (1996). Georeferencing of airborne laser altimeter measurements. *International Journal of Remote Sensing*, 17(11), 2185-2200.
- Vaze, J., Teng, J., & Spencer, G. (2010). Impact of DEM accuracy and resolution on topographic indices. *Environmental Modelling & Software*, 25(10), 1086-1098.
- Vosselman, G. (2008). Analysis of planimetric accuracy of airborne laser scanning surveys. *Silk Road for Information from Imagery*, Beijing. , XXXVII(Part B3a, Commission III, WG III/3) 99-104.
- Wagner, W., Ullrich, A., Melzer, T., Briese, C., & Kraus, K. (2004). From single-pulse to full-waveform airborne laser scanners: Potential and practical challenges. *XXth ISPRS Congress, 12-23 July 2004 Istanbul, Turkey Commission 3, Istanbul, Turkey. , XXXVI(III)*
- Wang, C., Menenti, M., Stoll, M., Feola, A., Belluco, E., & Marani, M. (2009). Separation of ground and low vegetation signatures in LiDAR measurements of salt-marsh environments. *IEEE Transactions on Geoscience & Remote Sensing*, 47(7), 2014-2023.
- Wang, J., Xu, L., Li, X., & Tian, X. (2011). Impact analysis of random measurement errors on airborne laser scanning accuracy. *Instrumentation and Measurement Technology Conference (I2MTC)*, Binjiang, China. 1-4.
- Webster, T. (2005). LiDAR validation using GIS: A case study in comparison between two LiDAR collection methods. *Geocarto International*, 20(4), 11-19.
- Wehr, A., & Lohr, U. (1999). Airborne laser scanning - An introduction and overview. *ISPRS Journal of Photogrammetry and Remote Sensing*, 54(2-3), 68-82.
- White, R., Dietterick, Mastin, T., & Strohmman, R. (2010). Forest roads mapped using LiDAR in steep forested terrain. *Remote Sensing*, 2, 1120-1141.
- Whittingham, M., Stephens, P., Bradbury, R., & Freckleton, R. (2006). Why do we still use stepwise modelling in ecology and behaviour? *Journal of Animal Ecology*, 75, 1182-1189.
- Wikipedia. (2012). *Accuracy and Precision*. [graphic illustration]. http://en.wikipedia.org/wiki/Accuracy_and_precision.
- Wulder, M., White, J., Nelson, R., Næsset, E., Ørka, H., Coops, N., ... Gobakken, T. (2012). LiDAR sampling for large-area forest characterization: A review. *Remote Sensing of Environment*, 121, 196-209.

- Xhardé, R., Long, B., & Forbes, D. (2006). Accuracy and limitations of airborne LiDAR surveys in coastal environments. Paper presented at the *2006 IEEE International Geoscience and Remote Sensing Symposium, IGARSS, July 31, 2006 - August 4, 2412-2415*.
- Yu, X., Hyyppä, H., Kaartinen, H., Hyyppä, J., Ahokas, E., & Kaasalainen, S. (2005). Applicability of first pulse derived digital terrain models for boreal forest studies. *Workshop "Laser Scanning 2005", September 12-14, 2005, Enschede, the Netherlands. , ISPRS WG III/3, III/4, V/3 97-102*.
- Zandbergen, P. (2008). Positional accuracy of spatial data: Non-normal distributions and a critique of the National Standard for Spatial Data Accuracy. *Transactions in GIS, 12*(1), 103-130.
- Zandbergen, P. (2011). Characterizing the error distribution of LiDAR elevation data for North Carolina. *International Journal of Remote Sensing, 32*(2), 409-430.